

<b>OCRWM</b>	<b>SCIENTIFIC ANALYSIS COVER SHEET</b>	1. QA:QA Page 1 of 124
--------------	--	---------------------------

2. Scientific Analyses Title  
**Characterize Framework for Igneous Activity at Yucca Mountain, Nevada**

3. DI (including Revision Number)  
**ANL-MGR-GS-000001 Revision 01**

4. Total Attachments  
 5. Attachment Numbers - Number of pages in each  
**Attachment I - 13; Attachment II-6; Attachment III-22**

	Printed Name	Signature	Date
6. Originator	F.V. Perry, R. Youngs, T. Vogt	SIGNATURE ON FILE	10/27/03 10/22/02
7. Checker	S. Baldrige	SIGNATURE ON FILE	10/30/03
8. QER	K. McFall	SIGNATURE ON FILE	11/3/03
9. Responsible Manager/Lead	M. Cline	SIGNATURE ON FILE	11/3/03
10. Responsible Manager	J. L. King	SIGNATURE ON FILE	11/3/03

11. Remarks  
**FINAL**

Technical Contact/Department: **F.V. Perry, Disruptive Events**

**Revision History**

12. Revision/ICN No.	13. Description of Revision/Change
REV 00	Initial issue
REV 00 ICN 01	<p>REV 00 ICN 01 of this AMR incorporates a calculations of the volcanic hazard using the 70,000 Metric Tons of Uranium (MTU) No-Backfill repository layout described in BRWMS M&amp;O (2000b). ICN 01 also modifies the approach for calculation of the conditional number of eruptive centers occurring within the potential repository footprint (1) using empirical distributions for the average spacing between eruptive centers rather than the expected values of these distributions, and (2) incorporating uncertainty in the effect of the repository opening on the conditional probability of the occurrence of an eruptive center within the potential repository footprint. Changes to the text are indicated in the document with change bars.</p> <p>New sections have been added to the document. Some sections were renumbered or renamed.</p> <p>Changes to figures:                      Part c was added to Figure 17a and b; Figures 16a, 16c, 20a, 21a, 22a, 23a, and 24a were added to the document. Figure 3 was modified as was Attachment I.</p> <p>Changes to tables:                      Tables 2a, 7a, 8a, 9a, 10a, 11a, 12a, and 13a were added to the document. In Table 13, a column was changed to indicate probability of at least one eruptive center. Table II-3 was added to Attachment II, and Table III-13 was added to Attachment III.</p> <p>Five new software routines were added to the document.</p>
REV 01	<p>Recalculated the frequency of intesection based on the new License Application footprint (Section 6.5.3); documented sensitivity of the 1999 USGS aeromagnetic data (Section 6.5.4); and documented the alternative <del>(REV 01C continued)</del> conceptual model of the hot spot beneath the Yucca Mountain region (Section 6.3.3). Change bars were not used because revisions were extensive due to the change in the repository footprint.</p>



**CONTENTS**

	<b>Page</b>
1. PURPOSE.....	11
2. QUALITY ASSURANCE.....	13
3. USE OF SOFTWARE .....	13
3.1 SOFTWARE TRACKED BY CONFIGURATION MANAGEMENT.....	13
3.1.1 Software Routines.....	14
3.1.2 Software Used in the Current Revision of this Scientific Analysis .....	17
3.2 EXEMPT SOFTWARE .....	20
4. INPUTS.....	21
4.1 DATA AND PARAMETERS .....	21
4.2 CRITERIA.....	21
4.3 CODES AND STANDARDS .....	22
5. ASSUMPTIONS.....	22
5.1 USE OF QUATERNARY VOLCANOES .....	22
5.2 ALL VOLCANIC EVENTS PRODUCE AT LEAST ONE ERUPTIVE CENTER....	23
5.3 LOCATION OF ERUPTIVE CENTERS ALONG THE LENGTH OF A DIKE OR DIKE SEGMENT.....	23
6. SCIENTIFIC ANALYSIS .....	24
6.1 INTRODUCTION .....	24
6.1.1 Features, Events, and Processes .....	25
6.2 VOLCANIC HISTORY OF THE YUCCA MOUNTAIN REGION.....	27
6.3 THE PROBABILISTIC VOLCANIC HAZARD ANALYSIS.....	30
6.3.1 The Probabilistic Volcanic Hazard Analysis Process .....	30
6.3.2 Definitions and Parameters of a Volcanic Event and Implications for Alternative Probability Calculations .....	37
6.3.3 Conceptual Models of Volcanism and Formulation of Probability Models .....	43
6.4 THE CRATER FLAT STRUCTURAL DOMAIN .....	48
6.4.1 Internal Structure and Boundaries of the Crater Flat Basin .....	50
6.4.2 Probabilistic Volcanic Hazard Analysis Volcanic Source Zones: Relationship to Crater Flat Structural Features and the Probability of Dike Intersection.....	55
6.5 RECALCULATION OF FREQUENCY OF INTERSECTION AND DEVELOPMENT OF DISTRIBUTIONS FOR LENGTH AND ORIENTATION OF DIKES AND FOR THE NUMBER OF ERUPTIVE CENTERS WITHIN THE PROPOSED REPOSITORY FOOTPRINT .....	58
6.5.1 Formulation.....	61
6.5.2 Implementation.....	76
6.5.3 Results .....	94
6.5.4 Impact of 1999 Aeromagnetic Data on Frequency of Intersection.....	105

**CONTENTS (Continued)**

	<b>Page</b>
7. CONCLUSIONS.....	113
7.1 SUMMARY OF SCIENTIFIC ANALYSIS .....	113
7.2 OUTPUTS BASED ON THE PROPOSED LICENSE APPLICATION FOOTPRINT (BLOCKS 1, 2, 3, AND 5) .....	114
7.3 UNCERTAINTIES .....	115
8. INPUTS AND REFERENCES .....	115
8.1 DOCUMENTS CITED.....	115
8.2 CODES, STANDARDS, REGULATIONS, AND PROCEDURES .....	122
8.3 DATA, LISTED BY DATA TRACKING NUMBER .....	122
8.4 SOFTWARE.....	123
8.5 OUTPUT DATA.....	124
ATTACHMENT I ADDRESSING <i>YUCCA MOUNTAIN REVIEW PLAN FINAL REPORT</i> ACCEPTANCE CRITERIA RELATED TO THE DEFINITION OF EVENTS WITH PROBABILITIES GREATER THAN $10^{-8}$ PER YEAR AND VOLCANIC DISRUPTION OF WASTE PACKAGES .....	I-1
ATTACHMENT II DEVELOPMENT OF FOOTPRINT POLYGON FOR THE PROPOSED REPOSITORY .....	II
ATTACHMENT III DEVELOPMENT OF DISTRIBUTIONS FOR NUMBER OF ERUPTIVE CENTERS PER VOLCANIC EVENT AND AVERAGE SPACING BETWEEN E.....	III-1

**FIGURES**

	<b>Page</b>
1. Flowchart for Computation of Frequency of Intersection of Proposed Repository by a Dike .....	15
2. Flowchart for Computation of Conditional Distributions for Length and Azimuth of Intersecting Dike and Number of Eruptive Centers Within the Proposed Repository Given Intersection of This Footprint by a Dike .....	18
3. Location and Age of Post-Miocene (< 5.3 million years (m.y.)) Volcanoes (or Clusters Where Multiple Volcanoes Have Indistinguishable Ages) in the Yucca Mountain Repository .....	27
4. Composite Distribution for Dike Length Averaged Across All 10 Probabilistic Volcanic Hazard Analysis Experts .....	39
5. Conceptual Diagram Comparing Event Definitions from the Probabilistic Volcanic Hazard Analysis and Reamer: Implications for Eruption and Intrusion Probabilities Based on Different Event Definitions .....	40
6. Composite Distribution for the Distance from the Point Volcanic Event to the End of the Dike Averaged Across All 10 PVHA Experts .....	44
7. Local Structural Domains and Domain Boundaries of the Yucca Mountain Repository and Internal Structures of the Crater Flat Basin and Selected Parts of Adjacent Domains.....	49
8. Schematic Cross Section of the Crater Flat Basin, from Seismic, Reflection Surficial Geology, and Borehole Information .....	51
9a. Local Structural Domains and Domain Boundaries of the Yucca Mountain Repository and Internal Structures of the Crater Flat Basin and Selected Parts of Adjacent Domains.....	56
9b. Local Structural Domains and Domain Boundaries of the Yucca Mountain Repository and Internal Structures of the Crater Flat Basin and Selected Parts of Adjacent Domains.....	57
10. Schematic Illustrating Procedure for Computing the Frequency of Intersection of the Proposed Repository by a Volcanic Event.....	60
11a. Logic Tree Structure Used to Characterize Uncertainty in Volcanic Hazard.....	62
11b. Logic Tree Structure for Subtrees Addressing Uncertainty in Volcanic Hazard from Specific Sources .....	62
12. Definition of Parameters Used to Compute the Probability of Intersection of the Proposed Repository Footprint by a Volcanic Event.....	64
13. Example Distributions for Dike Length, $L$ , (part a); Normalized Location of the Point Volcanic Event Relative to the Total Length of the Dike, $E^L$ , (part b); and the Resulting Distribution for Distance from the Point Volcanic Event to the End of the Dike, $d$ (part c) .....	65
14. Example Simulations of the Distribution of Eruptive Centers Along the Length of a Dike for: (a) the Independent, Uniformly Distributed Spatial Distribution and (b) the Uniformly Spaced, Randomly Distributed Spatial Distribution.....	71
15a. Probability for the Number of Eruptive Centers Within the Proposed Repository Footprint, $r^{EC}$ , as a Function of Dike Length, $L$ , for the Length of Intersection, $L^I = 1$ Kilometer and the Number of Eruptive Centers Associated with the Volcanic Event, $n^{EC} = 2$ .....	74

**FIGURES (Continued)**

	<b>Page</b>
5b. Probability for the Number of Eruptive Centers Within the Proposed Repository Footprint, $r^{EC}$ , as a Function of Dike Length, $L$ , for the Length of Intersection, $L^I = 1$ Kilometer and the Number of Eruptive Centers Associated with the Volcanic Event, $n^{EC} = 3$ .....	74
6a. Proposed License Application Emplacement Drifts and Footprint Polygon Encompassing Emplacement Panels 1, 2, 3, and 5 .....	78
6b. Location of Proposed License Application Repository Footprint Compared to Repository Footprint Used in the Probabilistic Volcanic Hazard Analysis.....	79
7. Spatial Distribution of Volcanic Hazard Defined by the Probabilistic Volcanic Hazard Analysis Expert Panel: (a) Map of Expected Volcanic Event Frequency and (b) Map of Spatial Disaggregation of Expected Intersection Frequency.....	84
8. Distributions for Number of Eruptive Centers per Volcanic Event, $n^{EC}$ , Derived from the Probabilistic Volcanic Hazard Analysis Experts' Interpretations (from Attachment III, Figure III-1).....	86
19. Probability for the Number of Eruptive Centers Within the Proposed Repository Footprint, $r^{EC}$ , Computed Using the Uniformly Spaced, Randomly Distributed Fixed Density Spatial Distribution of Eruptive Centers and for the Length of Intersection, $L^I = 1$ km, and an Average Spacing of 2.5 km Between Eruptive Centers Compared to the Results for the <i>IUD</i> and <i>USRD</i> Models Shown in Figure 15a.....	88
20. Annual Frequency of Intersecting the Proposed License Application Repository Footprint.....	97
21. Marginal Distributions for Dike Intersection Length, $L^I$ , for the 5th Percentile, Mean, and 95 <sup>th</sup> Percentile Frequency of Intersection.....	99
22. Marginal Distributions for Dike Intersection Azimuth, $f$ , for the 5th Percentile, Mean, and 95 <sup>th</sup> Percentile Frequency of Intersection for the Proposed License Application Footprint.....	101
23. Marginal Distributions for the Number of Eruptive Centers Within the Proposed Repository Footprint, $r^{EC}$ , for the 5 <sup>th</sup> Percentile, Mean, and 95 <sup>th</sup> Percentile Frequency of Intersection 104	
24. Locations of Potential Buried Basalt Inferred from Aeromagnetic Data .....	106
25. Composite Annual Frequency of Intersection of the Repository Footprint for Sensitivity Cases for the Primary-plus-Contingency Block Case of the 70,000-Metric Tons of Uranium No-Backfill Layout.....	111
26. Individual Expert Results for Annual Frequency of Intersection of the Proposed Repository Footprint for Sensitivity Cases for the Primary-plus-Contingency Block Case of the 70,000-Metric Tons of Uranium No-Backfill Layout.....	112

**TABLES**

	<b>Page</b>
1. Software Routines Used to Compute Frequency of Intersection of the Proposed Repository by a Dike.....	14
2. Software Routines Used to Compute Conditional Distributions for Dike Length, Azimuth, and Number of Eruptive Centers Within the Proposed Repository.....	15
3. Software Routines Used to Compute Conditional Distributions for Dike Length, Azimuth, and Number of Eruptive Centers Within the Proposed Repository, Incorporating an Empirical Distribution for Average Spacing Between Eruptive Centers .....	19
4. Software Used to Convert Emplacement Drift End Points for the Proposed LA Repository Footprint from Nevada State Plane Coordinates to Universal Transverse Mercator .....	20
5. Exempt Software.....	20
6. Input Data.....	21
7. Other Input to This Scientific Analysis .....	21
8. Project Requirements for This Scientific Analysis Report .....	21
9. Included Feature, Event, and Process for This Scientific Analysis Report and Its Disposition in Total System Performance Assessment for the License Application.....	26
10. Estimated Volume and <sup>40</sup> Ar/ <sup>39</sup> Ar Age <sup>a</sup> of Quaternary Volcanoes in the Yucca Mountain Repository .....	29
11. Probabilistic Volcanic Hazard Analysis Panel Members .....	30
12. Alternative Conceptual Models Not Considered in the Probabilistic Volcanic Hazard Analysis.....	34
13. Published Estimates of the Probability of Intersection of the Proposed Repository at Yucca Mountain by a Volcanic Event .....	37
14. Average Eruptive Center Spacing (from Attachment III, Table III-12) .....	87
15. Empirical Distribution for Average Spacing Between Eruptive Centers Calculation Results (from Attachment III, Table III-13 of this document) .....	93
16. Frequency of Intersection for the License Application Footprint (Blocks 1, 2, 3, and 5).....	95
17. Marginal Distributions for Dike Intersection Length for the 5th Percentile, Mean, and 95 <sup>th</sup> Percentile Frequency of Intersection of the Proposed License Application Footprint.....	100
18. Marginal Distribution for Intersecting Dike Azimuth for the 5th Percentile, Mean, and 95 <sup>th</sup> Percentile Frequency of Intersection of the Proposed License Application Footprint.....	102
19. Marginal Distribution for Number of Eruptive Centers Within the Proposed Repository for the 5th Percentile, Mean, and 95 <sup>th</sup> Percentile Frequency of Intersection of the Proposed License Application Footprint .....	104

**TABLES (Continued)**

	<b>Page</b>
20. Comparison of Mean Number of Volcanic Events for 1996 Probabilistic Volcanic Hazard Analysis Assessment with Sensitivity Analysis Values .....	109
21. Summary of Computed Frequency of Intersection for 70,000-Metric Tons of Uranium No-Backfill Repository Layout (primary + contingency blocks) from Sensitivity Cases .....	110
22. Summary Frequencies of Disruptive Volcanic Events for the License Application Footprint.....	114

## ACRONYMS AND ABBREVIATIONS

BSC	Bechtel SAIC Company, LLC
CDF	cumulative probability density function
DOE	U.S. Department of Energy
DTN	data tracking number
FEP	feature, event, and process
IUD-C	Independent, Uniformly Distributed, Correlated
IUD-UC	Independent, Uniformly Distributed, Uncorrelated
LA	License Application
MTU	metric tons of uranium
m.y.	million years
NRC	U.S. Nuclear Regulatory Commission
PA	performance assessment
PVHA	probabilistic volcanic hazard analysis
STN	software tracking number
SR	site recommendation
TSPA	total system performance assessment
TWP	technical work plan
USGS	U.S. Geological Survey
USRD-C	Uniformly Spaced, Randomly Distributed, Correlated
USRD-FD	Uniformly Spaced, Randomly Distributed Fixed Density
USRD-UC	Uniformly Spaced, Randomly Distributed, Uncorrelated
UTM	Universal Transverse Mercator
YMR	Yucca Mountain region
YMRP	<i>Yucca Mountain Review Plan, Final Report</i>

INTENTIONALLY LEFT BLANK

## 1. PURPOSE

The purpose of this scientific analysis report is threefold.

Present a conceptual framework of igneous activity in the Yucca Mountain region (YMR) consistent with the volcanic and tectonic history of this region and the assessment of this history by experts who participated in the probabilistic volcanic hazard analysis (PVHA) (CRWMS M&O 1996 [100116]\*). Conceptual models presented in the PVHA are summarized and applied in areas in which new information has been presented. Alternative conceptual models are discussed as well as their impact on probability models. The relationship between volcanic source zones defined in the PVHA and structural features of the YMR are described based on discussions in the PVHA and studies presented since the PVHA.

Present revised probability calculations, based on PVHA outputs, for the repository footprint currently proposed for the License Application (LA), rather than the footprint used at the time of the PVHA. This analysis report also calculates the probability of an eruptive center(s) forming within the current repository footprint using information developed in the PVHA. Probability distributions are presented for the length and orientation of volcanic dikes located within the repository footprint and for the number of eruptive centers (conditional on a dike intersecting the repository) located within the repository footprint.

Document sensitivity studies that analyze how the presence of potentially buried basaltic volcanoes impact the frequency of intersection of the proposed repository footprint by a basaltic dike. The sensitivity study was prompted by aeromagnetic data collected in 1999 indicating the possible presence of previously unrecognized buried volcanoes in the YMR (Blakely et al. 2000 [151881]; O'Leary et al. 2002 [158468]).

The U.S. Department of Energy (DOE) considers volcanism to be a potentially disruptive event in the total system performance assessment (TSPA) analysis supporting the LA for the proposed Yucca Mountain repository (DOE 1998 [100550]). The two volcanic scenarios (with individual probabilities and consequences) being modeled by the TSPA-LA are: (1) the ascent of a basaltic dike or dike system (i.e., a set or swarm of multiple dikes comprising a single intrusive event) to repository level where it intersects drifts; and (2) the development of a volcano within the repository footprint with one or more conduits that intersect waste packages. As a consequence of the first event, which is noneruptive, waste from breached packages may provide a source of radionuclides when groundwater moves through the damaged packages at some time in the future (igneous intrusion groundwater release). The potential consequence of the second event is that waste packages entrained within a conduit may be breached, releasing radionuclides to the erupting ash plume where they can be dispersed downwind to a reasonably maximally exposed individual (10 CFR 63 [156605], Section 63.2; 66 FR 55794) in the accessible environment at the controlled area boundary (10 CFR 63 [156605], Section 63.302; 66 FR 55813). According to 10 CFR Part 63 this location is to be approximately 18 kilometers (km) south of the repository.

---

\* In this report, a unique six-digit numerical identifier (the Document Input Reference System [DIRS] number) is placed in the text following the reference callout (e.g., BSC 2002 [155950]), the purpose of which is to assist the reader in locating a specific reference in the DIRS database. Within the reference list (Section 8), multiple sources by the same author and date (e.g., BSC2002) are sorted alphabetically by title.

The TSPA-LA requires consideration of both probability and consequence. The objective of the PVHA was to determine the probability of a basaltic dike intersecting the proposed repository (CRWMS M&O 1996 [100116]). The PVHA report was the outcome of an expert elicitation and forms the foundation of much of the igneous analysis for the LA. The PVHA included discussion of some aspects of the consequences of a volcanic event but not all the aspects required for the present analysis; therefore, additional analyses will be performed to support description of the volcanic risk. The risk from volcanism will be described by combining work from the PVHA (probability) and the present enhanced analysis of consequence.

This report, *Characterize Framework for Igneous Activity at Yucca Mountain, Nevada*, Revision 01, describes the conceptual framework for volcanism near Yucca Mountain and how the conceptual framework provides the basis for probability calculations. This report also presents the probability results and associated uncertainties for intersection of the proposed repository by a volcanic event and the probability of an eruption through the repository, conditional on a dike intersection. In the context of the PVHA, a volcanic event is a spatially and temporally distinct batch of magma ascending from the mantle through the crust as a dike or system of dikes (CRWMS M&O 1996 [100116], Appendix E). For the purposes of the probability models discussed in this report, a volcanic event is defined as a point (x,y) in space representing the expected midpoint of the dike system involved in the magma ascent. The dike system associated with the volcanic event is represented in probability model by a line element defined in terms of a length, azimuth and location relative to the point event (Figures 10 and 12). The term dike length used in the PVHA and in this report when discussing volcanic events, refers to the total length of the dike system associated with the volcanic event. The phrase intersection of the repository footprint by a dike refers to intersection of the emplacement area of the repository by the line element representing the dike system associated with the volcanic event. The possibility that a dike system (e.g., multiple dikes) has width or consists of multiple parallel dikes does not significantly affect the intersection probability and is not part of the calculations in this report. The width of the dikes and the number of parallel dikes does affect the consequences of an intersection and is included in *Number of Waste Packages Hit by Igneous Intrusion* (BSC 2003 [161851]).

The probability results documented in this report provide the basis for all further igneous consequence analysis. This report also provides direct input into the *Number of Waste Packages Hit by Igneous Intrusion* scientific analysis report, *Number of Waste Packages Hit by Igneous Intrusion* (BSC 2003 [161851]), and direct input to the TSPA-LA.

A recalculation of the volcanic hazard using the current proposed LA repository layout (BSC 2003 [162289]) is documented in this report. The current revision of this report (Revision 01) uses the same approach for calculation of the conditional number of eruptive centers occurring within the repository footprint that was used in the previous revision (CRWMS M&O 2000 [151551]). This approach is to calculate the conditional number of eruptive centers occurring within the repository footprint using empirical distributions for the average spacing between eruptive centers rather than the just the expected values of these distributions and to incorporate uncertainty in the effect of the repository opening on the conditional probability of the occurrence of an eruptive center within the repository footprint.

Consideration of the number of volcanic events that have occurred during selected periods of time in the YMR was one of the key parameters the PVHA used to calculate the probability of a basaltic dike intersecting the repository footprint. Volcanic features counted as volcanic events included individual volcanoes, alignments of volcanoes, and aeromagnetic anomalies in the region that are known (by drilling), or inferred to be, buried volcanoes. In 1999, three years after the PVHA was completed, a new aeromagnetic survey of the YMR was completed under the direction of the U.S. Geological Survey (USGS) (Blakely et al. 2000 [151881], O'Leary et al. 2002 [158468]). This report assesses the impact of new aeromagnetic data on the probability of intersection of the repository footprint by a basaltic dike using sensitivity studies that incorporate alternative conceptual models.

This report is governed by the OCRWM *Technical Work Plan For: Igneous Activity Analysis for Disruptive Events*, (BSC 2002 [161315]), Work Package ADEM03. The technical work plan (TWP) specifies the activities to be carried out in updating information in the revision of this report. The activities documented in this report do not deviate from those specified in the TWP.

## 2. QUALITY ASSURANCE

Development of this scientific analysis report and the supporting analyses have been determined to be subject to the Yucca Mountain Project's quality assurance program (BSC 2002 [161315], Section 8.1, Work Package ADEM03). Approved quality assurance procedures identified in the TWP (BSC 2002 [161315], Section 4) have been used to conduct and document the activities described in this report. The TWP also identifies the methods used to control the electronic management of data (BSC 2002, Section 8.4 [161315]).

An evaluation conducted per AP-SV.1Q, *Control of the Electronic Management of Information*, identifies that electronic data requiring controls are involved in this work (see Attachment 1, "Office of Civilian Radioactive Waste Management Process Control Evaluation for Supplement V"). Checksums and parity checks performed by computer operating systems during data transfer and storage using commonly available software and hardware, plus established computer security mechanisms, provide adequate assurance of the integrity of transferred data. Additional controls on electronic storage and transfer of data will be described in scientific notebooks documenting the work if scientific notebooks are used.

## 3. USE OF SOFTWARE

### 3.1 SOFTWARE TRACKED BY CONFIGURATION MANAGEMENT

The calculations presented in this scientific analysis report were performed with the set of software routines described below. This software has been qualified following procedure AP-SI.1Q, *Software Management*. The software and routines used in support of this work are appropriate for this application and are used within their range of validation as described in the qualification documentation. The software is written in FORTRAN77 and operates on a personal computer equipped with a 486 or Pentium processor under disk operating system or in a Windows Microsoft disk operating system window. The computations using these software routines were performed using the software routines acquired from Software Configuration

Management. The software was designed to perform the calculations defined by the PVHA (CRWMS M&O 1996 [100116]) and was used within the parameter limits defined by the PVHA.

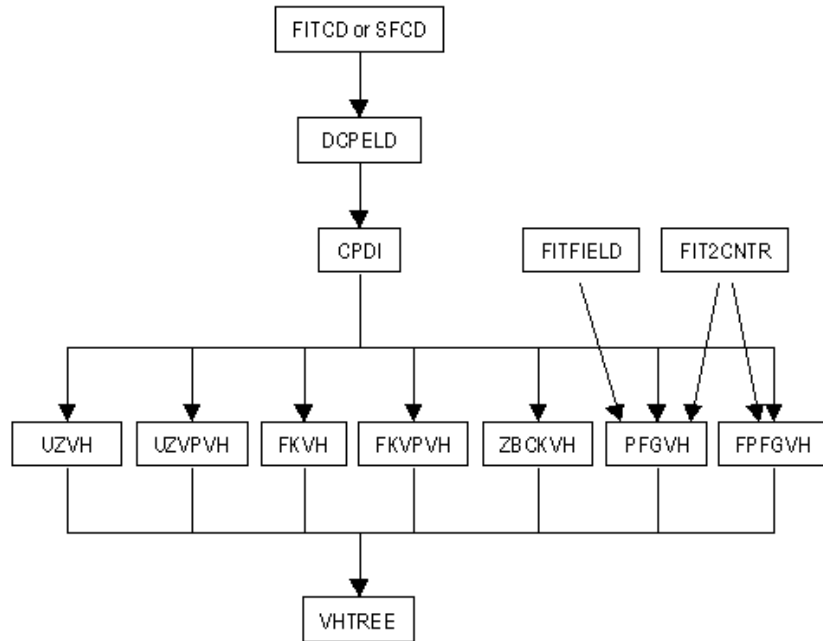
### 3.1.1 Software Routines

The software routine titles are listed with the *.FOR* extension in the Software Configuration Management database, the DIRS database, and in Section 8.3 of this report. The routines are listed by their titles without the *.FOR* extension in Tables 1 and 2, Figures 1 and 2, and in the text of this report.

Table 1 lists the software routines used to compute the frequency of intersection of the repository footprint by a volcanic event through full enumeration of the PVHA experts' logic trees. Figure 1 shows the data flow through the routines in Table 1. The software routines listed in Table 1 are qualified versions of the routines used in the PVHA calculation (CRWMS M&O 1996 [100116]).

Table 1. Software Routines Used to Compute Frequency of Intersection of the Proposed Repository by a Dike

Software Routine software tracking number (STN)	Function
FITCD V1.0 (10262-1.0-00) [148532]	Computes discrete cumulative probability distributions for dike length from cumulative probabilities specified at selected values of length.
SFCD V1.0 (10275-1.0-00) [148533]	Computes discrete cumulative probability distributions for dike length using user-specified distribution forms.
DCPELD V1.0 (10258-1.0-00) [148534]	Computes discrete probability distribution for dike length from expert-specified distributions (output of FITCD).
CPDI V1.0 (10257-1.0-00) [148535]	Computes conditional probability of intersection from volcanic events on a x,y grid using output of DCPELD and expert-specified azimuth distributions.
UZVH V1.0 (10277-1.0-00) [148536]	Computes frequency of intersection from volcanic source zones using output of CPDI.
FKVH V1.0 (10265-1.0-00) [148567]	Computes frequency of intersection using kernel density estimation with specified <i>h</i> and output of CPDI.
UZVPVH V1.0 (10279-1.0-00) [148537]	Computes frequency of intersection from volcanic source zones using volume predictable volcanic event rate model and output of CPDI.
FKVPVH V1.0 (10267-1.0-00) [148538]	Computes frequency of intersection using kernel density estimation using volume predictable volcanic event rate model and output of CPDI.
ZBCKVH V1.0 (10283-1.0-00) [148539]	Computes frequency of intersection using kernel density estimation with <i>h</i> constrained by a source zone boundary and output of CPDI.
FITFIELD V1.0 (10263-1.0-00) [148540]	Computes parameters of a bivariate Gaussian distribution that approximates boundaries of a defined polygon.
FIT2CNTR V1.0 (10261-1.0-00) [148541]	Computes parameters of a bivariate Gaussian distribution from locations of volcanic events.
PFGVH V1.0 (10273-1.0-00) [148542]	Computes frequency of intersection using a bivariate Gaussian distribution with specified field parameters and output of CPDI. Bivariate Gaussian distribution parameters obtained from programs FIT2CNTR or FITFIELD.
FPFGVH V1.0 (10269-1.0-00) [148543]	Computes frequency of intersection using a bivariate Gaussian distribution with parameters fit to volcanic event locations and output of CPDI.
VHTREE V1.0 (10282-1.0-00) [148544]	Computes mean and fractiles of frequency of intersection over an individual expert's volcanic hazard logic tree and aggregate over all experts using outputs of UZVH, UZVHB, FKVH, UZVPVH, FKVPVH, ZBCLVH, PFGVH, and FPFGVH.



N/A-For Illustration Purposes Only

NOTE: Names in the boxes denote software routines listed in Table 1.

Figure 1. Flowchart for Computation of Frequency of Intersection of Proposed Repository by a Dike

Table 2 lists the software routines used to compute the conditional distributions for the length and azimuth of an intersecting dike within the proposed repository footprint and the number of eruptive centers within this footprint. The data flow through the software routines for this calculation is shown in Figure 2.

Table 2. Software Routines Used to Compute Conditional Distributions for Dike Length, Azimuth, and Number of Eruptive Centers Within the Proposed Repository

Software Routine (STN Number)	Function
FITCD V1.0 (10262-1.0-00) [148532]	Computes discrete cumulative probability distributions for dike length from cumulative probabilities specified at selected values of length.
SFCV V1.0 (10275-1.0-00) [148533]	Computes discrete cumulative probability distributions for dike length using user-specified distribution forms.
DCPELD V1.0 (10258-1.0-00) [148534]	Computes discrete probability distribution for dike length from expert-specified distributions (output of FITCD).
CPDI V1.0 (10257-1.0-00) [148535]	Computes conditional probability of intersection from volcanic events on a x,y grid using output of DCPELD and expert-specified azimuth distributions.
UZVHLH V1.0 (10278-1.0-00) [148545]	Computes simulations of contributions to frequency of intersection on a x,y grid from volcanic source zones using Latin Hypercube sampling and output from CPDI.

Characterize Framework for Igneous Activity at Yucca Mountain, Nevada

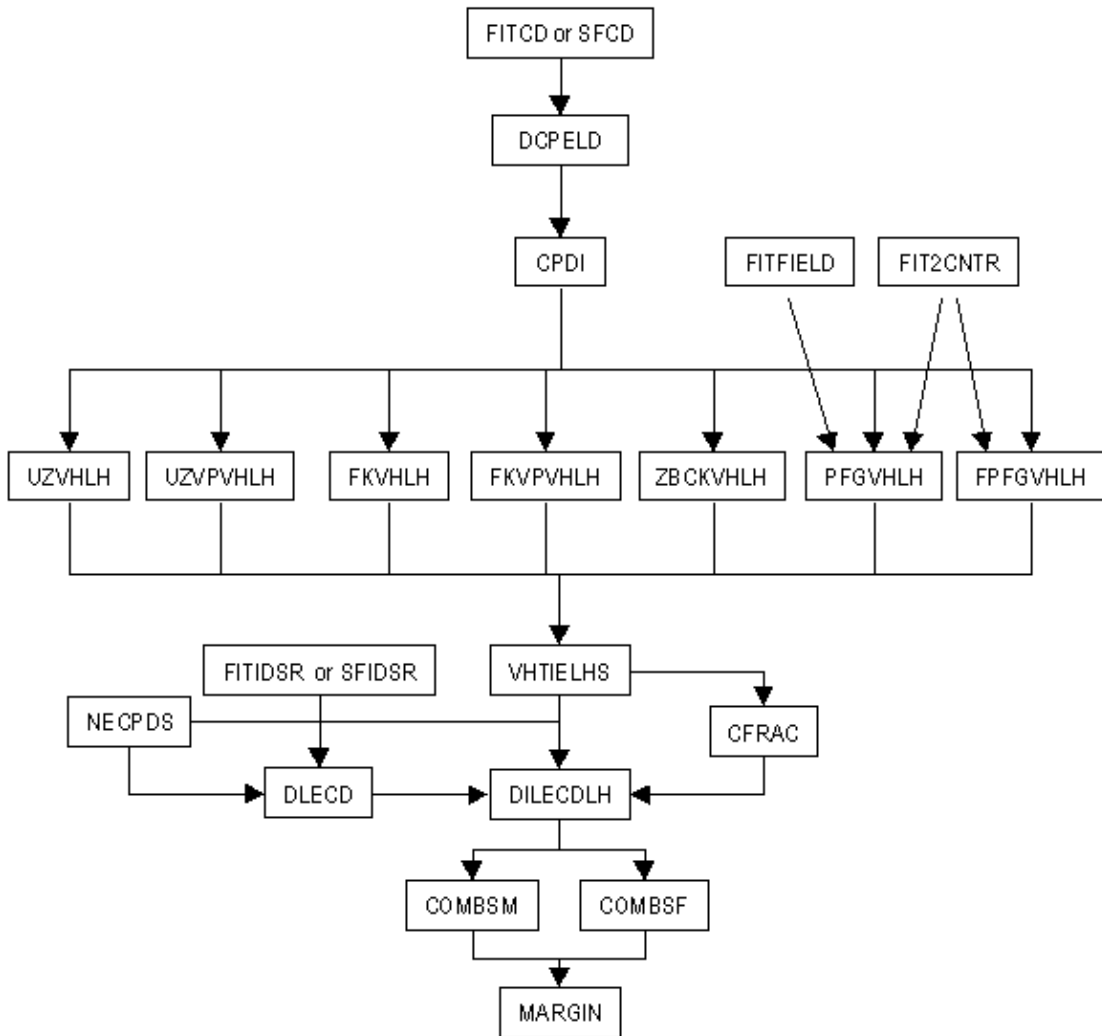
Table 2. Software Routines Used to Compute Conditional Distributions for Dike Length, Azimuth, and Number of Eruptive Centers Within the Proposed Repository (Continued)

Software Routine (STN Number)	Function
FKVHLH V1.0 (10266-1.0-00) [148546]	Computes simulations of contributions to frequency of intersection on an x,y grid using kernel density estimation with specified $h$ , Latin Hypercube sampling, and output from CPDI.
UZVPVHLH V1.0 (10280-1.0-00) [148547]	Computes simulations of contributions to frequency of intersection on an x,y grid from volcanic source zones using volume predictable volcanic event rate model, Latin Hypercube sampling, and output from CPDI.
FKVPVHLH V1.0 (10268-1.0-00) [148551]	Computes simulations of contributions to frequency of intersection on an x,y grid with kernel density estimation using volume predictable volcanic event rate model, Latin Hypercube sampling, and output from CPDI.
ZBCKVHLH V1.0 (10284-1.0-00) [148550]	Computes simulations of contributions to frequency of intersection on an x,y grid using kernel density estimation with $h$ constrained by a source zone boundary, Latin Hypercube sampling, and output from CPDI.
FITFIELD V1.0 (10263-1.0-00) [148540]	Computes parameters of a bivariate Gaussian distribution that approximates boundaries of a defined polygon.
FIT2CNTR V1.0 (10261-1.0-00) [148541]	Computes parameters of a bivariate Gaussian distribution from locations of volcanic events.
PFGVHLH V1.0 (10274-1.0-00) [148552]	Computes simulations of contributions to frequency of intersection on a x,y grid using a 2-D-Gaussian distribution with specified parameters, Latin Hypercube sampling, and output from CPDI. Gaussian distribution parameters obtained from programs FIT2CNTR or FITFIELD.
FPFGVHLH V1.0 (10270-1.0-00) [148553]	Computes simulations of contributions to frequency of intersection on an x,y grid using a 2-D-Gaussian distribution with parameters fit to volcanic event locations, Latin Hypercube sampling, and output from CPDI.
VHTIELHS V1.0 (10281-1.0-00) [148554]	Computes mean and fractiles of simulations of contributions to frequency of intersection on an x,y grid over an individual expert's volcanic hazard logic tree using Latin Hypercube sampling and output from UZVHLH, FKVHLH, UZVPVHLH, FKVPVHLH, ZBCLVHLH, PFGVHLH, and FPFGVHLH.
NECPDS V1.0 (10272-1.0-00) [148555]	Computes distributions for number of eruptive centers per volcanic event and average spacing between eruptive centers.
SFIDSR V1.0 (10276-1.0-00) [148571]	Computes discrete incremental probability distributions for dike length using input to SFCD.
DLECD V1.0 (10260-1.0-00) [148558]	Computes joint discrete probability distributions for dike length and number of eruptive centers per volcanic event using output from FITIDSR.
DILECDLH V1.0 (10259-1.0-00) [148559]	Computes joint conditional distribution of dike intersection length, dike azimuth, and number of eruptive centers within the repository footprint from outputs of program VHTIELHS using Latin hypercube sampling of dike length and volcanic event location distributions from DIECDIST.
CFRAC V1.0 (10254-1.0-00) [148560]	Locates individual expert's simulation results that represent specified percentiles of the composite distribution for frequency of intersection from outputs of VHTIELHS.
COMBSM V1.0 (10256-1.0-00) [148561]	Computes composite joint distribution of dike intersection length, dike azimuth, and number of eruptive centers within the repository footprint across experts from outputs of DILECDLH and VHTIELHS for mean hazard.
COMBSF V1.0 (10255-1.0-00) [148562]	Computes composite joint distribution of dike intersection length, dike azimuth, and number of eruptive centers within the repository footprint across experts from outputs of DILECDLH for selected percentiles of the hazard.
MARGIN V1.0 (10271-1.0-00) [148563]	Computes marginal distributions for dike intersection length, dike azimuth, and number of eruptive centers within the repository footprint from output of COMBSM and COMBSF.

In addition, the software routine COMBDELD V1.0 (STN: 10288–1.0-00 [148617]) was used to calculate aggregate dike length and event length distributions across all 10 PVHA experts for display in Figures 4 and 6.

### **3.1.2 Software Used in the Current Revision of this Scientific Analysis**

The current revision of this scientific analysis (Revision 01) re-computes the probability distributions for frequency of intersection of the repository footprint using the current proposed LA repository footprint (BSC 2003 [162289]). This calculation is performed using the software routines listed in Table 1. Revision 01 also re-computes the conditional probability for length and azimuth of intersecting dikes and the number of eruptive centers within the repository footprint. These calculations are performed using the software routines listed in Table 3. Five of the software routines in Table 3 are modified from those listed in Table 2 to incorporate the empirical distribution for the average spacing between eruptive centers. Software used to convert Nevada State Plane coordinates to Universal Transverse Mercator (UTM) coordinates for the proposed LA footprint is listed in Table 4.



N/A-For Illustration Purposes Only

NOTE: Names in boxes denote software routines listed in Table 2.

Figure 2. Flowchart for Computation of Conditional Distributions for Length and Azimuth of Intersecting Dike and Number of Eruptive Centers Within the Proposed Repository Given Intersection of This Footprint by a Dike

Table 3. Software Routines Used to Compute Conditional Distributions for Dike Length, Azimuth, and Number of Eruptive Centers Within the Proposed Repository, Incorporating an Empirical Distribution for Average Spacing Between Eruptive Centers

Software Routine (STN Number)	Function
FITCD V1.0 (10262-1.0-00) [148532]	Computes discrete cumulative probability distributions for dike length from cumulative probabilities specified at selected values of length.
SFCD V1.0 (10275-1.0-00) [148533]	Computes discrete cumulative probability distributions for dike length using user-specified distribution forms.
DCPELD V1.0 (10258-1.0-00) [148534]	Computes discrete probability distribution for dike length from expert-specified distributions (output of FITCD).
CPDI V1.0 (10257-1.0-00) [148535]	Computes conditional probability of intersection from volcanic events on a x,y grid using output of DCPELD and expert-specified azimuth distributions.
UZVHLH V1.0 (10278-1.0-00) [148546]	Computes simulations of contributions to frequency of intersection on a x,y grid from volcanic source zones using Latin Hypercube sampling and output from CPDI.
FKVHLH V1.0 (10266-1.0-00) [148545]	Computes simulations of contributions to frequency of intersection on an x,y grid using kernel density estimation with specified $h$ , Latin Hypercube sampling, and output from CPDI.
UZVPVHLH V1.0 (10280-1.0-00) [148547]	Computes simulations of contributions to frequency of intersection on an x,y grid from volcanic source zones using volume predictable volcanic event rate model, Latin Hypercube sampling, and output from CPDI.
FKVPVHLH V1.0 (10268-1.0-00) [148551]	Computes simulations of contributions to frequency of intersection on an x,y grid with kernel density estimation using volume predictable volcanic event rate model, Latin Hypercube sampling, and output from CPDI.
ZBCKVHLH V1.0 (10284-1.0-00) [148550]	Computes simulations of contributions to frequency of intersection on an x,y grid using kernel density estimation with $h$ constrained by a source zone boundary, Latin Hypercube sampling, and output from CPDI.
FITFIELD V1.0 (10263-1.0-00) [148540]	Computes parameters of a bivariate Gaussian distribution that approximates boundaries of a defined polygon.
FIT2CNTR V1.0 (10261-1.0-00) [148541]	Computes parameters of a bivariate Gaussian distribution from locations of volcanic events.
PFGVHLH V1.0 (10274-1.0-00) [148552]	Computes simulations of contributions to frequency of intersection on a x,y grid using a 2D-Gaussian distribution with specified parameters, Latin Hypercube sampling, and output from CPDI. Gaussian distribution parameters obtained from programs FIT2CNTR or FITFIELD.
FPFGVHLH V1.0 (10270-1.0-00) [148553]	Computes simulations of contributions to frequency of intersection on an x,y grid using a 2D-Gaussian distribution with parameters fit to volcanic event locations, Latin Hypercube sampling, and output from CPDI.
VHTIELHS V1.0 (10281-1.0-00) [148554]	Computes mean and fractiles of simulations of contributions to frequency of intersection on an x,y grid over an individual expert's volcanic hazard logic tree using Latin Hypercube sampling and output from UZVHLH, FKVHLH, UZVPVHLH, FKVPVHLH, ZBCLVHLH, PFGVHLH, and FPFGVHLH.
NECPDS V1.1 (10272-1.1-00) [148555]	Computes distributions for number of eruptive centers per volcanic event and average spacing between eruptive centers.

Table 3. Software Routines Used to Compute Conditional Distributions for Dike Length, Azimuth, and Number of Eruptive Centers Within the Proposed Repository, Incorporating an Empirical Distribution for Average Spacing Between Eruptive Centers (Continued)

Software Routine (STN Number)	Function
FITIDSR V1.0 (10264-1.0-00) [148557]	Computes discrete incremental probability distributions for dike length using input to FITCD.
SFIDSR V1.0 (10276-1.0-00) [148571]	Computes discrete incremental probability distributions for dike length using input to SFCD
DLECD V1.0 (10260-1.0-00) [148558]	Computes joint discrete probability distributions for dike length and number of eruptive centers per volcanic event using output from FITIDSR
DILECDLH V1.1 (10259-1.1-00) [148559]	Computes joint conditional distribution of dike intersection length, dike azimuth, and number of eruptive centers within the repository footprint from outputs of program VHTIELHS using Latin hypercube sampling of dike length and volcanic event location distributions from DIECDIST
CFRAC V1.0 (10254-1.0-00) [148560]	Locates individual expert's simulation results that represent specified percentiles of the composite distribution for frequency of intersection from outputs of VHTIELHS
COMBSM V1.1 (10256-1.1-00) [148561]	Computes composite joint distribution of dike intersection length, dike azimuth, and number of eruptive centers within the repository footprint across experts from outputs of DILECDLH and VHTIELHS for mean hazard
COMBSF V1.1 (10255-1.1-00) [148562]	Computes composite joint distribution of dike intersection length, dike azimuth, and number of eruptive centers within the repository footprint across experts from outputs of DILECDLH for selected percentiles of the hazard
MARGIN V1.1 (10271-1.1-00) [148563]	Computes marginal distributions for dike intersection length, dike azimuth, and number of eruptive centers within the repository footprint from output of COMBSM and COMBSF

Table 4. Software Used to Convert Emplacement Drift End Points for the Proposed LA Repository Footprint from Nevada State Plane Coordinates to Universal Transverse Mercator

Software Name and Version (V)	STN	Description	Computer and Platform Identification
EarthVision 5.1 [152614]	10174-5.1-00	Commercial GIS software used for coordinate conversion	Silicon Graphics/ IRIX 6.5

### 3.2 EXEMPT SOFTWARE

Commercial, off-the-shelf software used in support of this scientific analysis is listed in Table 5. This software is exempt from the requirements of AP-SI.1Q, *Software Management*.

Table 5. Exempt Software

Software Name and Version (V)	STN	Description	Computer and Platform Identification
Microsoft Excel, 97	N/A	The commercial software, Microsoft Excel, 97 was used for plotting graphs and preparing tables. No software routines or macros were used with this software to prepare this report. The output was visually checked for correctness.	PC, Windows 98

## 4. INPUTS

### 4.1 DATA AND PARAMETERS

The location, a brief description, and the data tracking numbers (DTNs) used as input for this scientific analysis report are listed in Table 6. The qualification status of data input is indicated in the electronic DIRS database.

The source of input data for this analysis is the PVHA expert interpretations presented in *Probabilistic Volcanic Hazard Analysis for Yucca Mountain, Nevada* (CRWMS M&O 1996 [100116]). Because this report is an analysis of the PVHA (CRWMS M&O 1996 [100116]), the use of the PVHA as input to this report is appropriate. The PVHA expert interpretations are used as inputs to the calculations described in Section 6.5 and Attachment III. The interpretations are also discussed in the conceptual framework described in Sections 6.1 through 6.4.

Table 6. Input Data

Data Name	Data Source	DTN
PVHA (CRWMS M&O 1996 [100116]): Expert Assessment of Volcanic Hazard in the YMR	CRWMS M&O 1996 [100116]	MO0002PVHA0082.000 [148234]

Other input to this analysis is listed in Table 7.

Table 7. Other Input to This Scientific Analysis

Name	Description	Uncertainty
LA repository footprint	Repository footprint determined from information described in BSC (2003 [162289])	N/A

All other DTNs presented in this scientific analysis report are not used as direct input to this report and are used as reference only.

### 4.2 CRITERIA

The Yucca Mountain *Projects Requirements Document* (Canori and Leitner 2003 [161770]) identifies the high-level requirements for the Project. The requirements that pertain to this scientific analysis report, and its link to 10 CFR Part 63 [156605], are shown in Table 8.

Table 8. Project Requirements for This Scientific Analysis Report

Requirement Number	Title	10 CFR Part 63 link [156605]	<i>Yucca Mountain Review Plan, Final Report (YMRP) (NRC 2003 [163274]) Acceptance Criteria</i>
PRD-002/T-015	Requirements for Performance Assessment (PA)	10 CFR 63.114	2.2.1.3.10.3, criteria 1 to 3

The YMRP (NRC 2003 [163274]) lists acceptance criteria pertaining to the above requirements. Criteria that are applicable to this scientific analysis report are described in Attachment I.

The YMRP Acceptance Criteria are intended to assure that the requirements at 10 CFR 63.114(a)–(c) and (e)–(g) [156605] are met.

### 4.3 CODES AND STANDARDS

No specific formally established codes or standards have been identified as applying to this activity. This activity does not directly support LA design.

## 5. ASSUMPTIONS

This section describes the assumptions used for the analyses in Section 6.5 and Attachment III.

The calculation of the updated distribution for frequency of intersection of the proposed repository footprint by a basaltic dike requires no assumptions because it uses the outputs defined by the PVHA (CRWMS M&O 1996 [100116]) without modification. The update involves only a change in the proposed repository footprint.

The calculation of conditional distributions for the length and azimuth of intersecting dikes within the proposed repository requires no assumptions because it involves only a modification of the software to output an intermediate step of the “frequency of intersection of the proposed repository footprint by a dike” calculation.

The calculation of conditional distributions for the number of eruptive centers within the proposed repository footprint requires an assessment of the number of eruptive centers associated with a volcanic event and the spatial distribution for eruptive centers along the length of the dike. As explained in Section 6.5.2.2, this analysis uses the PVHA experts’ assessment of volcanic event counts and the number of separate eruptive centers to develop a distribution for the number of eruptive centers per volcanic event. The number of eruptive centers associated with a volcanic event is derived using the following assumptions.

### 5.1 USE OF QUATERNARY VOLCANOES

**Assumption:** The mapped Quaternary volcanoes in the YMR are representative of the type being characterized for calculation of the consequences of an eruptive event through the proposed repository. For the purposes of this analysis report and for PA calculations, each eruptive center or vent equates to one subsurface conduit.

**Basis:** The characteristics of Quaternary volcanoes in the YMR are used to define the distributions for the characteristics of future volcanic events (BSC 2003 [161838]). The assumption that each volcano is associated with a conduit is consistent with the description of the eruptive process for YMR volcanoes described in Characterize Eruptive Processes at Yucca Mountain, Nevada (BSC 2003 [161838]). Volcanoes were also used by the PVHA experts as indicators of the occurrence of past volcanic events.

**Use in the Analysis:** This assumption is used in Attachment III to derive distributions for the number of eruptive centers per volcanic event and the average spacing between eruptive centers.

**Confirmation Status:** This assumption needs no further confirmation.

## **5.2 ALL VOLCANIC EVENTS PRODUCE AT LEAST ONE ERUPTIVE CENTER**

**Assumption:** Each hypothetical volcanic event for which the associated dike intersects the repository has at least one eruptive center located somewhere along the length of the dike.

**Basis:** This assumption is justified on the basis of the PVHA expert panel's general belief that magma that ascends to within a few hundred meters of the surface will produce a surface manifestation of the volcanic event (CRWMS M&O 1996 [100116], Appendix E, e.g., pp. RC-10, BC-6, WD-6, WH-6, MK-12). The assumption is conservative in that the PVHA experts allowed for the possibility that not all past volcanic events reached the surface in assessing the rate of volcanic events. The rate of volcanic events used to compute the frequency of intersection of the proposed repository footprint by a dike was obtained by multiplying the rate based on past volcanic events with observed surface manifestations by a "hidden events factor" greater than or equal to 1.0. Assuming all future volcanic events will produce an eruptive center produces the maximum rate of eruptive center occurrence.

**Use in the Analysis:** This assumption is used in Attachment III to develop distributions for the number of eruptive centers per volcanic event and in Section 6.5.2.2 in the computation of the conditional distribution for number of eruptive centers within the repository.

**Confirmation Status:** The assumption is consistent with the expert panel's general consideration that magma ascending to within a few hundred meters of the surface would erupt and need not be confirmed.

## **5.3 LOCATION OF ERUPTIVE CENTERS ALONG THE LENGTH OF A DIKE OR DIKE SEGMENT**

**Assumption:** The location of an eruptive center along the length of a dike or dike segment is defined by a uniform probability distribution.

**Basis:** This assumption is justified on the basis that it is the minimum information assumption that maximizes the uncertainty in location of the eruptive center. Any other form of a probability distribution requires more information than the range of possible locations (in this case, the end points of a dike or dike segment). The assumption is conservative because it maximizes the probability for the occurrence of multiple eruptive centers within the proposed repository.

**Use in the Analysis:** This assumption is used in Section 6.5.2.2 in the computation of the conditional distribution for number of eruptive centers within the proposed repository.

**Confirmation Status:** The assumption does not need to be confirmed because it does not impose any additional information beyond the length of the dike, which is obtained from the PVHA experts' interpretations. Furthermore, in this report an alternative assumption is used in

which the presence of the repository cavity results in a probability of 1.0 of at least one eruptive center, given an intersection by a volcanic event.

## 6. SCIENTIFIC ANALYSIS

### 6.1 INTRODUCTION

In this report, a conceptual framework for volcanism at Yucca Mountain consistent with output and results of the PVHA is described. This report describes how this framework and alternative conceptual frameworks influence the results of estimations of the probability of dike intersection and volcanic eruption at the proposed geologic repository at Yucca Mountain.

This report summarizes and extends the findings of the PVHA (CRWMS M&O 1996 [100116]). For the PVHA, an expert panel was convened in 1995 to review all pertinent data relating to volcanism at Yucca Mountain and, based on these data, to quantify both the annual probability and associated uncertainty of a volcanic event intersecting a proposed repository sited at Yucca Mountain. The data the experts reviewed was comprehensive, consisting of two decades of data collected by volcanologists who conducted studies to quantify the probability that a future volcanic eruption would disrupt the proposed repository (e.g., CRWMS M&O 1998 [105347] and references therein). This report also describes the relationship between volcanic source zones defined in the PVHA and the current understanding of structural controls on volcanism in the YMR.

The results of the PVHA are a set of alternative models for assessing the volcanic hazard at Yucca Mountain, probabilities that each model is the appropriate model, and probability distributions for the parameters of the models. As such, the PVHA defines the scientific uncertainty in applying models to assess the volcanic hazard. The PVHA experts documented the basis for their assessments of the validity of the alternative models in *Probabilistic Volcanic Hazard Analysis for Yucca Mountain, Nevada* (CRWMS M&O 1996 [100116], Appendix E). Therefore, the results of the PVHA are considered valid for assessing the uncertainty in the volcanic hazard at Yucca Mountain.

In the context of the PVHA the volcanic hazard is defined as the annual frequency of intersection of the repository by a volcanic event. A volcanic event was defined in the PVHA to be a spatially and temporally distinct batch of magma ascending from the mantle through the crust as a dike or system of dikes (CRWMS M&O 1996 [100116], Appendix E). For the purposes of the probability models developed in the PVHA and discussed in this report, a volcanic event is defined as a point (x,y) in space representing the expected midpoint of the dike system involved in the magma ascent. The dike system associated with the volcanic event is represented in probability model by a line element defined in terms of a length, azimuth and location relative to the point event. The term 'dike length' used in the PVHA and in this report when discussing volcanic events, refers to the total length of the dike system associated with the volcanic event. The phrase 'intersection of the repository footprint by a dike' refers to intersection of the emplacement area of the repository by the line element representing the dike system associated with the volcanic event. The possibility that a dike system (e.g., multiple dikes) has width or consists of multiple parallel dikes does not significantly affect the intersection probability and is

not part of the calculations in this report. The width of the dikes and the number of parallel dikes does affect the consequences of an intersection and is included in the consequence analyses presented in *Number of Waste Packages Hit by Igneous Intrusion* (BSC 2003 [161851]).

Based on the PVHA outputs and assumptions in Section 5 of this report, probability distributions are developed for the length and orientation of intersecting dikes within the proposed repository footprint and for the number of eruptive centers located within the repository footprint (conditional on a dike intersecting the repository). Lastly, the probability of dike intersection is recalculated based on the current proposed repository footprint, and the probability of an eruptive center(s) forming within the current proposed repository footprint is calculated (the latter is a calculation that was not included in the PVHA).

### **6.1.1 Features, Events, and Processes**

The development of a comprehensive list of feature, event, and process (FEPs) potentially relevant to postclosure performance of the proposed Yucca Mountain repository is an ongoing, iterative process based on site-specific information, design, and regulations. The approach for developing an initial list of FEPs in support of the TSPA-for the site recommendation (SR) (CRWMS M&O 2000 [153246]) was documented in Freeze et al. (2001 [154365]). The initial FEPs list contained 328 FEPs, of which 176 were included in TSPA-SR models (CRWMS M&O 2000 [153246], Tables B-9 through B-17). To support the TSPA-LA, the FEPs list was reevaluated in accordance with the Enhanced FEP Plan (BSC 2002 [158966], Section 3.2).

Tables 2 and 3 of the TWP for igneous activity analysis (BSC 2002 [161315]) provide a listing of both included and excluded FEPs for each of the disruptive events analysis and model reports. One FEP that was listed as included in the TWP, 1.2.04.01.00 Igneous Activity, was deleted during the FEPs review for TSPA-LA and conducted as part of the Enhanced FEPs Plan. The description of the FEP was found to be entirely redundant with more specific igneous related FEPs. The FEPs 1.2.04.02.0A, Igneous Activity Causes Changes to Rock Properties, and 1.2.10.02.00, Hydrologic Response to Igneous Activity, were previously, and continue to be, excluded. The technical basis for exclusion of these FEPs was previously provided in (CRWMS M&O 2000 [151553]). Although this analysis report may provide information cited in the technical basis for exclusion, the following discussion addresses only implementation (either implicit or explicit) within the TSPA-LA model, consistent with guidance provided in Appendix C of the *Scientific Processes and Guidelines Manual* (BSC 2002 [160313]).

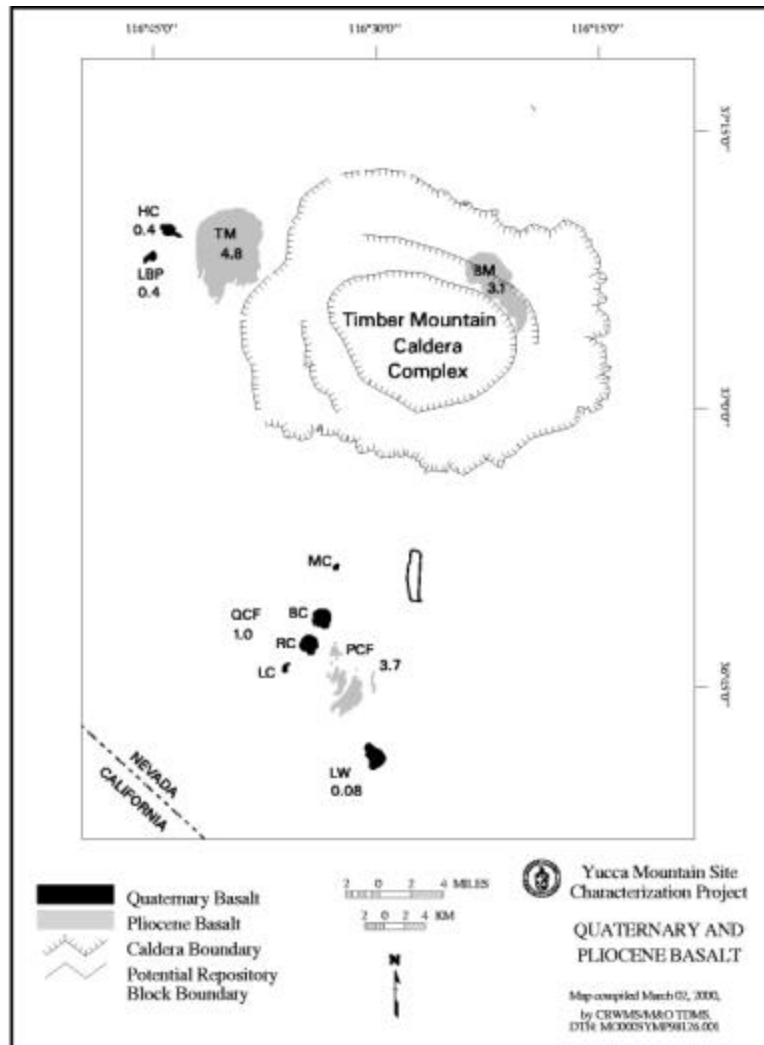
Table 9 describes the FEP that is included in the TSPA-LA through the use of the results of the analysis described in this document. Details of the implementation of this FEP are summarized in Section 6.5. The implementation of that included FEP in TSPA-LA is described in this analysis report. Details of the implementation are summarized here in the table, including specific reference to sections within this document. The parameters that address the included FEP are also listed. The sources of input for these parameters are described in Section 4 for input parameters and elsewhere in Section 6 if they were specifically developed within this document. Consequently, the supporting data, the alternative conceptual models considered by the PVHA, the findings and results, and the uncertainties documented in the PVHA as they relate to the listed FEP are considered to be implicitly included in the TSPA-LA (see Section 6.3.1).

Table 9. Included Feature, Event, and Process for This Scientific Analysis Report and Its Disposition in Total System Performance Assessment for the License Application

TSPA-SR FEP Number, Name, and Description	TSPA-LA FEP Number, Name and Description	Section Where Disposition Is Described	Summary of TSPA-LA Disposition
<p>1.2.04.03.00 Igneous Intrusion into Repository <i>Magma from an igneous intrusion flows into the drifts and extends over a large portion of the repository site, forming a sill. The sill could be limited to the drifts or a continuous sill could form along the plane of the repository, bridging between adjacent drifts.</i></p>	<p>1.2.04.03.0A Igneous Intrusion into Repository <i>Magma from an igneous intrusion flows into the drifts and extends over a large portion of the repository site, forming a sill, dike, or dike swarm depending on the stress conditions. This could involve multiple drifts. The sill could be limited to the drifts or a continuous sill could form along the plane of the repository, bridging between adjacent drifts.</i></p>	<p>Section 6.5</p>	<p>The technical basis for the inclusion of this FEP is provided in this analysis report by documenting the probability of a basaltic dike intersecting the repository footprint, the number of eruptive centers (conduits) within the repository footprint, and the length and azimuth of intersecting dikes within the repository footprint – each of these aspects is related to defining the consequence of an igneous intrusion into the repository.</p> <p>Parameters developed in this document that are a direct output to the <i>Number of Waste Packages Hit by Igneous Intrusion</i> scientific analysis report, <i>Number of Waste Packages Hit by Igneous Intrusion</i> (BSC 2003 [161851]), and implicitly included in the TSPA-LA include the following:</p> <ul style="list-style-type: none"> <li>• Conditional joint probability distribution for length and azimuth (within the repository) of an intersecting dike</li> <li>• Conditional joint probability distribution of the number of eruptive centers within the repository</li> <li>• Conditional marginal distributions for length of intersecting dike and number of eruptive centers within the repository footprint.</li> </ul> <p>The results of the probability analysis are used in the analyses of the number of waste package hit during an igneous intrusion and affected by conduit formation. The cumulative probability density function (CDF) of the number of waste packages hit is then used by the TSPA-LA model to determine the amount of waste released via an eruptive event and to determine the number of waste packages affected and the volume of waste subject to release via the groundwater pathway. Because the CDF for the number of waste packages hit is dependent on the underlying inputs, the underlying inputs and related FEPs are considered to be included implicitly in the TSPA-LA model.</p> <p>Parameters developed in this document that are direct outputs to and explicitly included in the TSPA-LA include the following:</p> <ul style="list-style-type: none"> <li>• Probability distribution for annual frequency of intersection of repository footprint by a dike</li> <li>• Summary frequencies of disruptive volcanic events.</li> </ul> <p>The TSPA-LA uses the probability distributions directly to weight the igneous contribution to annual dose. The results of this analysis report address this FEP by providing the basis for determining the mean probabilities used to weight igneous groundwater and eruptive dose. The values developed in this report represent full distributions, which are then binned together to generate a CDF of less than 100 points for the primary and contingency block values.</p>

## 6.2 VOLCANIC HISTORY OF THE YUCCA MOUNTAIN REGION

Because several Quaternary basaltic volcanoes exist within 20 km of the proposed Yucca Mountain repository (Figure 3), volcanism must be assessed as a possible future disruptive event in TSPA. Two major types of volcanism have occurred in the YMR: an early phase of Miocene silicic volcanism, the recurrence of which is considered unlikely and not of regulatory concern, and a more recent phase of Miocene and post-Miocene basaltic volcanism that is of regulatory concern (Reamer 1999 [119693], p. 5).



DTNs: LAFP831811AQ97.001 [144279]; MO003YMP98126.001 [149605] (both are used for reference only).

Source: Numbers by each volcano indicate approximate age in millions of years (CRWMS M&O 1998 [105347], Chapter 2, Tables 2.B and 2.C; DTN: LAFP831811AQ97.001).

NOTE: TM =Thirsty Mesa; PCF = Pliocene Crater Flat; BM = Buckboard Mesa; QCF = Quaternary Crater Flat; (MC = Makani Cone; BC = Black Cone; RC = Red Cone; LC = Little Cones); HC = Hidden Cone; LBP = Little Black Peak; LW = Lathrop Wells.

Figure 3. Location and Age of Post-Miocene (< 5.3 million years (m.y.) Volcanoes (or Clusters Where Multiple Volcanoes Have Indistinguishable Ages) in the Yucca Mountain Repository

The earliest volcanism in the YMR was dominated by a major episode of caldera-forming, silicic volcanism that occurred primarily between ~15 and 11 m.y., forming the southwestern Nevada volcanic field (Sawyer et al. 1994 [100075]). Silicic volcanism was approximately coincident with a major period of extension, which occurred primarily between 13 and 9 m.y. (Sawyer et al. 1994 [100075], Figure 4). Yucca Mountain is an uplifted, erosional remnant of voluminous ash-flow tuff deposits formed during the early phase of silicic volcanism.

The commencement of basaltic volcanism occurred during the latter part of the caldera-forming phase, as extension rates waned, and small-volume basaltic volcanism has continued into the Quaternary. In terms of eruption volume, the 15-m.y. history of volcanism in the YMR is viewed as a magmatic system that peaked between 13 and 11 m.y., with the eruption of over 5000 km<sup>3</sup> of ash flow tuffs, and has been in decline since, with relatively minor volumes of basalt erupted since 11 m.y. ago (CRWMS M&O 1998 [100129], Figure 3.9-2). Approximately 99.9 percent of the volume of the southwestern Nevada volcanic field erupted by about 7.5 m.y. ago with the eruption of tuffs from the Stonewall Mountain volcanic center, which is the last active caldera system of the southwestern Nevada volcanic field. The last 0.1 percent of eruptive volume of the volcanic field consists entirely of basalt erupted since 7.5 m.y. ago (CRWMS M&O 1998 [100129], Figure 3.9-5). Based on eruption volume, the southwestern Nevada volcanic field is considered to have virtually ceased eruptive activity since about 7.5 m.y. Considered in terms of total eruption volume, frequency of eruptions, and duration of volcanism, basaltic volcanic activity in the YMR defines one of the least active basaltic volcanic fields in the western United States (e.g., CRWMS M&O 1998 [105347], Chapter 4, Figure 4-2, for post-Miocene basalts of Crater Flat).

Post-caldera basalts in the YMR can be divided into two episodes: Miocene (eruptions between ~9 and 7.3 m.y.) and post-Miocene (eruptions between ~4.8 and 0.08 m.y.). The time interval of about 2.5 m.y. between these episodes is the longest eruptive hiatus of basalt in the YMR during the last 9 m.y. (CRWMS M&O 1998 [105347], Chapter 3, Table 3.1). This eruptive hiatus also marks a distinct shift in the locus of post-caldera basaltic volcanism in the YMR to the southwest (CRWMS M&O 1998 [100129], Figure 3.9-6). The Miocene basalts and post-Miocene basalts are, thus, both temporally and spatially distinct. This observation emphasizes the importance of considering the age and location of the post-Miocene basalts (~ the past 5 m.y. of the volcanic history of the YMR) when calculating the volcanic hazard to the proposed Yucca Mountain repository. The PVHA experts almost exclusively considered the time period of interest to be pos-5 m.y. (with significant weight given to the post-1 m.y. period) as the time period of interest in assessing volcanic hazard at Yucca Mountain (CRWMS M&O 1996 [100116], Figure 3-62).

The post-Miocene basalts formed during at least six episodes of volcanism (based on age groupings) that occurred within 50 km of the proposed Yucca Mountain repository (Figure 3). These six episodes, in order of decreasing age, consist of the (1) basalt of Thirsty Mesa, (2) Pliocene Crater Flat and Amargosa Valley, (3) Buckboard Mesa, (4) Quaternary Crater Flat, (5) Hidden Cone and Little Black Peak (the Sleeping Butte centers), and (6) Lathrop Wells. Three basalt episodes are in or near the Crater Flat topographic basin, within 20 km of Yucca Mountain. Several aeromagnetic anomalies in the Amargosa Valley have characteristics that indicate buried basaltic volcanic centers (Langenheim et al 1993 [148622], p. 1840). One of these anomalies (Anomaly B of Langenheim et al. 1993 [148622]) was drilled and basalt cuttings

dated at 3.85 m.y. using the  $^{40}\text{Ar}/^{39}\text{Ar}$  method (CRWMS M&O 1998 [105347], Chapter 2, Table 2.B). Because of the similarity in age to the 3.75 m.y. Pliocene Crater Flat episode, the buried basalts of Amargosa Valley are considered here as part of the same episode.

The total eruption volume of the post-Miocene basalts is about  $6 \text{ km}^3$ . The volume of individual episodes has decreased progressively through time, with the three Pliocene episodes having volumes of approximately 1 to  $3 \text{ km}^3$  each and the three Quaternary episodes having a total volume of only  $\sim 0.5 \text{ km}^3$  (CRWMS M&O 1998 [100129], Figure 3.9-2; Table 3). All of the Quaternary volcanoes are similar in that they are of small volume ( $\sim 0.1 \text{ km}^3$  or less, Table 10) and typically consist of a single main scoria cone surrounded by a small field of *aa* basalt flows, which commonly extend  $\sim 1 \text{ km}$  from the scoria cone.

The seven or eight (if Little Cones is counted as two volcanoes) Quaternary volcanoes in the YMR occur to the south, west, and northwest of Yucca Mountain in a roughly linear zone defined as the Crater Flat Volcanic Zone (Crowe and Perry 1990 [100973], p. 328). Five of seven Quaternary volcanoes are in or near Crater Flat and lie within 20 km of the Yucca Mountain site (Figure 3). Models that attempt to relate volcanism and structural features in the YMR have emphasized the Crater Flat basin because of the frequency of volcanic activity associated with Crater Flat and its proximity to the proposed Yucca Mountain repository (e.g Smith et al. 1990 [101019], p. 84; Connor and Hill 1995 [102646], p. 10122).

Table 10. Estimated Volume and  $^{40}\text{Ar}/^{39}\text{Ar}$  Age<sup>a</sup> of Quaternary Volcanoes in the Yucca Mountain Repository

Volcano	Volume (km <sup>3</sup> ) <sup>b</sup>	Volume (km <sup>3</sup> ) <sup>c</sup>	Age (m.y.) <sup>e</sup>
Makani Cone	0.006		1.16-1.17
Black Cone	0.105	0.07	0.94-1.10
Red Cone	0.105		0.92-1.08
Little Cones	0.002	>0.01 <sup>d</sup>	0.77-1.02
Hidden Cone	0.03		0.32-0.56
Little Black Peak	0.03		0.36-0.39
Lathrop Wells Cone	0.14		0.074-0.084

DTNS: LA0004FP831811.002 [149593]; LAFP831811AQ97.001 [144279] (BOTH ARE USED FOR REFERENCE ONLY).

NOTES <sup>a</sup> $^{40}\text{Ar}/^{39}\text{Ar}$  dates provide the most complete and self-consistent chronology data set for Quaternary volcanoes of the YMR. A full discussion of other chronology methods used to date basaltic rocks in the YMR can be found in CRWMS M&O (1998 [105347], Chapter 2). Other chronology methods may not provide consistent or accurate estimates of the time of eruption.

<sup>b</sup>CRWMS M&O (1998 [105347], Chapter 3, Table 3.1), (DTN: LA0004FP831811.002 [149593]).

<sup>c</sup>Stamatakis et al. (1997 [138819], p. 327).

<sup>d</sup>Accounts for volume of buried flows detected by ground magnetic surveys.

<sup>e</sup>Range of ages from CRWMS M&O (1998 [105347], Chapter 2, Table 2.B). Lathrop Wells ages (Heizler et al. 1999 [107255], Table 3) represent the range of plateau ages measured, except for sample LW157, a statistical outlier (DTN: LAFP831811AQ97.001 [144279]).

### 6.3 THE PROBABILISTIC VOLCANIC HAZARD ANALYSIS

In 1995 to 1996, the DOE sponsored the PVHA project to assess the probability of a future volcanic event intersecting the proposed repository at Yucca Mountain. To ensure that a wide range of approaches was considered for the PVHA, the DOE identified 10 experts in the field to participate in the project and evaluate the data. Their evaluations (elicitations) were then combined to produce an integrated assessment of the volcanic hazard that reflects a range of alternative scientific interpretations. This assessment, which focused on the volcanic hazard at the site expressed as the probability of intersection of the proposed repository by a basaltic dike, provided input to an assessment of volcanic risk.

#### 6.3.1 The Probabilistic Volcanic Hazard Analysis Process

The major procedural steps in the PVHA were selecting the expert panel members, identifying the technical issues, eliciting the experts' judgments, applying temporal and spatial aspects of probability models, and compiling and presenting the results.

##### 6.3.1.1 Selecting the Expert Panel Members

From more than 70 nominees, 10 individuals were selected to participate in the PVHA project. Efforts were made to balance the panel with respect to technical expertise (geology, geochemistry, and geophysics) and institutional/organizational affiliation. The 10 experts and their affiliations are listed in Table 11 (CRWMS M&O 1996 [100116], Table 1-2).

Table 11. Probabilistic Volcanic Hazard Analysis Panel Members

Expert	Abbreviation	Affiliation
Dr. Richard W. Carlson	RC	Carnegie Institute of Washington
Dr. Bruce M. Crowe	BC	Los Alamos National Laboratory
Dr. Wendell A. Duffield	WD	United States Geological Survey, Flagstaff
Dr. Richard V. Fisher	RF	University of California, Santa Barbara (Emeritus)
Dr. William R. Hackett	WH	WRH Associates, Salt Lake City
Dr. Mel A. Kuntz	MK	United States Geological Survey, Denver
Dr. Alexander R. McBirney	AM	University of Oregon (Emeritus)
Dr. Michael F. Sheridan	MS	State University of New York, Buffalo
Dr. George A. Thompson	GT	Stanford University
Dr. George P. L. Walker	GW	University of Hawaii, Honolulu

DTN: MO0002PVHA0082.000

##### 6.3.1.2 Identifying Technical Issues

The PVHA panel of experts convened between February and December 1995. A technical facilitator/integrator led carefully structured, intensive interactions among the panel members. The experts participated in workshops, field trips, and other interactions, which were used to identify sources of agreement and disagreement among them. Each expert played the role of an informed technical evaluator of data, rather than a proponent of a particular interpretation. On occasion, however, some experts were asked to present particular interpretations to facilitate discussion and consideration of alternative interpretations. In all the interactions, it was made

clear that the purpose of the PVHA was to identify and understand uncertainty, not to eliminate it. It was also emphasized that the purpose was not necessarily to achieve consensus. Instead, disagreement was expected and accepted.

At the core of the PVHA project were four workshops. The primary objective of the workshops was to ensure the experts' understanding of the issues, alternative volcanic hazard models, and the data available on which they would base their technical assessments. The first three workshops focused on the data, volcanic hazard models, and interpretations relevant to the PVHA. The workshops included presentations of data and interpretations by technical specialists from the Los Alamos National Laboratory, the USGS, the University of Nevada, Las Vegas, and the Center for Nuclear Waste Regulatory Analysis, as well as from some PVHA experts. During the fourth workshop, the experts reviewed the preliminary assessments developed by the panel members, after which the individual elicitations were revised, based on feedback received. Two field trips held during the course of the PVHA provided the opportunity for the panel members to observe geologic relationships pertaining to eruptive style, the definition of volcanic events, and the distribution and timing of volcanic activity in the YMR.

### **6.3.1.3 Temporal and Spatial Aspects of Probability Models**

Before the third PVHA workshop, an interactive meeting was held for the benefit of the expert panel, in order to focus on the methods available to calculate volcanic hazard. The methods were used to calculate the two main aspects of volcanic hazard probability models: the temporal and spatial aspects.

Temporal models describe the frequency of occurrence of volcanic activity and include homogeneous and nonhomogeneous models. Many of the experts used homogeneous Poisson models to define the temporal occurrence of volcanic events, which assumes a uniform rate of volcanism based on the number of volcanic events that occurred during various periods in the past. Nonhomogeneous models were used by some experts to consider the possibility that volcanic events are clustered in time or to describe the possible waning or waxing of volcanic activity in the region during the period of time the experts believed was relevant to hazard analysis.

Spatial models describe the spatial distribution (location) of future volcanic activity. The most common PVHA models considered the future occurrence of volcanoes to be homogeneous within particular defined regions or "source zones" (CRWMS M&O 1996 [100116], Figure 3-62). Source zones were defined based on several criteria: the spatial distribution of observed basaltic volcanoes (especially post-5 m.y. volcanoes), structurally-controlled regions, regions defined based on geochemical affinities, tectonic provinces, and other criteria. Nonhomogeneous parametric spatial distributions of future volcano occurrences were also modeled, for example, that the location of future volcanoes will follow a bivariate Gaussian distribution based on the location of volcanoes in Crater Flat. Finally, nonhomogeneous, nonparametric spatial density models were used by some experts to assess the spatial distribution of future volcanoes. These models make use of a kernel density function and smoothing parameter based on locations of existing centers to obtain the spatial distribution for location of future volcanoes.

#### 6.3.1.4 Eliciting the Experts' Judgments

Formal elicitation followed the third workshop. The process consisted of a two-day individual interview with each expert. To provide consistency, the same interview team was used for all elicitations. Following the elicitation interview, each expert was provided with a written summary of his elicitation, which was prepared by the interview team. The expert reviewed and clarified the summary and had the opportunity to revise any assessments. To promote a full understanding of each individual's judgment, the preliminary assessments made by each member of the expert panel were presented and discussed at the fourth workshop. Following this workshop, each expert had a final opportunity to revise his assessments before the results of the PVHA were finalized (CRWMS M&O 1996 [100116], Appendix E). A summary of input parameters for the PVHA probability models is found in CRWMS M&O (1998 [106102], Table 10-5).

#### 6.3.1.5 Probabilistic Volcanic Hazard Analysis Results and Uncertainty

The product of the PVHA was a quantitative assessment of the probability of a volcanic event intersecting the proposed repository and the uncertainty associated with the assessment (CRWMS M&O 1996 [100116], Figure 4-32). Specifically, a probability distribution of the annual frequency of intersection of a basaltic dike with the proposed repository footprint was defined. The contributions to uncertainty from each of the PVHA components is described in *Probabilistic Volcanic Hazard Analysis for Yucca Mountain, Nevada* (CRWMS M&O 1996 [100116], Section 4.2).

Each of the 10 experts independently arrived at a probability distribution for the annual frequency of intersection of the proposed repository footprint by a dike that typically spanned ~2 orders of magnitude (CRWMS M&O 1996 [100116], Figure 4-31). From these individual probability distributions, an aggregate probability distribution for the annual frequency of intersection of the proposed repository footprint by a dike was computed that reflected the uncertainty across the entire expert panel (CRWMS M&O 1996 [100116], Figure 4-32). The individual expert's distributions were combined using equal weights to obtain the aggregate probability distribution. The mean value of the aggregate probability distribution was  $1.5 \cdot 10^{-8}$  dike intersections per year, with a 90 percent confidence interval of  $5.4 \cdot 10^{-10}$  to  $4.9 \cdot 10^{-8}$  (CRWMS M&O 1996 [100116], p. 4-10). Note that these values are updated in this report for the proposed LA repository footprint in Section 6.5.3. The composite distribution spanned about three orders of magnitude for intersection frequency. The range in the mean frequencies of intersection for the individual expert's interpretations spanned about one order of magnitude (CRWMS M&O 1996 [100116], Figure 4-32). The variance for frequency of intersection defined by the composite distribution was disaggregated to identify the contributions from each of the sources of uncertainty, including variability between the experts' interpretations (CRWMS M&O 1996 [100116], Figure 4-33). Most of the uncertainty in characterizing the hazard arose from uncertainty in an individual expert's interpretations of the hazard rather than differences in scientific interpretation between the experts (CRWMS M&O 1996 [100116], p. 4-10, Figure 4-33). The probability distribution arrived at by the PVHA accounted for undetected events (buried volcanic events, or intrusive events that never reached the surface). The undetected event frequency ranged from 1 to 5 times that of observed events, with most estimates in the range of 1.1 to 1.5 (CRWMS M&O 1996 [100116], Figure 3-62).

The PVHA results indicated that the statistical uncertainty in estimating the event rate was the largest component of intra-expert uncertainty (CRWMS M&O 1996 [100116], Figure 4-33). The next largest uncertainty was uncertainty in the appropriate spatial model. Other important spatial uncertainties included the spatial smoothing distance, Gaussian field parameters, zonation models, and event lengths. The temporal issues of importance included the time period of interest, event counts at a particular center, and the frequency of hidden events (CRWMS M&O 1996 [100116], Figure 4-33).

#### **6.3.1.6 Consideration of Alternative Conceptual Models**

The PVHA was in essence an exercise in combining multiple alternative conceptual models (ACMs) into a single distribution that captured the uncertainty in the expert's conceptual models of the physical behavior of volcanism in the YMR. ACMs incorporated into the results of the PVHA consisted primarily of alternative temporal and spatial models that describe expected behavior (based on past behavior) of volcanism in the YMR. No single base-case conceptual model is appropriate in the area of volcanism because the underlying physical processes that control the precise timing and location of volcanic events within a particular region remain largely unknown to science.

Although numerous ACMs were incorporated in the PVHA, several alternative models not considered in the PVHA have emerged since the PVHA was completed in 1996. These models are summarized in Table 12 and are discussed in detail in Section 6 of this report.

#### **6.3.1.7 Significance of Buried Volcanic Centers on Probabilistic Volcanic Hazard Analysis Results**

The uncertainty in the event rate accounted for about 40 percent of the total intra-expert uncertainty (CRWMS M&O 1996 [100116], Figure 4-33). The event rate depends on the number of events estimated for a particular time period and for a particular source zone, and can be expressed as events/year/square kilometer (CRWMS M&O 1996 [100116], p. 3-2; Figure 17a of this report). A key parameter for estimating event rates is, therefore, an estimate of the number of volcanic events that have occurred in the YMR, particularly since the Miocene. Since all post-Miocene volcanic centers observable at the surface in the YMR have been identified (Figure 3), the only factor that could significantly change PVHA estimates of event counts and the event rate would be evidence not considered by the PVHA of a significant number of previously unidentified buried volcanic centers or intrusions.

Table 12. Alternative Conceptual Models Not Considered in the Probabilistic Volcanic Hazard Analysis

Alternative Models	Key Assumptions	Assessment
Anomalous strain rate in the YMR (Wernicke et al. 1998 [103485])	Anomalously high current strain rate based on GPS measurements indicates volcanic event rate may be underestimated by factor of 10.	Not considered plausible based on later measurements from Savage et al. (1999 [118952]) that show low strain rate as well as questionable assumptions about links between strain rate and volcanic event rate.
Mantle hotspot beneath the YMR (Smith et al. 2002 [158735])	Anomalously high mantle basalt source temperatures lead to underestimation of future volcanic event rate.	Not considered plausible based on weight of documented scientific opinion showing that mantle hotspot is not present beneath YMR.
Tectonically weighted probability models (Connor et al. 2000 [149935], p. 427)	Weighting of certain tectonic elements in probability models lead to probability estimates as high as $10^{-7}$ .	Not considered plausible based on observation that tectonically weighted probability models are poor predictors of location of volcanism in YMR.
Significant number of buried or undetected volcanic centers in the YMR (Hill and Stamatakos 2002 [159500])	Aeromagnetic anomalies suggest that significant number of volcanic events were unaccounted for in the PVHA, underestimating the volcanic hazard.	Significance of buried volcanoes on probability estimates cannot be assessed without further data collection and update of the PVHA. Sensitivity studies documented in Section 6.5.4 of this report are for information purposes only. The results of the 1996 PVHA, as summarized in Section 7.2 of this report, are the results that will be used in TSPA-LA.

Langenheim et al. (1993 [148622]) presented data for aeromagnetic anomalies in the Amargosa Valley and interpreted them as shallowly buried basaltic volcanic centers. These data were available to the PVHA experts (CRWMS M&O 1996 [100116], p. B-4), and data and interpretations concerning the Amargosa Valley anomalies were also presented by Langenheim during Workshop 1 of the PVHA project (CRWMS M&O 1996 [100116], p. C-3). In the PVHA, 9 of 10 experts included volcanic events of the Amargosa Valley in their YMR event counts (CRWMS M&O 1996 [100116], Appendix E, pp. RC-8, BC-17, WD-5, WH-7, MK-10, AM-8, MS-8, GT-6, GW-6). The only expert who did not include events of the Amargosa Valley in their YMR event counts considered only the past 2 m.y. to be the relevant time period (CRWMS M&O 1996 [100116], Appendix E, RF-6), thus, excluding the period of time during which the anomalies were probably formed. The most common expert assessment of the number of volcanic events represented by the aeromagnetic anomalies in Amargosa Valley was 5, with slightly less weight assigned to 3, 4, and 6 events (CRWMS M&O 1996 [100116], Figure 3-63). In addition, the PVHA experts assessed a hidden event factor, allowing for additional undetected events not counted in the total YMR event counts that already included the Amargosa Valley event counts (CRWMS M&O 1996 [100116], Figure 3-62, 3-63). These factors typically resulted in an increase of 10 to 50 percent in the rate of volcanic events over that computed from the observed volcanic events.

New data that could potentially change the assessment of the number of volcanic events by the PHVA experts include an analysis of existing aeromagnetic data for the YMR (Earthfield Technology 1995 [147778]) and new ground magnetic surveys of aeromagnetic anomalies (Connor et al. 1997 [135969]; Magsino et al. 1998 [147781]). A map presented by Earthfield Technology (1995 [147778], Appendix II) indicates the presence of as many as 40 to 60 aeromagnetic anomalies within ~35 to 40 km of Yucca Mountain that are interpreted as

intrusive bodies; six of these lie within ~5 km of the proposed repository site. The Earthfield Technology (1995 [147778]) results were based on the merging of three aeromagnetic data sets: the Timber Mountain, Lathrop Wells, and Yucca Mountain surveys. Subsequent to release of the Earthfield Technology (1995 [147778]) report, it was discovered that the report “was flawed by an incomplete and mislocated Timber Mt. Survey” (Feighner and Majer 1996 [105078], p. 1). Inspection of the flight survey map in Earthfield Technology (1995 [147778], Figure 2) and a corresponding map enclosed in *Results of the Analysis of the Timber Mt., Lathrop Wells, and Yucca Mt. Aeromagnetic Data* (Feighner and Majer (1996 [105078], Appendix I) indicates that the Timber Mountain Survey, which encompasses about 50 percent of the coverage area and the majority of the aeromagnetic anomalies, was mislocated approximately 20 km to the south-southwest of its correct location. For this reason, further analysis of the anomalies as presented by Earthfield Technology (1995 [147778], Appendix II), and that lie within the Timber Mountain survey, is not warranted. The six anomalies located within 5 km of the proposed repository site (the Yucca Mountain survey) are associated with mapped faults and are probably due to magnetic variation resulting from fault-controlled juxtaposition of rock masses with differing magnetic properties (Feighner and Majer 1996 [105078], p. 2; Reamer 1999 [119693], p. 32).

The most reliable and detailed data available for magnetic anomalies in the YMR is presented in Connor et al. (1997 [135969]) and Magsino et al. (1998 [147781]). These data were obtained using ground magnetic surveys of 14 selected aeromagnetic anomalies located to the north, east, west, and south of the proposed repository site (Magsino et al. 1998 [147781], Figure 1-1). Collectively, these surveys represent a comprehensive assessment of aeromagnetic anomalies nearest the proposed repository site and provide confidence that the geologic record of basaltic volcanism near Yucca Mountain is adequately understood. Of the 14 surveys, seven provide no evidence of buried basalt and three were conducted over areas with known surface exposures of basalt, partly to enhance understanding of the relationship between volcanism and geologic structure (Magsino et al. 1998 [147781], Section 4). Four of the 14 surveys provide evidence of buried volcanic centers. Two of these (Anomalies A and F/G of the PVHA) were known to the PVHA experts as possible buried basaltic volcanic centers (from the data of Langenheim et al. 1993 [148622]; Crowe et al. 1995 [100110], Figure 2.5), but the data presented in Connor et al. (1997 [135969]) and Magsino et al. (1998 [147781]) provide increased detail and confidence of their volcanic origin. Of the two remaining surveys, anomalies in the Steve’s Pass area on the southwest margin of Crater Flat are interpreted as buried basalt. Interpretation of a buried, reversely magnetized body of rock southwest of Northern (or Makani) Cone is less certain and may be either a basalt body or Miocene tuff (Magsino et al. 1998 [147781], Sections 4.4 and 4.11). Each of the four anomalies representing probable buried volcanic centers occur within volcanic source zones previously specified by the PVHA experts (CRWMS M&O 1996 [100116], Appendix E), except for the anomalies in the Steve’s Pass area, which lie slightly to the southwest of most experts’ volcanic source zones, in a direction away from Yucca Mountain.

On the basis of evidence for buried volcanic centers presented in Connor et al. (1997 [135969]), Brocoum (1997 [147772]) conducted sensitivity analyses to assess the potential impact on the PVHA results of increased event counts in Amargosa Valley and Crater Flat. Considering the experts’ method for assessment of event counts, particularly for northeast alignments of vents (as in the case of Amargosa anomaly F/G), the mean value for the number of buried volcanic centers

was increased from the original PVHA value of 4.7 events to 6.1 events (Brocoum 1997 [147772], Enclosure 1, p. 5). The mean annual frequency of intersection of a dike with the proposed repository footprint was recalculated using the revised event count distributions, resulting in an increase in the mean annual frequency of intersection of 4 percent (Brocoum 1997 [147772], Enclosure 1, p. 5). Given the uncertainty factored into the PVHA by assessment of alternative event counts and hidden event factors, small changes in the PVHA event counts have a minor impact on the annual frequency of intersection distribution derived from the PVHA. A later sensitivity analysis presented by *Synthesis of Volcanism Studies for the Yucca Mountain Site Characterization Project* (CRWMS M&O 1998 [105347], Chapter 6, pp. 6-83 and 6-84) conservatively assumed that all known aeromagnetic anomalies in Crater Flat and the Amargosa Valley were Quaternary age, instead of Pliocene. Using this assumption, the most likely number of Quaternary volcanic events near Yucca Mountain based on PVHA event counts was increased from 3.8 to 8 events. This increase in the Quaternary event count resulted in a disruption probability of  $\sim 2.5 \cdot 10^{-8}$  per year (CRWMS M&O 1998 [105347], Chapter 6, p. 6-84), a result not significantly different from the mean PVHA result of  $1.5 \cdot 10^{-8}$  per year (CRWMS M&O 1996 [100116], pp. 4-10, 4-14).

The data presented by Connor et al. (1997 [135969]) and Magsino et al. (1998 [147781]) provide stronger evidence that Anomalies A and F/G (as defined in the PHVA) represent buried volcanic centers, and that at least one anomaly not considered by the PVHA experts represents a probable buried volcanic center. Sensitivity studies (Brocoum 1997 [147772]; CRWMS M&O 1998 [105347], Chapter 6) show that the addition of several volcanic events located within already defined volcanic source zones does not significantly impact the results of the PVHA. Significantly, the four anomalies east of Yucca Mountain (Magsino et al. 1998 [147781], Figure 1-1) show no evidence of buried volcanic centers and provide confirmatory evidence that the volcanic source zones specified by the experts to the south and west of Yucca Mountain are a valid representation of the spatial distribution of post-Miocene volcanism in the YMR.

In 1999, the USGS conducted a regional aeromagnetic survey for the purpose of assessing potential hydrologic pathways in the Yucca Mountain/Death Valley region (Blakely et al 2000 [151881]). Subsequent interpretation of these data indicated that 20 to 24 aeromagnetic anomalies present to the west and south of Yucca Mountain could potentially represent buried basalt (O'Leary et al. 2002 [158468]; Hill and Stamatakos 2002 [159500]). Section 6.5.4 of this report documents an assessment of how the potential presence of additional buried volcanoes in the YMR could impact the frequency of intersection.

### **6.3.1.8 Alternative Estimates of the Intersection Probability**

Several alternative estimates of the intersection probability (the annual probability of a volcanic event intersecting the proposed repository footprint) were presented between 1982 and 1998 (Table 13). As discussed in the following section (6.3.2), volcanic events in hazard calculations have been represented as both points and lines (Table 13). For point events, volcanic source zone areas or the proposed repository area have generally been increased to account for the fact that volcanic events have dimension due to the length of associated dikes. The shorter the event length, the more comparable intersection probability results are for calculations representing volcanic events as either points or lines. Intersections probabilities near  $10^{-7}$  intersections/year

(Ho and Smith 1998 [140152], pp. 507 and 508; Reamer 1999, p. 61 [119693]) reflect unusually small volcanic source zone areas or unusually long event lengths (Table 13).

Most of the published intersection probabilities, including the mean intersection probability estimated in the PVHA, cluster at values slightly greater than  $10^{-8}$  per year (Table 13), indicating that this probability estimate is fairly robust, given the range of alternative temporal and spatial models, and event geometries considered in probability calculations.

Table 13. Published Estimates of the Probability of Intersection of the Proposed Repository at Yucca Mountain by a Volcanic Event

Reference	Intersection Probability (per year)	Comment	Event Representation
Crowe et al. (1982 [102741]), pp. 184 through 185	$3.3 \cdot 10^{-10} - 4.7 \cdot 10^{-8}$	Range of alternative probability calculations.	point
Crowe et al. (1993 [100026]), p. 188	$2.6 \cdot 10^{-8}$	Median value of probability distribution.	point
Connor and Hill (1995 [102646]), p. 10121	$1-5 \cdot 10^{-8}$	Range of 3 alternative models.	point
Crowe et al. (1995 [100110]), Table 7.22	$1.8 \cdot 10^{-8}$	Median value of 22 alternative probability models.	point
Ho and Smith (1998 [140152]), pp. 507 through 508	(1) $1.5 \cdot 10^{-8}$ , (2) $1.09 \cdot 10^{-8}$ , $2.83 \cdot 10^{-8}$ , (3) $3.14 \cdot 10^{-7}$	3 alternative models; 3 <sup>rd</sup> model assumes a spatial intersection ratio (using a Bayesian prior) of 8/75 or 0.11, approximately one order of magnitude higher than other published estimates, because volcanic events are forced to occur within a small zone enclosing Yucca Mountain.	point
CRWMS M&O (1998 [105347]), Chapter 6, p. 6-84	$2.5 \cdot 10^{-8}$	Sensitivity analysis that conservatively assumes all aeromagnetic anomalies in Amargosa Valley are Quaternary age.	point
Connor et al. (2000 [149935]), p. 427	$10^{-8}-10^{-7}$	Value of $10^{-7}$ assumes maximum event length of 20 km, regional recurrence rates of 5 events/m.y., and that crustal density variations contribute to event location.	line

### 6.3.2 Definitions and Parameters of a Volcanic Event and Implications for Alternative Probability Calculations

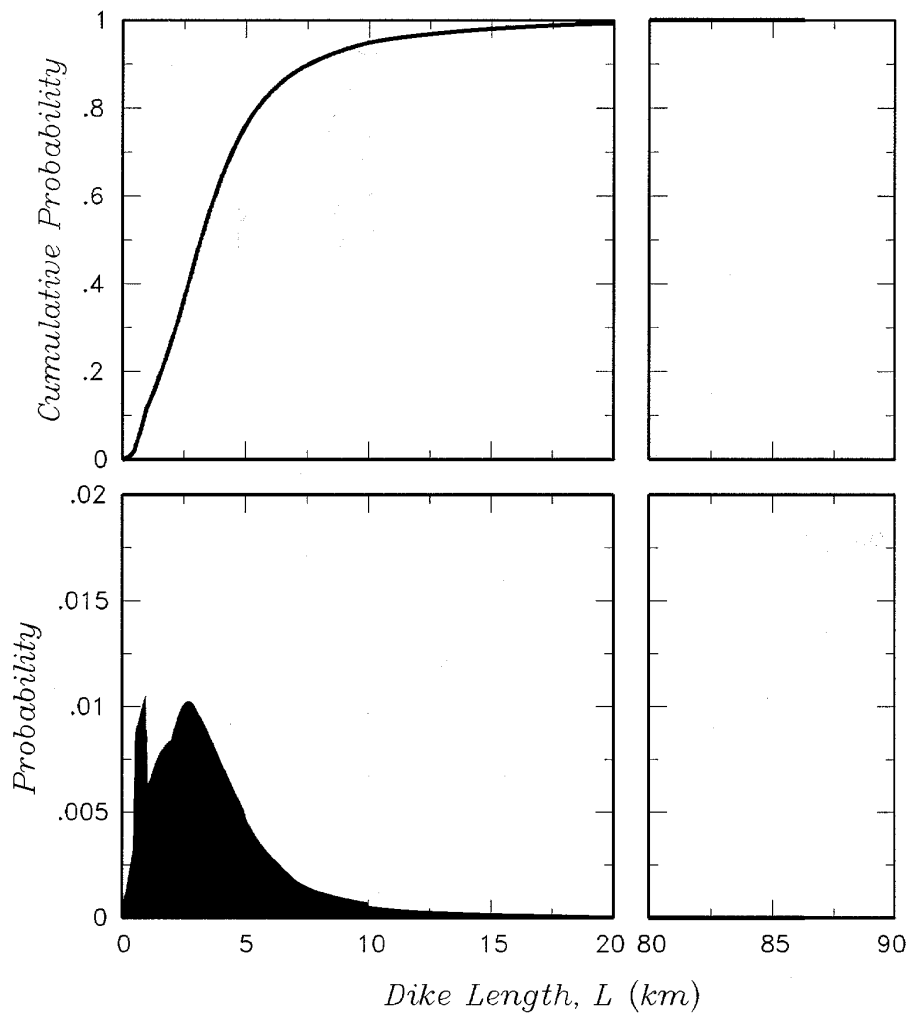
An important issue in the PVHA and in alternative volcanic hazard assessments of the proposed Yucca Mountain repository is the definition of a “volcanic event.” The definition of a volcanic event can affect the outcome of probability calculations and must be clearly understood to compare the results of alternative probability calculations meaningfully. The PVHA experts defined a volcanic event to be a spatially and temporally distinct batch of magma ascending from the mantle through the crust as a dike or system of dikes (CRWMS M&O 1996 [100116], Appendix E). The physical manifestations of a volcanic event include the dike or dike system, and any surface eruption deposits. For the purposes of probability models discussed in this

report (Section 6.5), a volcanic event is defined as a point (x,y) in space representing the expected midpoint of the dike system involved in the magma ascent. The dike system associated with the volcanic event is represented in probability model by a line element defined in terms of a length, azimuth and location relative to the point event (Figures 10 and 12). The term 'dike length' used in the PVHA and in this report when discussing volcanic events refers to the total length of the dike system associated with the volcanic event. The phrase 'intersection of the repository footprint by a dike' refers to intersection of the emplacement area of the repository by the line element representing the dike system associated with the volcanic event. The possibility that a dike system (e.g., multiple dikes) has width or consists of multiple parallel dikes does not significantly affect the intersection probability and is not part of the calculations in this report. The width of the dikes and the number of parallel dikes does affect the consequences of an intersection and is incorporated into the igneous intrusion scenario presented in *Number of Waste Packages Hit by Igneous Intrusion* (BSC 2003 [161851]). Although the PVHA assumed volcanic events to have both an extrusive and intrusive component (volcano and dike), the output of the PVHA was the annual frequency of intersection of the proposed repository by an intrusive basaltic dike (CRWMS M&O 1996 [100116], Section 4.2, Figure 4-32). The PVHA did not calculate the conditional probability that a dike intersecting the proposed repository would result in an extrusive volcanic eruption through the repository.

Typical dike dimensions assigned by the experts were a dike width of one meter and a dike length (the total length of the dike system associated with a volcanic event) of 1 to 5 km (CRWMS M&O 1996 [100116], Appendix E; Figure 4). The most likely values for maximum dike lengths were estimated to be in the range of 17 to 22 km (CRWMS M&O 1996 [100116], Figure 3-62). The values of maximum dike length represent tails of distributions that have a small impact on the probability of dike intersection. The individual PVHA expert dike length distributions can be aggregated to derive a PHVA aggregate dike length distribution. The aggregate dike-length distribution derived from the PVHA has 5<sup>th</sup>-percentile, mean, and 95<sup>th</sup>-percentile values of 0.6, 4.0, and 10.1 km, respectively (Figure 4). The most commonly assigned dike orientation centers around N30°E (CRWMS M&O 1996 [100116], Figure 3-62).

Prior to the PVHA, most assessments of volcanic hazard to the proposed repository represented volcanic events as points having no physical dimension (CRWMS M&O 1996 [100116], p. 3-16). The physical dimension of events was generally taken into account by appropriately expanding the area of the proposed repository or of volcanic source zones (e.g., Crowe et al. 1995 [100110], p. 7-64). The PVHA and probability calculations presented by the U.S. Nuclear Regulatory Commission (NRC) since the PVHA have represented volcanic events as having both length and orientation (Reamer 1999 [119693]). It is important to compare the different representations of volcanic events in order to compare probability results meaningfully. The PVHA intersection probability represents the probability of a dike intersecting the repository footprint (CRWMS M&O 1996 [100116], Section 3.1.6). The NRC intersection probability represents the intersection of the repository footprint by a vent or vent alignment (Reamer 1999 [119693], Sections 4.1.6.3.2 and 4.1.6.3.3, Figures 29 and 30), and assumes that all vents along the alignment are contemporaneous and represent a single volcanic event (e.g., the alignment of Quaternary vents from Makani Cone to Little Cones [Figure 3]). In contrast, the PVHA allowed that an alignment of volcanoes could represent one to several volcanic events that are not necessarily contemporaneous. Conceptually, use of either the PVHA or NRC volcanic event should result in the same intersection probability, if the same temporal/spatial models and

assumptions are used, as well as the same probability distributions for event length and orientation (Figure 5). However, these probabilities represent different physical occurrences, and PVHA and NRC model parameters are not equivalent. Since the PVHA intersection probability represents the probability of a dike intersection, the probability of an eruption (conditional on dike intersection) through the proposed repository is equal to or lower than the intersection probability (Figure 5). The NRC intersection probability values are based on the interpretation that every intersection of a vent alignment with the proposed repository footprint results in an eruption through the proposed repository (Reamer 1999 [119693], p. 57), and that the probability of intersection by shallow intrusive events that do not erupt is necessarily higher, possibly by a factor of 2-5 (Reamer 1999 [119693], p. 60, Figure 5).

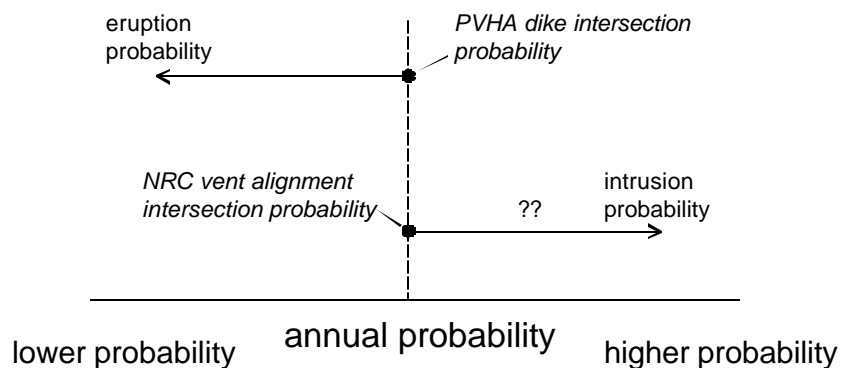


Output Data. DTN: LA0009FP831811.001 [164712]

NOTE: The 5<sup>th</sup>-percentile, mean, and 95<sup>th</sup>-percentile values are 0.6, 4.0, and 10.1, km, respectively. The distribution contains a very long upper tail extending to 86 km. The irregular shape of the probability mass function in the lower plot reflects the variation in the distributions defined by the individual experts.

Figure 4. Composite Distribution for Dike Length Averaged Across All 10 Probabilistic Volcanic Hazard Analysis Experts

The NRC assumes that every vent alignment intersection will result in an eruption through the proposed repository because they conclude that vent spacings along alignments are small compared to the proposed repository footprint (Reamer 1999 [119693], Sections 4.1.4.3.3 and 4.1.6.3.2). The technical basis for this conclusion is unclear. In Section 6.5.1.3, a number of alternative approaches for the number and spatial distribution of vents along the dike associated with a volcanic event are formulated, based on PVHA expert output and observed vent spacing in the YMR, to test for sensitivity of model choice. Using these approaches, the eruption probability is approximately 78 percent of the dike intersection probability, because of cases where no vents form within the repository footprint (Table 19).



N/A - For Illustration Purposes Only

Source:Reamer 1999 [119693]

Figure 5. Conceptual Diagram Comparing Event Definitions from the Probabilistic Volcanic Hazard Analysis and Reamer: Implications for Eruption and Intrusion Probabilities Based on Different Event Definitions

### 6.3.2.1 Intrusive Versus Extrusive Events: Evidence from Analog Sites

Another issue requiring discussion is whether dikes or dike systems can reach the near surface without any portion of the system erupting. The NRC (Reamer 1999 [119693]) assumption that all vent alignment intersections result in eruption through the proposed repository implies that intrusive events that intersect the proposed repository and do not erupt represent entirely separate temporal events. Using the San Rafael volcanic field as an analog, the NRC assumes for PA purposes that the probability of separate intrusive events that do not erupt is 2 to 5 times higher than the probability of eruptive events (Reamer 1999 [119693], Section 4.1.6.4). Thus, for example, if 5 volcanic events resulting in volcanic eruptions have occurred in the YMR in the past 1 m.y., the NRC's assumption requires that 10 to 25 additional intrusive events have also occurred, independent in time and location from the events that produced the volcanic eruptions. In the PVHA definition of a volcanic event, intrusive and extrusive events, in the YMR are generally considered to be linked on a one-to-one basis—a volcanic event is defined as an extrusive volcano and its associated intrusive dike or dike system. Dikes that reach depths of < 0.5 to 1 km are thought to erupt at some point along the length of the dike, mainly because of volatile exsolution (CRWMS M&O 1996 [100116], Appendix E, pp. RC-10, BC-6, WH-6, MK-12). The most common multiplier assigned for undetected intrusive events was 1.1 to

1.2 times that of known volcanic events (CRWMS M&O 1996 [100116], Figure 3-62), which is a number lower than the NRC multiplier of 2 to 5.

An appropriate analog in the YMR for understanding the relationship between intrusive and extrusive components of a volcanic event is the Paiute Ridge intrusive/extrusive center (Byers and Barnes 1967 [101859]) on the northeastern margin of the Nevada Test Site. Paiute Ridge is a small-volume Miocene volcanic center comparable in volume and composition to Quaternary volcanoes near Yucca Mountain (CRWMS M&O 1998 [105347], Chapter 5, p. 5-29). Paleomagnetic, geochronologic, and geochemical data indicate that the entire intrusive/extrusive complex formed during a brief magmatic pulse and, thus, represent a single volcanic event (Ratcliff et al. 1994 [106634]; CRWMS M&O 1998 [105347], Chapter 5, p. 5-29). The vents and associated dike system formed within an NNW-trending extensional graben provide excellent exposures of a variety of depths of the system including remnants of surface lava flows, volcanic conduits, and dikes and sills intruded into tuff country rock at depths of up to 300 meters (CRWMS M&O 1998 [105347], Chapter 5, pp. 5-27 through 5-41). There is evidence of shallow structural control of dike emplacement at Paiute Ridge, including dike emplacement along fault planes (Byers and Barnes 1967 [101859]; CRWMS M&O 1998 [105347], Chapter 5, pp. 5-27 through 5-28). Dike lengths at Paiute Ridge range from < 1 to 5 km (CRWMS M&O 1998 [105347], Chapter 5, p. 5-31), comparable to the range estimated for post-Miocene volcanism near Yucca Mountain (Figure 4).

Field observations at Paiute Ridge clearly show that, while some portions of individual dikes stagnated within about 100 meters of the surface without erupting, other portions of the same volcanic event did erupt, as evidenced by associated lava flows and volcanic conduits (Byers and Barnes 1967 [101859]; CRWMS M&O 1998 [105347], Chapter 5, pp. 5-29 through 5-33). During the time period considered most significant by the PVHA experts for evaluating volcanic hazard (the past 5 m.y., CRWMS M&O 1996 [100116], Figure 3-62), there is no known episode of dike intrusion to within a few hundreds meters of the surface in the YMR that has not been accompanied by an extrusive component. Thus, there is no evidence in the YMR geologic record to suggest that dike intrusions without accompanying eruptions occur 2 to 5 times more frequently than eruptions (Reamer 1999 [119693], Figure 5, Sections 4.1.6.3.4 and 4.1.6.4).

The NRC assumption of higher intrusion probabilities in the YMR is based on analogy to the San Rafael volcanic field on the western Colorado Plateau, where an extensive system of shallowly intruded dikes is well exposed (Delaney and Gartner 1997 [145370]). Delaney and Gartner (1997 [145370], p. 1180) estimate that 174 dikes are represented in the San Rafael dike swarm. Breccias are present along portions of 45 of these dikes, which are interpreted to represent the subsurface beneath eruptive centers (Delaney and Gartner 1997 [145370], pp. 1178 and 1191). No attempt is made in Delaney and Gartner (1997 [145370]) to estimate the frequency of temporally discrete intrusive versus eruptive events. They suggest only that at least 45 dikes show evidence of eruption along some segment of a dike; other parts of the same dike, or other parts of the same dike system, may have erupted, as is observed at Paiute Ridge. Given the Paiute Ridge analogy and the Delaney and Gartner (1997 [145370]) interpretation that the San Rafael swarm likely represents the subsurface beneath a large volcanic field active for about a million years (Delaney and Gartner 1997 [145370], pp. 1177, 1178, and 1179), it is likely that many individual intrusive/extrusive events are represented at San Rafael, with some portion of a dike system erupting during each event, and other portions of the same dike system not erupting.

Thus, while the data and discussion presented in Delaney and Gartner (1997 [145370]) have been used to argue that intrusive events without an eruptive component occur 2 to 5 times more frequently than intrusive events with an eruptive component, an alternative interpretation is that the intrusion/extrusion ratio is closer to 1. This alternative interpretation is more consistent with the geologic record of the YMR, as demonstrated at the Paiute Ridge analog site.

### 6.3.2.2 Alternative Event Lengths

The length of dikes or vent alignments (Reamer 1999 [119693], Figure 30) can significantly affect intersection probabilities, depending partly on how far areas of high-event frequency are from the proposed repository. When volcanic events primarily occur far from the proposed repository, they must have sufficient length to intersect the repository, and longer event lengths will result in higher intersection probabilities. When volcanic events occur more frequently nearer the proposed repository, volcanic events with shorter lengths are able to intersect the repository with higher frequency.

As evaluated by experts in the PVHA, the mean dike length associated with a volcanic event in the YMR is 4 km, and 95 percent of dikes are shorter than 10.1 km (Figure 4). These values are consistent with observed volcanic features in the YMR. For instance, the maximum vent spacing in the YMR is 5.4 km between Black and Makani Cones, and volcanic vent alignments lengths are typically in the range of 2 to 5 km (e.g., Hidden Cone-Little Black Peak, Amargosa Aeromagnetic Anomaly A, Red Cone-Black Cone). The longest proposed vent alignment in the YMR, assuming it represents one volcanic event, is the Quaternary Crater Flat alignment with a length of about 11 km (Figure 3). Observed dikes, such as at Paiute Ridge, range in length from < 1 to 5 km. Dike and vent alignments of the 3.7 m.y. basalts in southeast Crater Flat (Figure 3) are no more than 4 km in length.

Event lengths used in probability models by researchers from the University of Nevada, Las Vegas (e.g., Smith et al. 1990 [101019]) and the NRC (Reamer 1999 [119693], Figures 29 and 30) are significantly longer than those assessed by the experts in the PVHA. For example, Smith et al. (1990 [101019], p. 81) based the dimensions of “high-risk” volcanic source zones, used as a spatial control on event distribution in probability models, on the length of volcanic vent alignments at analog sites. The analog site chosen to define the dimensions of the “high-risk” zone is the relatively large-volume Fortification Hill volcanic field near Lake Mead, 200 km southeast of Yucca Mountain. In terms of volume, Smith et al. (1990 [101019], p. 85) acknowledge that this volcanic field is not analogous to Quaternary volcanism near Yucca Mountain. The vent alignment length defined at Fortification Hill is 25 km (Smith et al. 1990 [101019], p. 85). Smith et al. (1990 [101019], p. 87) consider this length to be an upper bound, and it corresponds to the > 99<sup>th</sup>-percentile value of the PVHA event length distribution (Figure 4).

Vent alignment lengths are used directly in NRC probability calculations (Reamer 1999 [119693], Sections 4.1.6.3.2 and 4.1.6.3.3, Figures 29 and 30) and have a maximum half-length range of 5.2 to 10.2 km, corresponding to a total-length range of 10.4 to 20.4 km. These values are based on the half-length of the Quaternary Crater Flat vent alignment (5.6 km, the longest half-length observed in the YMR), and the observation that vent alignment half-lengths of 10 km or more occur in other volcanic fields (Reamer 1999 [119693], p. 40). It is notable that

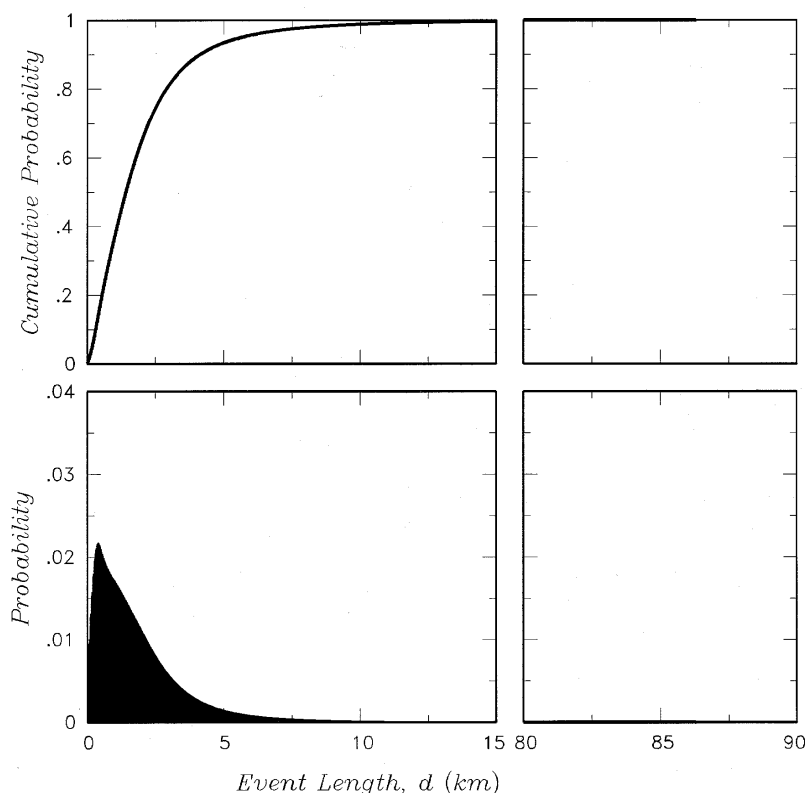
~97 percent of the 174 dike lengths measured in the San Rafael volcanic field (discussed above), which the NRC uses as a YMR analog, have total lengths of < 5 km (Delaney and Gartner 1997 [145370], Figure 4). The median of the length distribution at San Rafael is ~1.1 km, and the maximum dike length is 8 to 9 km (Delaney and Gartner 1997 [145370], Figure 4), a distribution not dissimilar to that used in the PVHA (Figure 4).

A measure comparable to dike half-length, the distance from the end of the dike nearest the proposed repository to the point of origin of the volcanic event, can be derived from information elicited in the PVHA (Figure 6). This distribution has a 5<sup>th</sup>-percentile, mean, and 95<sup>th</sup>-percentile values of 0.2, 2, and 5.6 km, which, given the previous discussions of observed dike lengths, vent spacings, and maximum observed half-length vent alignment of 5.6 km, is in excellent agreement with observed volcanic event features in the YMR. Note that the range of maximum event length values (10 to 20 km) used in NRC probability models (Reamer 1999 [119693], Figures 29 and 30), are comparable to the maximum dike lengths assessed by the PVHA experts. However, the NRC's use of a uniform distribution for dike half-length results in a much greater weighting in NRC probability models for dike lengths that represent the > 95<sup>th</sup>-percentile values assessed by the 10 PVHA experts (Figure 4). The NRC intersection probability value of  $10^{-7}$  per year, assumed for purposes of NRC PA (Reamer 1999 [119693], p. 61), depends on a maximum vent alignment length of 20 km (Reamer 1999 [119693], Figure 30).

### **6.3.3 Conceptual Models of Volcanism and Formulation of Probability Models**

In the PVHA and alternative assessments of volcanic hazard to the proposed Yucca Mountain repository, the conceptual model of volcanism—how and where magmas form and what processes control the timing and location of magma ascent through the crust to form volcanoes—has a fundamental impact on how probability models are formulated and the consequent results of probability models (e.g., Smith et al. 1990 [101019]; CRWMS M&O 1996 [100116]; Reamer 1999 [119693]).

In general, the PVHA experts viewed the YMR as part of the same extensional tectonic and volcanic regime as the rest of the southern Great Basin portion of the Basin and Range province, but several members of the panel noted the possible additional influence on volcanism of the Walker-Lane structural zone (CRWMS M&O 1996 [100116], Appendix E, e.g., pp. WD-1 and WH-1). The smaller volumes of basalt erupted in the YMR since the Miocene reflects waning of both tectonism and magmatism in this part of the Basin and Range Province (CRWMS M&O 1996 [100116], Appendix E, e.g., pp. RC-1, BC-3, WD-2, RF-3, WH-1, MK-1, AM-3).



Output data. DTN: LA0009FP831811.001 [164712]

NOTE: This distribution is obtained by convolving the distributions for dike length with those for the location of the point event relative to the dike. The 5<sup>th</sup>-percentile, mean, and 95<sup>th</sup>-percentile values are 0.2, 2.0, and 5.6, km, respectively. The distribution contains a very long upper tail extending to 86 km.

Figure 6. Composite Distribution for the Distance from the Point Volcanic Event to the End of the Dike Averaged Across All 10 PVHA Experts

Some PVHA experts distinguished between deep (mantle source) and shallow (upper crustal structure and stress field) processes when considering different scales (regional and local) of spatial control on volcanism (CRWMS M&O 1996 [100116], Appendix E, e.g., pp. MK-2 and AM-1). The PVHA experts generally view volcanism in the YMR as a regional-scale phenomenon because of melting processes in the upper lithospheric mantle that produce small volumes of alkali basalt, which is a basalt type generated by relatively small percentages of mantle melting compared to other basalt types (CRWMS M&O 1998 [105347], Chapter 4, p. 4-4). The exact mechanism of mantle melting in the YMR is poorly understood but may be controlled by a complex combination of processes including the effect of residual heat in the lithospheric mantle from previous episodes of volcanism and the presence of a plate subduction system, local variations in volatile (water) content, variations in mantle mineralogy and chemistry, and the effect of regional lithospheric extension (CRWMS M&O 1996 [100116], Appendix E). Researchers who have analyzed magmatic processes in the YMR generally agree that the magnitude of mantle melting has drastically decreased since the middle Miocene and that all melts in the past few million years have been generated within relatively cool (compared to asthenospheric mantle) ancient lithospheric mantle, which is a factor that may contribute to the

relatively small and decreasing volume of basaltic melt erupted in the YMR since the Miocene (Farmer et al. 1989 [105284]; Yogodzinski and Smith 1995 [136262]; CRWMS M&O 1996 [100116], Appendix E; Reamer 1999 [119693], pp. 17 and 47).

An alternative to the hypothesis of melting within lithospheric mantle was presented by Smith et al. (2002 [158735]), who hypothesized instead that basaltic melts beneath the YMR are generated within hot upwelling asthenospheric mantle (mantle “hotspot” model). This model raises the possibility that the recurrence rate of basaltic volcanism near Yucca Mountain (the Crater Flat volcanic field) could increase in the next few thousand years to a level comparable to the more active Lunar Crater volcanic field, 100 miles to the north. This hypothesis is based on a proposed correlation between the timing of volcanic episodes between the Lunar Crater and Crater Flat fields, and a proposal that anomalously hot mantle underlies the region beneath both volcanic fields, providing a common mechanism that controls the timing of volcanic activity. If this hypothesis were valid, probability models that estimate the probability of volcanic disruption of the repository might need to be revised to account for the possibility of higher recurrence rates in the future.

The hypothesis that recurrence rates of volcanism could suddenly increase because of anomalously hot mantle beneath the Yucca Mountain area is inconsistent with the following observations:

- The Crater Flat volcanic field is one of the *least* active volcanic fields in the western United States, while the Lunar Crater field is one of the *most* active fields within the Basin and Range interior. This fundamental difference in eruptive behavior does not suggest a common physical mechanism that links the two fields. Basaltic volcanic fields are common throughout the western United States, with at least 20 to 30 fields active in the last 5 m.y. Many of these volcanic fields consist of 50 to 100 individual volcanoes, with several of the largest containing more than 300 individual volcanoes. Eruption rates for most fields range from 10 to more than 100 km<sup>3</sup>/m.y. (Perry and Bowker 1998 [159502]). The Lunar Crater field consists of 70 to 100 individual volcanoes, with an eruption rate of approximately 20 km<sup>3</sup>/m.y. over the past 4 m.y. In contrast, the Crater Flat field consists of about 10 to 15 individual volcanoes, with an eruption rate of < 1 km<sup>3</sup>/m.y. over the past 4 m.y. (Perry and Bowker 1998 [159502]). These data indicate a recurrence rate in the Lunar Crater field that is approximately an order of magnitude greater than in the Crater Flat field. If, as proposed, the common link between the two fields is anomalously hot mantle, the lower volume, eruption rate, and recurrence rate of the Crater Flat field indicates that the underlying mantle is not as hot, or prone to melt, as mantle beneath Lunar Crater. Indeed, the low activity of the Crater Flat field compared to nearly every other volcanic field in the western U.S. indicates that the underlying mantle is not particularly hot. Therefore, there is no evidence to indicate that the recurrence rate of volcanism near Yucca Mountain will ever reach values equivalent to those at Lunar Crater.
- Neodymium isotopic compositions of basalts in the Lunar Crater and Crater Flat volcanic fields are significantly different, indicating fundamentally different mantle sources or fundamental differences in processes that produced the basalts. Smith et al. (2002 [158735]) recognized the isotopic differences between the two

volcanic fields and speculated that the unusual Nd isotopic compositions of basalt near Yucca Mountain are due to (1) contamination of asthenospheric melts passing through lithospheric mantle or (2) modification of asthenospheric mantle by fluids or melts derived from subducted crust. Either mechanism would not be expected to affect the basalts near Yucca Mountain selectively, but would instead operate on a much larger scale. For example, because subducted crust existed beneath most of the western United States for tens of millions of years, modifying fluids or melts derived from subducted crust would be expected to modify asthenospheric mantle on a continental scale, not just the small region surrounding Yucca Mountain. Basalts from Lunar Crater have isotopic compositions similar to ocean island basalts, indicating a source in relatively warm and convecting asthenospheric mantle. The unusual Nd isotopic composition of basalts in the Crater Flat field indicate derivation from a lithospheric mantle source that is old, stable, and cold (nonconvecting) compared to asthenospheric mantle (Perry et al. 1987 [162311]; Farmer et al. 1989 [105284]; Livaccari and Perry 1993 [162310]). Wernicke et al. (1987 [107250]), citing tectonic evidence, suggested that the relative lack of volcanism in the YMR until 15 m.y. ago left the lithosphere cold and difficult to extend compared to more volcanically active and earlier extended regions of the Basin and Range province. The preponderance of evidence indicates that the small volume of basalt and limited volcanic activity near Yucca Mountain reflect an underlying mantle source that is cold and unable to produce significant volcanic activity.

On a more local and shallow crustal scale, most researchers conclude that (1) volcanism is correlated with zones of past or present crustal extension, and (2) once dikes feeding volcanoes enter the shallow upper crust, their location and orientation is influenced by the orientation of the local stress field and the presence of faults that may locally control vent location and alignment. The evidence cited for these two conclusions includes several northeast-oriented vent alignments in the YMR and the association of eruptive centers with known or inferred faults (Smith et al. 1990 [101019], p. 83; CRWMS M&O 1996 [100116], Appendix E, e.g., p. AM-4; Connor et al. 1997 [135969], p. 78; Reamer 1999 [119693], Section 4.1.3.3.3; Fridrich et al. 1999 [107333], p. 211).

A mechanistic model relating mantle melting and lithospheric extension has recently been proposed for the YMR by Connor et al. (2000 [149935]) and, additionally, is used as the geologic basis for weighting spatial density models based on crustal density variations across the YMR (Reamer 1999 [119693], Section 4.1.6.3.3). The conceptual basis of the model is that crustal density variations across the YMR control variations in lithostatic pressure at the base of the crust. These pressure variations, in turn, control the location of decompression melting within the mantle, which, in turn, controls the location of future igneous activity within the YMR (Connor et al. 2000 [149935], pp. 419 through 422).

As formulated, a finite-element model that calculates lateral pressure changes in the YMR based on upper crustal density variations (Connor et al. 2000 [149935], p. 420) is a poor predictor of volcano distribution in the YMR. The model predicts that maximum melting (and, hence, more frequent occurrence of volcanism) will occur farthest from the region of high crustal density (Connor et al. 2000 [149935], Figure 3), but note that this model predicts the opposite of what is observed for the occurrence of post-Miocene volcanism in the YMR because volcanism is

concentrated near high-density crust of the Bare Mountain domain rather than farther to the east (Figure 7).

Inspection of a map of apparent crustal density variation (Connor et al. 2000 [149935], Plate 1) shows that low average crustal density extends fairly uniformly for a distance of at least 50 km east of the Bare Mountain Fault. Within the context of the conceptual model proposed by Connor et al., (2000 [149935] (i.e., crustal density exerts a primary control on location of volcanism), post-Miocene volcanism should occur somewhat randomly across this broad region. Instead, all post-Miocene volcanism near Yucca Mountain is located within 5 to 10 km of the Bare Mountain fault or near the southern ends of the Windy Wash and Stagecoach Road faults (Fridrich et al. 1999 [107333], p. 211), indicating that local zones of extension and upper crustal faulting may exert more direct control on the location of volcanism than the effect of shallow crustal processes on deep mantle processes (CRWMS M&O 1996 [100116], Appendix E, e.g., pp. AM-5 and MS-2; Fridrich et al. 1999 [107333], p. 211; Reamer 1999 [119693], Section 4.1.5.3.3). This is not to say that areas of low crustal density and volcanism do not often coincide, but instead that both are independently influenced or caused by upper crustal faulting and extension.

Connor et al. (2000 [149935]) uses crustal density as a primary “tectonic” or “geologic” control on volcano distribution (Reamer 1999 [119693], Section 4.1.6.3.3), even though volcano distribution is not randomly distributed over broad areas of low crustal density as predicted by this model. An alternative method of weighting spatial density models would be to weight by estimated percent of extension within the Crater Flat basin (e.g., Fridrich et al. 1999 [107333], Figure 5), thereby tying probability models more directly to a geologic process (faulting and extension) that many researchers agree exerts an important geologic control on volcano location (Smith et al. 1990 [101019], p. 83; CRWMS M&O 1996 [100116], Appendix E, e.g., pp. AM-5 and MS-2; Connor et al. 1997 [135969], p. 78; Reamer 1999 [119693], Section 4.1.3.3.3, p. 47). The strong southward and westward increase in extension rate across the Crater Flat basin corresponds well to sites of most recent volcanism in the basin (Fridrich et al. 1999 [107333], Figures 1 and 5), as opposed to crustal density variations that are hypothesized to control volcano location but do not correspond well with volcano location (Reamer 1999 [119693], Figure 22). In terms of alternative conceptual models, models based on observable geologic features in the YMR provide a more defensible framework and technical basis for probability calculations than models relying on unobservable processes that remain largely speculative (i.e., Reamer 1999 [119693], Section 4.1.5.3.2; see also Probability Acceptance Criteria 3, Reamer 1999 [119693], p. 24).

In summary, the probability model proposed by Connor et al. (2000 [149935]) that relies on spatial density functions weighted by crustal density is not well supported based on observations of volcano distribution within the YMR. Significantly, this probability model is the basis for calculating the highest annual probability value for a volcanic eruption within the proposed repository boundary ( $9 \cdot 10^{-8}$  per year, Reamer 1999 [119693], Figure 30), which is the value (rounded up to “ $10^{-7}$ ” per year) that the NRC will use for the purposes of PA (Reamer 1999 [119693], p. 61). It should also be noted that this probability model results in an approximately two-fold increase in the intersection probability compared to unweighted spatial density models (Reamer 1999 [119693], Figure 29). As discussed previously in Section 6.3.2.2, the results of

this probability model also depend to a large extent on dike lengths that are inconsistent with the geologic record of the YMR.

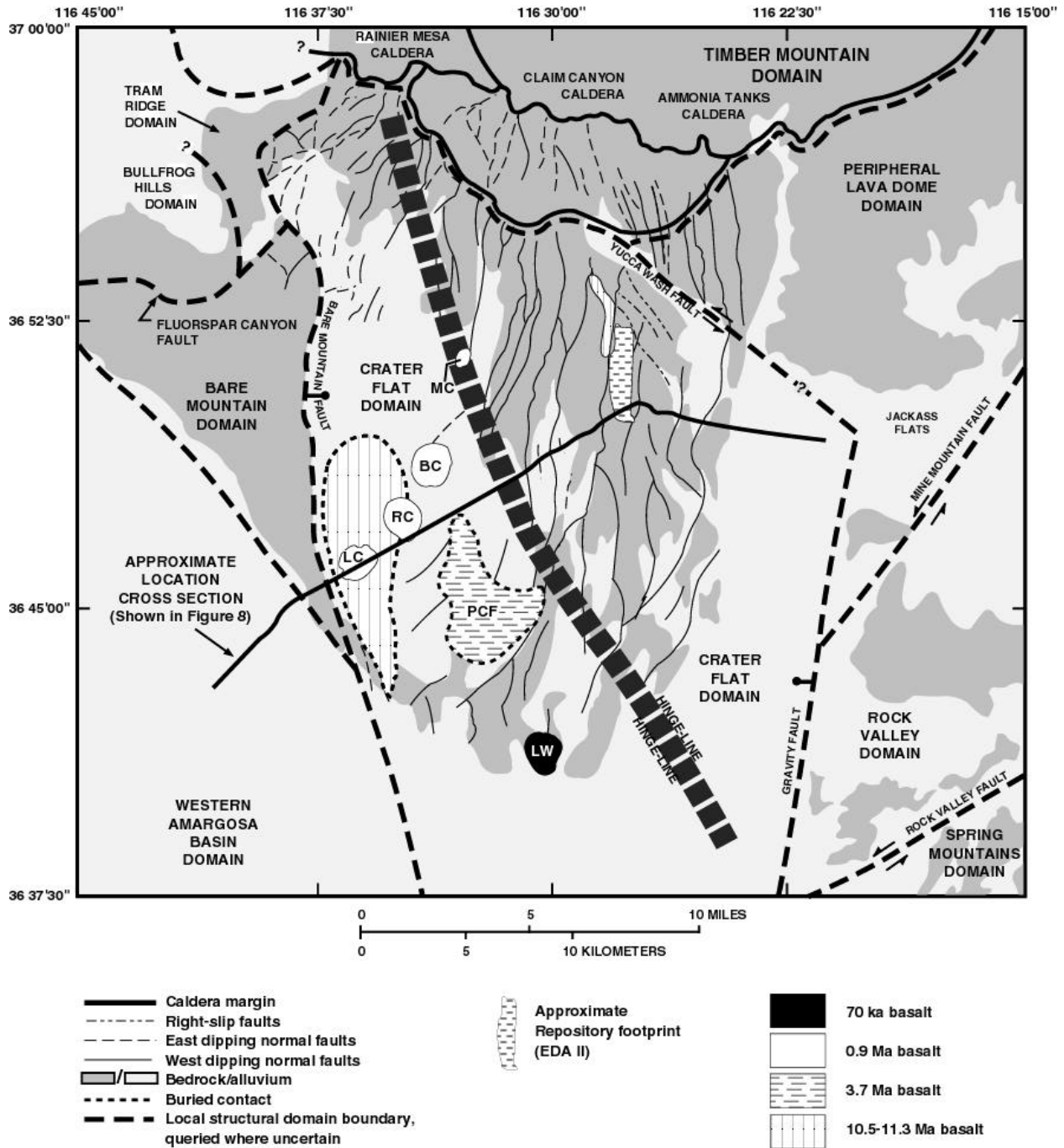
#### **6.4 THE CRATER FLAT STRUCTURAL DOMAIN**

Clearly, post-Miocene volcanoes in the YMR are spatially clustered (Crowe et al. 1995 [100110], Chapter 3; Connor and Hill 1995 [102646], Figure 2). For probability models that incorporate clustering of volcanoes (Connor and Hill 1995 [102646]) or specify volcanic source zones based primarily on the location or clustering of volcano centers (CRWMS M&O 1996 [100116]), estimation of the hazard to Yucca Mountain is often dominated by the presence of the Crater Flat cluster. This is due to the relatively high occurrence and Quaternary age of volcanoes in the Crater Flat basin (including Lathrop Wells, which lies within the Crater Flat structural domain and is the youngest volcano in the YMR), and because of the close proximity of Crater Flat volcanoes to Yucca Mountain, compared to other volcanic clusters in the YMR (Figure 3).

The Crater Flat structural domain as defined by Fridrich (1999 [118942], pp. 170 through 178) is a structural basin or graben. It is bounded on the west by the Bare Mountain fault and on the east by structures buried beneath Jackass Flats (Figure 7). It includes the Crater Flat topographic basin on the west and Yucca Mountain near the center of the structural basin (Figure 7). Because the proposed Yucca Mountain repository lies within the Crater Flat structural basin, the structural and geophysical features of the basin, and to what degree they influence the location of volcanism within the basin, have been a key factor in conceptual models of volcanism that provide the geologic framework for assessing hazards to the proposed repository.

The following sections describe the internal structure of the Crater Flat basin, as well as how the PVHA experts and subsequent investigators have interpreted the influence of structural characteristics of the basin in estimating the locations of future volcanic events. Based largely on work published since the PVHA, the evidence that the northeastern and southwestern portions of the basin have different extensional histories that may have influenced the location of basaltic volcanism within the basin is summarized below.

# Characterize Framework for Igneous Activity at Yucca Mountain, Nevada



Source: Basalts of different ages are shown in relation to basin structure (modified from Fridrich et al. 1999 [118942], Figure 1). The 70-ka age of the Lathrop Wells volcano indicated in the legend was estimated based on preliminary data subsequently published in Heizler et al. (1999) [107255], which indicates an age closer to 80 k.y.

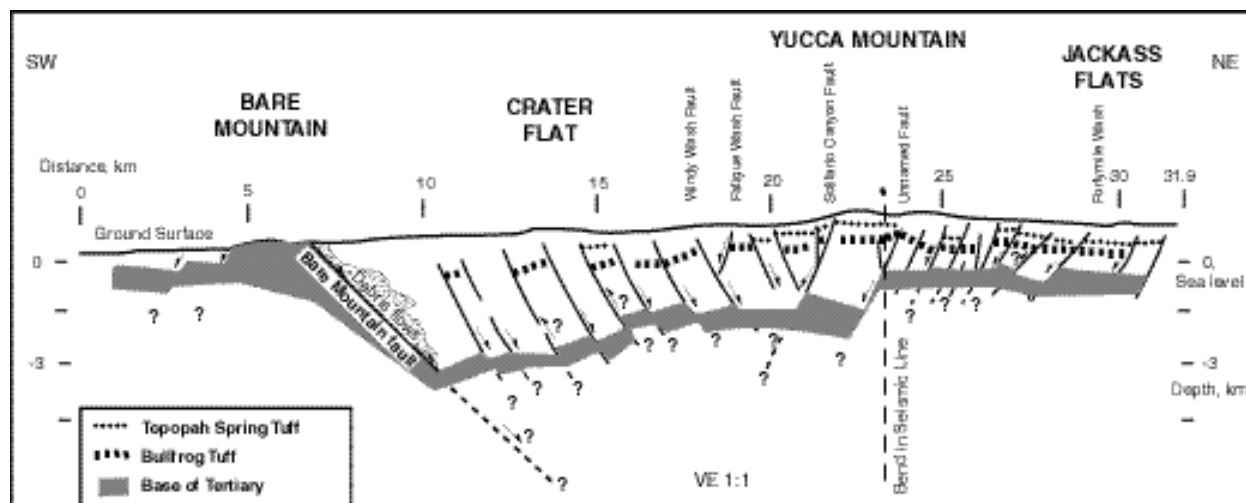
NOTE: PCF = Pliocene Crater Flat; MC = Makani Cone; BC = Black Cone; RC = Red Cone; LC = Little Cones; LW = Lathrop Wells.

Figure 7. Local Structural Domains and Domain Boundaries of the Yucca Mountain Repository and Internal Structures of the Crater Flat Basin and Selected Parts of Adjacent Domains

#### **6.4.1 Internal Structure and Boundaries of the Crater Flat Basin**

The Crater Flat structural domain (also referred to herein as the “Crater Flat basin”) comprises the Crater Flat topographic basin (west of Yucca Mountain), Yucca Mountain, and the western part of Jackass Flats. Based on geologic mapping and interpretation of subsurface structures from geophysical surveys (discussed below), the Crater Flat structural domain appears to comprise a single, westward-sloping, faulted basin (Figure 8). The western boundary of the Crater Flat basin coincides with the Bare Mountain fault and the northward extension of the fault into the Tram Ridge and Tate’s Wash faults (Fridrich 1999 [118942], p. 174). The Bare Mountain fault dips steeply ( $64^{\circ} \pm 5^{\circ}$  near the southern end) and can be imaged by seismic reflection to depths of at least 3.5 km and possibly to depths of 6 km (Brocher et al. 1998 [100022], pp. 956 and 966). Logically, this major fault probably extends to the brittle-ductile transition in the middle crust. The northern boundary consists of a gradational termination of intrabasin structure at the perimeter of the Timber Mountain caldera complex (Fridrich 1999 [118942], p. 174). As defined by Fridrich (1999 [118942], pp. 174 and 176), the northeastern boundary coincides with Yucca Wash, which is an alluvium-filled valley inferred to be underlain by a small northwest-striking right-lateral strike slip fault or zone of faults (Fridrich 1999 [118942], pp. 174 and 176). The fault is nowhere exposed but is inferred from the fact that Yucca Wash is a linear valley separating Yucca Mountain from a domain to the northeast in which the 12.7- to 12.8-m.y. Paintbrush Group and older rocks are more extended than on northern Yucca Mountain (Fridrich 1999 [118942], p. 176). Day et al. (1998 [100027], p. 11) summarize evidence indicating that a major fault is not present beneath Yucca Wash.

The eastern and southern margins of the domain are not physiographically distinct but, rather, merge with adjacent portions of the Basin and Range. The eastern margin of the Crater Flat basin is probably a buried, down-to-the-west fault known as the Gravity Fault (Fridrich 1999 [118942], p. 176, Figure 7). The southern margin is inferred from gravity and magnetic data, and from discontinuous outcrops, to be a fault structure buried beneath young alluvium. It is typically drawn in a northwestern direction along the Amargosa Valley (Fridrich 1999 [118942], p. 176). Fundamental changes in the style, timing, and magnitude of extension and other deformation occur across all of the boundaries of the Crater Flat basin.



Source: Modified from Brocher et al. 1998 [100022]

NOTE: Location of cross section is indicated in Figure 7.

Figure 8. Schematic Cross Section of the Crater Flat Basin, from Seismic, Reflection Surficial Geology, and Borehole Information

#### 6.4.1.1 Fault Orientations, Dip Directions, and Displacements

In the center of the Crater Flat basin, a sequence of 12.7 to 12.8 m.y. ash-flow tuffs (primarily the Tiva Canyon and Topopah Spring Tuffs of the Paintbrush Group) crop out. These exposed tuff units comprise Yucca Mountain and adjacent mesas. Much of the information about orientation, offset, and timing of faulting is based on examination of faults that cut through the exposed tuffs. Because both Crater Flat and Jackass Flats are basins that have undergone alluviation in the late Quaternary, much of the structure of these basins is not accessible to direct observation. Information on structures beneath Crater Flat and Jackass Flats is derived mainly from seismic, gravity, and aeromagnetic and ground magnetic data.

The Crater Flat basin is characterized by an array of closely spaced, small-to-moderate sized extensional faults that generally dip towards the center of the basin (Figure 8). Normal faults within the Crater Flat basin strike northerly in the northeastern part of the basin but change to increasingly northeasterly to the south and west across the basin (Figure 7). These orientations can be measured directly where faults are exposed on Yucca Mountain and can be inferred from the strike of aeromagnetic and gravity anomalies where buried beneath young basin fill. In general, the fault pattern within Crater Flat basin is roughly radial to the caldera complex to the north and curved from north to south across the basin. Based on the strike directions of faults within the Crater Flat basin, a northwest-trending “hinge line” can be defined (Fridrich et al. 1999 [107333], p. 208) that separates an area of predominantly north-striking faults on the northeast from an area of predominantly northeast-striking faults on the southwest (Figure 7). The hinge line marks the approximate location of (1) the 20° contour of clockwise rotation of the Tiva Canyon Tuff, (2) a subtle yet abrupt decline in elevation to the southwest, and (3) an increase in Quaternary displacement for faults southwest of the hinge line (Fridrich et al. 1999 [107333], p. 208; Stamatakos et al. 1997 [138819], p. 327). These observations are consistent with a division of the Crater Flat basin into two portions, separated at

the approximate position of the hinge line (Figure 7): (1) a northeastern, less extended portion, and (2) a southwestern, more extended portion (Fridrich et al. 1999 [107333], p. 208; Stamatakos et al. 1997 [138819], pp. 327 through 328).

Seismic reflection surveys show that the Crater Flat basin is deepest to the west (Brocher et al. 1998 [100022], Figure 6; see also Ferrill et al. 1996 [105315], Figure 1b), implying that extension is also greatest to the west. Stratigraphic thickening of Miocene volcanic rocks to the west support this interpretation (Fridrich et al. 1999 [107333], p. 198). Thus, Crater Flat basin is a single, westward-dipping graben, with less fault displacement in the eastern half, within which no major faults dominate (Figure 8).

Nearly all faults of the Crater Flat basin have at least a small component of oblique offset (Fridrich 1999 [118942], p. 177). Stratal tilts increase strongly to the west and south from an area of minimum tilts in the northeastern part of the basin on north Yucca Mountain. Faults in the southern part of the basin have a shallower dip and generally greater hanging wall tilt. In the northeastern part of the basin, cumulative extension is 7 to 15 percent. In contrast, cumulative extension in the southwestern part of the basin is at least 50 to 100 percent. This greater extension results from decreased spacing between the intrabasin faults and to increased average throw of the major faults (Fridrich et al. 1999 [107333], pp. 197 through 198).

#### **6.4.1.2 Rotation of Faults**

The curved pattern of faults and the difference in orientation of faults from northeast to southwest in the Crater Flat basin is attributed to southward increasing clockwise vertical-axis rotation, whereby fault blocks together with their bounding faults were rotated from their original positions. On the scale of the basin as a whole, the spatial variation of declination (i.e., interpreted as vertical-axis rotation) is very smooth (Rosenbaum et al. 1991 [106708], pp. 1976 and 1977; Hudson et al. 1996 [106194]; Fridrich et al. 1999 [107333], Figure 8). The hinge line that is defined from the strike directions of faults corresponds approximately to the contour of 20° clockwise rotation of the Tiva Canyon Tuff. In general, more than 20° of clockwise rotation is present southwest of this line, and less than 20° of rotation is present northeast of the hinge line. In the northeastern part of the basin, cumulative clockwise rotation is generally < 5°; in contrast, cumulative rotation in the southwestern part of the basin is > 45° (Fridrich et al. 1999 [107333], p. 197). Paleomagnetic data from the Crater Flat basin are interpreted to show that older stratigraphic units are rotated more than younger units and that the major pulse of vertical-axis rotation followed the major episode of extension by about 1 m.y. The major pulse of rotation occurred between 11.6 and 11.45 m.y. (Hudson et al. 1996 [106194]; Fridrich et al. 1999 [107333], p. 210). The close association in the areal pattern of vertical axis rotation with the magnitude of extension in the Crater Flat basin suggests that the rotation and extension are related as a consequence of fan-like opening of the basin (Fridrich et al. 1999 [107333], p. 210).

#### **6.4.1.3 Quaternary Slip Rate**

Based on the areal variation in the pattern of late Quaternary extension in the Crater Flat basin, a strong southward increase in deformation rate exists. Slip rates determined on individual faults generally increase to the south (Fridrich et al. 1999 [107333], pp. 197 and 208; Fridrich 1999

[118942], p. 177). In addition, cumulative late Quaternary (900 to 100 k.y.) extension measured along three profiles yields 0.025, 0.1, and 0.2 percent per m.y. from north to south across the basin (Fridrich et al. 1999 [107333], p. 207). Thus, the original fan-like pattern of basin opening established in the Miocene still persists. The continuing pattern of oblique basin opening indicates that vertical-axis rotation must still be occurring at a rate that is significant relative to the rate of extension (Fridrich et al. 1999 [107333], pp. 207 and 208).

Wernicke et al. (1998 [103485], p. 2098) presented data from global positioning system surveys that they interpreted as indicating a strain rate near Yucca Mountain three to four times the Basin and Range average. Based on this conclusion, they suggested that the volcanic hazard at Yucca Mountain may have been underestimated by an order of magnitude (Wernicke et al. 1998 [103485], p. 2099). A more recent study (Savage et al. 1999 [118952]) using data covering a longer time period than Wernicke et al. (1998 [103485]) interpreted the data to suggest that within the error of the measurements, the strain rate near Yucca Mountain measured between 1983 to 1998 was not significantly different from zero (Savage et al. 1999 [118952], p. 17631).

The suggestion that postulated anomalous strain rates near Yucca Mountain would lead to an order-of-magnitude increase in the volcano recurrence rate is not consistent with the post-Miocene volcanic record of the YMR. The total volume of basalt erupted during the past million years near Yucca Mountain is less than  $0.5 \text{ km}^3$ , and is part of a systematic decline in the volume of basalt erupted over the past 5 m.y. (CRWMS M&O 1998 [105347], Chapter 4, p. 4-12). This million-year record of low-volume volcanism is inconsistent with the hypothesis that approximate 100,000 year time intervals within this period have involved particularly high strain rates that would lead to an order-of-magnitude increase in magmatic activity, as stated by Wernicke et al. (1998 [103485], p. 2099). Furthermore, the youngest episode of volcanism near Yucca Mountain occurred as a temporally isolated event ~80 k.y. ago at Lathrop Wells, with no volcanism occurring since (CRWMS M&O 1998 [105347], Chapter 2, Sections III and IV). This observation is inconsistent with the Wernicke et al. (1998 [103485], p. 2099) hypothesis that Lathrop Wells may represent the onset of a cluster of volcanic events that may continue for several tens of thousands of years. Savage et al. (1998 [145359], p. 1007b) calculated that an order-of-magnitude increase in the volcano recurrence rate would result in a 90 percent probability of a new volcano forming since 80 ka. No such event has occurred. Savage et al. (1998 [145359], Figure 1) also presented fault displacement data showing that deformation rates in the YMR have decreased since about 60 k.y. ago, suggesting that the region is not currently within a period of anomalous strain rate that would couple to increased volcano recurrence rate.

#### **6.4.1.4 Basin Subsidence and Fault Displacement**

A greater subsidence in the southwestern part of the Crater Flat basin can be inferred from a lower elevation and, therefore, a greater sedimentation rate compared to the northeastern part of the basin. A subtle topographic decline (lower on the southwest side) corresponds with the hinge line, defined from the strike directions of faults (discussed above), along most of its length. The lower elevation is a function of greater total amount of extension to the southwest of the hinge line. Most faults that cross the hinge line show a pronounced southward increase in both Quaternary displacement and total bedrock displacement across it (Fridrich et al. 1999 [107333], pp. 197 and 208; Fridrich 1999 [118942], p. 177), especially near the western margin (Bare

Mountain fault) and central part (southern Yucca Mountain) of the basin. Miocene and Pliocene sediments are only slightly offset at the northern end of the Bare Mountain fault, whereas Holocene sediments are significantly offset near the southern end of the fault (Stamatakos et al. 1997 [138819], p. 327). Also, growth of alluvial fans is greater along the southern part of the fault. Differences in fan growth are indicative of increased fault slip in the southwestern part of the basin and are compatible with measured slip rates along the Bare Mountain fault from 0.02 mm/yr in the north to 0.21 mm/yr along the southern part of the fault (Ferrill et al. 1996 [105315], p. 562). Along the eastern side of Crater Flat, cumulative offset on the Solitario Canyon fault is approximately 1000 m greater to the south compared to the north (Stamatakos et al. 1997 [138819], p. 327). Greater differential subsidence in the southwestern part of the Crater Flat basin is correlated with a greater thickness of Quaternary alluvium in this part of the basin compared to adjacent parts. For example, lava flows associated with Little Cones are buried beneath approximately 15 meters of alluvium, whereas Red and Black Cones, of approximately the same age, are more completely exposed.

To summarize, a variety of structural data, including fault orientations, direction of dip, total and late Quaternary extension, vertical-axis rotation, and basin subsidence, are interpreted to show that the northeastern part of the Crater Flat basin is significantly different from the southwestern part of the basin. That is, each part of the basin has a distinctive style of deformation; the two regions of the basin can be distinguished from each other across a well-defined though gradational boundary, the hinge line extending obliquely across the Crater Flat basin (Figure 7). Thus, the northeastern and southwestern parts of the Crater Flat basin comprise structurally distinct portions of the basin with the southwestern portion characterized by a history of greater extension.

#### **6.4.1.5 Correlation with Volcanism**

The post-Miocene basaltic centers of the Crater Flat basin lie within the southwestern part of the basin (Figure 7). This portion of the basin is coincident with the zone of greatest transtensional deformation, between the hinge line of the basin and the Bare Mountain fault, suggesting that this extensional zone controlled the ascent of basalt through the upper crust (Fridrich et al. 1999 [107333], p. 210). The youngest volcano in the Crater Flat basin, the 80-ka Lathrop Wells volcano, lies between the southern ends of the Windy Wash and Stagecoach Road faults, the most active site of late Quaternary faulting in the Crater Flat basin (Fridrich et al. 1999 [107333], p. 211). Thus, there is a close spatial and temporal relationship between sites of extension and volcanism throughout the Crater Flat basin (Fridrich et al. 1999 [107333], p. 211). The restriction of three episodes of post-Miocene volcanism to the transtensional zone in the Crater Flat basin suggests that volcanism is less likely to occur at Yucca Mountain, which lies outside of the transtensional zone, in an area where no post-Miocene volcanism has occurred (Fridrich et al. 1999 [107333], p. 210, Figure 17a). As discussed in the next section, the PVHA experts recognized the close association between volcanism and areas of maximum extension in the YMR (CRWMS M&O 1996 [100116], pp. RC-5, BC-12, AM-5, MS-2, GT-2). Subsequent geologic and geophysical studies provide corroborative evidence that areas of maximum extension in the Crater Flat basin correspond closely to volcanic source zones defined in the PVHA (Stamatakos et al. 1997 [138819]; Brocher et al. 1998 [100022]; Fridrich et al. 1999 [107333]).

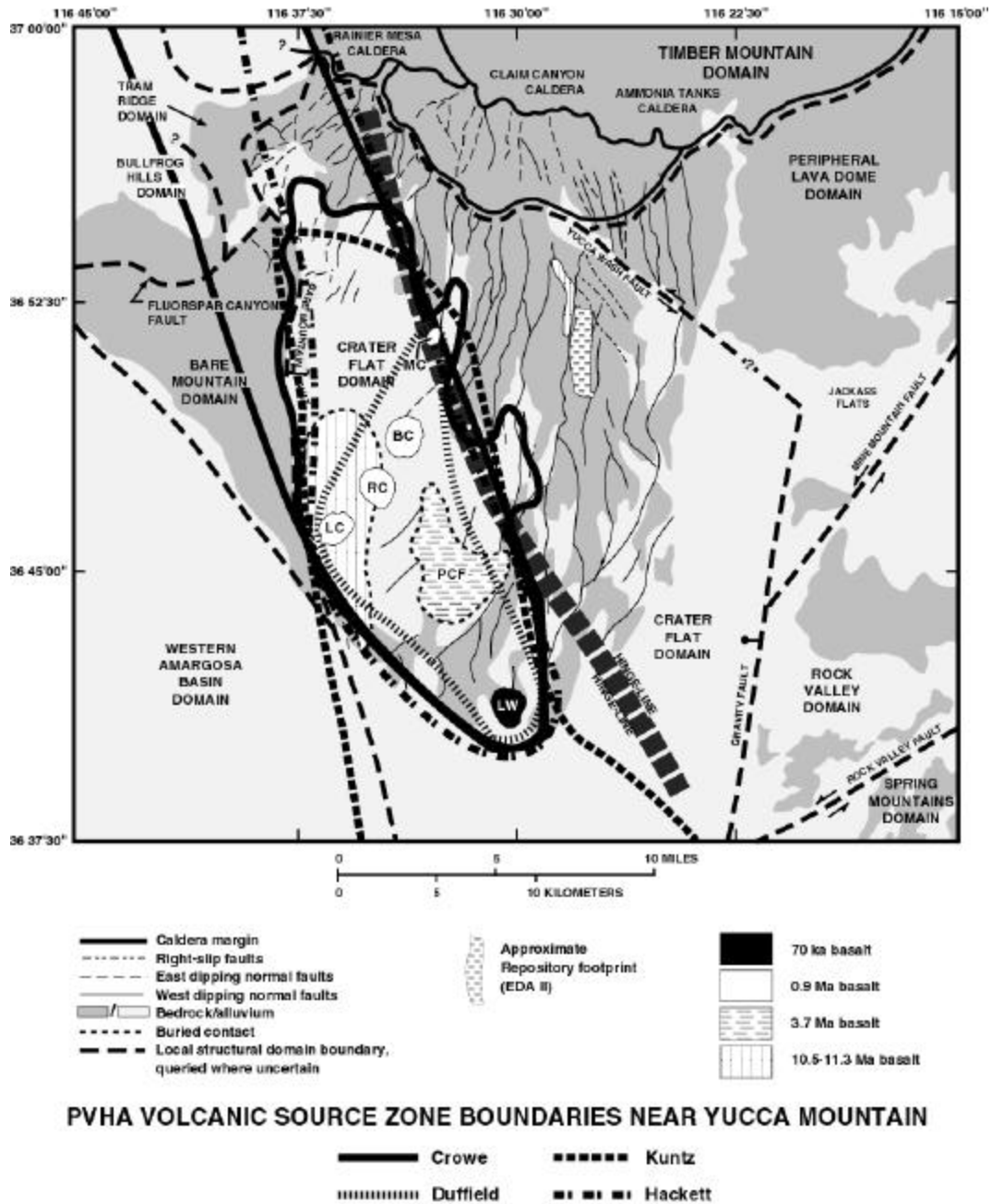
#### **6.4.2 Probabilistic Volcanic Hazard Analysis Volcanic Source Zones: Relationship to Crater Flat Structural Features and the Probability of Dike Intersection**

The correlation between the structurally active portion of the Crater Flat basin and sites of volcanism within the basin indicate that Yucca Mountain is near, but not within, a local volcanic zone that may produce small volumes of future volcanism (CRWMS M&O 1996 [100116], Appendix E, expert zone maps). Although local source zones were chosen by PVHA experts based largely on the location of past volcanic events, they correspond to the areas of highest cumulative extension and most active faulting in the Crater Flat basin (Fridrich et al. 1999 [107333], Figures 5 and 6), an association recognized by several of the PHVA experts (CRWMS M&O 1996 [100116], pp. RC-5, BC-12, AM-3 through 5, GT-2). In all cases in which local zones were defined, they were restricted to the southwestern portion of the Crater Flat basin or defined elongated, northwest-trending belts that included the southwestern portion and stretched to the Timber Mountain area (Figures 9a and 9b). All of the local zones excluded the northeastern portion of the Crater Flat basin, in which the proposed Yucca Mountain repository is located (Figures 9a and 9b). Based on structural arguments, therefore, and the past patterns of the close association of volcanism and extension, the eastern boundaries of local volcanic source zones defined in the PVHA separate more tectonically active and less tectonically active portions of the Crater Flat basin and may be reasonable predictors of the eastern extent of volcanism expected in the future.

In terms of probability calculations, the volcanic source zones defined in the PVHA represent local regions of higher event frequency (southwestern Crater Flat), whereas northeastern Crater Flat (which includes Yucca Mountain) falls within a regional background source zone of lower event frequency (Figure 17a). According to the intersection probability models used in the PVHA, two mechanisms can generate a disruptive event at Yucca Mountain: either a volcanic event is generated within a local source zone (higher probability event) to the west of Yucca Mountain and has the appropriate location and dike characteristics (length and azimuth) to intersect the proposed repository, or a volcanic event is generated within a regional background zone (lower probability event) and intersects the repository. Because the probability of intersection of a volcanic event with the proposed repository includes components of both mechanisms, the intersection probability estimated for the repository should reflect spatial event frequencies that lie between local source zone values and regional background values, consistent with the results of the PVHA, and appropriate for a site that lies outside of a local volcanic source zone but near enough possibly to be affected by dikes generated within the source zone.

In summary, many models of the experts related the areas of greatest likelihood for future volcanic activity to the region where previous volcanism has occurred and in which extensional deformation has been and continues to be greatest, i.e., to the southwestern portion of the Crater Flat basin (CRWMS M&O 1996 [100116], pp. RC-5, BC-12, AM-5, MS-2, GT-2, and expert zone maps; Figures 9a and b). Analysis by the NRC also indicates that the highest likelihood of future volcanic activity is in southwestern Crater Flat (Reamer 1999 [119693], Sections 4.1.5.4 and 4.1.6.3.3; Figure 28). Given that the southern and southwestern portion of the Crater Flat basin is the most extended (Ferrill et al. 1996 [105315]; Stamatakos et al. 1997 [138819]; Fridrich et al. 1999 [107333]; Reamer 1999 [119693], p. 47) and that the locus of post-Miocene volcanism in the Crater Flat basin lies in the south and southwestern portion of the basin (Fridrich et al. 1999 [107333]; Reamer 1999 [119693], p. 47), volcanic source zones defined in

the PVHA and centered in southwestern Crater Flat are consistent with the tectonic history and structural features of the Crater Flat structural domain (Figures 9a and b, Figure 17a).

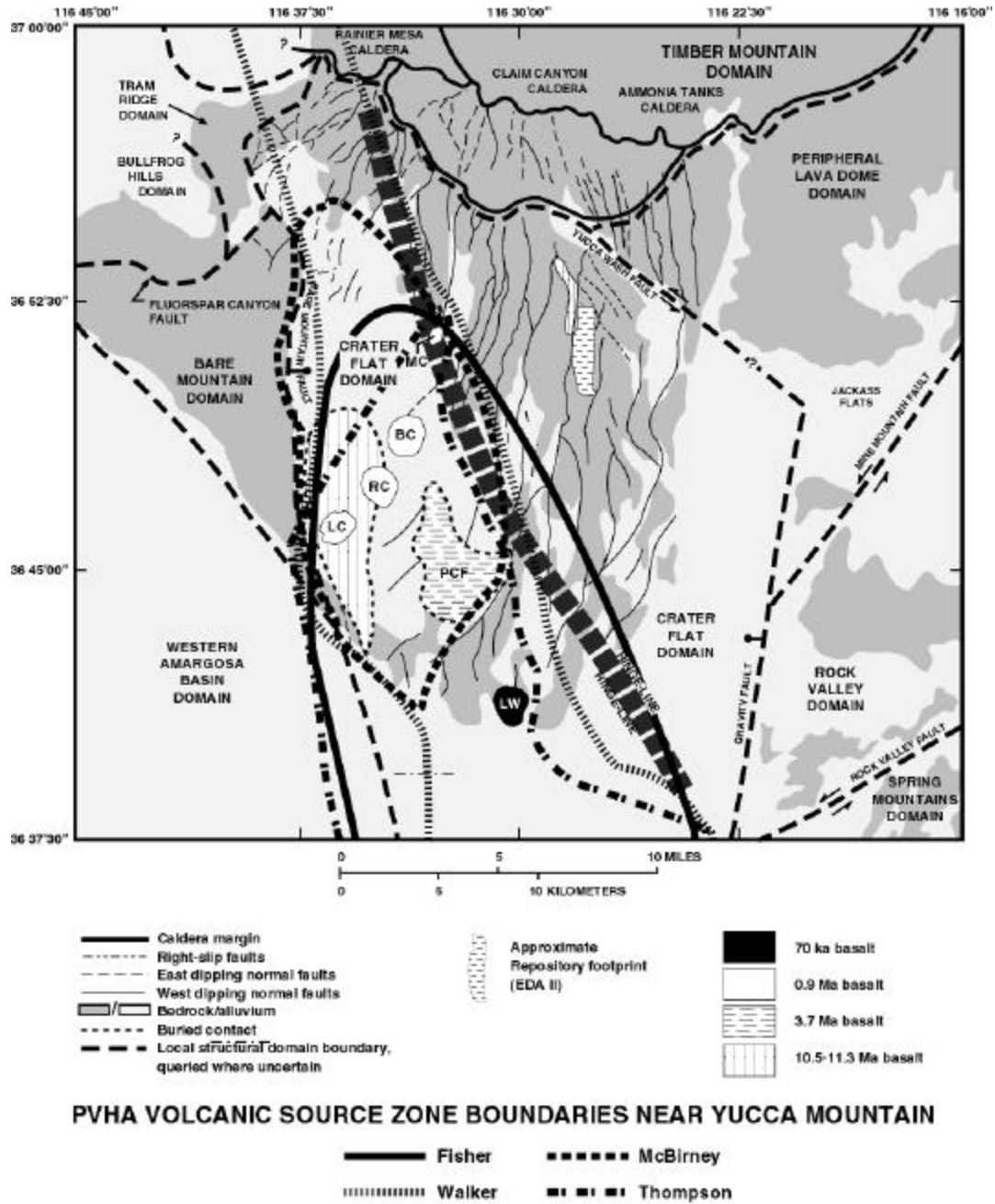


DTN: MO0002PVHA0082.000 [148234] (for zone boundaries only)

Source: Superimposed on the Fridrich et al. (1999 [107333], Figure 1) map are boundaries of selected volcanic source zones (locally homogeneous spatial and temporal model, CRWMS M&O 1996 [100116], Section 3.13) defined by the PVHA experts that lie within the Crater Flat basin (CRWMS M&O 1996 [100116], Appendix E).

NOTE: MC = Makani Cone; BC = Black Cone; RC = Red Cone; LC = Little Cones; LW = Lathrop Wells.

Figure 9a. Local Structural Domains and Domain Boundaries of the Yucca Mountain Repository and Internal Structures of the Crater Flat Basin and Selected Parts of Adjacent Domains



DTN: MO0002PVHA0082.000 [148234] (FOR ZONE BOUNDARIES ONLY)

Source: Superimposed on the Fridrich et al. (1999 [107333], Figure 1) map are boundaries of selected volcanic source zones (locally homogeneous spatial and temporal model, CRWMS M&O 1996 [100116], Section 3.13) defined by the PVHA experts that lie within the Crater Flat basin (CRWMS M&O 1996 [100116], Appendix E).

NOTE: MC = Makani Cone; BC = Black Cone; RC = Red Cone; LC = Little Cones; LW = Lathrop Wells.

Figure 9b. Local Structural Domains and Domain Boundaries of the Yucca Mountain Repository and Internal Structures of the Crater Flat Basin and Selected Parts of Adjacent Domains

## **6.5 RECALCULATION OF FREQUENCY OF INTERSECTION AND DEVELOPMENT OF DISTRIBUTIONS FOR LENGTH AND ORIENTATION OF DIKES AND FOR THE NUMBER OF ERUPTIVE CENTERS WITHIN THE PROPOSED REPOSITORY FOOTPRINT**

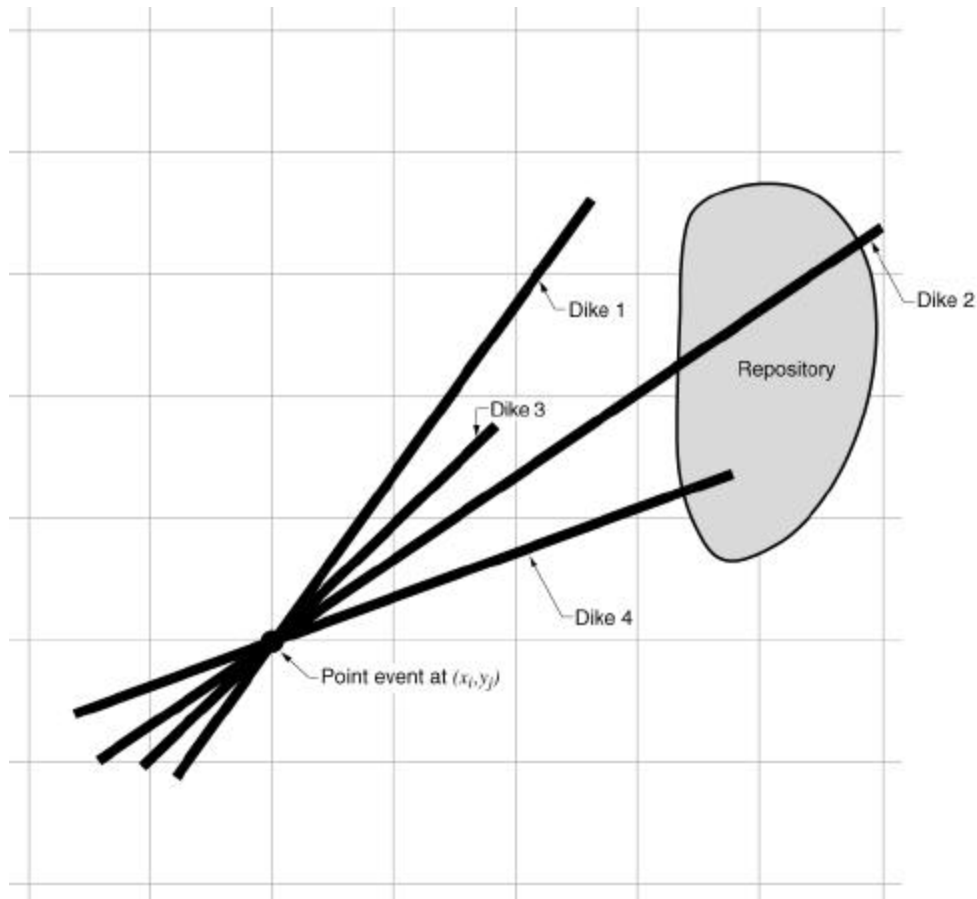
The PVHA (CRWMS M&O 1996 [100116]) presented a methodology for calculating the frequency of intersection of the proposed repository by a volcanic event and presented interpretations of 10 experts that were used to compute a distribution for the frequency of intersection that quantified the scientific uncertainty in the PVHA assessment. To evaluate the consequences of an intersection, information is needed on the length and orientation of the intersecting dike or dikes and the probability that an eruptive center (the vent above the conduit feeding an erupting volcano) forms within the emplacement area of the repository. This section of the report develops these assessments. In addition, the current configuration of the proposed LA repository emplacement area has a different outline from that used in the PVHA (CRWMS M&O 1996 [100116]). Consequently, the distribution for frequency of intersection was recalculated as part of this report, using the proposed repository footprint for the LA.

In the context of the PVHA, a volcanic event is a spatially and temporally distinct batch of magma ascending from the mantle through the crust as a dike or system of dikes (CRWMS M&O 1996 [100116], Appendix E). For the purposes of the probability models discussed in this report, a volcanic event is defined as a point  $(x,y)$  in space representing the expected midpoint of the dike system involved in the magma ascent. The dike system associated with the volcanic event is represented in probability model by a line element defined in terms of a length, azimuth and location relative to the point event (Figures 10 and 12). The term ‘dike length’ used in the PVHA and in this report when discussing volcanic events, refers to the total length of the dike system associated with the volcanic event. The phrase ‘intersection of the repository footprint by a dike’ refers to intersection of the emplacement area of the repository by the line element representing the dike system associated with the volcanic event. The possibility that a dike system (e.g., multiple dikes) has width or consists of multiple parallel dikes does not significantly affect the intersection probability and is not part of the calculations in this report. The width of the dikes and the number of parallel dikes does affect the consequences of an intersection and is included in *Number of Waste Packages Hit by Igneous Intrusion* (BSC 2003 [161851]).

The approach used to compute the frequency of intersection of the proposed repository by a volcanic event is illustrated in Figure 10. The PVHA experts specified spatial and temporal models that define the frequency of occurrence of volcanic events in the region around Yucca Mountain. A grid is constructed over this region with a spacing of 0.5 kilometer in the  $x$  (east-west) and  $y$  (north-south) directions (a 1-kilometer spacing was used in the original PVHA calculation, CRWMS M&O 1996 [100116]). At each location in the grid,  $x$  and  $y$ , the annual frequency of occurrence of volcanic events,  $I(x,y,t)$ , is computed from the experts’ spatial and temporal models. The variable  $t$  indicates that this rate is defined to be the present day rate. The volcanic events occurring at point  $(x,y)$  will have an associated dike. The experts defined distributions for the length and orientation of the possible dike or dike system that may be associated with volcanic events. Shown schematically on Figure 10 are four possible alternative representations of the dike system associated with the volcanic event. Of these four, two are at the proper orientation and of sufficient length to intersect the proposed repository. Using the

distributions for dike length and orientation, the fraction of all the possible alternative dike systems associated with volcanic events at point  $(x,y)$  that intersect the proposed repository is computed. This is defined as the conditional probability of intersection for volcanic events at point  $(x,y)$ ,  $P^I(x,y)$ . The frequency of intersecting volcanic events at point  $(x,y)$  is then the frequency of volcanic events,  $I(x,y,t)$ , multiplied by the conditional probability of intersection. The process is repeated for all locations in the grid, producing the frequency of intersection at each point. The sum of these values over all locations in the grid is the annual frequency of intersection of the proposed repository by volcanic events, the computed result of the PVHA.

The PVHA analysis did not make any assessment of the consequences of an intersection of the proposed repository footprint by a dike. Consequently, a potential dike that extended all the way through the proposed repository, such as dike 2 on Figure 10, has the same contribution to the frequency of intersection as a shorter dike that only extends part way into the proposed repository, such as dike 4 on Figure 10. However, an assessment of consequences requires information on the length and orientation of the intersecting dikes within the proposed repository. Consequently, the PVHA calculation process was modified to provide this information. This is accomplished by a straightforward disaggregation of the intersection frequency into relative frequencies for discrete increments of length and azimuth. A series of bins with length increments of 0.05 kilometer and azimuth increments of  $5^\circ$  were set up. This discretization is sufficiently fine to provide an accurate picture of the distribution of lengths and azimuths of intersecting dikes. Then, when a volcanic event produces an intersection in the hazard calculation, the resulting length and azimuth within the proposed repository footprint are computed, and the event is assigned to the appropriate bin. At the end of the calculation, the value in each bin represents the frequency of intersections that produce the specific values of length and azimuth represented by the bin. The sum of the numbers in all of the length-azimuth bins equals the frequency of intersection. The values in each bin divided by the frequency of intersection provide a conditional distribution for length and azimuth given an intersection. This calculation is completely defined by the interpretations developed by the PVHA expert panel (CRWMS M&O 1996 [100116], Appendix E) and requires no additional assumptions.



N/A - For Illustration Purposes Only

Figure 10. Schematic Illustrating Procedure for Computing the Frequency of Intersection of the Proposed Repository by a Volcanic Event

The additional evaluation needed for consequence analyses is a conditional distribution for the number of eruptive centers that occur within the proposed repository footprint given that there is an intersection by a dike associated with a volcanic event. Evaluation of this distribution requires an assessment of the number of eruptive centers associated with a volcanic event and the spatial distribution for eruptive centers along the length of the dike. The PVHA experts were not asked to make these assessments as part of their characterization of the volcanic hazard. The PVHA experts did assess the number of volcanic events represented by the observed eruptive centers in the YMR. These assessments, together with the characteristics of Quaternary volcanoes in the YMR and a limited number of assumptions (described in Section 5), are used to derive empirical distributions for the number of eruptive centers per volcanic event (presented in Attachment III). Application of these assessments in the calculation of the number of eruptive centers within the proposed repository requires assessment of the possible correlation between number of eruptive centers and dike length and on the spatial distribution of eruptive centers along the length of the dike. Calculations are performed in this report using a range of possible assessments to incorporate these uncertainties into the analysis.

The assessments of the distributions for length and orientation of intersecting dikes developed in this report use the geometric representation of a dike employed in the PVHA (CRWMS M&O 1996 [100116]). As such, dikes are linear features having only length and orientation. The evaluation of the consequences of a dike intersection of the proposed repository footprint requires additional information on the width of the intersecting feature. Assessments of the width of intersecting dikes is presented in BSC (2003 [161838]).

### 6.5.1 Formulation

This section describes the mathematical formulation required to compute the conditional distributions for the length and azimuth of intersecting dikes within the proposed repository footprint and the number of eruptive centers within this footprint. The formulation is an extension of the mathematical formulation used to compute the frequency of intersection of the proposed repository footprint by a dike in the PVHA (CRWMS M&O 1996 [100116], Section 3).

#### 6.5.1.1 Frequency of Intersection of the Proposed Repository Footprint by a Dike

This section restates the PVHA formulation (CRWMS M&O 1996 [100116], Section 3) to introduce terms and notation.

The PVHA study provided a distribution for the annual frequency of intersection of the proposed repository,  $n^I(t)$ , computed using the relationship (CRWMS M&O 1996 [100116], p. 3-2):

$$n^I(t) = \iint_R I(x, y, t) \cdot P^I(|x, y) dx dy \quad (\text{Eq. 1})$$

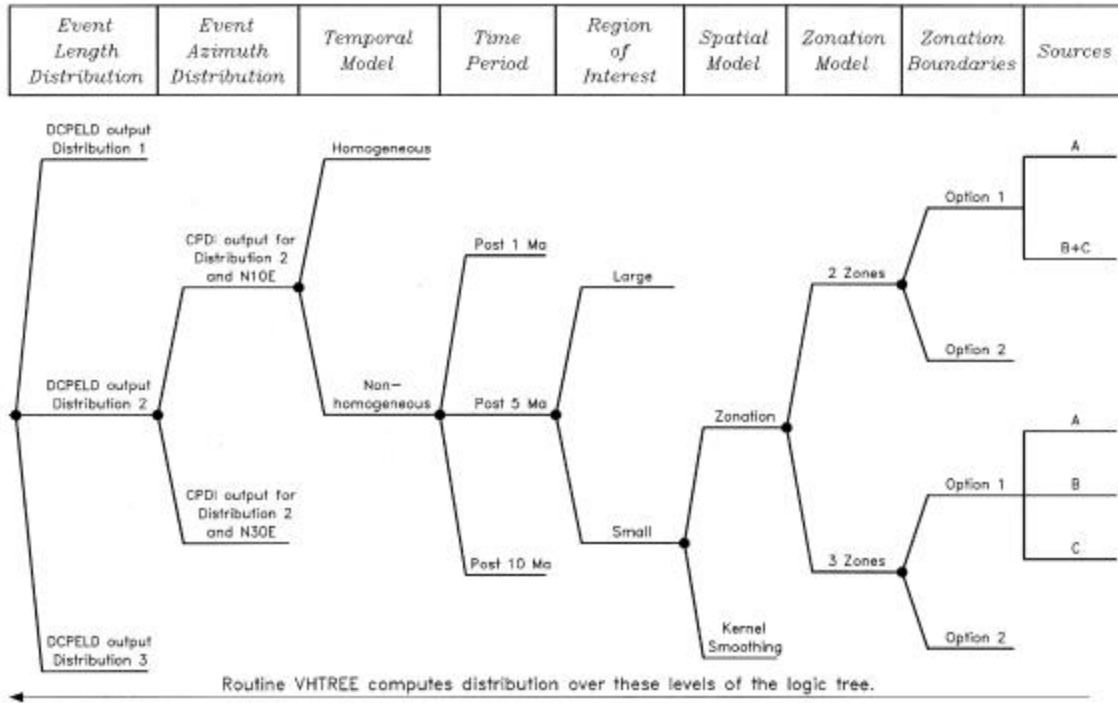
where  $I(x, y, t)$  is the rate of volcanic events at location  $(x, y)$  for the current time  $t$ ;  $P^I(|x, y)$  is the conditional probability that a dike associated with the volcanic event at point  $(x, y)$  intersects the proposed repository boundary; and  $R$  is the region surrounding the proposed repository. Note that the notation for intersection has been changed from a subscript  $I$  in CRWMS M&O (1996 [100116]) to a superscript  $I$  in this report for clarity.

The actual calculation was performed on a 0.5-km  $\times$  0.5-km grid spacing using the numerical summation:

$$n^I(t) = \sum_i \sum_j I(x_i, y_j, t) \cdot P^I(|x_i, y_j) \Delta x \Delta y \quad (\text{Eq. 2})$$

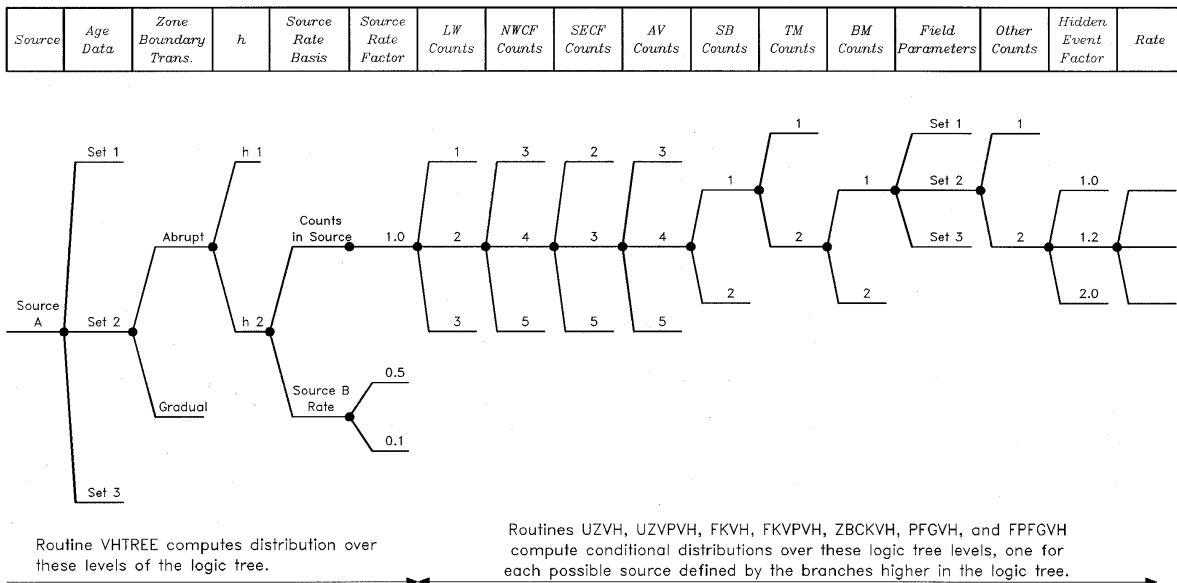
The PVHA experts quantified the uncertainty in  $n^I(t)$  by developing a set of alternative probability models and model parameters for all aspects of the hazard calculation. These were organized in the logic tree format shown in Figures 11a and 11b.

# Characterize Framework for Igneous Activity at Yucca Mountain, Nevada



Source: Modified from CRWMS M&O 1996 [100116].

Figure 11a. Logic Tree Structure Used to Characterize Uncertainty in Volcanic Hazard



Source: Modified from CRWMS M&O 1996 [100116].

NOTE: These subtrees are attached to the overall logic tree shown on Figure 11a.

Figure 11b. Logic Tree Structure for Subtrees Addressing Uncertainty in Volcanic Hazard from Specific Sources

The end branches of these logic trees define a discrete joint distribution for the parameters,  $\Theta$ , required to perform the calculation. Thus, Equation 2 becomes:

$$\mathbf{n}^I(t|\mathbf{q}_S) = \sum_i \sum_j \mathbf{I}(x_i, y_j, t|\mathbf{q}_S) \cdot P^I(x_i, y_j, \mathbf{q}_S) \Delta x \Delta y \quad (\text{Eq. 3})$$

where  $\mathbf{q}_S$  is the parameter set associated with an individual end branch of one expert's logic tree. The probability that  $\mathbf{n}^I(t|\mathbf{q}_S)$  is the correct frequency of intersection, given the expert's characterization of the uncertainty in the process, is given by the probability that the parameter set  $\Theta$  takes on the specific values defined by  $\mathbf{q}_S$ ,  $P(\Theta = \mathbf{q}_S)$ . This discrete probability is obtained by multiplying all of the conditional probabilities at each node along the path through the logic tree that leads to  $\mathbf{q}_S$ . The mean or expected frequency of intersection is given by:

$$E[\mathbf{n}^I(t)] = \sum_s \mathbf{n}^I(t|\mathbf{q}_S) \cdot P(\Theta = \mathbf{q}_S) \quad (\text{Eq. 4})$$

and the percentiles of the distribution for  $\mathbf{n}^I(t)$  are obtained by ordering the values of  $\mathbf{n}^I(t|\mathbf{q}_S)$  and then summing the probabilities  $P(\Theta = \mathbf{q}_S)$  until the desired percentiles are reached.

### 6.5.1.2 Conditional Distribution for Length and Azimuth of an Intersecting Dike

The above formulation for the PVHA hazard computation gives the overall frequency of intersection,  $\mathbf{n}^I(t)$ . However, to compute the consequences of an intersection, one needs to know the distribution for length and orientation of the intersecting dikes. This distribution is developed by breaking down (disaggregating) the total frequency,  $\mathbf{n}^I(t|\mathbf{q}_S)$ , into frequencies for specific values of intersecting dike length,  $L_m^I$ , and dike azimuth,  $\mathbf{f}_n$ . The process involves computing the spatial disaggregation of the frequency of intersection into the contributions from each location  $(x_i, y_j)$  in the spatial grid around the proposed repository,  $\mathbf{n}_{x_i, y_j}^I(t|\mathbf{q}_S)$  (see Figure 10).

At each point  $(x_i, y_j)$ , the conditional probability of intersection is the probability that dikes of all lengths and azimuths will intersect the proposed repository. The conditional probability of intersection is divided into probabilities for intersection from dikes with specific lengths and azimuths. As a result, the frequency of intersection from volcanic events at point  $(x_i, y_j)$  is divided into the frequency of intersection from volcanic events at point  $(x_i, y_j)$  that produce specific values of length,  $L_m^I$ , and azimuth,  $\mathbf{f}_n$ , within the proposed repository footprint,  $\mathbf{n}_{x_i, y_j}^I(t, L_m^I, \mathbf{f}_n|\mathbf{q}_S)$ . Summing these frequencies over all locations gives the frequency of intersection with a specific value of length and azimuth from all volcanic events,  $\mathbf{n}^I(t, L_m^I, \mathbf{f}_n|\mathbf{q}_S)$ . Dividing this frequency by the total frequency of intersection,  $\mathbf{n}^I(t|\mathbf{q}_S)$ , gives the conditional probability that an intersecting dike will produce a specific value of length and azimuth within the proposed repository.

The conditional probability of intersection,  $P^I(x, y, \mathbf{q}_S)$ , in Equation 3 is computed using the relationship (CRWMS M&O 1996 [100116], p. 3-17):

$$P^I(x_i, y_j, \mathbf{q}_S) = \int_0^{L_{max}|\mathbf{q}_S} f(d|\mathbf{q}_S) \cdot \left[ \int_{f_1|x,y,d}^{f_2|x,y,d} f(\mathbf{f}|\mathbf{q}_S) d\mathbf{f} \right] dd \quad (\text{Eq. 5})$$

where:

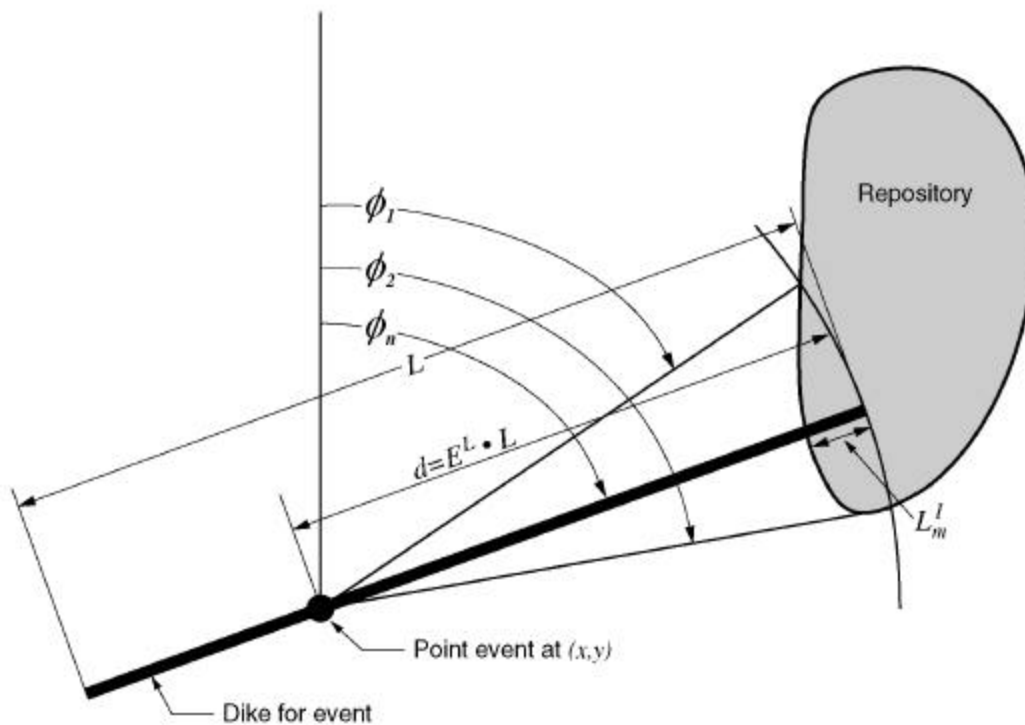
$f(d|\mathbf{q}_S)$  is the probability that a dike associated with a volcanic event at  $(x, y)$  will extend a distance  $d$  toward the proposed repository

$L_{max}$  is the maximum length of a dike

$f(\mathbf{f}|\mathbf{q}_S)$  is the density function for dike azimuth

$f_1|x,y,d$  and  $f_2|x,y,d$  define the range of azimuths over which a dike extending  $d$  from a volcanic event at  $(x, y)$  will intersect the footprint of the proposed repository.

These parameters are illustrated in Figure 12. The integration over dike length in Equation 5 is also computed by summation.

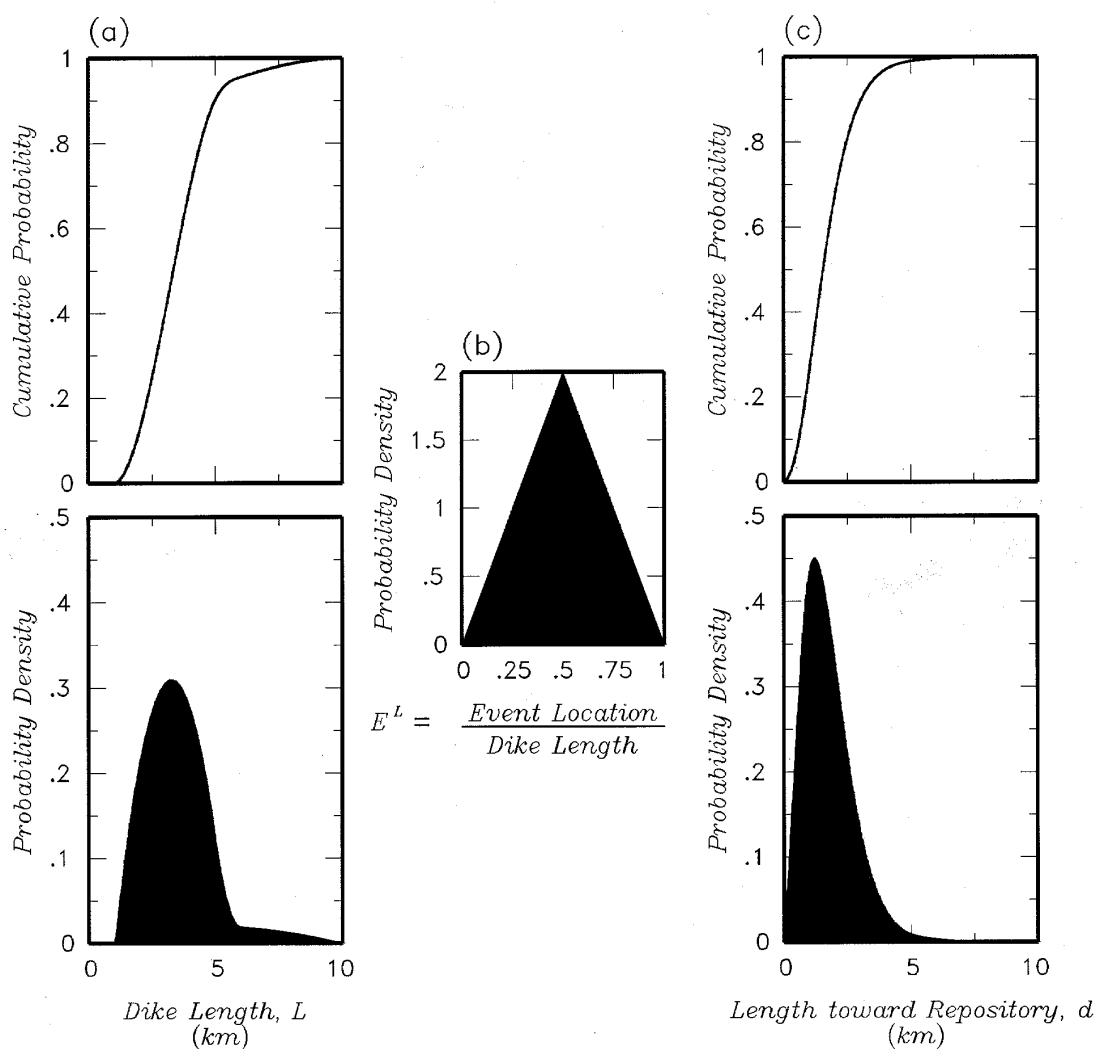


NA - For Illustration Purposes Only

NOTE: Parameters are defined in text preceding this figure, except  $L$  is the length of the dike,  $L^I$  and  $\phi$  are the length and azimuth, respectively for that portion of an intersecting dike within the proposed repository footprint, and  $L_m^I$  and  $\phi_n$  are specific bins of intersection length and azimuth.

Figure 12. Definition of Parameters Used to Compute the Probability of Intersection of the Proposed Repository Footprint by a Volcanic Event

The density function  $f(d|q_s)$  is computed by convolving the distribution for the total length of the dike,  $f(L|q_s)$ , with a distribution for the normalized location of the dike relative to the volcanic event,  $f(E^L|q_s)$ . Figure 13 illustrates the process using example distributions defined by one of the PVHA expert panel members. Part (a) of Figure 13 shows the probability distribution for the total length of the dike associated with a volcanic event,  $f(L|q_s)$ . Typically these were defined by the PVHA experts to be skewed distributions with long upper tails. Part (b) shows a distribution for the normalized location of the point event [point (x,y)] relative to the total length of the dike,  $f(E^L|q_s)$ . These were defined as symmetric distributions over the range of 0 to 1, typically with higher probability for locations at the midpoint [the dike centered on point (x,y)] than at the ends [the dike extending for its full length in one direction away from point (x,y)]. Part (c) shows the resulting probability and cumulative probability distributions for distance from the proposed repository to the end of the dike ( $d = E^L \times L$ ) obtained by convolving the distributions from (a) and (b).



NA - For Illustration Purposes Only

Figure 13. Example Distributions for Dike Length,  $L$ , (part a); Normalized Location of the Point Volcanic Event Relative to the Total Length of the Dike,  $E^L$ , (part b); and the Resulting Distribution for Distance from the Point Volcanic Event to the End of the Dike,  $d$  (part c)

Using these definitions, the summation form of Equation 5 becomes:

$$P^I(x_i, y_j, \mathbf{q}_S) = \sum_{L_p=0}^{L_p=L_{\max}} P(L_p | \mathbf{q}_S) \sum_{E_o^L=0}^{E_o^L=1} P(E_o^L | \mathbf{q}_S) \sum_{\mathbf{f}_n=\mathbf{f}_1 | x_i, y_j, E_o^L \times L_p}^{\mathbf{f}_n=\mathbf{f}_2 | x_i, y_j, E_o^L \times L_p} P(\mathbf{f}_n | \mathbf{q}_S) \quad (\text{Eq. 6})$$

where:

$P(L_p | \mathbf{q}_S)$  is a discrete probability mass function for dike length

$P(E_o^L | \mathbf{q}_S)$  is a discrete probability mass function for the relative location of the dike on the volcanic event

$P(\mathbf{f}_n | \mathbf{q}_S)$  is a discrete probability mass function for dike azimuth

$\mathbf{f}_1 | x_i, y_j, E_o^L \times L_p$  and  $\mathbf{f}_2 | x_i, y_j, E_o^L \times L_p$  again define the range of azimuths over which a dike extending  $d = E_o^L \times L_p$  from a volcanic event at  $(x, y)$  will intersect the proposed repository footprint.

The three probability mass functions are obtained by discretizing the continuous probability density functions developed for  $L$ ,  $E^L$ , and  $\mathbf{f}$  by the PVHA experts.

As the summation in Equation 6 is performed, it can be disaggregated into bins defined by azimuth increments,  $\mathbf{f}_n$ , and intersection length increments,  $L_m^I$ , where  $L^I$  is the length of penetration of a dike into the proposed repository (see Figure 12). As a result, Equation 6 can be rewritten as:

$$P^I(x_i, y_j, \mathbf{q}_S) = \sum_m \sum_n P^I(L_m^I, \mathbf{f}_n | x_i, y_j, \mathbf{q}_S) \quad (\text{Eq. 7})$$

The quantity  $P^I(L_m^I, \mathbf{f}_n | x_i, y_j, \mathbf{q}_S)$  is the probability that a dike associated with a volcanic event at location  $(x_i, y_j)$  will intersect the proposed repository with length  $L_m^I$  and azimuth  $\mathbf{f}_n$ , and is given by:

$$P^I(L_m^I, \mathbf{f}_n | x_i, y_j, \mathbf{q}_S) = \sum_{L_p=0}^{L_p=L_{\max}} P(L_p | \mathbf{q}_S) \sum_{E_o^L=0}^{E_o^L=1} P(E_o^L | \mathbf{q}_S) \cdot \mathbf{d}(L^I = L_m^I) \cdot P(\mathbf{f}_n | \mathbf{q}_S) \quad (\text{Eq. 8})$$

where  $\mathbf{d}(L^I = L_m^I) = 1$  for those combinations of  $L_p$ ,  $E_o^L$ , and  $\mathbf{f}_n$  that result in  $L^I = L_m^I$  for a volcanic event at  $(x, y)$ , and  $\mathbf{d}(L^I = L_m^I) = 0$  otherwise.

Multiplying Equation 8 by the frequency of volcanic events at  $(x_i, y_j)$  and summing over all locations yields the frequency of occurrence for intersections of the proposed repository of length  $L_m^I$  and azimuth  $f_n$ :

$$\mathbf{n}^I(t, L_m^I, \mathbf{f}_n | \mathbf{q}_S) = \sum_i \sum_j \mathbf{I}(x_i, y_j, t | \mathbf{q}_S) \cdot P^I(L_m^I, \mathbf{f}_n | x_i, y_j, \mathbf{q}_S) \quad (\text{Eq. 9})$$

Because the summation of  $\mathbf{n}^I(t, L_m^I, \mathbf{f}_n | \mathbf{q}_S)$  over the  $m \times n$   $L^I$  and  $\mathbf{f}$  intervals equals  $\mathbf{n}^I(t | \mathbf{q}_S)$   $\left[ \mathbf{n}^I(t | \mathbf{q}_S) = \sum_m \sum_n \mathbf{n}^I(t, L_m^I, \mathbf{f}_n | \mathbf{q}_S) \right]$ , the ratio  $\mathbf{n}^I(t, L_m^I, \mathbf{f}_n | \mathbf{q}_S) / \mathbf{n}^I(t | \mathbf{q}_S)$  defines the relative frequency of intersection events with length  $L_m^I$  and azimuth  $\mathbf{f}_n$ .

Equation 9 can be recast into the form:

$$\mathbf{n}^I(t, L_m^I, \mathbf{f}_n | \mathbf{q}_S) = \sum_i \sum_j \left[ \mathbf{I}(x_i, y_j, t | \mathbf{q}_S) \cdot P^I(x_i, y_j, \mathbf{q}_S) \right] \left[ \frac{P^I(L_m^I, \mathbf{f}_n | x_i, y_j, \mathbf{q}_S)}{P^I(x_i, y_j, \mathbf{q}_S)} \right]$$

or, if we define :  $\mathbf{n}_{x_i, y_j}^I(t | \mathbf{q}_S) = \mathbf{I}(x_i, y_j, t | \mathbf{q}_S) \cdot P^I(x_i, y_j, \mathbf{q}_S)$  (Eq. 10)

$$\mathbf{n}^I(t, L_m^I, \mathbf{f}_n | \mathbf{q}_S) = \sum_i \sum_j \left[ \mathbf{n}_{x_i, y_j}^I(t | \mathbf{q}_S) \right] \left[ \frac{P^I(L_m^I, \mathbf{f}_n | x_i, y_j, \mathbf{q}_S)}{P^I(x_i, y_j, \mathbf{q}_S)} \right]$$

The first term in brackets defines the contribution to the frequency of intersection from volcanic events occurring at point  $(x, y)$ ,  $\mathbf{n}_{x_i, y_j}^I(t | \mathbf{q}_S)$ . The second term in brackets defines the joint distribution for intersection length and azimuth from volcanic events at point  $(x, y)$  conditional on intersection occurring.

The only parameters of  $\mathbf{q}_S$  that affect the second term are the specification of the dike length, dike location on the volcanic event, and dike azimuth distributions. The PVHA experts specified these distributions to be independent of the distributions that characterized the spatial density and frequency of volcanic events. Thus  $\Theta$  can be broken into two independent sets:  $\Theta^D$  and  $\Theta^E$ . Parameters  $\Theta^D$  are those that define the distributions for total length, location relative to the point volcanic event, and azimuth of the dike associated with the volcanic event [the parameters used in the computation of the conditional probability  $P^I(\cdot|x,y)$ ]. These are defined by the first two levels of the logic tree shown on Figure 11a. Parameters  $\Theta^E$  are those that define the distribution for volcanic event frequency,  $I(x,y,t)$ . These are defined by all of the remaining levels of the logic trees shown on Figures 11a and 11b. Therefore, the expected or mean value of  $\mathbf{n}^I(t, L_m^I, \mathbf{f}_n | \mathbf{q}_S)$  (Equation 4) can be written as:

$$\mathbb{E}[\mathbf{n}^I(t, L_m^I, \mathbf{f}_n | \Theta)] = \sum_{\Theta^D} P(\Theta^D = \mathbf{q}_{S_D}^D) \left\{ \sum_i \sum_j \left[ \frac{P^I(L_m^I, \mathbf{f}_n | x_i, y_j, \mathbf{q}_{S_D}^D)}{P^I(x_i, y_j, \mathbf{q}_{S_D}^D)} \right] \times \sum_{\Theta^E} P(\Theta^E = \mathbf{q}_{S_E}^E) \cdot I(x_i, y_j, t | \mathbf{q}_{S_E}^E) \times P^I(L_m^I, \mathbf{f}_n | x_i, y_j, \mathbf{q}_{S_D}^D) \right\}$$

$$\text{or, again using } \mathbf{n}_{x_i, y_j}^I(t | \mathbf{q}_S) = I(x_i, y_j, t | \mathbf{q}_S) \cdot P^I(x_i, y_j, \mathbf{q}_S) \quad (\text{Eq. 11})$$

$$\mathbb{E}[\mathbf{n}^I(t, L_m^I, \mathbf{f}_n | \Theta)] = \sum_{\Theta^D} P(\Theta^D = \mathbf{q}_{S_D}^D) \left\{ \sum_i \sum_j \left[ \frac{P^I(L_m^I, \mathbf{f}_n | x_i, y_j, \mathbf{q}_{S_D}^D)}{P^I(x_i, y_j, \mathbf{q}_{S_D}^D)} \right] \mathbb{E}[\mathbf{n}_{x_i, y_j}^I(t | \mathbf{q}_{S_D}^D)] \right\}$$

where  $\mathbb{E}[\mathbf{n}_{x_i, y_j}^I(t | \mathbf{q}_{S_D}^D)]$  is the expected value of  $\mathbf{n}_{x_i, y_j}^I(t)$  conditional on the set of dike parameters  $\mathbf{q}_{S_D}^D$ . The form of Equation 11 greatly improves the efficiency of the calculation because the terms involving the conditional probability of intersection need to be computed only once for each dike parameter set,  $\mathbf{q}_{S_D}^D$ , rather than for every combination of the parameters  $\mathbf{q}_{S_E}^E$  that define the distribution for volcanic event frequency.

### 6.5.1.3 Conditional Distribution for the Number of Eruptive Centers

This section develops the mathematical formulation for assessing the conditional distribution for the number of eruptive centers within the footprint of the proposed repository. The development is based on the concept that eruptive centers will occur at uncertain locations along the length of the dike associated with a volcanic event. The length of intersection within the proposed repository footprint compared to the total length of the dike, the number of eruptive centers per volcanic event, and the spatial distribution of eruptive centers along the length of the dike provide the bases for assessing the likelihood that one or more eruptive centers will occur within the proposed repository footprint. The total length of the dike and the length of intersection within the proposed repository are computed as part of the formulation presented in Section 6.5.1.2 and are completely defined by the PVHA experts' interpretations. The number of

eruptive centers per volcanic event and the spatial distribution of eruptive centers along the length of a dike were not defined as part of the PVHA expert elicitation. However, with the limited set of assumptions (Section 5), these can be derived from the experts' interpretations. There are alternative ways that these assumptions can be applied. In keeping with the concept of uncertainty characterization employed in the PVHA, these alternatives were used to develop alternative assessments of the conditional distribution for the number of eruptive centers within the proposed repository footprint. These are then combined using relative weights assigned to each to produce a composite assessment.

The assumptions listed in Section 5.1 and 5.2 provide the basis for using the mapped volcanoes in the YMR to derive assessments of the number of eruptive centers per volcanic event from the PVHA experts' interpretations. Two alternative approaches are used. The first approach uses the number of mapped volcanoes to derive empirical distributions for the number of eruptive centers per volcanic event independent of any assessment of the total length of the dike system associated with the volcanic event. In this approach, volcanic events can have from 1 to 5 eruptive centers, the range in number of individual volcanoes associated with a single volcanic event by the PVHA experts using the YMR data. The second approach uses the number and location of the mapped volcanoes to derive an assessment of the spacing between eruptive centers. The spacing between eruptive centers combined with the total length of the dike system associated with a volcanic event determines the number of eruptive centers for a given volcanic event. Attachment III presents the assessments of the distributions for number of eruptive centers per volcanic event and the spacing between eruptive centers. The use of these results is described in greater detail in Section 6.5.2.2.

The calculation of the likelihood of one or more eruptive centers occurring within the proposed repository requires specification of the spatial distribution of eruptive centers along the length of the dike system. The minimum information model for the random location of a point on a line is the uniform distribution between the limits of the line length. The assumption listed in Section 5.3 applies the uniform distribution to eruptive center location. Two alternative applications of the uniform distribution were used to capture the range of possible behaviors when multiple eruptive centers occur along the length of the dike system for a single volcanic event.

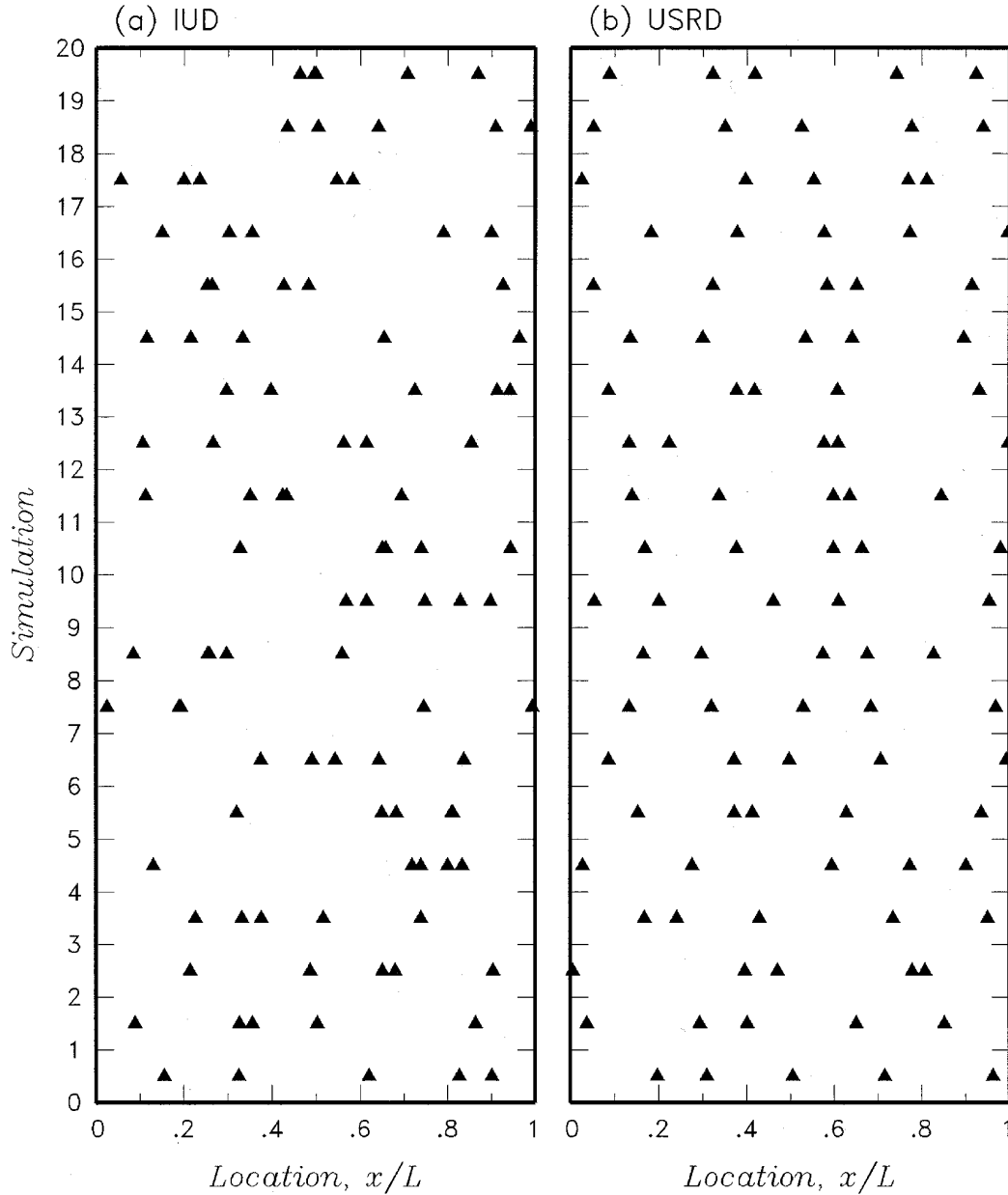
The first approach specifies the location of each eruptive center independently of the others. Over many volcanic events, this approach, on average, will produce eruptive centers spaced out over the total length of the volcanic events. However, for an individual event, a range of behaviors may occur. Part (a) of Figure 14 shows the results of 20 simulations using this approach, designated the independent, uniformly distributed (*IUD*) approach. Some of the simulations produce relatively uniform spaced eruptive centers and some produce highly clustered eruptive centers.

Dense clustering of multiple eruptive centers can be prevented by imposing a minimum spacing between the eruptive centers. Taking this approach to the limit would result in uniform spacing of eruptive centers along the length of the dike. Part (b) of Figure 14 shows the results of 20 simulations using a model in which the length of the dike is divided into equal length segments, one segment for each eruptive center. Applying the assumption listed in Section 5.3, each eruptive center is randomly located within its segment following a uniform distribution.

This approach, designated the uniformly spaced, randomly distributed (*USRD*) approach, produces a broader spread between the eruptive centers in each simulation compared with the *IUD* approach, while still allowing for clustering of two eruptive centers along the length of the dike. Some clustering is expected to occur on occasion, given the close spacing between Little Cones SW and Little Cones NE.

Using these two approaches for the spatial distribution of eruptive centers, the formulation from Section 6.5.1.2 is expanded to define the distribution for the number of eruptive centers that occur within the proposed repository. In the previous section, the contributions to the frequency of intersection from each location  $(x,y)$  in the spatial grid around the proposed repository,  $\mathbf{n}_{x,y}^I(t|\mathbf{q}_S)$ , were divided into probabilities for intersection with specific lengths and azimuths,  $\mathbf{n}_{x,y}^I(t, L_m^I, \mathbf{f}_n | \mathbf{q}_S)$ .

This calculation involved looping over the possible dike lengths and azimuths. During this calculation, the spatial models described above can be used to compute the number of volcanic events that produce 0, 1, 2, 3, etc., eruptive centers in the proposed repository. As a result,  $\mathbf{n}_{x,y}^I(t, L_m^I, \mathbf{f}_n | \mathbf{q}_S)$  is divided into the frequency of intersection from volcanic events at point  $(x,y)$  that produce specific numbers of eruptive centers within the proposed repository,  $\mathbf{n}_{x,y}^I(t, L_m^I, \mathbf{f}_n, r^{EC} | \mathbf{q}_S)$ . Summing these values over all locations  $(x,y)$  gives the frequency of intersection with a specific number of eruptive centers in the proposed repository,  $\mathbf{n}^I(t, L_m^I, \mathbf{f}_n, r^{EC} | \mathbf{q}_S)$ . Dividing this frequency by the total frequency of intersection,  $\mathbf{n}^I(t | \mathbf{q}_S)$ , gives the conditional probability that an intersecting event will produce a specific number of eruptive centers in the proposed repository.



N/A - For Illustration Purposes Only

NOTE: The solid triangles show the locations of five eruptive centers for each simulation.

Figure 14. Example Simulations of the Distribution of Eruptive Centers Along the Length of a Dike for: (a) the Independent, Uniformly Distributed Spatial Distribution and (b) the Uniformly Spaced, Randomly Distributed Spatial Distribution

The disaggregation of  $\mathbf{n}_{x_p, y_j}^I(t, L_m^I, \mathbf{f}_n | \mathbf{q}_S)$  into  $\mathbf{n}_{x_p, y_j}^I(t, L_m^I, \mathbf{f}_n, r^{EC} | \mathbf{q}_S)$  for  $r^{EC} = 0, 1, 2, \dots$  eruptive centers is accomplished by computing the conditional distribution for  $r^{EC}$ , given the total length of the dike,  $L$ , the length of intersection within the proposed repository footprint,  $L^I$ , the number

of eruptive centers associated with the volcanic event,  $n^{EC}$ , and the spatial distribution for the location of eruptive centers. Note that the assumption listed in Section 5.2 results in  $n^{EC} \geq 1$ .

*Independent, Uniformly Distributed (IUD) Spatial Distribution*

In this approach, the location of each eruptive center is uniformly distributed along the total length of the dike and the location of each eruptive center is independent of all of the others. Thus, the occurrence of each eruptive center within the footprint of the proposed repository is an independent Bernoulli trial with probability of success,  $p$ , equal to the length of intersecting dike within the proposed repository,  $L^I$ , divided by the total length of the dike,  $L$ . Under these conditions, the conditional probability distribution for the number of eruptive centers within the proposed repository footprint,  $r^{EC}$ , given  $n^{EC}$  eruptive centers associated with the volcanic event, is given by the binomial distribution:

$$P_{IUD}(r^{EC} | n^{EC}, L, L^I) = \binom{n^{EC}}{r^{EC}} \left(\frac{L^I}{L}\right)^{r^{EC}} \left(1 - \frac{L^I}{L}\right)^{n^{EC} - r^{EC}} \quad (\text{Eq. 12})$$

where  $\binom{n^{EC}}{r^{EC}}$  is the binomial coefficient and the subscript *IUD* refers to independent, uniformly distributed eruptive centers.

*Uniformly Spaced, Randomly Distributed (USRD) Spatial Distribution*

The alternative approach for the spatial distribution of eruptive centers is that they are spaced more or less equal-distant along the length of the dike. If  $n^{EC}$  eruptive centers are generated along the length of the dike, then each eruptive center is located within a segment of length  $L^s = L/n^{EC}$ . If the location of the eruptive center within each segment is defined by a uniform distribution, the probability that an eruptive center associated with segment  $q$  will occur within the proposed repository footprint is equal to the length of segment  $q$  within the boundary of the proposed repository,  $L^s_q$ , divided by the total length of the segment,  $L^s$ . There can be at most two segments of a dike that have partial penetration of the proposed repository footprint in one volcanic event (there may be more segments that lie entirely within the proposed repository footprint). If only the  $q^{\text{th}}$  segment penetrates into the proposed repository footprint, then the probabilities for zero or one eruptive center within the proposed repository are given by:

$$P_{USRD}(r^{EC} = 0 | n^{EC}, L, L^I) = 1 - \frac{L^s_q}{L^s} \quad (\text{Eq. 13})$$

$$P_{USRD}(r^{EC} = 1 | n^{EC}, L, L^I) = \frac{L^s_q}{L^s}$$

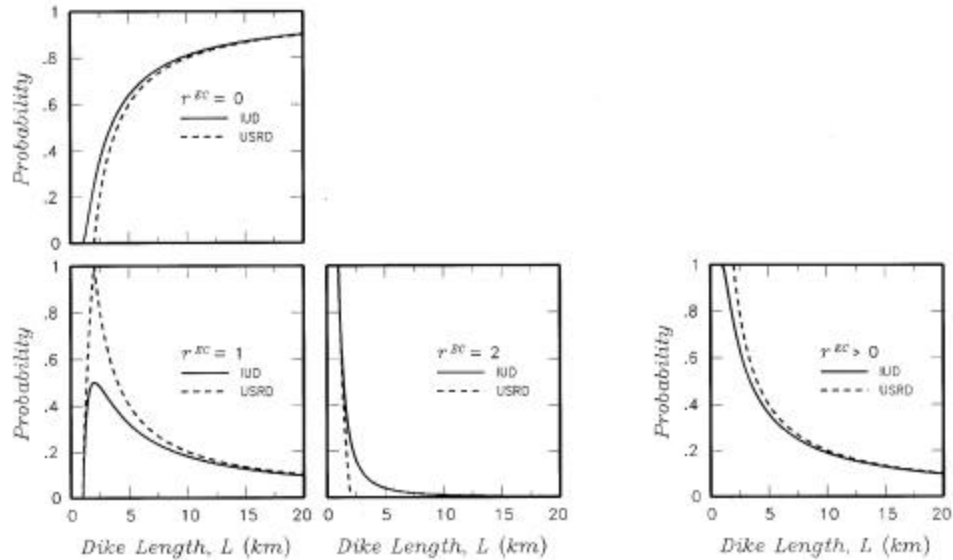
If the  $q^{\text{th}}$  and  $(q+1)^{\text{th}}$  segments penetrate into the proposed repository footprint, then the probabilities for zero, one, or two eruptive centers within the proposed repository are given by:

$$\begin{aligned}
 P_{USR D}(r^{EC} = 0 | n^{EC}, L, L^I) &= \left(1 - \frac{L_q^{sl}}{L_q^s}\right) \left(1 - \frac{L_{q+1}^{sl}}{L_{q+1}^s}\right) \\
 P_{USR D}(r^{EC} = 1 | n^{EC}, L, L^I) &= \left(\frac{L_q^{sl}}{L_q^s}\right) \left(1 - \frac{L_{q+1}^{sl}}{L_{q+1}^s}\right) + \left(1 - \frac{L_q^{sl}}{L_q^s}\right) \left(\frac{L_{q+1}^{sl}}{L_{q+1}^s}\right) \\
 P_{USR D}(r^{EC} = 2 | n^{EC}, L, L^I) &= \left(\frac{L_q^{sl}}{L_q^s}\right) \left(\frac{L_{q+1}^{sl}}{L_{q+1}^s}\right)
 \end{aligned} \tag{Eq. 14}$$

If one or more segments lie entirely within the proposed repository footprint, then the probability of an eruptive center occurring within the proposed repository is unity for these segments. In such a case, the value of  $r^{EC}$  in Equations 13 and 14 is increased by the number of wholly contained segments. For example, if one segment lies completely within the proposed repository and one spans the boundary of the proposed repository, then Equation 13 becomes:

$$\begin{aligned}
 P_{USR D}(r^{EC} = 0 | n^{EC}, L, L^I) &= 0 \\
 P_{USR D}(r^{EC} = 1 | n^{EC}, L, L^I) &= 1 - \frac{L_q^{sl}}{L_q^s} \\
 P_{USR D}(r^{EC} = 2 | n^{EC}, L, L^I) &= \frac{L_q^{sl}}{L_q^s}
 \end{aligned} \tag{Eq. 15}$$

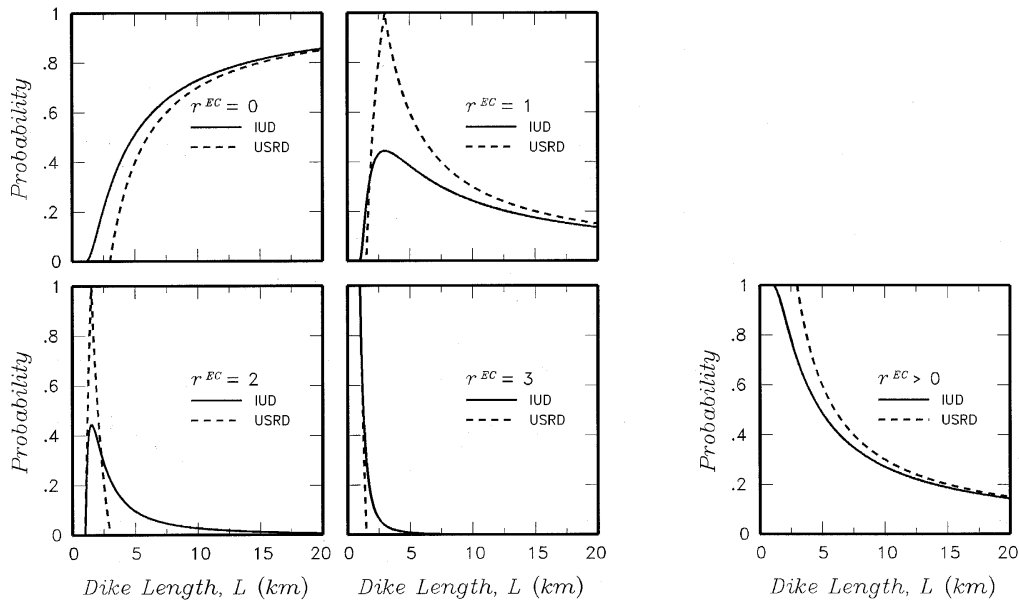
Figures 15a and 15b compare the probabilities obtained from these two approaches to the spatial distribution of eruptive centers as a function of dike length,  $L$ , for  $L^I = 1$  kilometer and  $n^{EC} = 2$  (Figure 15a) and for  $L^I = 1$  kilometer and  $n^{EC} = 3$  (Figure 15b). The figures show the computed probabilities for  $r^{EC}$  equal to from 0 to  $n^{EC}$ , and the probability for at least one eruptive center within the proposed repository  $P(r^{EC} > 0)$ . Note that  $P(r^{EC} > 0)$  is equal to the sum of the probabilities for  $r^{EC}$  equal to from 1 to  $n^{EC}$ , and is equal to  $1 - P(r^{EC} = 0)$ . For all total lengths, the *USR D* model produces a higher probability for  $r^{EC} > 0$ , with the difference between the two models diminishing as the dike length increases. Except for short dike lengths, use of the *IUD* spatial distribution produces a higher probability of multiple eruptive centers within the proposed repository footprint.



N/A - For Illustration Purposes Only

NOTE: Results are shown for the independent, uniformly distributed (IUD) (Equation 12) and the uniformly spaced, randomly distributed (USRD) (Equation 13) spatial distributions.

Figure 15a. Probability for the Number of Eruptive Centers Within the Proposed Repository Footprint,  $r^{EC}$ , as a Function of Dike Length,  $L$ , for the Length of Intersection,  $L^I = 1$  Kilometer and the Number of Eruptive Centers Associated with the Volcanic Event,  $n^{EC} = 2$



N/A - For Illustration Purposes Only

NOTE: Results are shown for the independent, uniformly distributed (IUD) (Equation 12) and the uniformly spaced, randomly distributed (USRD) (Equation 13) spatial distributions.

Figure 15b. Probability for the Number of Eruptive Centers Within the Proposed Repository Footprint,  $r^{EC}$ , as a Function of Dike Length,  $L$ , for the Length of Intersection,  $L^I = 1$  Kilometer and the Number of Eruptive Centers Associated with the Volcanic Event,  $n^{EC} = 3$

### Conditional Distribution

In evaluating the consequences of an intersection of the proposed repository footprint by the dike system associated with a volcanic event, it is more informative to define  $P(r^{EC})$  conditional on the length of intersection,  $L_m^I$ . Equation 8 defines the joint probability of intersection length and azimuth for a volcanic event at point  $(x_i, y_j)$ ,  $P^I(L_m^I, \mathbf{f}_n | x_i, y_j, \mathbf{q}_{S_D}^D)$ . As indicated in developing Equation 11, the only parameters that affect the calculation of the conditional probability of intersection are  $\mathbf{q}_{S_D}^D$ . Thus  $P^I(L_m^I, \mathbf{f}_n | x_i, y_j, \mathbf{q}_{S_D}^D)$  in Equation 8 can be rewritten as  $P^I(L_m^I, \mathbf{f}_n | x_i, y_j, \mathbf{q}_{S_D}^D)$ . In addition, the probability for the number of eruptive centers within the proposed repository, Equations 12, 13, and 14, is dependent on the number of eruptive centers per volcanic event,  $n^{EC}$ . Attachment III develops distributions for  $n^{EC}$ ,  $P(n^{EC} = \mathbf{h} | L_p, \mathbf{q}_{S_D}^D)$ , which may be conditional on the total length of the dike,  $L_p$ . The parameter set  $\mathbf{q}_{S_D}^D$  is expanded to include any alternatives for assessing  $P(n^{EC} = \mathbf{h})$ . Using these definitions, the joint probability of  $r^{EC}$  eruptive centers in the proposed repository for a volcanic event at  $(x, y)$  producing a length of intersection of  $L_m^I$  at an azimuth of  $\mathbf{f}_n$  is given by:

$$P^I(L_m^I, \mathbf{f}_n, r^{EC} | x_i, y_j, \mathbf{q}_{S_D}^D) = \sum_{L_p=0}^{L_p=L_{\max}^D} P(L_p | \mathbf{q}_{S_D}^D) \sum_{E_o^L=0}^{E_o^L=1} P(E_o^L | \mathbf{q}_{S_D}^D) \cdot \mathbf{d}(L^I = L_m^I) \cdot P(\mathbf{f}_n | \mathbf{q}_{S_D}^D) \times \sum_{h=1}^{h=n_{\max}^{EC}} P(n^{EC} = \mathbf{h} | L_p, \mathbf{q}_{S_D}^D) P(r^{EC} | L_p, L_m^I, n^{EC} = \mathbf{h}) \quad (\text{Eq. 16})$$

with  $P(r^{EC} | L_p, L_m^I, n^{EC} = \mathbf{h})$  given by either Equation 12 or Equations 13 and 14.

Multiplying Equation 16 by  $I(x_i, y_j, t | \mathbf{q}_{S_D}^D)$ , the frequency of volcanic events at  $(x_i, y_j)$ , and summing over all locations yields the frequency of occurrence for intersections of the proposed repository of length  $L_m^I$  and azimuth  $\mathbf{f}_n$  with  $r^{EC}$  eruptive centers within the repository:

$$\mathbf{n}^I(t, L_m^I, \mathbf{f}_n, r^{EC} | \mathbf{q}_S) = \sum_i \sum_j I(x_i, y_j, t | \mathbf{q}_{S_E}^E) \cdot P^I(L_m^I, \mathbf{f}_n, r^{EC} | x_i, y_j, \mathbf{q}_{S_D}^D) \quad (\text{Eq. 17})$$

Because the summation of  $\mathbf{n}^I(t, L_m^I, \mathbf{f}_n, r^{EC} | \mathbf{q}_S)$  over  $r^{EC} = 0$  to  $r^{EC} = n_{\max}^{EC}$  equals  $\mathbf{n}^I(t, L_m^I, \mathbf{f}_n | \mathbf{q}_S)$ , the ratio  $\mathbf{n}^I(t, L_m^I, \mathbf{f}_n, r^{EC} | \mathbf{q}_S) / \mathbf{n}^I(t, L_m^I, \mathbf{f}_n | \mathbf{q}_S)$  defines the relative frequency of intersection events with length  $L_m^I$  and azimuth  $\mathbf{f}_n$ , that produce  $r^{EC}$  eruptive centers within the proposed repository.

In the same manner that Equation 9 was recast as Equation 10, Equation 17 can be recast into the form:

$$\mathbf{n}^I(t, L_m^I, \mathbf{f}_n, r^{EC} | \mathbf{q}_S) = \sum_i \sum_j \mathbf{n}_{x_i, y_j}^I(t | \mathbf{q}_{S_E}^E, \mathbf{q}_{S_D}^D) \cdot \left[ \frac{P^I(L_m^I, \mathbf{f}_n, r^{EC} | x_i, y_j, \mathbf{q}_{S_D}^D)}{P^I(x_i, y_j, \mathbf{q}_{S_D}^D)} \right] \quad (\text{Eq. 18})$$

where the substitution  $\mathbf{n}_{x_i, y_j}^I(t | \mathbf{q}_{S_E}^E, \mathbf{q}_{S_D}^D) = \mathbf{I}(x_i, y_j, t | \mathbf{q}_{S_E}^E) \cdot P^I(x_i, y_j, \mathbf{q}_{S_D}^D)$  has been made. Equation 18 may be adapted in a manner similar to Equation 11 to improve the efficiency of the computation of the expected value of  $\mathbf{n}^I(t, L_m^I, \mathbf{f}_n, r^{EC} | \mathbf{q}_S)$ , producing:

$$E[\mathbf{n}^I(t, L_m^I, \mathbf{f}_n, r^{EC} | \Theta)] = \sum_{\Theta^D} P(\Theta^D = \mathbf{q}_{S_D}^D) \cdot \left\{ \sum_i \sum_j \left[ \frac{P^I(L_m^I, \mathbf{f}_n, r^{EC} | x_i, y_j, \mathbf{q}_{S_D}^D)}{P^I(x_i, y_j, \mathbf{q}_{S_D}^D)} \right] E[\mathbf{n}_{x_i, y_j}^I(t | \mathbf{q}_{S_D}^D)] \right\} \quad (\text{Eq. 19})$$

## 6.5.2 Implementation

This section describes the implementation of the formulation presented in Section 6.5.1. Equations 3 and 5 provide the relationships used to compute the frequency of intersection,  $\mathbf{n}^I(t)$ . Equations 10, 11, 18, and 19 provide the relationships used to compute the frequency of intersecting volcanic events that produce an intersection length of  $L_m^I$ , at an azimuth of  $\mathbf{f}_n$ , with  $r^{EC}$  eruptive centers occurring within the proposed repository footprint.

### 6.5.2.1 Frequency of Intersection of the Proposed Repository Footprint by a Dike

The computational scheme used in CRWMS M&O (1996 [100116]) and repeated in this report consists of the steps shown on Figure 1 (repeated for each expert's interpretation).

**Step 1:** Discrete cumulative distributions for dike length are developed from the experts' assessments using software routines FITCD V1.0 (STN: 10262-1.0-00 [148532]) or SFCD V1.0 (STN: 10275-1.0-00 [148533]) [e.g., part (a) of Figure 13]. These are then convolved with the event location of the dike on the volcanic event [e.g. part (b) of Figure 13] to produce distributions for volcanic event length [e.g. part (c) of Figure 13] using software routine DCPELD V1.0 (STN: 10258-1.0-00 [148534]).

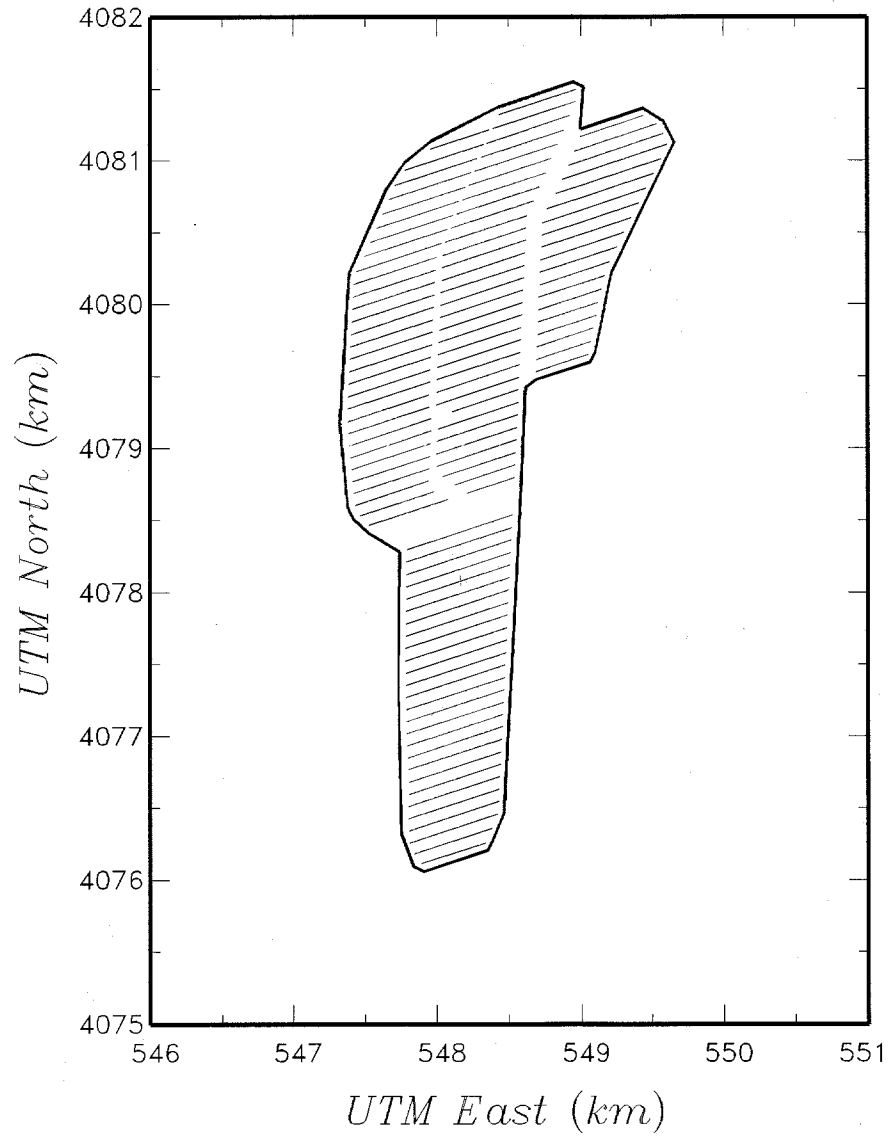
**Step 2:** The conditional probability of intersection,  $P^I(x_i, y_j, \mathbf{q}_{S_D}^D)$ , is computed for each set of parameters  $\mathbf{q}_{S_D}^D$  (defined by a unique event length distribution from step 1 and a unique azimuth distribution) using software routine CPDI V1.0 (STN: 10257-1.0-00 [148535]).

**Step 3:** The rate of intersection,  $\mathbf{n}^I(t)$ , is computed using software routines specific to the type of source [software routines UZVH V1.0 (STN: 10277-1.0-00 [148536]) and UZVPVH V1.0 (STN: 10279-1.0-00 [148537]) for source zones; routines FKVH V1.0 (STN: 10265-1.0-00 [148567]), FKVPVH V1.0 (STN: 10267-1.0-00 [148538]), and ZBCKVH V1.0 (STN: 10283-1.0-00 [148539]) for kernel density sources; and routines PFGVH V1.0 (STN: 10273-1.0-00 [144542]) and FPFVH V1.0 (STN: 10269-1.0-00 [148543]) for 2-D Gaussian field sources]. The characterization of individual volcanic sources is defined by a 12-parameter subset of  $\mathbf{q}_{S_E}^E$ . The distribution for these parameters depends upon the alternative source definitions, temporal models, and time periods of interest. To denote this breakdown of  $\mathbf{q}_{S_E}^E$ , the parameter set  $\mathbf{q}_{S_{ASM}}^E$  represents the alternative source models (including temporal models) and parameter set

$\mathbf{q}_{S_{ISP}}^E | \mathbf{q}_{S_{ASM}}^E$  represents the individual source parameters, which are conditional on the chosen source and temporal models  $\mathbf{q}_{S_{ASM}}^E$ . The software routines used to compute the hazard from an individual source contain a set of 12 nested DO loops to enumerate all of the alternative versions of  $\mathbf{q}_{S_{ISP}}^E | \mathbf{q}_{S_{ASM}}^E$  (see Figure 11b). Given a set of parameters, the frequency of volcanic events,  $\mathbf{l}_a(x_i, y_j, t | \mathbf{q}_{S_{ISP}}^E)$ , is computed for a specific source,  $\mathbf{a}$ , using the formulation appropriate for the source type. This is multiplied by the conditional probability of intersection,  $P^I(x_i, y_j, \mathbf{q}_{S_D}^D)$ , from the output of routine CPDI V1.0 and summed over all points within the source to obtain the frequency of intersection from volcanic events associated with source  $\mathbf{a}$ . The software routines store the mean frequency of intersection and the distribution in the frequency of intersection (computed over the distributions for  $\mathbf{q}_{S_{ISP}}^E | \mathbf{q}_{S_{ASM}}^E$  in output files for use in the final step of the computations. Separate output files are created for all of the alternative sets of source model parameters,  $\mathbf{q}_{S_{ASM}}^E$ , and for the alternative parameters that describe the associated dikes,  $\mathbf{q}_{S_D}^D$ .

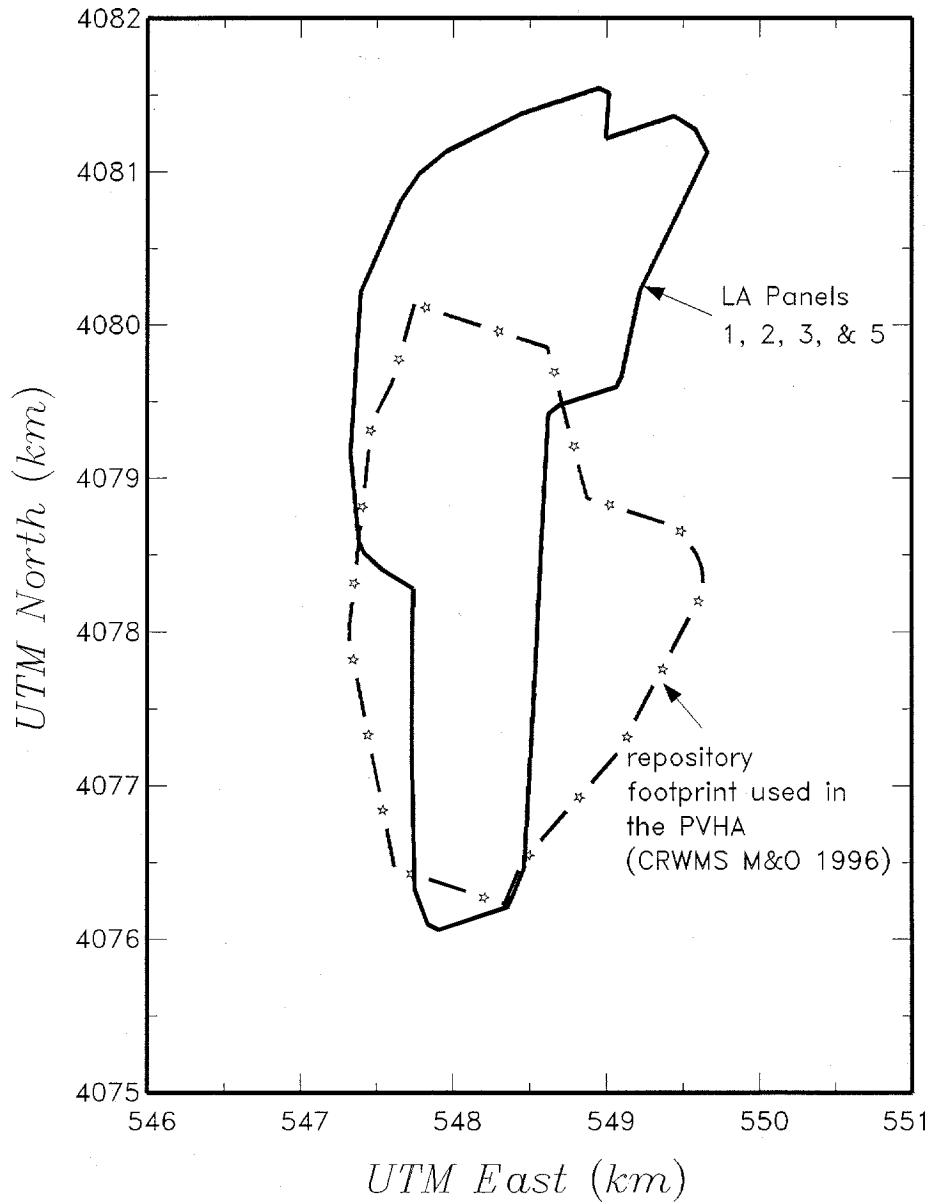
**Step 4:** The results from step 3 are combined over the distributions for  $\mathbf{q}_{S_{ASM}}^E$  and  $\mathbf{q}_{S_D}^D$  (see Figures 11a and 11b) to compute the full distribution for frequency of intersection specified by an individual PVHA expert's interpretations. The results for each expert are then combined to obtain the composite distribution. These calculations are performed using software routine VHTREE V1.0 (STN: 10282-1.0-00 [148544]). Complete enumeration of all of the alternative parameter sets  $\mathbf{q}_{S_{ASM}}^E$  is again achieved by a series of nested DO loops. The mean value and various percentiles of the distribution for frequency of intersection of the proposed repository footprint by a dike were computed from the discrete distribution for  $\mathbf{n}^I(t | \mathbf{q}_{S_D}^D, \mathbf{q}_{S_E}^E)$  as described above in Section 6.5.1.1. These are then combined using equal weights to produce a composite distribution for frequency of intersection.

The proposed LA repository footprint used for the calculations in this report is shown in Figure 16a. The calculations performed in the PVHA (CRWMS M&O 1996 [100116]) used the proposed repository footprint shown in Figure 16b. The LA repository design calls for a longer and narrower emplacement area compared to the design used at the time of the PVHA (Figure 16b). Attachment II presents the coordinates of the drifts in the proposed LA repository footprint and their transformation to UTM kilometers. The polygon used for calculations in this report was constructed to provide a clearance of approximately 55 m around the drift coordinates (see Figure 16a) to account for the effect of the size of eruptive centers in the calculations (see Attachment III). The polygon encompasses emplacement panels 1, 2, 3, and 5 of the current IED design (BSC 2003 [162289]) and was used to calculate the conditional distributions for intersection length, azimuth, and number of eruptive centers using the simulation approach developed in this report. This polygon was also used to calculate an updated mean and distribution for the frequency of intersection of the proposed LA repository footprint by a dike using the full enumeration approach employed in the PVHA (CRWMS M&O 1996 [100116]).



DTN: LA0303BY831811.001 [163985]

Figure 16a. Proposed License Application Emplacement Drifts and Footprint Polygon Encompassing Emplacement Panels 1, 2, 3, and 5



DTN: LA0303BY831811.001 [163985]

NOTE: PVHA reference in figure is CRWMS M&O (1996 [100116]).

Figure 16b. Location of Proposed License Application Repository Footprint Compared to Repository Footprint Used in the Probabilistic Volcanic Hazard Analysis

### 6.5.2.2 Distributions for Length, Azimuth, and Number of Eruptive Centers

The computations performed in CRWMS M&O (1996 [100116]) were made for all possible sets of  $\mathbf{q}_{S_D}^D$  and  $\mathbf{q}_{S_E}^E$  defined by the volcanic hazard characterization of each of the PVHA experts [full enumeration of the logic tree branches (CWRMS M&O 1996 [100116], Appendix E)]. However, the objective of this analysis is a disaggregation of the intersection frequency,  $\mathbf{n}^I(t|\mathbf{q}_{S_D}^D, \mathbf{q}_{S_E}^E)$ , into intersection frequencies with specific values of  $L_m^I$ ,  $\mathbf{f}_n$ , and  $r^{EC}$ . Repeating the calculation for the spatial disaggregation would require exhaustive computation and storage of the spatial disaggregation of the hazard,  $\mathbf{n}_{x,y}^I(t|\mathbf{q}_{S_E}^E, \mathbf{q}_{S_D}^D)$ , for all possible parameter sets  $\mathbf{q}_{S_E}^E$ . Therefore, a simulation approach was used to develop random sample parameter sets  $\mathbf{q}_{S_E}^E$  from the PVHA experts' logic trees to speed up the computation process. As discussed subsequently in the results (Section 6.5.3), the mean and distribution for the frequency of intersection of the proposed repository footprint by a dike computed by full enumeration and by simulation for each PVHA expert's interpretation and for the composite result generally agree within a few percent. The approach used to obtain the spatial disaggregation of the frequency of intersection consists of the following steps (see Figure 2).

**Step 1:** The conditional probability of intersection,  $P^I(x_i, y_j, \mathbf{q}_{S_D}^D)$ , was taken directly from the computation for the frequency of intersection discussed above. The files containing  $P^I(x_i, y_j, \mathbf{q}_{S_D}^D)$  for each set of parameters  $\mathbf{q}_{S_D}^D$  were created using routine CPDI V1.0 (STN: 10257-1.0-00 [148535]) using inputs processed through routines FITCD V1.0 (STN: 10262-1.0-00 [148532]), SFCD V1.0 (STN: 10275-1.0-00 [148533]), and DCPELD V1.0 (STN: 10258-1.0-00 [148534]).

**Step 2:** The second step in the calculation involved computation of the spatial disaggregation of frequency of intersection hazard for the individual sources specified by the alternative source parameter sets  $\mathbf{q}_{S_{ASM}}^E$  and for the alternative dike parameters  $\mathbf{q}_{S_D}^D$ . For the reasons discussed above, simulation is used to select random samples of the parameter subset  $\mathbf{q}_{S_{ISP}}^E | \mathbf{q}_{S_{ASM}}^E$  used to compute the frequency of intersection for an individual source type. The approach used to generate these parameter subsets is Latin hypercube sampling (McKay et al. 1979 [127905], pp. 243–245). The software routines used to compute the frequency of intersection replace the 12 nested DO loops with simulation of 50 parameter sets,  $\mathbf{q}_{sim_{ISP}}^E | \mathbf{q}_{S_{ASM}}^E$ ,  $sim_{ISP} = 1..50$ , using Latin hypercube sampling from the 12 independent, discrete parameter distributions that define  $\Theta_{ISP}^E | \mathbf{q}_{S_{ASM}}^E$ . Once a parameter subset is defined, the spatial distribution of  $I(x,y,t)$  for source  $\mathbf{a}$  is computed using the same algorithms employed for the PVHA calculation (CRWMS M&O 1996 [100116]). The disaggregated frequency of intersection,  $\mathbf{n}_{\mathbf{a},x_i,y_j}^I(t|\mathbf{q}_{sim_{ISP}}^E, \mathbf{q}_{S_{ASM}}^E, \mathbf{q}_{S_D}^D)$ , from each simulation for each source  $\mathbf{a}$  is output to a file along with the mean frequency of intersection for the source. Each simulated parameter set  $\mathbf{q}_{sim_{ISP}}^E | \mathbf{q}_{S_{ASM}}^E$  is an equally likely realization of the possible parameter sets from the joint distribution for  $\Theta_{ISP}^E | \mathbf{q}_{S_{ASM}}^E$ . Therefore, the mean frequency of intersection for source  $\mathbf{a}$ , given source model parameter set  $\mathbf{q}_{S_{ASM}}^E$  and dike parameters  $\mathbf{q}_{S_D}^D$ ,

$E[n_a^I(t|q_{S_{ASM}}^E, q_{S_D}^D)]$ , and its spatial disaggregation  $E[n_{a,x_i,y_j}^I(t|q_{S_{ASM}}^E, q_{S_D}^D)]$ , may be estimated by the average of the results from the 50 simulations.

$$E[n_a^I(t|q_{S_{ASM}}^E, q_{S_D}^D)] \sim \frac{1}{50} \sum_{sim_{ISP}=1}^{sim_{ISP}=50} n_a^I(t|q_{sim_{ISP}}^E, q_{S_{-ASM}}^E, q_{S_D}^D)$$

and (Eq. 20)

$$E[n_{a,x_i,y_j}^I(t|q_{S_{ASM}}^E, q_{S_D}^D)] \sim \frac{1}{50} \sum_{sim_{ISP}=1}^{sim_{ISP}=50} n_{a,x_i,y_j}^I(t|q_{sim_{ISP}}^E, q_{S_{-ASM}}^E, q_{S_D}^D)$$

The simulation software routines are designated UZVHLH V1.0 (STN: 10278-1.0-00 [1485454]), UZVPVHLH V1.0 (STN: 10280-1.0-00 [148547]), FKVHLH V1.0 (STN: 10266-1.0-00 [148546]), FKVPVHLH V1.0 (STN: 10268-1.0-00 [148551]), ZBCKVHLH V1.0 (STN: 10284-1.0-00 [148550]), PFGVHLH V1.0 (STN: 10274-1.0-00 [148552]), and FPGVHLH V1.0 (STN: 10270-1.0-00 [148553]). They use the same input files used to compute the frequency of intersection by full enumeration (Section 6.5.2.1).

**Step 3:** The third step in the calculation is computation of the distribution for the spatial disaggregation of the hazard for each the PVHA expert's interpretation. The full enumeration of the possible parameter sets  $q_{S_D}^D$  and  $q_{S_{ASM}}^E$  is again replaced by simulation of 50 equally likely parameter sets. The software routine VHTIELHS V1.0 (STN: 10281-1.0-00 [148554]) is used to perform the following operations for the interpretation developed by each of the PVHA experts.

Step 3a. First, all of the possible sets  $q_{S_D}^D, q_{S_{ASM}}^E$  in the joint distribution for  $\Theta^D$  and  $\Theta_{ASM}^E$  are enumerated. The joint probability of each set is computed from the PVHA expert's logic tree.

Step 3b. The mean frequency of intersection for each set of  $q_{S_D}^D, q_{S_{ASM}}^E$  and its spatial disaggregation are estimated from the sum of all the individual source results from Step 2, for those sources present in the parameter set  $q_{S_{ASM}}^E$ ,

$$E[n_a^I(t|q_{S_{ASM}}^E, q_{S_D}^D)] \sim \sum_{a|q_{S_{ASM}}^E} E[n_a^I(t|q_{S_{ASM}}^E, q_{S_D}^D)]$$

and (Eq. 21)

$$E[n_{x_i,y_j}^I(t|q_{S_{ASM}}^E, q_{S_D}^D)] \sim \sum_{a|q_{S_{ASM}}^E} E[n_{a,x_i,y_j}^I(t|q_{S_{ASM}}^E, q_{S_D}^D)]$$

Step 3c. The sets of  $\mathbf{q}_{S_D}^D, \mathbf{q}_{S_{ASM}}^E$  are then ranked in terms of increasing mean frequency of intersection,  $E[\mathbf{n}^I(t|\mathbf{q}_{S_{ASM}}^E, \mathbf{q}_{S_D}^D)]$ , defining a distribution for  $E[\mathbf{n}^I(t|\mathbf{q}_{S_{ASM}}^E, \mathbf{q}_{S_D}^D)]$ .

Step 3d. Then, 50 parameter sets,  $\mathbf{q}_{sim_D}^D, \mathbf{q}_{sim_{ASM}}^E$ , are selected using Latin hypercube sampling from the distribution for  $E[\mathbf{n}^I(t|\mathbf{q}_{S_{ASM}}^E, \mathbf{q}_{S_D}^D)]$ . For each of these, the frequency of intersection and its spatial disaggregation are computed for the 50 simulations of parameters  $\mathbf{q}_{sim_{ISP}}^E | (\mathbf{q}_{S_{ASM}}^E = \mathbf{q}_{sim_{ASM}}^E)$  by:

$$\mathbf{n}^I(t|\mathbf{q}_{sim_{ISP}}^E, \mathbf{q}_{sim_{ASM}}^E, \mathbf{q}_{sim_D}^D) \sim \sum_{\mathbf{a}|\mathbf{q}_{sim_{ASM}}^E} \mathbf{n}_{\mathbf{a}}^I(t|\mathbf{q}_{sim_{ISP}}^E, \mathbf{q}_{sim_{ASM}}^E, \mathbf{q}_{sim_D}^D)$$

and (Eq. 22)

$$\mathbf{n}_{x_i, y_j}^I(t|\mathbf{q}_{sim_{ISP}}^E, \mathbf{q}_{sim_{ASM}}^E, \mathbf{q}_{sim_D}^D) \sim \sum_{\mathbf{a}|\mathbf{q}_{sim_{ASM}}^E} \mathbf{n}_{\mathbf{a}, x_i, y_j}^I(t|\mathbf{q}_{sim_{ISP}}^E, \mathbf{q}_{sim_{ASM}}^E, \mathbf{q}_{sim_D}^D)$$

In Equation 22,  $\mathbf{n}_{\mathbf{a}}^I(t|\mathbf{q}_{sim_{ISP}}^E, \mathbf{q}_{sim_{ASM}}^E, \mathbf{q}_{sim_D}^D)$ , and its spatial disaggregation,  $\mathbf{n}_{\mathbf{a}, x_i, y_j}^I(t|\mathbf{q}_{sim_{ISP}}^E, \mathbf{q}_{sim_{ASM}}^E, \mathbf{q}_{sim_D}^D)$ , are the values for source  $\mathbf{a}$  for the simulated parameter set  $\mathbf{q}_{sim_{ISP}}^E | \mathbf{q}_{S_{ASM}}^E, \mathbf{q}_{S_D}^D$  from (2) with  $\mathbf{q}_{S_{ASM}}^E, \mathbf{q}_{S_D}^D = \mathbf{q}_{sim_{ASM}}^E, \mathbf{q}_{sim_D}^D$ , the source model and dike parameter set selected in one simulation. The result is 2,500 equally likely values for frequency of intersection. The resulting values of the spatial disaggregation of the frequency of intersection,  $\mathbf{n}_{x_i, y_j}^I(t|\mathbf{q}_{sim_{ISP}}^E, \mathbf{q}_{sim_{ASM}}^E, \mathbf{q}_{sim_D}^D)$ , are written to separate files for each of the 2,500 simulated parameter sets.

Step 3e. Finally, the expected value for the spatial disaggregation of the frequency of intersection for each of the possible dike parameter sets is estimated from the average of all of the results from step 3d for which  $\mathbf{q}_{sim_D}^D = \mathbf{q}_{S_D}^D$ .

$$E[\mathbf{n}_{x_i, y_j}^I(t|\mathbf{q}_{S_D}^D)] \sim \frac{\sum_{sim_{ISP, ASP, D}=1}^{sim_{ISP, ASP, D}=2500} \mathbf{n}_{x_i, y_j}^I(t|\mathbf{q}_{sim_{ISP}}^E, \mathbf{q}_{sim_{ASM}}^E, \mathbf{q}_{sim_D}^D) \cdot \mathbf{d}(\mathbf{q}_{sim_D}^D = \mathbf{q}_{S_D}^D)}{\sum_{sim_{ISP, ASP, D}=1}^{sim_{ISP, ASP, D}=2500} \mathbf{d}(\mathbf{q}_{sim_D}^D = \mathbf{q}_{S_D}^D)}$$

(Eq. 23)

where  $\mathbf{d}(\mathbf{q}_{sim_D}^D = \mathbf{q}_{S_D}^D) = 1$  for those simulations where  $\mathbf{q}_{sim_D}^D = \mathbf{q}_{S_D}^D$ , and zero otherwise. Note that

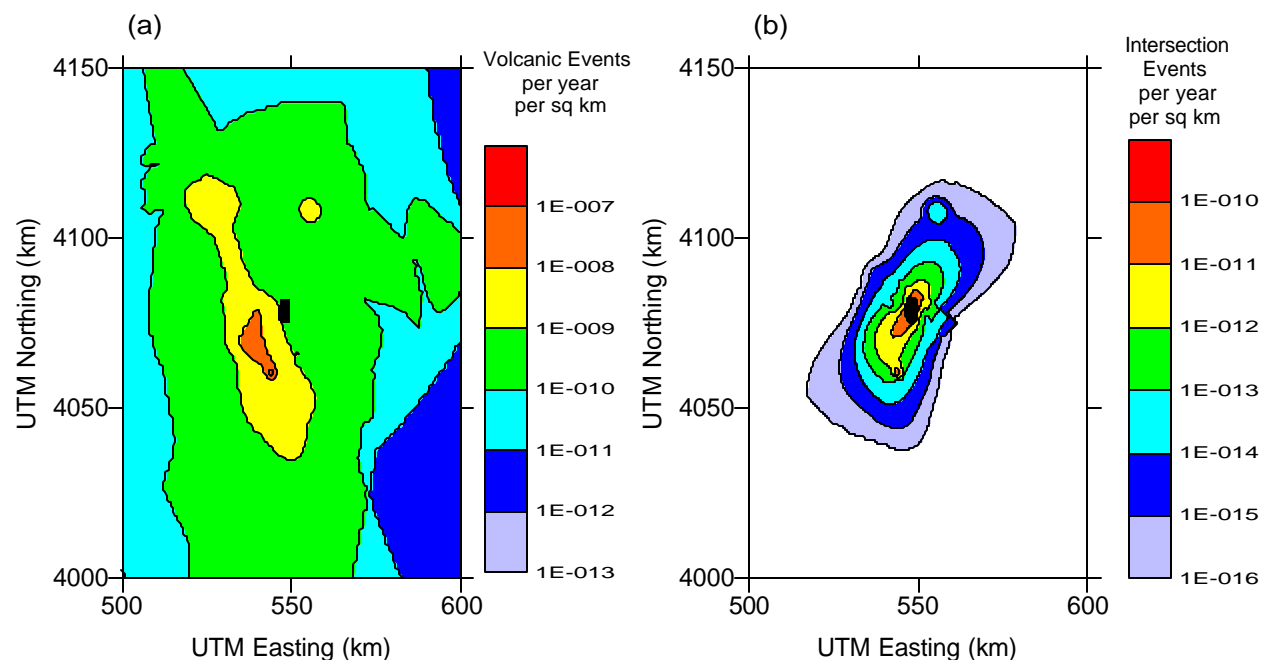
$$\frac{1}{2,500} \sum_{sim_{ISP, ASP, D}=1}^{sim_{ISP, ASP, D}=2500} \mathbf{d}(\mathbf{q}_{sim_D}^D = \mathbf{q}_{S_D}^D) \sim P(\Theta^D = \mathbf{q}_{S_D}^D) \cdot ]$$

Figure 17, part (b), shows a map of  $E[\mathbf{n}_{x_i,y_j}^I(t|\mathbf{q}_{S_D}^D)]$  averaged across all 10 experts. This figure indicates the locations of volcanic events that contribute to the frequency of intersection. Also shown on Figure 17, part (a), is a map of the expected frequency of volcanic events,  $E[\mathbf{I}(x_i,y_j,t|\mathbf{q}_{S_D}^D)]$ , averaged across all experts. This map was obtained by repeating the calculation for part (a) with the conditional probability of intersection,  $P^I(x_i,y_j,\mathbf{q}_{S_D}^D)$ , set to 1 at every point  $(x,y)$ .

The previous version of this analysis report (Revision 00 ICN 01) recalculates the frequency of intersection using the 70,000 metric tons of uranium (MTU) No-Backfill layout shown on Figure 16a. Figure 17a shows the revised map of  $E[\mathbf{n}_{x_i,y_j}^I(t|\mathbf{q}_{S_D}^D)]$  averaged across all 10 experts.

**Step 4:** The composite distribution for the frequency of intersection of the proposed repository footprint by a dike is now represented by the 2,500×10 simulation results for the 10 PVHA experts. Each expert's distribution was assigned equal weight in the PVHA aggregation process. Thus, the composite 25,000 simulations of  $\mathbf{n}^I(t)$  are all equally likely. The 25,000 simulations of  $\mathbf{n}^I(t)$  are ranked and the simulations that produce various percentile of the distribution for  $\mathbf{n}^I(t)$  are identified (e.g., the 95<sup>th</sup> percentile is the simulation with rank  $0.95 \times 25,000 = 23,750$ ). Simulation results that are close to each percentile (within a rank of  $\pm 250$ ) that are for different experts are also identified to capture the range of expert interpretations. These simulations are identified using software routine CFRAC V1.0 (STN: 10254-1.0-00 [148560]).

**Step 5:** Steps 1 through 4 provide the values of  $\mathbf{n}_{x_i,y_j}^I(t|\mathbf{q}_{simSP}^E, \mathbf{q}_{simASM}^E, \mathbf{q}_{simD}^D)$  and  $E[\mathbf{n}_{x_i,y_j}^I(t|\mathbf{q}_{S_D}^D)]$  needed for Equations 10, 11, 18, and 19. What remains is the calculation of  $P^I(L_m, \mathbf{f}_n | x_i, y_j, \mathbf{q}_{S_D}^D)$  and  $P^I(L_m, \mathbf{f}_n, r^{EC} | x_i, y_j, \mathbf{q}_{S_D}^D)$ , the discretization of the conditional probability of intersection into increments of intersection length, intersection azimuth, and number of eruptive centers within the proposed repository footprint for each volcanic event location  $(x,y)$ . Software routine DILECDLH V1.0 (STN: 10259-1.0-00 [148559]) is used to discretize the conditional probability of intersection,  $P^I(x_i, y_j, \mathbf{q}_{S_D}^D)$ , into the designated bins for length and azimuth within the proposed repository. The inputs to program DILECDLH are: (1) the spatial disaggregation of the frequency of intersection (either the mean result conditional on  $\mathbf{q}_{S_D}^D$  for one expert from Step 3 or for one of the hazard simulations representative of the 95<sup>th</sup> percentile of the composite distribution from Step 4); (2) the dike length and volcanic event location distributions for the corresponding parameter set  $\mathbf{q}_{S_D}^D$ ; (3) a joint distribution for dike length and the number of eruptive centers on a dike,  $P(n^{EC} = \mathbf{h} | L_p, \mathbf{q}_{S_D}^D)$  [computed using software routines FITIDSR V1.0 (STN: 10264-1.0-00) [148557], SFIDSR V1.0 (STN: 10276-1.0-00 [148571]), and DLECD V1.0 (STN: 10260-1.0-00 [148558]); and (4) the spatial distribution of eruptive centers along the dike. With the exception of the assessments for the number and spatial distribution of eruptive centers, all of the probability distributions required to perform this calculation are defined in CRWMS M&O (1996 [100116]).



Output DTN: (Figure 17a) LA0009FP831811.001 [164712]; DTN: (Figure 17b) LA0303BY831811.001 [163985].

NOTE: The maps represent the mean results averaged over 10 experts and over each expert's bgic tree (CRWMS M&O 1996 [100116], Appendix E). Black area in center of maps is the location of the proposed repository.

Figure 17. Spatial Distribution of Volcanic Hazard Defined by the Probabilistic Volcanic Hazard Analysis Expert Panel: (a) Map of Expected Volcanic Event Frequency and (b) Map of Spatial Disaggregation of Expected Intersection Frequency

Two alternative approaches are developed for the spatial distribution of eruptive centers in Section 6.5.1.3. In the first approach (designated *IUD*) the location of each eruptive center is specified by an independent, uniform distribution over the total length of the dike,  $L_p$ . In the second approach (designated *USRD*) the eruptive centers are spaced out over the full length of the dike with the location each of the  $n^{EC}$  eruptive centers uniformly distributed in a segment of length  $L_p/n^{EC}$ . Calculations of  $P^I(L_m^I, \mathbf{f}_n, r^{EC} | x_i, y_j, \mathbf{q}_{S_D}^D)$  are performed for both approaches. Distributions for the number of eruptive centers on a dike,  $P(n^{EC} = \mathbf{h} | L_p, \mathbf{q}_{S_D}^D)$ , are developed below from the PVHA experts' assessments of the number of eruptive centers associated with a volcanic event.

Each of the PVHA experts made assessments for the number of volcanic events represented by the observed Quaternary eruptive centers. For example, the observed five volcanoes in Crater Flat may have been caused by 1 to 5 volcanic events, with each expert providing a probability distribution for the number of volcanic events. These assessments can be used to produce a distribution for the number of eruptive centers per volcanic event. For example, if Crater Flat contains five individual volcanic events, then the data indicate one eruptive center per volcanic

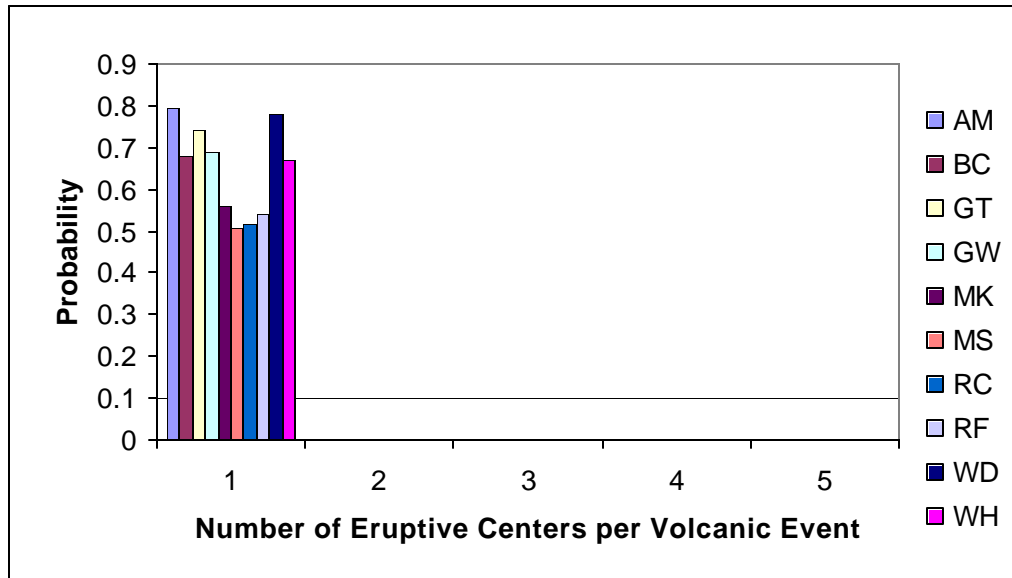
event. If, on the other hand, the five volcanoes (and their associated eruptive centers) were created by one volcanic event, then the data indicate five eruptive centers per volcanic event. Using each expert's assessments of volcanic event counts and the number of separate eruptive centers that have occurred in the Quaternary, distributions for the number of separate eruptive centers per volcanic event were developed. These are presented in Attachment III and shown in Figure 18.

The distributions for  $P(n^{EC} = \mathbf{h} | L_p, \mathbf{q}_{SD}^D)$  derived in Attachment III are marginal distributions in the sense that they are defined independent of assessments of dike length and are averaged over an expert's interpretations,  $\Theta^E$ . The experts' assessed distributions for dike length are also marginal distributions. However, the calculations need to use the conditional distribution of number of eruptive centers given dike length. The limiting conditions that define the relationship between two variable parameters are complete independence and complete dependence. These two limiting conditions are used to define the influence of dike length on  $P(n^{EC} = \mathbf{h} | L_p, \mathbf{q}_{SD}^D)$ . Complete independence implies that the conditional distribution for number of eruptive centers is equal to the marginal distribution, and  $P(n^{EC} = \mathbf{h} | L_p, \mathbf{q}_{SD}^D) = P(n^{EC} = \mathbf{h} | \Theta^E)$  is used in Equation 16. The resulting discretizations of the frequency of intersection are designated:  $\mathbf{n}_{IUD-UC}^I(t, L_m^I, \mathbf{f}_n, r^{EC} | \mathbf{q}_S)$  for independent, uniformly distributed spatial locations with the number of eruptive centers uncorrelated with dike length; and  $\mathbf{n}_{USRD-UC}^I(t, L_m^I, \mathbf{f}_n, r^{EC} | \mathbf{q}_S)$  for uniformly spaced, randomly distributed spatial locations with the number of eruptive centers uncorrelated with dike length.

Complete dependence implies that the number of eruptive centers varies directly with dike length (it is considered unrealistic to have a negative correlation). The correlation between dike length and number of eruptive centers per event was set to the maximum value by making the marginal distributions for dike length and number of eruptive centers per volcanic event rank correlated. This is achieved by specifying a one-to-one correspondence of the marginal CDF's for the two parameters. The resulting discretizations of the frequency of intersect are designated:  $\mathbf{n}_{IUD-C}^I(t, L_m^I, \mathbf{f}_n, r^{EC} | \mathbf{q}_S)$  for independent, uniformly distributed spatial locations and the number of eruptive centers correlated with dike length; and  $\mathbf{n}_{USRD-C}^I(t, L_m^I, \mathbf{f}_n, r^{EC} | \mathbf{q}_S)$  for uniformly spaced, randomly distributed spatial locations and the number of eruptive centers correlated with dike length. These two approaches span the range of correlation considered reasonable (zero to maximum).

The longest proposed single-event dike represented by the Quaternary volcanoes in the YMR is the 11.2-kilometer spacing between Little Cones SW and Makani Cone in Crater Flat. However, many of the PVHA experts specified distributions for dike length with upper tails that greatly exceed this length. Thus, the distributions presented in Attachment III may not be representative of conditions for very long dikes. To address this issue, an alternative approach for defining the number of eruptive centers was included in which the number of eruptive centers is defined as an average density per kilometer of dike length, or equivalently, by the average spacing between eruptive centers. For a given dike length, the number of eruptive centers is found by dividing the dike length by the average spacing (rounding to the nearest integer). Consistent with the number of eruptive centers being defined by an average spacing between eruptive centers, the *USRD*

spatial distribution is used. The resulting spatial distribution approach is designated Uniformly Spaced, Randomly Distributed Fixed Density (*USRD-FD*) for uniformly spaced, randomly distributed with fixed density.



OUTPUT DATA. DTN: LA0009FP831811.001 [164712]

NOTE: The two-letter code refers to the initials of the 10 PVHA experts in Table 11.

Figure 18. Distributions for Number of Eruptive Centers per Volcanic Event,  $n^{EC}$ , Derived from the Probabilistic Volcanic Hazard Analysis Experts' Interpretations (from Attachment III, Figure III-1)

The same process used to derive the distribution for number of eruptive centers per volcanic event from the PVHA experts' assessments was to be used to evaluate the average spacing between eruptive centers. For example, if the five volcanoes in Crater Flat are considered to constitute a single volcanic event, then the 11.2-km distance between Little Cones SE and Makani Cone in Crater Flat divided by 4 (the number of intervals between eruptive centers) gives an average spacing of 2.8 km. The other Quaternary volcano cluster with multiple cones is Hidden Cone and Little Black Peak near Sleeping Butte, 2.5 km apart. If these are considered to be the result of a single volcanic event, the average spacing between eruptive centers for this event is 2.5 km. If these are the only two volcanic events with multiple eruptive centers, then one obtains an average spacing for all volcanic events of 2.6 km. An alternative assessment might be that Crater Flat contains two volcanic events. One volcanic event may consist of Makani and Black Cones. These two cones are located 5.4 km apart. The other volcanic event would then consist of Red Cone and the two Little Cones. The distance between Red Cone and Little Cone SW is 3.2 km, resulting in an average spacing for this volcanic event of 1.6 km. The average eruptive center spacing for the three volcanic events would then be 3.1 km. Using each expert's assessments of volcanic event counts and the number of separate eruptive centers that have occurred in the Quaternary, the average spacing of eruptive centers was computed. These are presented in Attachment III and are summarized in Table 14.

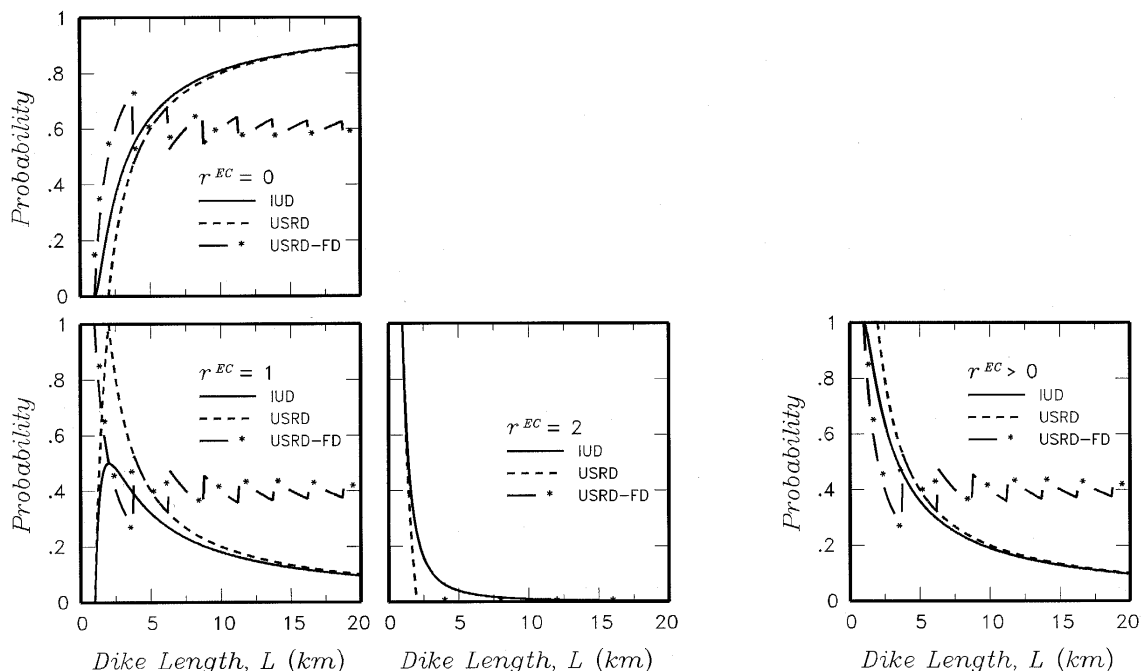
Table 14. Average Eruptive Center Spacing (from Attachment III, Table III-12)

PVHA Expert	Average Spacing Between Eruptive Centers (km)
Alex McBirney (AM)	2.7
Bruce Crowe (BC)	1.9
George Thompson (GT)	1.5
George Walker (GW)	1.4
Mel Kuntz (MK)	2.4
Michael Sheridan (MS)	2.5
Richard Carlson (RC)	2.4
Richard Fisher (RF)	2.5
Wendell Duffield (WD)	1.4
William Hackett (WH)	2.0

OUTPUT DATA. DTN: LA0009FP831811.001 [164712]

The values listed in Table 14 are used as an alternative approach to obtaining  $n^{EC}$ . For each simulation of a dike length,  $L_p$ , the value of  $n^{EC}$  is set to  $L_p$  divided by the average spacing from Table 14, with the quotient rounded to the nearest integer.

Figure 19 compares the probability of the occurrence of  $r^{EC} = 0, 1, 2,$  and  $r^{EC} > 0$  [ $P(r^{EC} > 0)$  is equal to  $1 - P(r^{EC} = 0)$  and is the sum of  $P(r^{EC} = 1), P(r^{EC} = 2), \dots$ ] eruptive centers computed using the *USRD-FD* spatial distribution and an average eruptive center spacing of 2.5 km with the probabilities shown on Figure 15a for the *IUD* and *URSD* spatial distribution approaches. For short dike lengths, the *USRD-FD* approach results in a lower probability for one or more centers within the proposed repository than the other two approaches. However, as the dike length increases, the *USRD-FD* approach reaches a nearly constant probability of 0.4 for  $r^{EC} = 1$  [ $0.4 = (L^I = 1)/2.5$  kilometer average spacing of eruptive centers]. The oscillations in the probability about 0.4 are a result of incremental changes in  $n^{EC}$  by integer values as the length of the dike increases. The *USRD-FD* approach produces a density of eruptive centers per volcanic event for all dike lengths that is similar to that observed for the Quaternary volcanoes in the YMR. The resulting discretization of the frequency of intersection is designated  $n_{USRD-FD}^I(t, L_m^I, \mathbf{f}_n, r^{EC} | \mathbf{q}_S)$  for uniformly spaced, randomly distributed spatial locations, with the number of eruptive centers determined by an average spacing between eruptive centers along a dike.



N/A - For Illustration Purposes Only

Figure 19. Probability for the Number of Eruptive Centers Within the Proposed Repository Footprint,  $r^{EC}$ , Computed Using the Uniformly Spaced, Randomly Distributed, Fixed Density Spatial Distribution of Eruptive Centers and for the Length of Intersection,  $L^I = 1$  km, and an Average Spacing of 2.5 km Between Eruptive Centers Compared to the Results for the *IUD* and *USRD* Models Shown in Figure 15a

The computation procedure used in software routine DILECDLH V1.0 is as follows:

Step 5a. An input file is created that contains the probability distributions for the length of the dike,  $L$ , and number of eruptive centers per volcanic event,  $n^{EC}$ . The probability distribution for  $L$  is discretized into the probability mass for  $L_p$  in 0.05 kilometer increments using module FITIDSR V1.0 (STN: 10264-1.0-00 [148557]) or SFIDSR V1.0 (STN: 10276-1.0-00 [148571]). The marginal distribution for  $n^{EC}$  is listed at the top of the file and the rank correlated value for  $n^{EC}$  is listed for each value of  $L$  by determining the value in the marginal distribution for  $n^{EC}$  that has the same cumulative probability as  $L_p$  in the marginal distribution for  $L$ .

Step 5b. For each of the dike parameter sets,  $\mathbf{q}_{S_D}^D$ , the spatial disaggregation of the hazard computed in Steps 3 and 4 is then input into the program. At each location  $(x,y)$  that contributes to the frequency of intersection  $\{n_{x,y}^I(t|\mathbf{q}_{sim_{SP}}^E, \mathbf{q}_{sim_{ASM}}^E, \mathbf{q}_{sim_D}^D)\}$  or  $E[n_{x,y}^I(t|\mathbf{q}_{S_D}^D)] > 0$ , the direction toward the proposed repository is sampled over  $5^\circ$  increments in azimuth, with the probability distribution for  $P^I(\mathbf{f}_n|\mathbf{q}_{S_D}^D)$  obtained by computing the probability mass in the interval  $\mathbf{f}_n - 2.5^\circ \leq \mathbf{f} \leq \mathbf{f}_n + 2.5^\circ$ . At each azimuth,  $\mathbf{f}_n$ , 100 simulations of  $L_{sim}$  and  $E_{sim}^L$  are created by Latin hypercube sampling from the distributions defined for each. For those combinations of  $L_p$  and  $E_o^L$  at azimuth  $\mathbf{f}_n$  that result in intersections with the proposed repository footprint,  $L^I$  is computed.

The probability  $P^I(L_m^I, \mathbf{f}_n | x_i, y_j, \mathbf{q}_{S_D}^D)$  defined in Equation 8 is now approximated by the expression:

$$P^I(L_m^I, \mathbf{f}_n | x_i, y_j, \mathbf{q}_S) \sim \frac{1}{100} \mathbf{d}(L^I = L_m^I) \cdot P(\mathbf{f}_n | \mathbf{q}_S) \quad (\text{Eq. 24})$$

and the probability  $P^I(r^{EC}, L_m^I, \mathbf{f}_n | x_i, y_j, \mathbf{q}_{S_D}^D)$  in Equation 16 is approximated by

$$P^I(r^{EC}, L_m^I, \mathbf{f}_n | x_i, y_j, \mathbf{q}_{S_D}^D) \sim \frac{1}{100} \sum_{sim=1}^{sim=100} \mathbf{d}(L^I = L_m^I) \cdot P(\mathbf{f}_n | \mathbf{q}_{S_D}^D) \times \sum_{h=1}^{h=n_{max}^{EC}} P(n^{EC} = \mathbf{h} | L_{sim}, \mathbf{q}_{S_D}^D) P(r^{EC} | L_{sim}, L_m^I, n^{EC} = \mathbf{h}) \quad (\text{Eq. 25})$$

where  $\mathbf{d}(L^I = L_m^I) = 1$  for those simulation values of  $L_{sim}$  and  $E_{sim}^L$  at azimuth  $\mathbf{f}_n$  that result in  $L^I = L_m^I$  for a volcanic event at  $(x, y)$ , and  $\mathbf{d}(L^I = L_m^I) = 0$  otherwise. An increment of 0.05 km is chosen for the intersection length bin size. This length bin size, together with the azimuth bin size of  $5^\circ$  are sufficient to define clearly the variability in the length and azimuth of intersecting dikes. (Note that the computation of the frequency of intersection is independent of these bin sizes.) Equation 25 is used five times for the five alternative approaches for  $P(n^{EC} = \mathbf{h} | L_{sim}, \mathbf{q}_{S_D}^D)$  and  $P(r^{EC} | L_{sim}, L_m^I, n^{EC} = \mathbf{h})$  described above.

Step 5c. The results of step 5b are then used in Equations 11 and 19 to estimate the expected frequencies of intersection  $E[\mathbf{n}^I(t, L_m^I, \mathbf{f}_n | \Theta)]$  and  $E[\mathbf{n}^I(t, L_m^I, \mathbf{f}_n, r^{EC} | \Theta)]$ , respectively for each of the PVHA expert's interpretations. The definition for  $P(\Theta^D = \mathbf{q}_{S_D}^D)$  used in Equation 23 is used in this calculation. The results for each expert are then averaged to obtain an estimate of the composite expected frequencies over all experts using the expressions:

$$E[\mathbf{n}^I(t, L_m^I, \mathbf{f}_n)] \sim \frac{1}{10} \sum_{\text{expert } 1}^{\text{expert } 10} E[\mathbf{n}^I(t, L_m^I, \mathbf{f}_n | \Theta)]$$

and

$$E[\mathbf{n}^I(t, L_m^I, \mathbf{f}_n, r^{EC})] \sim \frac{1}{10} \sum_{\text{expert } 1}^{\text{expert } 10} E[\mathbf{n}^I(t, L_m^I, \mathbf{f}_n, r^{EC} | \Theta)] \quad (\text{Eq. 26})$$

This calculation is performed using software routine COMBSM V1.0 (STN: 10256-1.0-00 [148561]). The resulting partial frequencies of intersection are then normalized to produce conditional distributions. At each value of  $L_m^I$  and  $\mathbf{f}_n$ , the computed vales of  $E[\mathbf{n}^I(t, L_m^I, \mathbf{f}_n, r^{EC})]$  are divided by  $E[\mathbf{n}^I(t, L_m^I, \mathbf{f}_n)]$  to produce a distribution for  $r^{EC}$  conditional on  $L_m^I$  and  $\mathbf{f}_n$ . The values of  $E[\mathbf{n}^I(t, L_m^I, \mathbf{f}_n)]$  are, in turn, divided by  $E[\mathbf{n}^I(t)]$  to produce a joint distribution for  $L_m^I$  and  $\mathbf{f}_n$  conditional on the mean frequency of intersection. Because Latin hypercube sampling

was used instead of full enumeration in (2), at a few of the points  $(x,y)$  that contribute to the frequency of intersection computed in Step 3, the 100 simulated values of  $L_{sim}$  and  $E_{sim}^L$  do not produce any intersections. These occur at locations where only the longest possible dikes combined with values of  $E^L$  very near 1.0 result in intersections of the proposed repository footprint. As a result, the sum of  $E[n^I(t, L_m^I, \mathbf{f}_n | \Theta)]$  over  $L_m^I$  and  $\mathbf{f}_n$  for each expert typically equaled about 97 percent to 99 percent of  $E[n^I(t | \Theta)]$ . Because the purpose of Step 5 is to obtain a conditional distribution, the computed values of  $E[n^I(t, L_m^I, \mathbf{f}_n | \Theta)]$  for each expert were normalized in software routine COMBSM V1.0 to sum to the value of  $E[n^I(t | \Theta)]$  computed in Step (3). [Note that the true value of  $E[n^I(t | \Theta)]$  was computed by full enumeration of the individual expert interpretations.]

Step 5d. Step 4 identified those simulation results that represented the 5<sup>th</sup> and 95<sup>th</sup> percentiles of the composite distribution for frequency of intersection. For these parameter sets, designated  $\mathbf{q}^{0.05}$  and  $\mathbf{q}^{0.95}$ , the results of step 5b are used in Equations 10 and 18 to compute the values of  $n^I(t, L_m^I, \mathbf{f}_n | \mathbf{q}^{0.05})$  and  $n^I(t, L_m^I, \mathbf{f}_n, r^{EC} | \mathbf{q}^{0.05})$ , respectively, for the 5<sup>th</sup> percentile hazard and  $n^I(t, L_m^I, \mathbf{f}_n | \mathbf{q}^{0.95})$  and  $n^I(t, L_m^I, \mathbf{f}_n, r^{EC} | \mathbf{q}^{0.95})$ , respectively, for the 95<sup>th</sup> percentile hazard. The results of the individual simulations are averaged using software routine COMBSF V1.0 (STN: 10255-1.0-00 [148562]) to produce the final values of  $n^I(t, L_m^I, \mathbf{f}_n | \mathbf{q}^{0.05})$ ,  $n^I(t, L_m^I, \mathbf{f}_n, r^{EC} | \mathbf{q}^{0.05})$ ,  $n^I(t, L_m^I, \mathbf{f}_n | \mathbf{q}^{0.95})$  and  $n^I(t, L_m^I, \mathbf{f}_n, r^{EC} | \mathbf{q}^{0.95})$ . Routine COMBSF V1.0 performed this calculation, including the normalization so that the sum of  $n^I(t, L_m^I, \mathbf{f}_n | \mathbf{q}^{0.xx})$  over  $L_m^I$  and  $\mathbf{f}_n$  equals  $n^I(t | \mathbf{q}^{0.xx})$  obtained in Step 4. The resulting disaggregated frequencies of intersection are then normalized to produce conditional distributions. At each value of  $L_m^I$  and  $\mathbf{f}_n$ , the computed values of  $n^I(t, L_m^I, \mathbf{f}_n, r^{EC} | \mathbf{q}^{0.05})$  are divided by  $n^I(t, L_m^I, \mathbf{f}_n | \mathbf{q}^{0.05})$  and the values of  $n^I(t, L_m^I, \mathbf{f}_n, r^{EC} | \mathbf{q}^{0.95})$  are divided by  $n^I(t, L_m^I, \mathbf{f}_n | \mathbf{q}^{0.95})$  to produce a distribution for  $r^{EC}$  conditional on  $L_m^I$  and  $\mathbf{f}_n$ . The values of  $n^I(t, L_m^I, \mathbf{f}_n | \mathbf{q}^{0.05})$  are, in turn, divided by  $n^I(t | \mathbf{q}^{0.05})$  and the values  $n^I(t, L_m^I, \mathbf{f}_n | \mathbf{q}^{0.95})$  are divided by  $n^I(t | \mathbf{q}^{0.95})$  to produce joint distributions for  $L_m^I$  and  $\mathbf{f}_n$  conditional on the 5<sup>th</sup> and 95<sup>th</sup> percentile values for the frequency of intersection.

In summary, the mathematical formulation for computing the conditional distribution for the length and azimuth of intersecting dikes within the proposed repository footprint is developed directly from the PVHA formulation presented in CRWMS M&O (1996 [100116], Section 3 and Appendix E) without invoking any additional assumptions. The formulation for computing the conditional distribution for the number of eruptive centers occurring within the proposed repository footprint requires additional assumptions in order to assess the number of eruptive centers per volcanic event and the spatial distribution of eruptive centers along the length of the dike. Five alternative approaches are developed to implement these assumptions to span the range of available approaches. Calculations are performed for all five approaches to indicate the

sensitivity of the results. As a final step, relative weights are assigned to the five approaches in order that a composite result can be obtained. The five approaches are summarized below:

1. The Independent, Uniformly Distributed, Uncorrelated (*IUD-UC*) approach. The distribution for the number of eruptive centers per volcanic event is derived from the PVHA experts' interpretations. These distributions are uncorrelated with the distributions for dike length. The location for each eruptive center is defined by a uniform distribution over the total length of the dike, and if multiple eruptive centers occur in a volcanic event, the distributions for their locations are independent.
2. The Independent, Uniformly Distributed, Correlated (*IUD-C*) approach. The distribution for the number of eruptive centers per volcanic event is derived from the PVHA experts' interpretations. These distributions are completely correlated with the distributions for dike length. The location for each eruptive center is defined by a uniform distribution over the total length of the dike, and if multiple eruptive centers occur in a volcanic event, the distributions for their locations are independent.
3. The Uniformly Spaced, Randomly Distributed, Uncorrelated (*USRD-UC*) approach. The distribution for the number of eruptive centers per volcanic event is derived from the PVHA experts' interpretations. These distributions are uncorrelated with the distributions for dike length. The total length of the dike is divided into equal segments for each eruptive center. Within each segment, the location of the eruptive center is defined by a uniform distribution over the length of the segment.
4. The Uniformly Spaced, Randomly Distributed, Correlated (*USRD-C*) approach. The distribution for the number of eruptive centers per volcanic event is derived from the PVHA experts' interpretations. These distributions are completely correlated with the distributions for dike length. The total length of the dike is divided into equal segments for each eruptive center. Within each segment, the location of the eruptive center is defined by a uniform distribution over the length of the segment.
5. The *USRD-FD* approach. The number of eruptive centers per volcanic event is determined by dividing the total length of the dike by an average distance between eruptive centers derived from the PVHA experts' interpretations. The total length of the dike is divided into equal segments for each eruptive center. Within each segment, the location of the eruptive center is defined by a uniform distribution over the length of the segment.

Application of the results of this report in assessing the impact of disruptive events will require a rule for combining the results for these five approaches. In the overall framework of the PVHA, this is accomplished by assigning weights to each model. These weights are derived by separately examining the three issues addressed by the alternative approaches.

The first issue is the overall approach for evaluating the number of eruptive centers per volcanic event. The two approaches are to define a distribution for the total number based on the observed Quaternary data or to define the average spacing using the Quaternary data and compute the number for each dike length. These two approaches are considered to be equally

credible. They both rely to an equal degree on the observed data and the PVHA experts' interpretations of these data to define the characteristics of volcanic events in the YMR. Thus, the two approaches are given equal weight.

The second issue is the appropriate spatial distribution for eruptive centers along the length of the dike or dike system. Two alternative approaches are used, one in which the location of each eruptive center is independent of the others (*IUD*) and one in which the eruptive centers are spaced out along the total length of the dike system (*USRD*). The simulations shown on Figure 14 indicate that the *IUD* spatial model often produces tight clustering of multiple eruptive centers. This is somewhat at odds with the limited observations for eruptive centers in the vicinity of Yucca Mountain. Therefore, the *USRD* model is strongly preferred over the *IUD* model by a ratio of 3:1, yielding weights of 0.75 for the *USRD* models and 0.25 for the *IUD* models. Note that this assessment applies to the cases where the number of eruptive centers is derived from the distributions shown on Figure 18. When the number of eruptive centers is derived from an average spacing, only the *USRD* model is applied because it is consistent with the basis for determining the number of eruptive centers.

The third issue addresses the correlation between the distributions for number of eruptive centers per volcanic event shown on Figure 18 and the distributions for the length of the dike associated with a volcanic event developed by the PVHA experts. Two alternatives were used: the two distributions are uncorrelated and the two distributions are fully correlated. It is likely that there is some degree of correlation because longer total dike lengths would provide more opportunity for the formation of vents and presumably result from volcanic events with larger volumes. Thus, the fully correlated model is slightly favored (0.6) to the uncorrelated model (0.4). Again, this assessment applies only to the cases where the number of eruptive centers is derived from the distributions shown in Figure 18. Determining the number of eruptive centers for a volcanic event using the average spacing and the total length produces full correlation between length and number of eruptive centers.

Combining these three sets of weights yields the following relative weighting of the five approaches for computing the conditional distribution for number of eruptive centers within the proposed repository footprint:

- The weight for the *IUD-UC* approach is equal to 0.5 for the approach for number of centers times 0.25 for the spatial approach times 0.4 for uncorrelated number of eruptive centers and dike length distributions, yielding a weight of 0.05.
- The weight for the *IUD-C* approach is equal to 0.5 for the approach for number of centers times 0.25 for the spatial approach times 0.6 for correlated number of eruptive centers and dike length distributions, yielding a weight of 0.075.
- The weight for the *USRD-UC* approach is equal to 0.5 for the approach for number of centers times 0.75 for the spatial approach times 0.4 for uncorrelated number of eruptive centers and dike length distributions, yielding a weight of 0.15.

- The weight for the *USRD-C* approach is equal to 0.5 for the approach for number of centers times 0.75 for the spatial approach times 0.6 for uncorrelated number of eruptive centers and dike length distributions, yielding a weight of 0.225.
- The weight for the *USRD-FD* approach is 0.5 for the approach, with only the *USRD* spatial approach applying and the correlation issue not pertinent, yielding a weight of 0.5.

These weights are used to combine the results of consequence evaluations for the five alternative approaches of number of eruptive centers in downstream analyses.

**Modification to the Uniformly Spaced, Randomly Distributed Fixed Density Approach**—In the previous version of this scientific analysis report (CRWMS M&O 2000 [151551]) and continued in this current version, the expected value of the average spacing between eruptive centers listed in Table 14 is replaced by the empirical distribution for the average spacing between eruptive centers in applying the *USRD-FD* approach. Table 15 lists the empirical distribution for the average spacing of eruptive centers derived in Attachment III from the PVHA experts’ interpretations. Note that the means of these distributions are equal to the expected values listed in Table 14. Using the full distribution for the average spacing of eruptive centers, rather than its expected value, makes the calculation for the *USRD-FD* approach consistent with those for the *IUD* and *USRD* approaches, which use empirical distributions for the number of eruptive centers per volcanic event. As a result of using the full distribution, there is an increase in the total number of eruptive centers that may occur within the repository footprint. The minimum value of the average spacing of eruptive centers in the empirical distributions is 0.46 km (the spacing between Little Cones NE and Little Cones SW). Using this average spacing and the maximum repository dimensions, the maximum possible number of eruptive centers within the proposed LA repository footprint is 13.

Table 15. Empirical Distribution for Average Spacing Between Eruptive Centers Calculation Results (from Attachment III, Table III-13 of this document)

PVHA Expert	Empirical Distribution for Average Spacing between Eruptive Centers (km)
Alex McBirney (AM)	0.46 (0.0272), 2.01 (0.0492), 2.45 (0.0253), 2.80 (0.8859), 2.88 (0.0124)
Bruce Crowe (BC)	0.46 (0.4031), 1.62 (0.0489), 2.45 (0.1874), 2.80 (0.0914), 2.88 (0.2203), 5.35 (0.0489)
George Thompson (GT)	0.46 (0.4720), 2.01 (0.1279), 2.45 (0.1839), 2.80 (0.1705), 2.88 (0.0457)
George Walker (GW)	0.46 (0.5916), 2.45 (0.1767), 2.80 (0.0800), 2.88 (0.1517)
Mel Kuntz (MK)	0.46 (0.0550), 2.01 (0.2100), 2.45 (0.2950), 2.80 (0.4200), 2.88 (0.0200)
Michael Sheridan (MS)	0.46 (0.0388), 2.01 (0.1330), 2.45 (0.3238), 2.80 (0.4656), 2.88 (0.0388)

Table 15. Empirical Distribution for Average Spacing Between Eruptive Centers Calculation Results (from Attachment III, Table III-13 of this document) (Continued)

PVHA Expert	Empirical Distribution for Average Spacing between Eruptive Centers (km)
Richard Carlson (RC)	0.46 (0.1186), 2.45 (0.3608), 2.80 (0.4020), 2.88 (0.1186)
Richard Fisher (RF)	0.46 (0.0842), 1.62 (0.0192), 2.45 (0.3383), 2.80 (0.5199), 2.88 (0.0192), 5.35 (0.0192)
Wendell Duffield (WD)	0.46 (0.6445), 2.45 (0.0322), 2.80 (0.0833), 2.88 (0.1560), 4.09 (0.0840)
William Hackett (WH)	0.46 (0.4078), 2.45 (0.1844), 2.80 (0.0851), 2.88 (0.1844), 4.09 (0.1383)

OUTPUT DATA. DTN: LA0009FP831811.004 [152659]

NOTE: The values in ( ) are the empirical probability for the preceding value of average spacing.

**Incorporation of Potential Effect of Repository Openings**—The approaches developed above for assessing the spatial distribution of eruptive centers along the length of the dike or dikes associated with a volcanic event assume that the presence of the repository drifts has no impact on the likelihood of an eruptive conduit forming within the repository footprint. Therefore, for the calculation in the previous version of this scientific analysis report (Revision 00 ICN 01) (CRWMS M&O 2000 [151551]) and continued in this current version (Revision 01), two approaches are used to address the effect of the repository openings. The first approach considers the repository openings to have no effect and uses the weighted combination of the five approaches described above to develop the conditional distributions for  $r^{EC} = 0, 1, 2, 3, \dots$ . The second approach considers that the repository openings will induce at least one eruptive center. For this approach the distribution for  $r^{EC}$  is derived from the results of the first approach by setting the conditional probability of  $r^{EC} = 0$  to zero and renormalizing the probabilities for  $r^{EC} = 1, 2, 3, \dots$  to sum to unity. For example, if the first approach resulted in a distribution for  $r^{EC}$  of {0 (0.4), 1 (0.3), 2 (0.2), 3 (0.1)}, then the second approach would result in the distribution for  $r^{EC}$  of {1 (0.5), 2 (0.333), 3 (0.167)}. Because there has not been significant study of the issue and the PVHA experts were not elicited on this question, maximum uncertainty weights of 0.5 are applied to these two approaches for assessing the effect of the repository openings. As a result, the composite distribution for  $r^{EC}$  in the above example would be {0 (0.2), 1 (0.4), 2 (0.267), 3 (0.133)}.

### 6.5.3 Results

#### 6.5.3.1 Frequency of Intersection of the Proposed Repository Footprint by a Dike for the License Application Footprint

Table 16 lists the mean annual frequency of intersection of the proposed repository footprint and percentiles of the distribution for the frequency of intersection computed by full enumeration and by simulation with Latin hypercube sampling for the LA footprint. The results are listed for each expert, indicated by the expert’s initials from Table 11, and for the composite distribution over all 10 experts, with equal weight assigned to the individual expert assessments. The results computed by full enumeration of the experts’ logic trees are indicated by the suffix—FEn in the

column headings (e.g., AM-FEn) and the results computed by simulation are indicated by the suffix-Sim in the column headings (e.g., AM-Sim). The percent difference in the frequency of intersection is also listed in the tables. The differences between the frequencies of intersection computed by full enumeration and by simulation are generally small, ranging from -25.7 percent to +20.5 percent, indicating that simulation with Latin hypercube sampling reliably represents the full distribution for frequency of intersection.

Table 16. Frequency of Intersection for the License Application Footprint (Blocks 1, 2, 3, and 5)

	<b>AM<sup>1</sup>-FEn<sup>2</sup></b>	<b>AM-Sim<sup>2</sup></b>	<b>% difference<sup>3</sup></b>	<b>BC-FEn</b>	<b>BC-Sim</b>	<b>% difference</b>	<b>GT-FEn</b>	<b>GT-Sim</b>	<b>% difference</b>
Mean	0.696E-08	0.698E-08	0.2	0.136E-07	0.135E-07	-0.3	0.379E-07	0.374E-07	-1.3
0.05	0.199E-08	0.212E-08	6.3	0.118E-08	0.118E-08	-4.9	0.123E-07	0.117E-07	-4.8
0.1	0.245E-08	0.253E-08	3.0	0.195E-08	0.179E-08	-8.5	0.148E-07	0.149E-07	0.7
0.15	0.282E-08	0.303E-08	7.5	0.251E-08	0.238E-08	-5.1	0.174E-07	0.172E-07	-0.9
0.2	0.316E-08	0.318E-08	0.4	0.295E-08	0.278E-08	-5.8	0.204E-07	0.192E-07	-5.8
0.3	0.363E-08	0.364E-08	0.2	0.398E-08	0.389E-08	-2.3	0.229E-07	0.226E-07	-1.2
0.4	0.407E-08	0.402E-08	-1.3	0.550E-08	0.542E-08	-1.4	0.263E-07	0.265E-07	0.6
0.5	0.457E-08	0.467E-08	2.1	0.832E-08	0.819E-08	-1.5	0.316E-07	0.322E-07	1.8
0.6	0.549E-08	0.529E-08	-3.7	0.132E-07	0.136E-07	3.5	0.372E-07	0.387E-07	4.3
0.7	0.676E-08	0.646E-08	-4.4	0.178E-07	0.176E-07	-1.2	0.447E-07	0.436E-07	-2.3
0.8	0.851E-08	0.827E-08	-2.8	0.240E-07	0.240E-07	-0.2	0.525E-07	0.501E-07	-4.6
0.85	0.102E-07	0.111E-07	8.6	0.263E-07	0.265E-07	0.6	0.617E-07	0.575E-07	-6.7
0.9	0.141E-07	0.138E-07	-2.7	0.309E-07	0.307E-07	-0.8	0.676E-07	0.656E-07	-3.0
0.95	0.209E-07	0.214E-07	2.4	0.417E-07	0.402E-07	-3.6	0.776E-07	0.756E-07	-2.6
	<b>GW-FEn</b>	<b>GW-Sim</b>	<b>% difference</b>	<b>MK-FEn</b>	<b>MK-Sim</b>	<b>% difference</b>	<b>MS-FEn</b>	<b>MS-Sim</b>	<b>% difference</b>
Mean	0.675E-08	0.695E-08	3.1	0.123E-07	0.120E-07	-2.0	0.190E-07	0.186E-07	-1.7
0.05	0.126E-08	0.121E-08	-3.9	0.437E-09	0.468E-09	7.3	0.324E-08	0.341E-08	5.3
0.1	0.174E-08	0.180E-08	3.6	0.912E-09	0.103E-08	13.4	0.468E-08	0.436E-08	-6.8
0.15	0.219E-08	0.216E-08	-1.5	0.174E-08	0.186E-08	7.0	0.589E-08	0.539E-08	-8.4
0.2	0.257E-08	0.233E-08	-9.2	0.251E-08	0.247E-08	-1.8	0.708E-08	0.629E-08	-11.2
0.3	0.331E-08	0.312E-08	-5.7	0.398E-08	0.390E-08	-2.1	0.977E-08	0.841E-08	-13.9
0.4	0.407E-08	0.401E-08	-1.6	0.603E-08	0.576E-08	-4.4	0.126E-07	0.110E-07	-12.4
0.5	0.501E-08	0.493E-08	-1.7	0.813E-08	0.791E-08	-2.7	0.155E-07	0.148E-07	-4.3
0.6	0.631E-08	0.587E-08	-7.0	0.107E-07	0.106E-07	-0.9	0.195E-07	0.188E-07	-3.4
0.7	0.794E-08	0.791E-08	-0.4	0.141E-07	0.139E-07	-1.7	0.234E-07	0.238E-07	1.4
0.8	0.102E-07	0.104E-07	1.4	0.186E-07	0.186E-07	0.0	0.282E-07	0.286E-07	1.6
0.85	0.120E-07	0.123E-07	2.2	0.219E-07	0.216E-07	-1.3	0.316E-07	0.318E-07	0.7
0.9	0.138E-07	0.139E-07	0.4	0.275E-07	0.265E-07	-3.7	0.363E-07	0.366E-07	0.8
0.95	0.174E-07	0.155E-07	-10.6	0.363E-07	0.357E-07	-1.7	0.447E-07	0.443E-07	-0.8
	<b>RC-FEn</b>	<b>RC-Sim</b>	<b>% difference</b>	<b>RF-FEn</b>	<b>RF-Sim</b>	<b>% difference</b>	<b>WD-FEn</b>	<b>WD-Sim</b>	<b>% difference</b>
Mean	0.157E-07	0.151E-07	-3.7	0.199E-07	0.197E-07	-0.8	0.166E-08	0.200E-08	20.5
0.05	0.123E-08	0.130E-08	5.8	0.437E-08	0.437E-08	0.1	0.138E-09	0.134E-09	-3.0
0.1	0.191E-08	0.177E-08	-7.3	0.617E-08	0.573E-08	-7.0	0.204E-09	0.205E-09	0.3
0.15	0.251E-08	0.237E-08	-5.8	0.759E-08	0.687E-08	-9.5	0.257E-09	0.256E-09	-0.4
0.2	0.339E-08	0.310E-08	-8.4	0.891E-08	0.816E-08	-8.4	0.339E-09	0.352E-09	3.9

Table 16. Frequency of Intersection for the License Application Footprint (Blocks 1, 2, 3, and 5) (Continued)

	RC-FEn	RC-Sim	% difference	RF-FEn	RF-Sim	% difference	WD-FEn	WD-Sim	% difference
0.3	0.468E-08	0.439E-08	-6.1	0.112E-07	0.111E-07	-1.2	0.537E-09	0.539E-09	0.3
0.4	0.741E-08	0.736E-08	-0.7	0.138E-07	0.141E-07	2.5	0.100E-08	0.743E-09	-25.7
0.5	0.977E-08	0.992E-08	1.5	0.170E-07	0.173E-07	1.8	0.123E-08	0.124E-08	0.7
0.6	0.129E-07	0.130E-07	0.5	0.200E-07	0.196E-07	-1.8	0.123E-08	0.124E-08	0.8
0.7	0.174E-07	0.176E-07	1.2	0.234E-07	0.234E-07	-0.3	0.151E-08	0.153E-08	0.9
0.8	0.229E-07	0.230E-07	0.4	0.282E-07	0.283E-07	0.3	0.263E-08	0.229E-08	-12.9
0.85	0.309E-07	0.303E-07	-2.0	0.316E-07	0.321E-07	1.5	0.295E-08	0.293E-08	-0.7
0.9	0.372E-07	0.348E-07	-6.4	0.363E-07	0.379E-07	4.4	0.380E-08	0.382E-08	0.4
0.95	0.525E-07	0.437E-07	-16.7	0.457E-07	0.444E-07	-2.8	0.457E-08	0.535E-08	16.9
	WH-FEn	WH-Sim	% difference	Composite <sup>4</sup> Fen	Composite <sup>4</sup> Sim	% difference			
Mean	0.353E-07	0.357E-07	0.9	0.169E-07	0.168E-07	-0.6			
0.05	0.692E-08	0.702E-08	1.5	0.741E-09	0.743E-09	0.2			
0.1	0.871E-08	0.874E-08	0.4	0.148E-08	0.149E-08	0.4			
0.15	0.102E-07	0.102E-07	-0.1	0.229E-08	0.227E-08	-1.1			
0.2	0.120E-07	0.120E-07	-0.5	0.302E-08	0.296E-08	-2.0			
0.3	0.170E-07	0.164E-07	-3.5	0.457E-08	0.449E-08	-1.8			
0.4	0.234E-07	0.233E-07	-0.6	0.692E-08	0.673E-08	-2.7			
0.5	0.295E-07	0.299E-07	1.3	0.100E-07	0.992E-08	-0.8			
0.6	0.355E-07	0.363E-07	2.2	0.145E-07	0.142E-07	-1.9			
0.7	0.437E-07	0.440E-07	0.8	0.204E-07	0.203E-07	-0.8			
0.8	0.537E-07	0.542E-07	0.9	0.269E-07	0.276E-07	2.6			
0.85	0.603E-07	0.607E-07	0.8	0.331E-07	0.330E-07	-0.5			
0.9	0.692E-07	0.696E-07	0.5	0.407E-07	0.410E-07	0.7			
0.95	0.871E-07	0.891E-07	2.3	0.550E-07	0.533E-07	-3.0			

Output data. DTN: LA0303BY831811.001 [163985]

NOTES: <sup>1</sup>AM = Alex McBirney, BC = Bruce Crowe, GT = George Thompson, GW = George Walker, MK = Mel Kuntz, MS = Michael Sheridan, RC = Richard Carlson, RF = Richard Fisher, WD = Wendell Duffield, WH = William Hackett.

<sup>2</sup>FEn = results from full enumeration, Sim = results from simulations with Latin hypercube sampling.

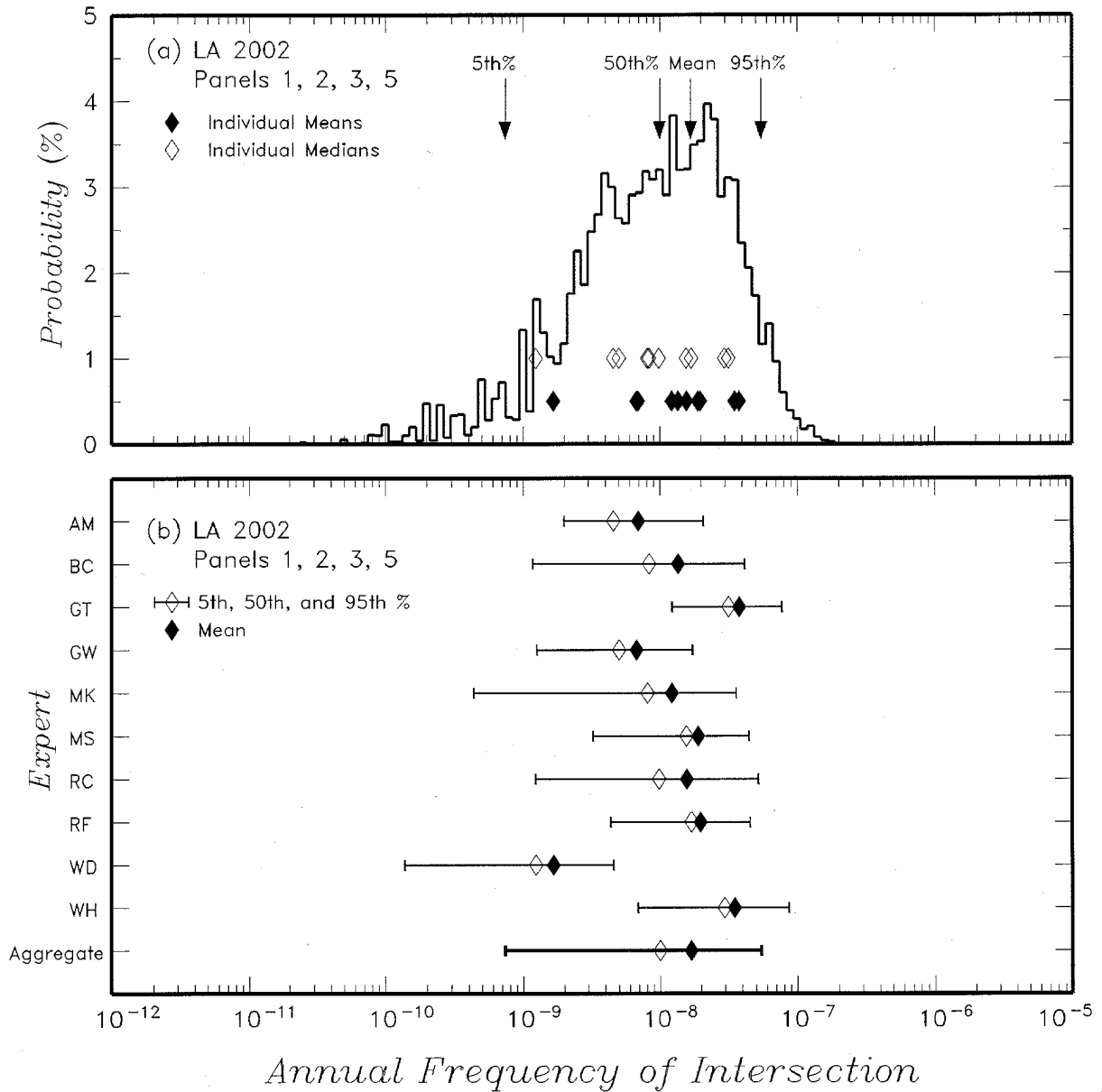
<sup>3</sup>The percent difference is computed as (Sim – FEn)/FEn. It represents the percent difference between the frequency of intersection computed by full enumeration and by simulation.

<sup>4</sup>The composite distributions are computed giving equal weight to the individual expert’s distributions.

The computed distribution for the annual frequency of intersection of the proposed repository footprint by a dike is shown in Figure 20 for the proposed LA repository footprint. Part (a) of Figure 20 shows the computed distributions for the frequency of intersection aggregated over all of the 10 PVHA experts’ interpretations together with the median and mean values obtained for each expert’s interpretation. Part (b) of Figure 20 compares the 5<sup>th</sup> to 95<sup>th</sup> percentile range for frequency of intersection obtained for each expert’s interpretation with that for the aggregate distributions.

The computed mean annual frequency of intersection of the proposed repository footprint by a dike is  $1.7 \times 10^{-8}$  for the LA footprint as compared to  $1.5 \times 10^{-8}$  obtained in the PVHA (CRWMS

M&O 1996 [100116], p. 410). The computed 5<sup>th</sup> and 95<sup>th</sup> percentiles of the uncertainty distribution for frequency of intersection are  $7.4 \times 10^{-10}$  and  $5.5 \times 10^{-8}$ , respectively, as compared to  $5.4 \times 10^{-10}$  and  $4.9 \times 10^{-8}$  obtained in the PVHA (CRWMS M&O 1996 [100116], p. 4-10).



Output Data. DTN: LA0303BY831811.001 [163985]

NOTE: (a) Aggregate distribution and median and means for individual PVHA expert interpretations. (b) Range for 5<sup>th</sup> to 95<sup>th</sup> percentiles for results from individual PVHA expert interpretations compared to range for aggregate distribution. Two-letter code indicates initials of experts from Table 11.

Figure 20. Annual Frequency of Intersecting the Proposed License Application Repository Footprint

The composite uncertainty distributions for frequency of intersection that are the output of these calculations for the proposed LA footprint are located in the output file PVHA-4P.DST in DTN: LA0302BY831811.001 [162670]. The file consists of a title record, a record giving the number of points in the composite distribution, and  $n$  records containing the  $n$  discrete values of frequency of intersection, the associated probability mass, and the cumulative probability (CDF).

### **6.5.3.2 Conditional Distributions for Intersection Length, Azimuth, and Number of Eruptive Centers Within the Proposed License Application Repository Footprint**

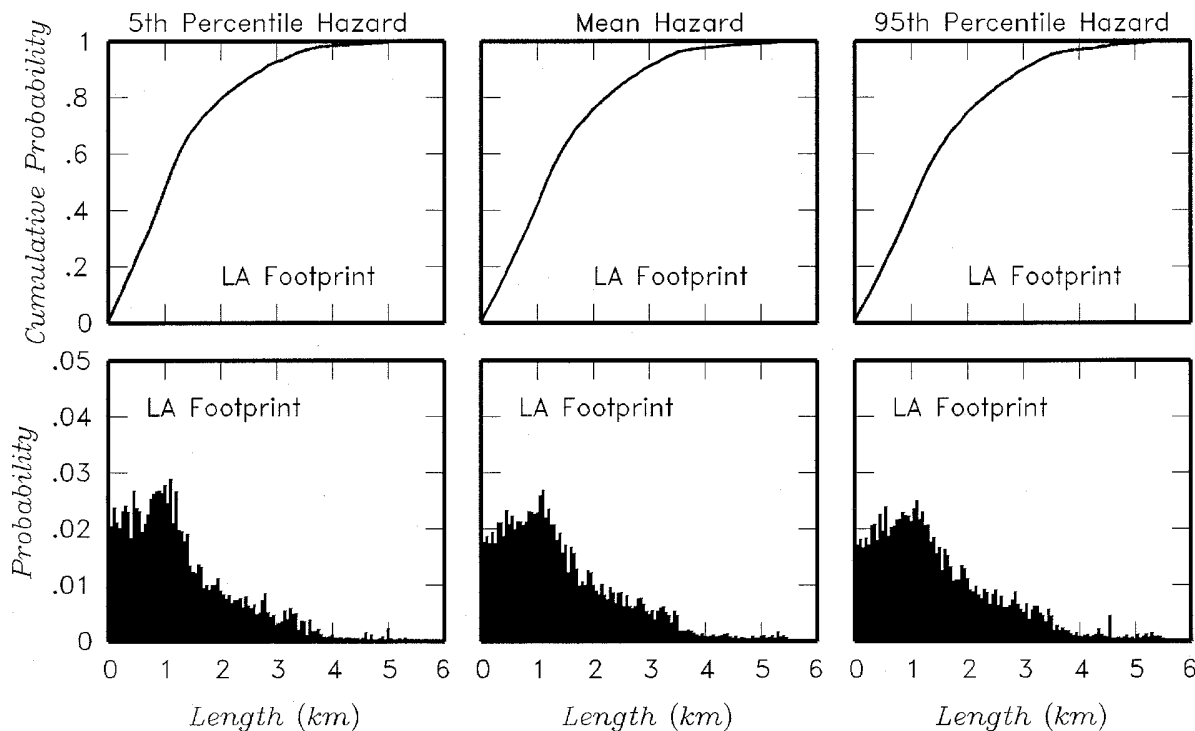
The Latin hypercube sampling process described in Section 6.5.2.2 was used to compute joint distributions for length and azimuth of dike intersection at the mean, 5<sup>th</sup>, and 95<sup>th</sup> frequencies of intersection. At each of these frequencies of intersection distributions for the number of eruptive centers within the proposed repository LA footprint conditional on the length and azimuth within the repository of the intersecting dike system were developed. The joint distributions are listed in three output files (DTN: LA0303BY831811.001 [163985]): file CCSM-LA.CMP provides the joint distribution for length and azimuth of dike intersection and conditional distributions for the number of eruptive centers corresponding to the mean frequency of intersection; file CC05-LA.CMP provides the joint distribution for length and azimuth of dike intersection and conditional distributions for the number of eruptive centers corresponding to the 5<sup>th</sup>-percentile frequency of intersection; and file CC95-LA.CMP provides the joint distribution for length and azimuth of dike intersection and conditional distributions for the number of eruptive centers corresponding to the 95<sup>th</sup>-percentile frequency of exceedance. Each file consists of a title record, a record giving the number of points in the joint distribution for dike intersection length and azimuth, and  $n$  records containing the  $n$  pairs of intersection length and azimuth ( $L_m^I$  and  $f_n$ ) and the joint probability of an intersection having that length and azimuth within the proposed repository. Also listed for each  $L_m^I$  and  $f_n$  pair is the composite conditional distribution for the number of eruptive centers within the proposed repository given the pair  $L_m^I$  and  $f_n$ .

Figures 21, 22, and 23 show the marginal distributions for intersection length, intersection azimuth, and number of eruptive centers for the LA footprint, respectively, computed from the joint distributions described above. These results are also summarized in Tables 17, 18, and 19. The marginal distributions are computed from the joint distributions using software routine MARGIN V1.1 (STN: 10271-1.1-00 [148563]) (Figure 2). The results indicate the degree to which the distributions for length and azimuth of intersecting dikes and the number of eruptive centers vary with frequency of intersection. For example, results listed in Table 17 indicated that similar marginal distributions for dike intersection length are obtained at the 5<sup>th</sup>, mean, and 95<sup>th</sup> frequencies of intersection. The marginal distributions for intersection azimuth obtained at the 5<sup>th</sup>, mean, and 95<sup>th</sup> frequencies of intersection (Table 18) are also similar.

Figure 23 shows the marginal distributions for the number of eruptive centers within the repository footprint obtained using the five alternative approaches for the number and spatial distribution of eruptive centers along the length of the dike system. The *IUD-UC* approach produces the lowest probability of one or more eruptive centers within the proposed repository, approximately 0.4, and the *USRD-FD* approach produces the highest probability, approximately 0.6. The values plotted in Figure 23 are those computed using the five alternative approaches for evaluating the number and spatial distribution of eruptive centers under the assumption that the presence of the proposed repository opening has no effect on the location of eruptive centers.

These distributions are listed in the second through sixth columns of Table 19 under the overall subheading of “Random Location” for the formulation of eruptive center spatial distribution. The seventh column of Table 19 shows the marginal distribution for the weighted average results of the five approaches using the weights described at the end of Section 6.5.2.2 and indicated in the column headings. The eighth column of Table 19 shows the marginal distribution for number of eruptive centers within the proposed repository footprint under the assumption that the presence of the repository openings results in at least one eruptive center within the proposed repository footprint given an intersection. The last column of Table 19 lists the final composite marginal distribution, which represents an equally weighted average of the random location assumption and the renormalized random distributions with  $P(r^{EC} = 0) = 0$  (eighth column). Similar marginal distributions for the number of eruptive centers are obtained at the 5<sup>th</sup>, mean, and 95<sup>th</sup> frequencies of intersection.

The results summarized in Tables 17, 18, and 19 indicated that the distributions for intersecting dike length, intersecting dike azimuth, and number of eruptive centers within the repository footprint show little variation between the 5<sup>th</sup>, mean, and 95<sup>th</sup> frequencies of intersection. Therefore, the results obtained for the mean frequency of intersection can be used to assess the consequences of intrusive and extrusive distribution for all frequencies of intersection.



Output Data. DTN: LA0303BY831811.001 [163985]

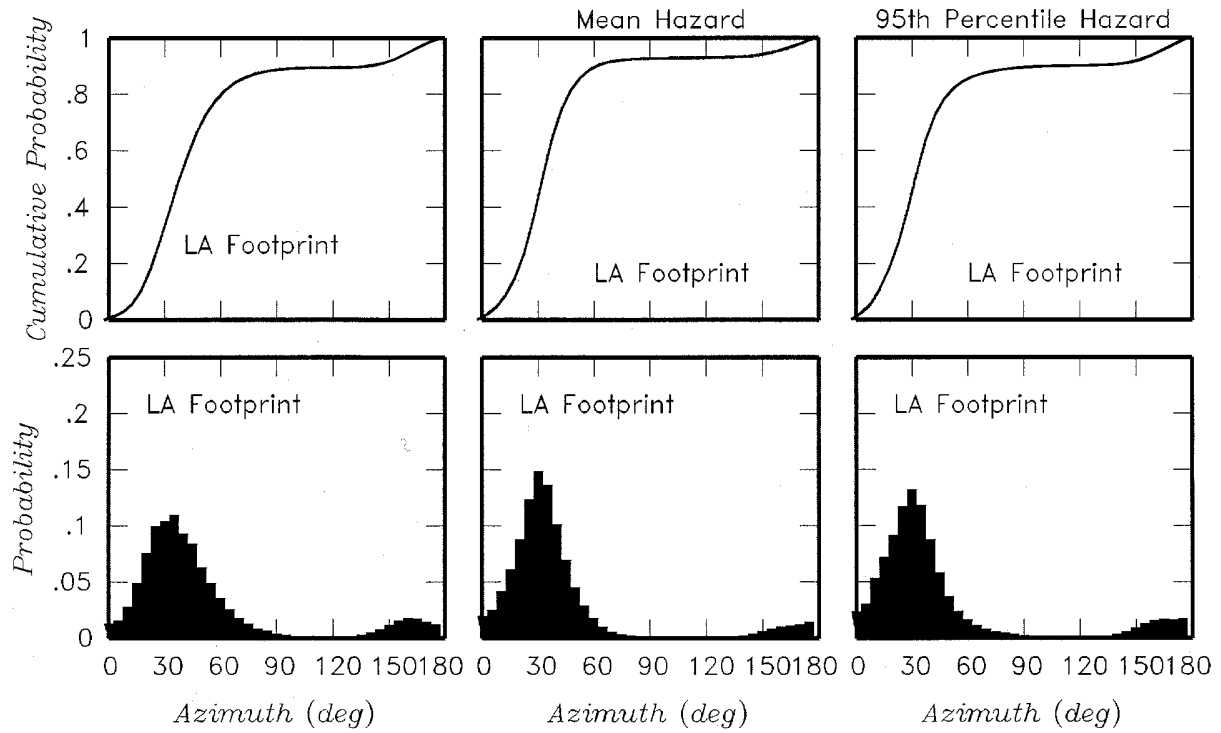
NOTE: These distributions are conditional on the occurrence on an intersection.

Figure 21. Marginal Distributions for Dike Intersection Length,  $L'$ , for the 5th Percentile, Mean, and 95<sup>th</sup> Percentile Frequency of Intersection

Table 17. Marginal Distributions for Dike Intersection Length for the 5th Percentile, Mean, and 95<sup>th</sup> Percentile Frequency of Intersection of the Proposed License Application Footprint

Dike Intersection Length (km)	Probability Mass		
	5 <sup>th</sup> Percentile Frequency of Intersection	Mean Frequency of Intersection	95 <sup>th</sup> Percentile Frequency of Intersection
0.0-0.255	0.1288	0.1088	0.1051
>0.255-0.505	0.1159	0.1048	0.1012
>0.505-0.755	0.1114	0.1054	0.1047
>0.755-1.005	0.1336	0.1128	0.1105
>1.005-1.255	0.1208	0.1189	0.1137
>1.255-1.505	0.0821	0.0909	0.0888
>1.505-1.755	0.0583	0.0674	0.0679
>1.755-2.005	0.0492	0.0553	0.0591
>2.005-2.255	0.0382	0.0430	0.0433
>2.255-2.505	0.0353	0.0421	0.0417
>2.505-2.755	0.0296	0.0323	0.0324
>2.755-3.005	0.0255	0.0318	0.0334
>3.005-3.255	0.0219	0.0263	0.0285
>3.255-3.505	0.0190	0.0226	0.0230
>3.505-3.755	0.0104	0.0089	0.0106
>3.755-4.005	0.0044	0.0055	0.0065
>4.005-4.255	0.0028	0.0043	0.0046
>4.255-4.505	0.0025	0.0050	0.0062
>4.505-4.755	0.0036	0.0028	0.0066
>4.755-5.005	0.0039	0.0033	0.0031
>5.005-5.255	0.0016	0.0036	0.0044
>5.255-5.505	0.0013	0.0042	0.0043
>5.505-5.755	0.0001	0.0003	0.0003

Output data. DTN: LA0307BY831811.001 [164713]



Output Data. DTN: LA0303BY831811.001 [163985]

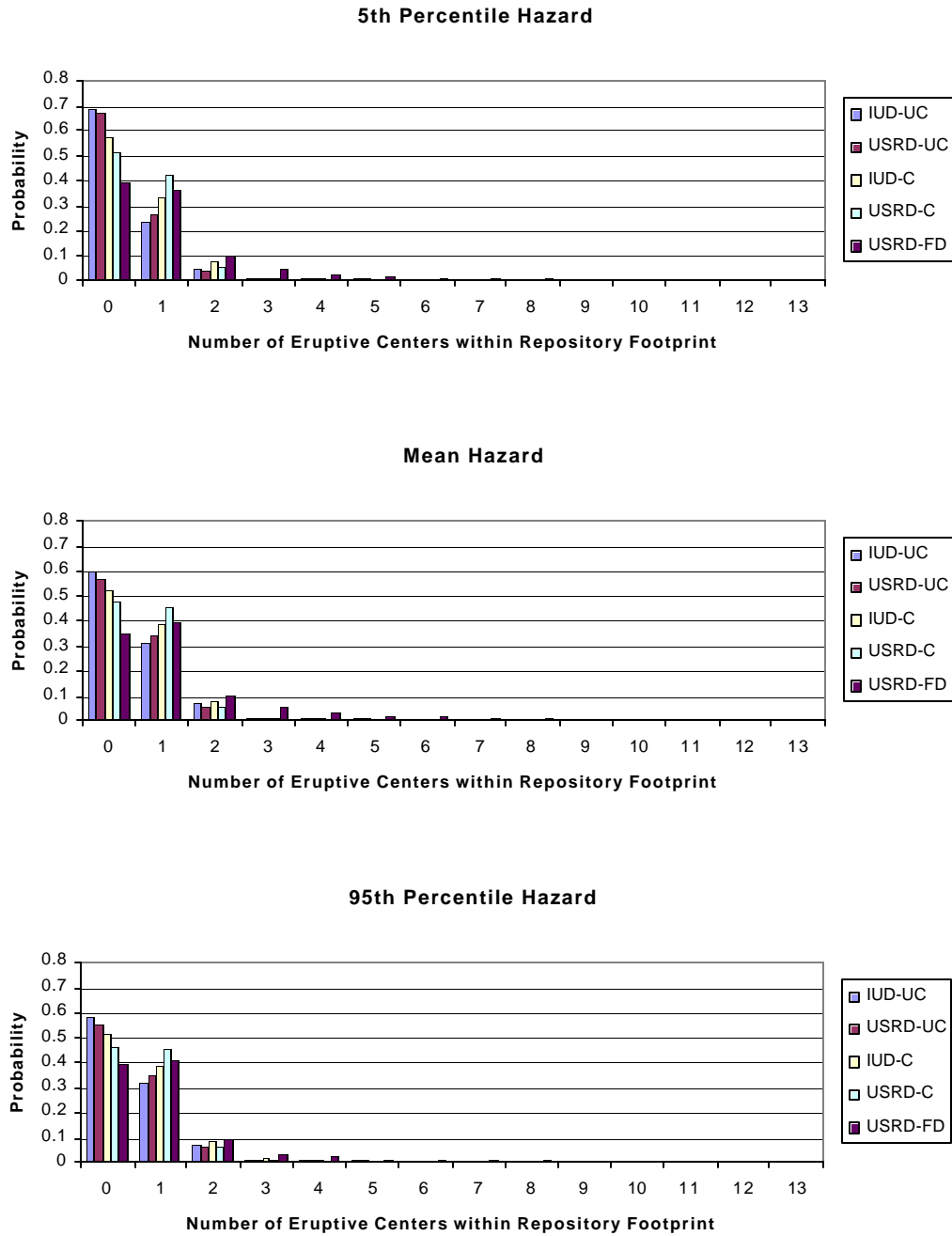
NOTE: These distributions are conditional on the occurrence on an intersection.

Figure 22. Marginal Distributions for Dike Intersection Azimuth,  $f$ , for the 5th Percentile, Mean, and 95<sup>th</sup> Percentile Frequency of Intersection for the Proposed License Application Footprint

Table 18. Marginal Distribution for Intersecting Dike Azimuth for the 5th Percentile, Mean, and 95<sup>th</sup> Percentile Frequency of Intersection of the Proposed License Application Footprint

Intersecting Dike Azimuth (°)	Probability Mass		
	5 <sup>th</sup> percentile Frequency of Intersection	Mean Frequency of Intersection	95 <sup>th</sup> percentile Frequency of Intersection
>-2.5-12.5	0.0560	0.0861	0.1072
>12.5-22.5	0.1240	0.1485	0.1636
>22.5-32.5	0.2030	0.2717	0.2491
>32.5-42.5	0.2015	0.2372	0.2060
>42.5-52.5	0.1463	0.1146	0.0955
>52.5-62.5	0.0841	0.0464	0.0402
>62.5-72.5	0.0431	0.0157	0.0188
>72.5-82.5	0.0209	0.0053	0.0099
>82.5-92.5	0.0102	0.0023	0.0055
>92.5-102.5	0.0043	0.0011	0.0031
>102.5-112.5	0.0013	0.0005	0.0017
>112.5-122.5	0.0005	0.0004	0.0009
>122.5-132.5	0.0019	0.0011	0.0015
>132.5-142.5	0.0072	0.0037	0.0049
>142.5-152.5	0.0193	0.0100	0.0145
>152.5-162.5	0.0327	0.0182	0.0280
>162.5-172.5	0.0316	0.0230	0.0325
>172.5-177.5	0.0121	0.0142	0.0170

Output data. DTN: LA0307BY831811.001 [164713]



Output Data. DTN: LA0303BY831811.001 [163985]

NOTE: IUD = independent; uniformly distributed; USRD = uniformly spaced; randomly distributed; UC = uncorrelated length and number of eruptive centers per volcanic event distributions; C = correlated length and number of eruptive centers per volcanic event distributions; FD = fixed density for number of eruptive centers per volcanic event.

Figure 23. Marginal Distributions for the Number of Eruptive Centers Within the Proposed Repository Footprint,  $r^{FC}$ , for the 5<sup>th</sup> Percentile, Mean, and 95<sup>th</sup> Percentile Frequency of Intersection

Table 19. Marginal Distribution for Number of Eruptive Centers Within the Proposed Repository for the 5th Percentile, Mean, and 95th Percentile Frequency of Intersection of the Proposed License Application Footprint

Number of Eruptive Centers with Proposed Repository $r^{EC}$	Formulation for Eruptive Center Spatial Distribution							Repository Induces Eruptive Center (weight 0.5)	Final Composite Marginal Probability	
	Random Location (weight 0.5)						Weighted Average For Random Location			Renormalized such that $P(r^{EC}=0)=0$
	Independent, Uniformly Distributed, Uncorrelated, <i>IUD-UC</i> (weight 0.05)	Uniformly Spaced, Randomly Distributed, Uncorrelated, <i>USRD-UC</i> (weight 0.15)	Independent, Uniformly Distributed, Correlated, <i>IUD-C</i> (weight 0.075)	Uniformly Spaced, Randomly Distributed, Correlated, <i>USRD-C</i> (weight 0.225)	Uniformly Spaced, Randomly Distributed, Fixed Density, <i>USRD-FD</i> (weight 0.5)					
<b>5<sup>th</sup> Percentile Frequency of Intersection</b>										
0	0.693	0.672	0.571	0.516	0.391	0.490	0	0.245		
1	0.232	0.264	0.328	0.419	0.369	0.355	0.738	0.546		
2	0.0489	0.0414	0.0775	0.0537	0.102	0.0775	0.140	0.109		
3	0.0108	0.0098	0.0171	0.0088	0.0495	0.0300	0.0539	0.0419		
4	0.00688	0.00566	0.00520	0.00159	0.0301	0.0170	0.0273	0.0222		
5	0.00903	0.00728	0.00105	0.00015	0.0186	0.0109	0.0157	0.0133		
6	0	0	0	0	0.0151	0.00755	0.00985	0.00870		
7	0	0	0	0	0.0120	0.00598	0.00762	0.00680		
8	0	0	0	0	0.00677	0.00339	0.00423	0.00381		
9	0	0	0	0	0.00227	0.00114	0.00134	0.00124		
10	0	0	0	0	0.00269	0.00135	0.00166	0.00151		
11	0	0	0	0	0.00078	0.00039	0.00044	0.00041		
12	0	0	0	0	0.00033	0.00016	0.00018	0.00017		
13	0	0	0	0	0.00005	0.00002	0.00003	0.00002		
<b>Mean Frequency of Intersection</b>										
0	0.590	0.568	0.521	0.477	0.348	0.435	0	0.218		
1	0.312	0.347	0.383	0.454	0.390	0.394	0.740	0.567		
2	0.0661	0.0576	0.0756	0.0585	0.104	0.0829	0.134	0.108		
3	0.0140	0.0129	0.0148	0.0085	0.0540	0.0327	0.0533	0.0430		
4	0.00746	0.00616	0.00477	0.00137	0.0349	0.0194	0.0282	0.0238		
5	0.0103	0.00833	0.00097	0.00012	0.0240	0.0139	0.0187	0.0163		
6	0	0	0	0	0.0181	0.00903	0.0111	0.0101		
7	0	0	0	0	0.01271	0.00636	0.00763	0.00699		
8	0	0	0	0	0.00617	0.00308	0.00362	0.00335		
9	0	0	0	0	0.00269	0.00135	0.00154	0.00144		
10	0	0	0	0	0.00171	0.00086	0.00098	0.00092		
11	0	0	0	0	0.00149	0.00075	0.00086	0.00080		
12	0	0	0	0	0.00084	0.00042	0.00049	0.00045		
13	0	0	0	0	0.00010	0.00005	0.00006	0.00005		
<b>95<sup>th</sup> Percentile Frequency of Intersection</b>										
0	0.576	0.551	0.511	0.464	0.393	0.451	0	0.225		
1	0.316	0.355	0.385	0.459	0.410	0.406	0.789	0.597		
2	0.0699	0.0628	0.0795	0.0648	0.087	0.0768	0.118	0.0972		
3	0.0169	0.0155	0.0177	0.0102	0.0362	0.0249	0.0393	0.0321		
4	0.00948	0.00765	0.00591	0.00188	0.0242	0.0146	0.0209	0.0177		

Table 19. Marginal Distribution for Number of Eruptive Centers Within the Proposed Repository for the 5th Percentile, Mean, and 95<sup>th</sup> Percentile Frequency of Intersection of the Proposed License Application Footprint (Continued)

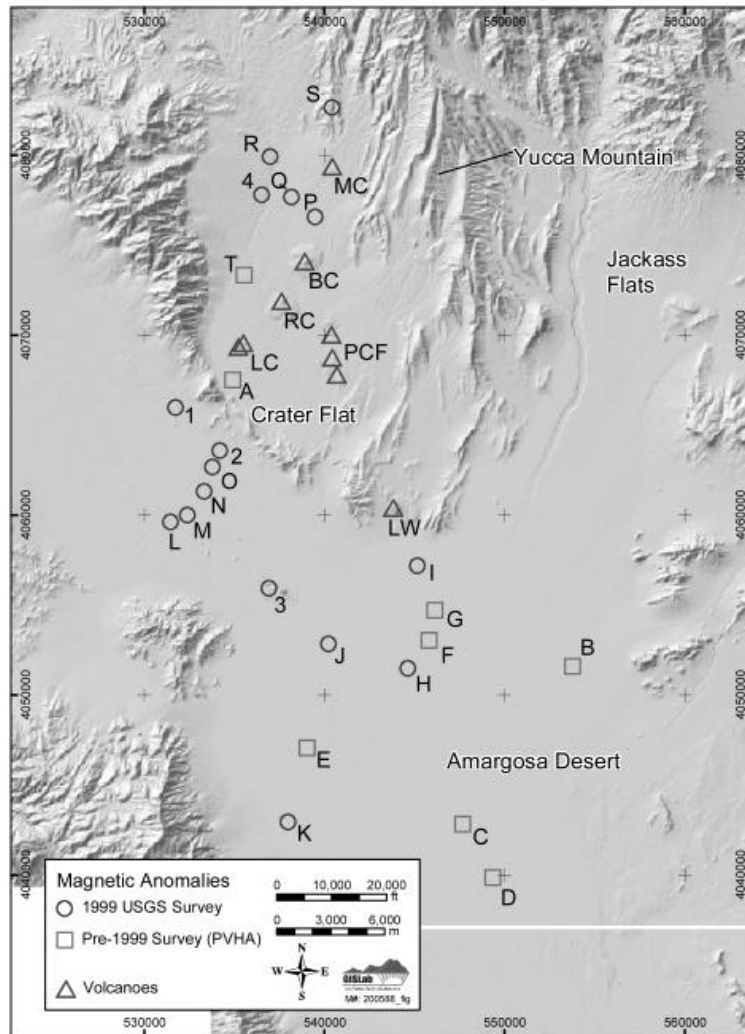
Number of Eruptive Centers with Proposed Repository $r^{EC}$	Formulation for Eruptive Center Spatial Distribution							Final Composite Marginal Probability
	Random Location (weight 0.5)						Repository Induces Eruptive Center (weight 0.5)	
	Independent, Uniformly Distributed, Uncorrelated, <i>IUD-UC</i> (weight 0.05)	Uniformly Spaced, Randomly Distributed, Uncorrelated, <i>USRD-UC</i> (weight 0.15)	Independent, Uniformly Distributed, Correlated, <i>IUD-C</i> (weight 0.075)	Uniformly Spaced, Randomly Distributed, Correlated, <i>USRD-C</i> (weight 0.225)	Uniformly Spaced, Randomly Distributed, Fixed Density, <i>USRD-FD</i> (weight 0.5)	Weighted Average For Random Location	Renormalized such that $P(r^{EC}=0)=0$	
5	0.0114	0.00893	0.00126	0.00017	0.0167	0.0104	0.0142	0.0123
6	0	0	0	0	0.0126	0.00629	0.00764	0.00696
7	0	0	0	0	0.00940	0.00470	0.00558	0.00514
8	0	0	0	0	0.00469	0.00234	0.00271	0.00253
9	0	0	0	0	0.00225	0.00113	0.00126	0.00119
10	0	0	0	0	0.00173	0.00086	0.00098	0.00092
11	0	0	0	0	0.00145	0.00073	0.00082	0.00077
12	0	0	0	0	0.00079	0.00040	0.00045	0.00042
13	0	0	0	0	0.00007	0.00003	0.00004	0.00004

Output data. DTN: LA0307BY831811.001 [164713]

NOTE: Results presented in this table were rounded to at most three significant digits after calculation.

### 6.5.4 Impact of 1999 Aeromagnetic Data on Frequency of Intersection

Anomalies observed in aeromagnetic and ground magnetic data gathered by the USGS and the CNWRA, respectively, since completion of the PVHA suggest the possibility that a number of basaltic volcanic centers are buried beneath alluvium in Crater Flat and the northern Amargosa Desert (Blakely et al. 2000 [151881]; O’Leary et al. 2002 [158468]; Hill and Stamatakos 2002 [159500]). Interpretation of these data indicates that 20 to 24 magnetic anomalies occur within Crater Flat and the northern Amargosa Desert that could represent buried basaltic volcanoes (O’Leary et al. 2002 [158468]; Hill and Stamatakos 2002 [159500]). Of these anomalies, eight were known at the time of the PVHA from previous surveys and were considered as possible volcanic events as part of the PVHA (Figure 24).



Source: Magnetic Anomaly designations are from Hill and Stamatakos 2002. [159500]; (Coordinates from Hill and Stamatakos 2002 [159500])

NOTE: MC = Makani Cone; BC = Black Cone; RC = Red Cone; LC = Little Cones; LW = Lathrop Wells. PCF = Pliocene Crater Flat.

Figure 24. Locations of Potential Buried Basalt Inferred from Aeromagnetic Data

This section summarizes the methodology and results of an evaluation carried out as part of this report to determine the effect of the possible presence of buried volcanic centers on the results of the PVHA. The results of the evaluation are considered non-Q because the input data (O’Leary et al. 2002 [158468]; Hill and Stamatakos 2002 [159500]) were not obtained using Yucca Mountain Project quality procedures. The results are for information only and are not to be used for purposes of assessing repository performance.

Evaluation of the effect on the probability estimate from potential buried volcanic centers requires an estimate of the age of possible buried centers and an assessment of the likelihood that anomalies or groups of anomalies represent buried basaltic volcanic centers.

The probable age range of potential buried volcanic centers was estimated by using a range of calculated sedimentation rates in Crater Flat and the Amargosa Valley and the modeled depth of anomalies from O'Leary et al. 2002 [158468]. For two cases, the basalt in Crater Flat encountered in drill hole VH-2 and the basalt of Anomaly B, sedimentation rates were calculated by dividing the known depth (from drilling) of the buried basalt by the measured age of the basalt. These calculations give sedimentation rates of 0.03 and 0.04 mm/yr, respectively. A third case, Little Cones, has buried flows that have been characterized by ground magnetic surveys (Stamatokos et al. 1997 [138819]). Using a modeled depth to the top of the flows of 15 m, a flow thickness of 10 m, and an age of 0.77-0.98 m.y. (Stamatokos et al. 1997 [138819], p. 328), the calculated sedimentation rate is 0.025-0.32 mm/yr.

Using the range of calculated sedimentation rates discussed above and the modeled burial depth of anomalies (O'Leary et al. 2002 [158468]), minimum and maximum ages were estimated for individual anomalies. Maximum ages for anomalies range from 2.5 to 8.3 m.y., and minimum ages range from 1.25 to 6.25 m.y. The exception to this age range is Anomaly T, which was estimated to be approximately 11 m.y. in age. Consideration of magnetic polarity data adds another age constraint, and a "most likely" age was chosen for each anomaly within the age range estimated for that anomaly. This approach leads to most likely ages for the anomalies that range from 2.6 to 6.3 m.y. All age ranges represent minimum ages (and, thus, are conservative for the purposes of volcanic hazard analysis) because they do not account for the thickness of the basalt bodies in calculating the depth of sediments deposited after basalt was emplaced.

The PVHA experts made evaluations of the likelihood that the magnetic anomalies identified at that time represented buried volcanic centers. An individual expert's confidence that an anomaly represented buried basalt generally depended on the expert's interpretation of the shape, magnetic signature, and geologic setting of the anomaly (CRWMS M&O 1996 [100116]). O'Leary et al. (2002 [158468]) and Hill and Stamatokos (2002 [159500]) used similar criteria to rank their confidence that the 20 to 24 anomalies identified in their reports represent buried basalt using a scale of one to four (O'Leary et al. 2002 [158468]) and high, medium, and low (Hill and Stamatokos 2002 [159500]). Qualitatively, the rankings used in these two reports lead to similar conclusions regarding scientific confidence that particular anomalies represent buried basalt. The number of magnetic anomalies identified in these reports that may represent buried basalt depends upon the resolution of the aeromagnetic data. Hill and Stamatokos (2002 [159500]) suggest that basaltic features with areas smaller than 1 km<sup>2</sup> are generally undetectable using the data presented in O'Leary et al. (2002 [158468]).

The potential impact of the aeromagnetic and ground magnetic data on the probability of igneous disruption of the proposed repository was assessed by developing distributions for the number of volcanic events represented by the anomalies, assigning these events to the volcanic sources defined by the experts in the 1996 PVHA, and calculating the annual frequency of intersection of the proposed repository footprint. The distributions for the number of volcanic events were developed using the tendency of each expert to group, or not group, aligned anomalies into single or multiple volcanic events. Two cases were developed. In the 1996 PVHA, the experts

did not consider all of the anomalies identified at that time to be buried volcanic centers. Instead, to varying degrees, they factored the likelihood that the anomalies represented buried volcanic centers into their assessments of the number of volcanic events that have occurred. Case 1 for this study was developed to be consistent with this approach. The distributions for the number of volcanic events represented by the magnetic anomalies for Case 1 were developed by the authors of this scientific analysis report using the qualitative likelihood that the anomalies represent buried volcanic centers discussed above and using each expert's tendency for including anomalies with various levels of confidence into those experts' distributions for volcanic events. In Case 2, all anomalies were assumed to be buried volcanic centers, and the distributions for the number of volcanic events were developed by the authors of this report based only on each expert's tendency for grouping aligned volcanic centers into events.

The PVHA experts considered the time period of interest for computing the rate of volcanic events in the YMR to range from the past 1 m.y. to the past 10 m.y., with the most likely time period to be the past 4.5 to 5 m.y. With the exception of Anomaly T, the age estimates for the anomalies generally fall within the past 6 m.y. For purposes of these sensitivity analyses, it was assumed that the ages of 22 anomalies (A, B, C, D, E, F, G, H, I, J, K, L, M, N, O, P, Q, R, 1, 2, 3, and 4) fall within the past 4.5- to 5-m.y. time period. The age of Anomaly T was assumed to fall within the past 9 to 10-m.y. time period. Two of the PVHA experts considered a time period of the past 2 m.y. The range in age estimates for Anomalies O, 1, and 2 overlaps the 2-m.y. time period, and, for these sensitivity analyses, these anomalies were given a 50 percent probability of being less than 2 m.y. in age.

Table 20 lists the results of the sensitivity analyses in terms of the mean number of volcanic events occurring within the time period used by the experts to define the rate of volcanic events. For those experts who considered a 5-m.y. time period, the sensitivity analyses indicate an approximate 50 percent increase in the mean number of events for Case 1 (which incorporates the likelihood that the anomalies represent buried volcanic centers) and an approximate 100 percent increase in the mean number of events for Case 2 (which assumes that all of the anomalies represent buried volcanic centers).

Table 20. Comparison of Mean Number of Volcanic Events for 1996 Probabilistic Volcanic Hazard Analysis Assessment with Sensitivity Analysis Values

Expert <sup>a</sup>	Time Period					
	Quaternary			Plio-Quaternary		
	1996	Case 1 <sup>b</sup>	Case 2 <sup>b</sup>	1996	Case 1 <sup>b</sup>	Case 2 <sup>b</sup>
AM	-	-	-	14.5	21.8	27.2
BC	-	-	-	16.7	24.0	29.7
GT	-	-	-	14.5	22.3	29.0
GW	-	-	-	14.8	22.8	30.6
MK	4.1	4.6	5.6	11.1	17.9	25.6
MS	-	-	-	14.4	24.5	25.6
RC	-	-	-	12.0	18.5	24.4
RF	4.4	5.1	5.9	-	-	-
WD	6.6	6.6	6.6	-	-	-
WH	-	-	-	15.7	18.4	30.4
Average	5.0	5.4	6.0	14.2	21.3	27.8

N/A – For Reference Only

NOTES <sup>a</sup> AM = Alexander McBirney; BC = Bruce Crowe; GT = George Thompson; GW = George Walker; MK = Mel Kuntz; MS = Michael Sheridan; RC = Richard Carlson; RF = Richard Fisher; WD = Wandell Duffield; WH = William Hackett.

<sup>b</sup> Case 1 and Case 2 were developed by the authors of this report based on the 1996 PVHA experts' preferences for grouping aligned volcanic centers into volcanic events.

For the two experts who considered a 2-m.y. time period, the sensitivity analyses result in increases of 10 and 20 percent for Case 1 and Case 2, respectively. Duffield considered only a 1-m.y. time period but assigned low probabilities that some of the anomalies are less than 1 m.y. in age (CRWMS M&O 1996 [100116]). Applying this assessment to the larger population of anomalies results in less than a 1-percent increase in the mean number of volcanic events.

For each expert in this sensitivity study, the distributions for the number of volcanic events developed were assigned to the appropriate volcanic sources defined by the PVHA experts. In general, the magnetic anomalies lie within or slightly to the west of the experts' Crater Flat and Amargosa Valley sources. Therefore, for these sensitivity analyses, the volcanic events represented by the magnetic anomalies were assigned to the experts' Crater Flat and Amargosa Valley sources (i.e., source zones, Gaussian fields, kernel density functions) rather than to larger background source zones.

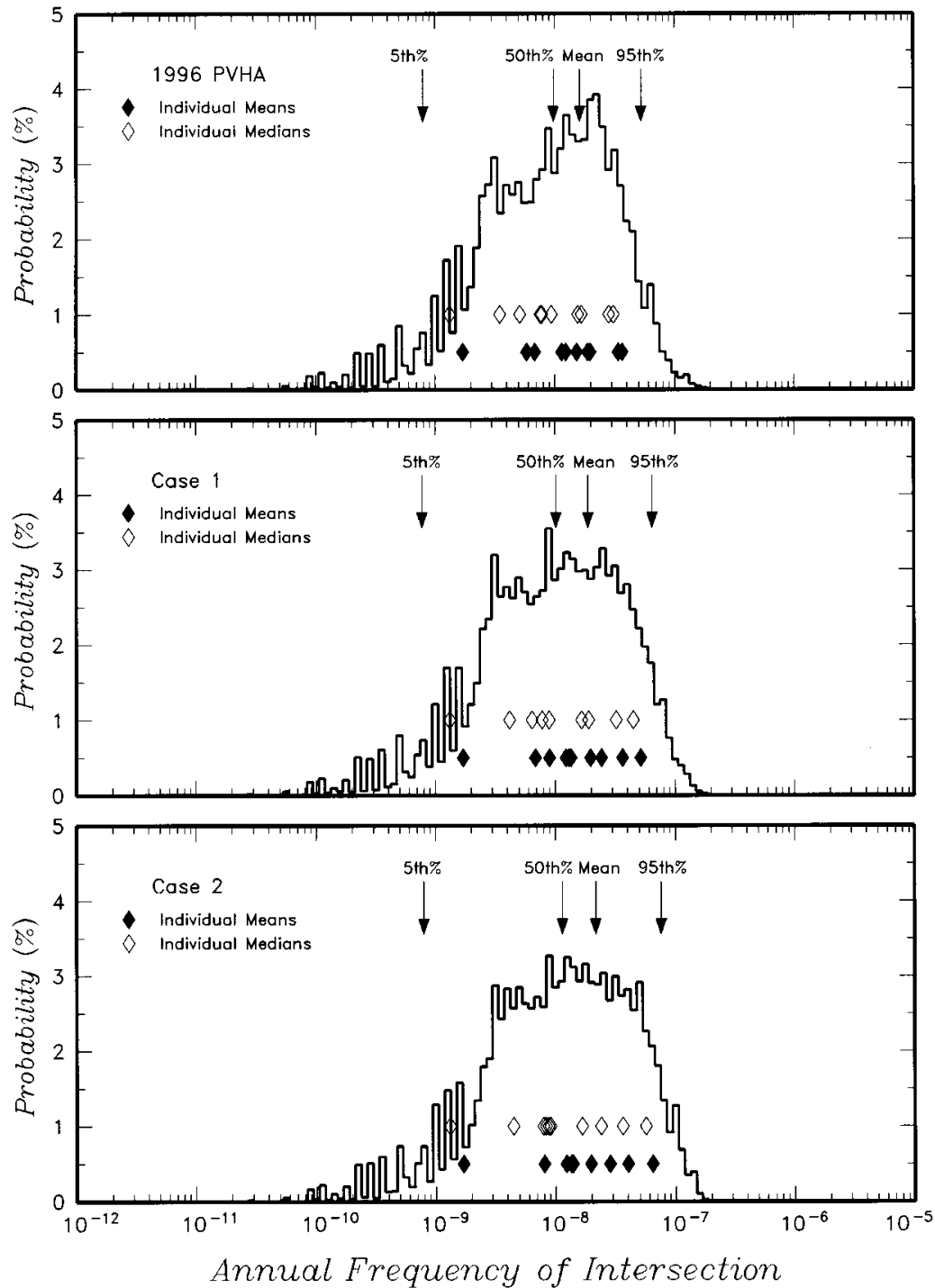
Figures 25 and 26 show the results of the sensitivity analyses in terms of the computed distributions for the frequency of intersection of the proposed repository footprint by a basaltic dike. The footprint used for these analyses is the 70,000-MTU no-backfill repository layout (primary-plus-contingency blocks) used in the previous version (Revision 00 ICN 01) of this report (CRWMS M&O 2000 [151551]). Use of this footprint results in approximately 6 percent lower frequencies of intersections than if the proposed LA footprint had been used to assess the impact (based on comparison of the mean annual frequency of intersection from the two footprints). The results are summarized in Table 21. The volcanic event count distributions developed for sensitivity Case 1 result in a 22-percent increase in the mean annual frequency of intersection, and those for sensitivity Case 2 result in a 40-percent increase. The increase in the frequency of intersection is less than the increase in the mean number of volcanic events because

the additional events are located in the more active volcanic sources to the west of the site. As indicated in Figure 17, a significant portion of the volcanic hazard results from the occurrence of volcanic events near or to the northeast of the proposed repository, areas in which the estimated rate of volcanic events is not greatly affected by inclusion of the additional magnetic anomalies in the volcanic event count distributions.

Table 21. Summary of Computed Frequency of Intersection for 70,000-Metric Tons of Uranium No-Backfill Repository Layout (primary + contingency blocks) from Sensitivity Cases

Input Parameters	Annual Frequency of Intersection			
	5 <sup>th</sup> percentile	50 <sup>th</sup> percentile	Mean	95 <sup>th</sup> percentile
1996 PVHA	7.9E-10	9.8E-09	1.6E-08	5.2E-08
Sensitivity Case 1	7.8E-10	1.0E-08	1.9E-08	6.5E-08
Sensitivity Case 2	7.9E-10	1.1E-08	2.2E-08	7.6E-08

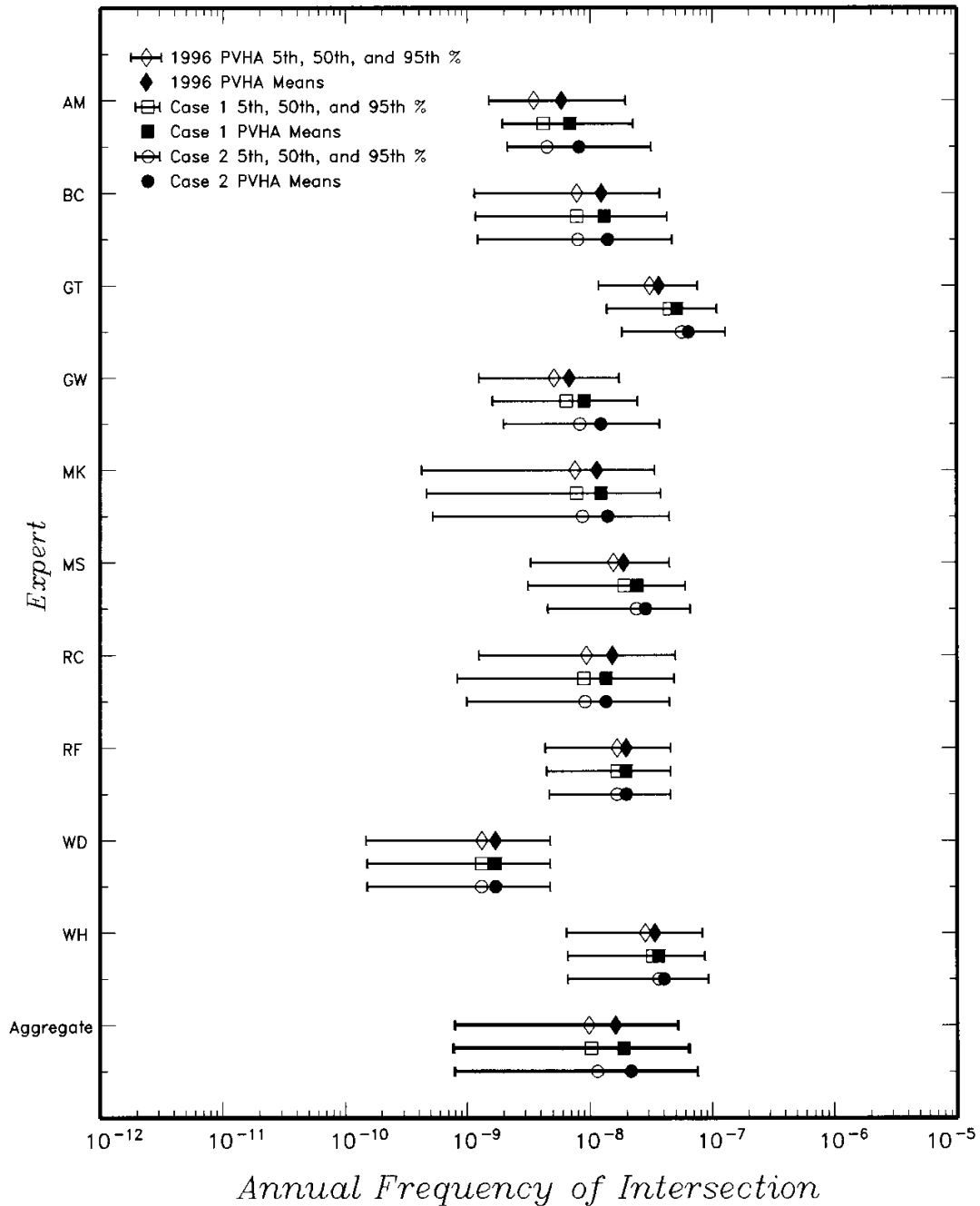
NOTE: N/A - Reference only



N/A -For Reference Only

NOTE: Results labeled 1996 use the PVHA volcanic event counts; results labeled Case 1 and Case 2 use the volcanic event counts developed in this sensitivity analysis.

Figure 25. Composite Annual Frequency of Intersection of the Repository Footprint for Sensitivity Cases for the Primary-plus-Contingency Block Case of the 70,000-Metric Tons of Uranium No-Backfill Layout



N/A – For Reference Only

NOTE: Results labeled 1996 use the PVHA volcanic event counts; results labeled Case 1 and Case 2 use the volcanic event counts developed for the sensitivity cases.

Figure 26. Individual Expert Results for Annual Frequency of Intersection of the Proposed Repository Footprint for Sensitivity Cases for the Primary-plus-Contingency Block Case of the 70,000-Metric Tons of Uranium No-Backfill Layout

## 7. CONCLUSIONS

### 7.1 SUMMARY OF SCIENTIFIC ANALYSIS

The result of the PVHA (CRWMS M&O 1996 [100116]) has been recalculated using PVHA outputs to account for the proposed LA repository footprint (the outline of the waste emplacement area) and extended to include the probability of an eruption within the proposed LA repository footprint, conditional on a dike intersection (Table 22). A conceptual framework for the probability calculations, based on PVHA outputs and subsequent studies, accounts for deep (mantle) and shallow (structural control) processes that influence volcanic event distribution and recurrence rate in the YMR. The framework presented here emphasizes the close correlation between the distribution of volcanic events and areas of crustal extension and faulting in the YMR, and within this context, the appropriateness of volcanic source zone boundaries defined in the PVHA. It also emphasizes the appropriate selection of parameter distributions that affect probability models and provides support for comparison of alternative scenarios and parameter selection, within the framework of the volcanic history of the YMR. Alternative models presented by Connor et al. (2000 [149935]) that result in higher eruption probabilities ( $10^{-7}$  versus  $1.3 \times 10^{-8}$  per year) than those presented here are found to employ input parameters that either represent extreme values (e.g., event length) or assume a specific geologic control (i.e., crustal density) on spatial distribution while not considering more defensible and observable controls (i.e., crustal extension and structure). Spatial density models weighted by crustal density result in higher event frequencies at the proposed repository site, while the same models weighted by an alternative geologic control such as cumulative crustal extension across the Crater Flat structural domain would likely lead to decreased event frequencies at the site. Connor et al. (2000 [149935]) state that the highest value ( $10^{-7}$  per year) in their range of calculated probability values ( $10^{-8}$ – $10^{-7}$  per year) cannot be considered more or less likely than any other value they have calculated using alternative probability models. The analysis in this report suggests that the choice of input parameters used by Connor et al. (2000 [149935]) compared to those used in the PVHA logically places their highest probability value at the extreme upper tail of a probability distribution.

The annual frequency of intersection of the proposed repository footprint by a dike or dike system associated with a volcanic event and the annual frequency of a volcanic event producing one or more eruptive centers within the proposed repository have been recalculated, based on the current proposed repository footprint. These results are summarized in Table 22. The annual frequency of disruption of the repository by one or more eruptive centers is obtained by multiplying the frequency of intersection from Figure 20 by the conditional probability of the occurrence of at least one eruptive center (1 minus the conditional probability of 0 centers) from the right-hand column of Table 19. It is important to note that the reported values represent the annual frequencies of intrusive and extrusive disruption of the repository waste emplacement footprint by a volcanic event includes the possibility for multiple parallel dikes (see definition of volcanic event at the beginning of Section 6.5). For assessing the consequences of igneous intrusion, users of the results of this scientific analysis must consider the distribution for the number of parallel dikes associated with a volcanic event.

Conditional distributions for the length and azimuth of the intersecting dike and the number of eruptive centers occurring within the proposed repository footprint are developed for the three values of frequency of intersection in Table 22. These distributions are very similar for the three levels of frequency of intersection. Because of this similarity, it is appropriate to use the conditional distributions obtained for the mean frequency of intersection to perform consequence analyses and as input to TSPA, as described below in Section 7.2.

The inputs to this scientific analysis report are the results of an expert elicitation conducted in a manner consistent with the guidance in the Branch Technical Position on Expert Elicitation (Kotra et al. 1996 [100909]). The PVHA experts explicitly quantified the uncertainties in their interpretations and they are represented in the outputs of this report in the form of probability distributions. Thus, it is concluded that the results of this report form an appropriate basis for the evaluation of the consequences of volcanic hazards in the YMR. YMRP (NRC 2003 [163274]) acceptance criteria have been met as described in Attachment I of this report.

Table 22. Summary Frequencies of Disruptive Volcanic Events for the License Application Footprint

Annual Frequency of Intersection of Proposed Repository by a Volcanic Event	Composite Conditional Probability of at Least One Eruptive Center	Annual Frequency of Occurrence of One or More Eruptive Centers within Proposed Repository
$7.4 \times 10^{-10}$ (5 <sup>th</sup> percentile)	0.75	$5.6 \times 10^{-10}$
$1.7 \times 10^{-8}$ (mean)	0.78	$1.3 \times 10^{-8}$
$5.5 \times 10^{-8}$ (95 <sup>th</sup> percentile)	0.77	$4.3 \times 10^{-8}$

DTN: LA0307BY831811.001 [164713] (Output data)

NOTE: Results presented in this table were rounded to two significant digits after calculation.

## 7.2 OUTPUTS BASED ON THE PROPOSED LICENSE APPLICATION FOOTPRINT (BLOCKS 1, 2, 3, AND 5)

The outputs of this scientific analysis report based on the proposed LA Footprint are described in detail in Section 6.5.3. They are summarized as the following.

1. A discrete probability distribution for the annual frequency of intersection of the proposed repository emplacement area footprint by a dike or dike system. This distribution is given in output file PVHA-4PA.DST (DTN: LA0307BY831811.001 [164713]). The file contains three columns of data. The first column contains discrete values for the annual frequency of intersection. The second column contains the probability mass associated with each frequency of intersection. The third column contains the cumulative probability that the frequency of intersection is equal to or lower than the corresponding value in the third first.
2. A discrete probability distribution for the annual frequency of disruption of the proposed repository emplacement area footprint by one or more eruptive centers. This distribution is obtained by multiplying the first column of output file PVHA-4PA.DST (DTN: LA0302BY831811.001 [162670]) by 0.782, the conditional probability of disruption by at least one eruptive center, given intersection of the repository. As

discussed in Sections 6.5.3.2 and 7.1, it is considered appropriate to use the conditional probability obtained for the mean frequency of intersection to define the full distribution for frequency of extrusive disruption.

3. Conditional joint probability distributions for length and azimuth of an intersecting dike, and number of eruptive centers within the proposed repository LA footprint, output files CCSM-LA.CMP, CC05-LA.CMP, and CC95-LA.CMP (DTN: LA0302BY831811.001 [162670]). As discussed in Sections 6.5.3.2 and 7.1, it is considered appropriate to use the distributions obtained for the mean frequency of intersection (output file CCSM-LA.CMP) to evaluate consequences at all frequencies of intersection.

Because the proposed LA footprint is the current proposed repository design, the outputs from the calculations based on this particular repository layout and presented in this report will be used as input to revisions of the *Number of Waste Packages Hit by Igneous Intrusion* report (BSC 2003 [161851]) and as inputs to TSPA-LA.

### 7.3 UNCERTAINTIES

The data and parameter inputs to the PVHA, as well as their uncertainty, were defined as part of the expert elicitation process. All of the uncertainties defined by the elicitation process were fully propagated through the probability models and are reflected in the final probability distribution. Selection of particular parameter values, ranges, and bounding assumptions for conceptual models were arrived at through the process of expert elicitation. The contributions to uncertainty from each of the PVHA components are described in CRWMS M&O (1996 [100116], Section 4.2) and Section 6.3.1.5 of this scientific analysis report.

## 8. INPUTS AND REFERENCES

### 8.1 DOCUMENTS CITED

The following is a list of the references cited in this document. Column 1 represents the unique six-digit numerical identifier (the Document Input Reference System [DIRS] number), which is placed in the text following the reference callout (e.g., BSC 2002 [155950]). The purpose of these numbers is to assist the reader in locating a specific reference in the DIRS database. Within the reference list, multiple sources by the same author and date (e.g., BSC 2002) are alphabetically by title.

- 160533 AP-SV.1Q, Rev. 0, ICN 3. *Control of the Electronic Management of Information*. Washington, D.C.: U.S. Department of Energy, Office of Civilian Radioactive Waste Management. ACC: MOL.20020917.0133.
- 151881 Blakely, R.J.; Langenheim, V.E.; Ponce, D.A.; and Dixon, G.L. 2000. *Aeromagnetic Survey of the Amargosa Desert, Nevada and California: A Tool for Understanding Near-Surface Geology and Hydrology*. Open-File Report 00-188. Denver, Colorado: U.S. Geological Survey. TIC: 248767.

- 100022 Brocher, T.M.; Hunter, W.C.; and Langenheim, V.E. 1998. "Implications of Seismic Reflection and Potential Field Geophysical Data on the Structural Framework of the Yucca Mountain-Crater Flat Region, Nevada." *Geological Society of America Bulletin*, 110 (8), 947-971. Boulder, Colorado: Geological Society of America. TIC: 238643.
- 147772 Brocoum, S.J. 1997. "Evaluation of Data Provided at U.S. Department of Energy (DOE) and U.S. Nuclear Regulatory Commission (NRC) Igneous Activity Technical Exchange, February 25-26, 1997." Letter from S.J. Brocoum (DOE/OCRWM) to J.T. Greeves (NRC), June 4, 1997, with enclosure. ACC: MOL.19970722.0276; MOL.19970722.0277.
- 160313 BSC (Bechtel SAIC Company) 2002. *Scientific Processes Guidelines Manual*. MIS-WIS-MD-000001 REV 01. Las Vegas, Nevada: Bechtel SAIC Company. ACC: MOL.20020923.0176.
- 159527 BSC 2002. *Repository Design, Repository/PA IED Subsurface Facilities Plan Sht. 1 of 5, Sht. 2. of 5, Sht. 3 of 5, Sht. 4 of 5, and Sht. 5 of 5*. DWG-MGR-MD-000003 REV A. Las Vegas, Nevada: Bechtel SAIC Company. ACC: MOL.20020601.0194.
- 158966 BSC 2002. *The Enhanced Plan for Features, Events, and Processes (FEPs) at Yucca Mountain*. TDR-WIS-PA-000005 REV 00. Las Vegas, Nevada: Bechtel SAIC Company. ACC: MOL.20020417.0385.
- 161315 BSC 2002. *Technical Work Plan for: Igneous Activity Analysis for Disruptive Events*. TWP-WIS-MD-000007 REV 02. Las Vegas, Nevada: Bechtel SAIC Company. ACC: MOL.20030107.0009.
- 161838 BSC 2003. *Characterize Eruptive Processes at Yucca Mountain, Nevada*. ANL-MGR-GS-000002 REV 01. Las Vegas, Nevada: Bechtel SAIC Company.
- 161851 BSC 2003. *Number of Waste Packages Hit by Igneous Intrusion*. ANL-MGR-GS-000003 REV 00. Las Vegas, Nevada: Bechtel SAIC Company.
- 162289 BSC (Bechtel SAIC Company) 2003. *Repository Design, Repository/PA IED Subsurface Facilities*. 800-IED-EBS0-00401-000-00C. Las Vegas, Nevada: Bechtel SAIC Company. ACC: ENG.20030303.0002.
- 101859 Byers, F.M., Jr. and Barnes, H. 1967. *Geologic Map of the Paiute Ridge Quadrangle, Nye and Lincoln Counties, Nevada*. Map GQ-577. Washington, D.C.: U.S. Geological Survey. ACC: HQS.19880517.1104.
- 161770 Canori, G.F. and Leitner, M.M. 2003. *Project Requirements Document*. TER-MGR-MD-000001 REV 01. Las Vegas, Nevada: Bechtel SAIC Company. ACC: DOC.20030404.0003.

- 102646 Connor, C.B. and Hill, B.E. 1995. "Three Nonhomogeneous Poisson Models for the Probability of Basaltic Volcanism: Application to the Yucca Mountain Region, Nevada." *Journal of Geophysical Research*, 100 (B6), 10,107-10,125. Washington, D.C.: American Geophysical Union. TIC: 237682.
- 135969 Connor, C.B.; Stamatakos, J.; Ferrill, D.; Hill, B.E.; Magsino, S.B.L.; La Femina, P.; and Martin, R.H. 1997. "Integrating Structural Models into Probabilistic Volcanic Hazard Analyses: An Example from Yucca Mountain, NV." *Abstracts with Programs – Geological Society of America*, 28, (7), A-192. Boulder, Colorado: Geological Society of America. TIC: 247409.
- 149935 Connor, C.B.; Stamatakos, J.A.; Ferrill, D.A.; Hill, B.E.; Ofoegbu, G.I.; Conway, F.M.; Sagar, B.; and Trapp, J. 2000. "Geologic Factors Controlling Patterns of Small-Volume Basaltic Volcanism: Application to a Volcanic Hazards Assessment at Yucca Mountain, Nevada." *Journal of Geophysical Research*, 105, (B1), 417–432. Washington, D.C.: American Geophysical Union. TIC: 247906.
- 100973 Crowe, B.M. and Perry, F.V. 1990. "Volcanic Probability Calculations for the Yucca Mountain Site: Estimation of Volcanic Rates." *Proceedings of the Topical Meeting on Nuclear Waste Isolation in the Unsaturated Zone, FOCUS '89, September 17-21, 1989, Las Vegas, Nevada*. Pages 326-334. La Grange Park, Illinois: American Nuclear Society. TIC: 212738.
- 102741 Crowe, B.M.; Johnson, M.E.; and Beckman, R.J. 1982. "Calculation of the Probability of Volcanic Disruption of a High-Level Radioactive Waste Repository Within Southern Nevada, USA." *Radioactive Waste Management and the Nuclear Fuel Cycle*, 3 (2), 167–190. New York, New York: Harwood Academic Publishers. TIC: 222179.
- 100026 Crowe, B.M.; Perry, F.V.; Valentine, G.A.; Wallmann, P.C.; and Kossik, R. 1993. "Simulation Modeling of the Probability of Magmatic Disruption of the Potential Yucca Mountain Site." *Proceedings of the Topical Meeting on Site Characterization and Model Validation, Focus '93, September 26-29, 1993*. Pages 182-191. La Grange Park, Illinois: American Nuclear Society. TIC: 102245.
- 100110 Crowe, B.; Perry, F.; Geissman, J.; McFadden, L.; Wells, S.; Murrell, M.; Poths, J.; Valentine, G.A.; Bowker, L.; and Finnegan, K. 1995. *Status of Volcanism Studies for the Yucca Mountain Site Characterization Project*. LA-12908-MS. Los Alamos, New Mexico: Los Alamos National Laboratory. ACC: HQO.19951115.0017.
- 100116 CRWMS M&O (Civilian Radioactive Waste Management System Management and Operating Contractor). 1996. *Probabilistic Volcanic Hazard Analysis for Yucca Mountain, Nevada*. BA0000000-01717-2200-00082, Rev 0. Las Vegas, Nevada: CRWMS M&O. ACC: MOL.19971201.0221.

- 106102 CRWMS M&O 1998. "Disruptive Events." Chapter 10 of *Total System Performance Assessment–Viability Assessment (TSPA-VA) Analyses Technical Basis Document*. B00000000-01717-4301-00010, REV 00. Las Vegas, Nevada: CRWMS M&O. ACC: MOL.19980724.0399.
- 100129 CRWMS M&O 1998. "Geochemistry." Book 3 - Section 6 of *Yucca Mountain Site Description*. B00000000-01717-5700-00019 REV 00. Las Vegas, Nevada: CRWMS M&O. ACC: MOL.19980729.0052.
- 105347 CRWMS M&O 1998. *Synthesis of Volcanism Studies for the Yucca Mountain Site Characterization Project*. Deliverable 3781MR1. Las Vegas, Nevada: CRWMS M&O. ACC: MOL.19990511.0400.
- 151551 CRWMS M&O 2000. *Characterize Framework for Igneous Activity at Yucca Mountain, Nevada*. ANL-MGR-GS-000001 REV 00 ICN 01. Las Vegas, Nevada: CRWMS M&O. ACC: MOL.20001221.0001.
- 151553 CRWMS M&O 2000. *Features, Events, and Processes: Disruptive Events*. ANL-WIS-MD-000005 REV 00 ICN 1. Las Vegas, Nevada: CRWMS M&O. ACC: MOL.20001218.0007.
- 153246 CRWMS M&O 2000. *Total System Performance Assessment for the Site Recommendation*. TDR-WIS-PA-000001 REV 00 ICN 01. Las Vegas, Nevada: CRWMS M&O. ACC: MOL.20001220.0045.
- 100027 Day, W.C.; Dickerson, R.P.; Potter, C.J.; Sweetkind, D.S.; San Juan, C.A.; Drake, R.M., II; and Fridrich, C.J. 1998. *Bedrock Geologic Map of the Yucca Mountain Area, Nye County, Nevada*. Geologic Investigations Series I-2627. Denver, Colorado: U.S. Geological Survey. ACC: MOL.19981014.0301.
- 145370 Delaney, P.T. and Gartner, A.E. 1997. "Physical Processes of Shallow Mafic Dike Emplacement Near the San Rafael Swell, Utah." *Geological Society of America Bulletin*, 109 (9), 1177–1192. Boulder, Colorado: Geological Society of America. TIC: 247421.
- 100550 DOE (U.S. Department of Energy). 1998. *Total System Performance Assessment*. Volume 3 of *Viability Assessment of a Repository at Yucca Mountain*. DOE/RW-0508. Washington, D.C.: U.S. Department of Energy, Office of Civilian Radioactive Waste Management. ACC: MOL.19981007.0030.
- 147778 Earthfield Technology. 1995. *Summary Report: Magnetic and Gravity Study of the Yucca Mountain Area, Nevada*. Houston, Texas: Earthfield Technology. ACC: MOL.20000228.0374.
- 105284 Farmer, G.L.; Perry, F.V.; Semken, S.; Crowe, B.; Curtis, D.; and DePaolo, D.J. 1989. "Isotopic Evidence on the Structure and Origin of Subcontinental Lithospheric Mantle in Southern Nevada." *Journal of Geophysical Research*, 94, (B6), 7885-7898. Washington, D.C.: American Geophysical Union. TIC: 201800.

- 105078 Feighner, M.A. and Majer, E.L. 1996. *Results of the Analysis of the Timber Mt., Lathrop Wells, and Yucca Mt. Aeromagnetic Data*. Milestone SPT23KM4. Berkeley, California: Lawrence Berkeley National Laboratory. ACC: MOL.19971204.0767.
- 105315 Ferrill, D.A.; Stamatakos, J.A.; Jones, S.M.; Rahe, B.; McKague, H.L.; Martin, R.H.; and Morris, A.P. 1996. "Quaternary Slip History of the Bare Mountain Fault (Nevada) from the Morphology and Distribution of Alluvial Fan Deposits." *Geology*, 24, (6), 559–562. Boulder, Colorado: Geological Society of America. TIC: 234557.
- 154365 Freeze, G.A.; Brodsky, N.S.; and Swift, P.N. 2001. *The Development of Information Catalogued in REV00 of the YMP FEP Database*. TDR-WIS-MD-000003 REV 00 ICN 01. Las Vegas, Nevada: Bechtel SAIC Company. ACC: MOL.20010301.0237.
- 118942 Fridrich, C.J. 1999. "Tectonic Evolution of the Crater Flat Basin, Yucca Mountain Region, Nevada." Chapter 7 of *Cenozoic Basins of the Death Valley Region*. Wright, L.A. and Troxel, B.W., eds. Special Paper 333. Boulder, Colorado: Geological Society of America. TIC: 248054.
- 107333 Fridrich, C.J.; Whitney, J.W.; Hudson, M.R.; and Crowe, B.M. 1999. "Space-Time Patterns of Late Cenozoic Extension, Vertical Axis Rotation, and Volcanism in the Crater Flat Basin, Southwest Nevada." Chapter 8 of *Cenozoic Basins of the Death Valley Region*. Wright, L.A., and Troxel, B.W., eds. Special Paper 333. pp. 197-212. Boulder, Colorado: Geological Society of America. TIC: 248054.
- 107255 Heizler, M.T.; Perry, F.V.; Crowe, B.M.; Peters, L.; and Appelt, R. 1999. "The Age of Lathrop Wells Volcanic Center: An  $^{40}\text{Ar}/^{39}\text{Ar}$  Dating Investigation." *Journal of Geophysical Research*, 104 (B1), 767–804. Washington, D.C.: American Geophysical Union. TIC: 243399.
- 159500 Hill, B.E. and Stamatakos, J.A. 2002. *Evaluation of Geophysical Information Used to Detect and Characterize Buried Volcanic Features in the Yucca Mountain Region*. San Antonio, Texas: Center for Nuclear Waste Regulatory Analyses. TIC: 252846.
- 140152 Ho, C.-H. and Smith, E.I. 1998. "A Spatial-Temporal/3-D Model for Volcanic Hazard Assessment: Application to the Yucca Mountain Region, Nevada." *Mathematical Geology*, 30 (5), 497–510. New York, New York: Plenum Publishing Corporation. TIC: 245110.
- 106194 Hudson, M.R.; Minor, S.A.; and Fridrich, C.J. 1996. "The Distribution, Timing, and Character of Steep-Axis Rotations in a Broad Zone of Dextral Shear in Southwestern Nevada." *Abstracts with Programs*, 28, (7), A-451. Boulder, Colorado: Geological Society of America. TIC: 234723.

- 100909 Kotra, J.P.; Lee, M.P.; Eisenberg, N.A.; and De Wispelare, A.R. 1996. *Branch Technical Position on the Use of Expert Elicitation in the High-Level Radioactive Waste Program*. NUREG-1563. Washington, D.C.: U.S. Nuclear Regulatory Commission. TIC: 226832.
- 148622 Langenheim, V.E.; Kirchoff-Stein, K.S., and Oliver, H.W. 1993. "Geophysical Investigations of Buried Volcanic Centers Near Yucca Mountain, Southwest Nevada." *High-Level Radioactive Waste Management, Proceedings of the Fourth Annual International Conference, Las Vegas, Nevada, April 26-30, 1993*. 2, 1840-1846. La Grange Park, Illinois: American Nuclear Society. TIC: 208542.
- 162310 Livaccari, R.F. and Perry, F.V. 1993. "Isotopic Evidence for Preservation of Cordilleran Lithospheric Mantle During the Sevier-Laramide Orogeny, Western United States." *Geology*, 21, 719–722.
- 147781 Magsino, S.L.; Connor, C.B.; Hill, B.E.; Stamatakos, J.A.; La Femina, P.C.; Sims, D.A.; and Maratin, R.H. 1998. *CNWRA Ground Magnetic Surveys in the Yucca Mountain Region, Nevada (1996-1997)*. CNWRA 98-001. San Antonio, Texas: Center for Nuclear Waste Regulatory Analyses. TIC: 247807.
- 127905 McKay, M.D.; Beckman, R.J.; and Conover, W.J. 1979. "A Comparison of Three Methods for Selecting Values of Input Variables in the Analysis of Output from a Computer Code." *Technometrics*, 21, (2), 239–245. Alexandria, Virginia: American Statistical Association. TIC: 221741.
- 163274 NRC (U.S. Nuclear Regulatory Commission) 2003. *Yucca Mountain Review Plan, Final Report*. NUREG-1804, Rev. 2. Washington, D.C.: U.S. Nuclear Regulatory Commission, Office of Nuclear Material Safety and Safeguards. TIC: 254568.
- 158468 O’Leary, D.W.; Mankinen, E.A.; Blakely, R.J.; Langenheim, V.E.; and Ponce, D.A. 2002. *Aeromagnetic Expression of Buried Basaltic Volcanoes Near Yucca Mountain, Nevada*. Open-File Report 02-020. Denver, Colorado: U.S. Geological Survey. ACC: MOL.20020627.0225.
- 159502 Perry, F.V. and Bowker, L.M. 1998. "Petrologic and Geochemical Constraints on Basaltic Volcanism in the Great Basin." Chapter 4 of *Volcanism Studies: Final Report for the Yucca Mountain Project*. Perry, F.V.; Crowe, B.M.; Valentine, G.A.; and Bowker, L.M., eds. LA-13478. Los Alamos, New Mexico: Los Alamos National Laboratory. TIC: 247225.
- 162311 Perry, F.V.; Baldrige, W.S.; and DePaolo, D.J. 1987. "Role of Asthenosphere and Lithosphere in the Genesis of Late Cenozoic Basaltic Rocks from the Rio Grande Rift and Adjacent Regions of the Southwestern United States." *Journal of Geophysical Research*, 92, 9193–9213.

- 106634 Ratcliff, C.D.; Geissman, J.W.; Perry, F.V.; Crowe, B.M.; and Zeitler, P.K. 1994. "Paleomagnetic Record of a Geomagnetic Field Reversal from Late Miocene Mafic Intrusions, Southern Nevada." *Science*, 266, 412-416. Washington, D.C.: American Association for the Advancement of Science. TIC: 234818.
- 119693 Reamer, C.W. 1999. "Issue Resolution Status Report (Key Technical Issue: Igneous Activity. Revision 2.)" Letter from C.W. Reamer (NRC) to Dr. S. Brocoum (DOE/YMSCO), July 16, 1999 with enclosure. ACC: MOL.19990810.0639.
- 106708 Rosenbaum, J.G.; Hudson, M.R.; and Scott, R.B. 1991. "Paleomagnetic Constraints on the Geometry and Timing of Deformation at Yucca Mountain, Nevada." *Journal of Geophysical Research*, 96, (B2), 1963–1979. Washington, D.C.: American Geophysical Union. TIC: 225126.
- 145359 Savage, J.C.; Connor, C.B.; Stamatakos, J.A.; Ferrill, D.A.; Hill, B.E.; Davis, J.L.; Wernicke, B.P.; and Bennett, R.A. 1998. "Detecting Strain in the Yucca Mountain Area, Nevada." *Science*, 282, (5391), 1007b. Washington, D.C.: American Association for the Advancement of Science. TIC: 243445.
- 118952 Savage, J.C.; Svarc, J.L.; and Prescott, W.H. 1999. "Strain Accumulation at Yucca Mountain, Nevada, 1983–1998." *Journal of Geophysical Research*, 104 (B8), 17627–17631. Washington, D.C.: American Geophysical Union. TIC: 245645.
- 100075 Sawyer, D.A.; Fleck, R.J.; Lanphere, M.A.; Warren, R.G.; Broxton, D.E.; and Hudson, M.R. 1994. "Episodic Caldera Volcanism in the Miocene Southwestern Nevada Volcanic Field: Revised Stratigraphic Framework,  $^{40}\text{Ar}/^{39}\text{Ar}$  Geochronology, and Implications for Magmatism and Extension." *Geological Society of America Bulletin*, 106, (10), 1304–1318. Boulder, Colorado: Geological Society of America. TIC: 222523.
- 101019 Smith, E.I.; Feuerbach, D.L.; Nauman, T.R.; and Faulds, J.E. 1990. "The Area of Most Recent Volcanism Near Yucca Mountain, Nevada: Implications for Volcanic Risk Assessment." *High-Level Radioactive Waste Management, Proceedings of the International Topical Meeting, Las Vegas, Nevada, April 8-12, 1990*. 1, 81–90. La Grange Park, Illinois: American Nuclear Society. TIC: 202058.
- 158735 Smith, E.I.; Keenan, D.L.; and Plank, T. 2002. "Episodic Volcanism and Hot Mantle: Implications for Volcanic Hazard Studies at the Proposed Nuclear Waste Repository at Yucca Mountain, Nevada." *GSA Today*, 12, (4), 4–10. Boulder, Colorado: Geological Society of America. TIC: 253146.
- 138819 Stamatakos, J.A.; Connor, C.B.; and Martin, R.H. 1997. "Quaternary Basin Evolution and Basaltic Volcanism of Crater Flat, Nevada, from Detailed Ground Magnetic Surveys of the Little Cones." *Journal of Geology*, 105, 319-330. Chicago, Illinois: University of Chicago. TIC: 245108.

- 107250 Wernicke, B.P.; Christiansen, R.L.; England, P.C.; and Sonder, L.J. 1987. "Tectonomagmatic Evolution of Cenozoic Extension in the North American Cordillera." *Continental Extensional Tectonics*. Coward, M.P.; Dewey, J.F.; and Hancock, P.L., eds. Special Publication No. 28, Pages 203–221. Oxford, England: Geological Society. TIC: 225180.
- 103485 Wernicke, B.; Davis, J.L.; Bennett, R.A.; Elosegui, P.; Abolins, M.J.; Brady, R.J.; House, M.A.; Niemi, N.A.; and Snow, J.K. 1998. "Anomalous Strain Accumulation in the Yucca Mountain Area, Nevada." *Science*, 279, 2096–2100. New York, New York: American Association for the Advancement of Science. TIC: 235956.
- 136262 Yogodzinski, G.M. and Smith, E.I. 1995. "Isotopic Domains and the Area of Interest for Volcanic Hazard Assessment in the Yucca Mountain Area." *Transactions of the American Geophysical Union*, 76 (46), F669. Washington, D.C.: American Geophysical Union. TIC: 237939.

## 8.2 CODES, STANDARDS, REGULATIONS, AND PROCEDURES

- 164105 AP-SI.1Q, Rev. 5, ICN 1. *Software Management*. Washington, D.C.: U.S. Department of Energy, Office of Civilian Radioactive Waste Management. ACC: DOC.20030708.0001.
- 164179 AP-SIII.9Q, Rev. 1, ICN 0. *Scientific Analyses*. Washington, D.C.: U.S. Department of Energy, Office of Civilian Radioactive Waste Management. ACC: DOC.20030708.0002.
- 156605 10 CFR 63. Energy: Disposal of High-Level Radioactive Wastes in a Geologic Repository at Yucca Mountain, Nevada. Readily available.

## 8.3 DATA, LISTED BY DATA TRACKING NUMBER

- 149593 LA0004FP831811.002. Volume of Volcanic Centers in the Yucca Mountain Region. Submittal date: 04/14/2000. (Data are used for reference only).
- 164712 LA0009FP831811.004. Summary Frequencies of Disruptive Volcanic Events. Submittal date; 09\05\2000.
- 152659 LA0009FP831811.004. Data Summaries Supporting Computation of Volcanic Event Intersection Frequencies for the 70,000 MTU Repository Layout. Submittal date: 09/14/2000.
- 144279 LAFP831811AQ97.001. Chemical and Geochronology Data for the Revision and Final Publication of the Volcanism Synthesis Report. Submittal date: 08/29/1997. (Data are used for reference only).
- 148234 MO0002PVHA0082.000. Probabilistic Volcanic Hazard Analysis for Yucca Mountain, Nevada. Submittal date: 02/17/2000.

149605 MO0003YMP98126.001. Quaternary and Pliocene Basalt. Submittal date: 03/02/2000. (Data are used for reference only).

#### 8.4 SOFTWARE

- 152614 Dynamic Graphics. 1998. *Software Code: EARTHVISION*. 5.1. Silicon Graphics Indigo R4000. 10174-5.1-00.
- 148560 LANL (Los Alamos National Laboratory). 2000. *Software Routine: CFRAC.FOR V1.0*. V1.0. 10254-1.0-00.
- 148617 LANL. 2000. *Software Routine: COMBDELD.FOR V1.0*. V1.0. 10288-1.0-00.
- 148562 LANL. 2000. *Software Routine: COMBSF.FOR V1.0*. V1.0. 10255-1.0-00.
- 148561 LANL. 2000. *Software Routine: COMBSM.FOR V1.0*. V1.0. 10256-1.0-00.
- 148535 LANL. 2000. *Software Routine: CPDI.FOR V1.0*. V1.0. 10257-1.0-00.
- 148534 LANL. 2000. *Software Routine: DCPELD.FOR V1.0*. V1.0. 10258-1.0-00.
- 148559 LANL. 2000. *Software Routine: DILECDLH.FOR V1.0*. V1.0. 10259-1.0-00.
- 148558 LANL. 2000. *Software Routine: DLECD.FOR V1.0*. V1.0. 10260-1.0-00.
- 148541 LANL. 2000. *Software Routine: FIT2CNTR.FOR V1.0*. V1.0. 10261-1.0-00.
- 148532 LANL. 2000. *Software Routine: FITCD.FOR V1.0*. V1.0. 10262-1.0-00.
- 148540 LANL. 2000. *Software Routine: FITFIELD.FOR V1.0*. V1.0. 10263-1.0-00.
- 148557 LANL. 2000. *Software Routine: FITIDSR.FOR V1.0*. V1.0. 10264-1.0-00.
- 148567 LANL. 2000. *Software Routine: FKVH.FOR V1.0*. V1.0. 10265-1.0-00.
- 148546 LANL. 2000. *Software Routine: FKVHLH.FOR V1.0*. V1.0. 10266-1.0-00.
- 148538 LANL. 2000. *Software Routine: FKVPVH.FOR V1.0*. V1.0. 10267-1.0-00.
- 148551 LANL. 2000. *Software Routine: FKVPVHLH.FOR V1.0*. V1.0. 10268-1.0-00.
- 148543 LANL. 2000. *Software Routine: FPFVH.FOR V1.0*. V1.0. 10269-1.0-00.
- 148553 LANL. 2000. *Software Routine: FPFVHLH.FOR V1.0*. V1.0. 10270-1.0-00.
- 148563 LANL. 2000. *Software Routine: MARGIN.FOR V1.0*. V1.0. 10271-1.0-00.
- 148555 LANL. 2000. *Software Routine: NECPDS.FOR V1.0*. V1.0. 10272-1.0-00.

- 148542 LANL. 2000. *Software Routine: PFGVH.FOR V1.0.* V1.0. 10273-1.0-00.
- 148552 LANL. 2000. *Software Routine: PFGVHLH.FOR V1.0.* V1.0. 10274-1.0-00.
- 148533 LANL. 2000. *Software Routine: SFCD.FOR V1.0.* V1.0. 10275-1.0-00.
- 148571 LANL. 2000. *Software Routine: SFIDSR.FOR V1.0.* V1.0. 10276-1.0-00.
- 148536 LANL. 2000. *Software Routine: UZVH.FOR V1.0.* V1.0. 10277-1.0-00.
- 148545 LANL. 2000. *Software Routine: UZVHLH.FOR V1.0.* V1.0. 10278-1.0-00.
- 148537 LANL. 2000. *Software Routine: UZVPVH.FOR V1.0.* V1.0. 10279-1.0-00.
- 148547 LANL. 2000. *Software Routine: UZVPVHLH.FOR V1.0.* V1.0. 10280-1.0-00.
- 148554 LANL. 2000. *Software Routine: VHTIELHS.FOR V1.0.* V1.0. 10281-1.0-00.
- 148544 LANL. 2000. *Software Routine: VHTREE.FOR V1.0.* V1.0. 10282-1.0-00.
- 148539 LANL. 2000. *Software Routine: ZBCKVH.FOR V1.0.* V1.0. 10283-1.0-00.
- 148550 LANL. 2000. *Software Routine: ZBCKVHLH.FOR V1.0.* V1.0. 10284-1.0-00.

## 8.5 OUTPUT DATA

- 164712 LA0009FP831811.001. Compilation and Summaries of Data Supporting Computation of Volcanic Event Intersection Frequencies. Submittal date: 09/01/2000.
- 164714 LA0009FP831811.002. Summary Frequencies of Disruptive Volcanic Events. Submittal date: 09/05/2000.
- 162670 LA0302BY831811.001. Summary Frequencies of Disruptive Volcanic Events. Submittal date: 02/05/03.
- 163985 LA0303BY831811.001. Data for tables and figures used in ANL-MGR-GS-000001, REV01. Submittal date: 04/07/03.
- 164713 LA0307BY831811.001. Formatted output data for TSPA. Submittal date: 07/29/03

**ATTACHMENT I**

**ADDRESSING *YUCCA MOUNTAIN REVIEW PLAN FINAL REPORT* ACCEPTANCE  
CRITERIA RELATED TO THE DEFINITION OF EVENTS WITH PROBABILITIES  
GREATER THAN  $10^{-8}$  PER YEAR AND VOLCANIC DISRUPTION OF WASTE  
PACKAGES**

INTENTIONALLY LEFT BLANK

## ATTACHMENT I

### **ADDRESSING YUCCA MOUNTAIN REVIEW PLAN FINAL REPORT ACCEPTANCE CRITERIA RELATED TO THE DEFINITION OF EVENTS WITH PROBABILITIES GREATER THAN $10^{-8}$ PER YEAR AND VOLCANIC DISRUPTION OF WASTE PACKAGES**

The probability of intersection of the repository by an ascending basaltic dike has been estimated to be  $1.7 \times 10^{-8}$  per year. Hence, to meet the requirements of 10 CFR 63.114(d), the probability of intersection has been identified as an event that must be evaluated as part of the analysis of repository postclosure performance. Section 1.5.2 of the YMRP (NRC 2003 [163274]) describes the review methods that apply to the description of site characterization activities, and Section 1.5.3 provides the acceptance criteria. Section 2.2.1.2.2.3 contains Acceptance Criteria related to the review of LA information about identification of events with probabilities greater than  $10^{-8}$  per year. The following information identifies sections of this report that contain information relevant to future igneous events at Yucca Mountain.

#### Section 1.5.2 Review Method 2: Summary of Site Characterization Results

Review Method specifies that the LA must contain an overview of geology, consistent with other site characterization summaries, that includes

- (f) A summary of regional geomorphic, tectonic, seismic, and volcanic models (i.e., conceptual, technical basis, interpretation of data), with particular emphasis on those features, events, and processes that may have an effect on the repository operations and safety.

FEPs associated with igneous activity and addressed by information in this report are identified in Section 6.1.2. The analysis report describes the volcanic history of the YMR and separates the Miocene eruptions of huge volumes of silicic tephra from the Pliocene and Quaternary eruptions of very modest amounts of basalt that ended with the eruption(s) at the Lathrop Wells cone about 80,000 years ago. Characteristics of the Crater Flat structural domain are described in Section 6.4.1. The correlation of volcanism with features of the structural domain is described in Section 6.4.1.5. The relationship of volcanic source zones described in the Probabilistic Volcanic Hazards Analysis for Yucca Mountain, Nevada (PVHA) to the structural domain are described in Section 6.4.2.

- (i) A summary evaluation of volcanic probability

The PVHA established that the annual probability of intersection of the repository by a basaltic dike is very low but still large enough that volcanism must be considered in the TSPA-LA. The estimate of the annual probability of intersection of the repository by an ascending basaltic dike was done using an expert elicitation process described in the PVHA. Topics of special interest include (a) discussion of PVHA results and uncertainty (Section 6.3.1.5), (b) consideration of alternative conceptual models (Section 6.3.1.6), (c) discussion of the significance of buried volcanic centers on PVHA results (Section 6.3.1.7), (d) discussion of alternative estimates of intersection probabilities, (e) discussion of the definitions and parameters of a volcanic event and

implications for alternative probability calculations (Section 6.3.2), and (f) discussion of conceptual models of volcanism and formulation of probability models (Section 6.3.3).

Section 1.5.3: Acceptance Criterion 2: The “General Information” Section of the License Application contains an adequate description of site characterization results.

- (1) A sufficient understanding is provided of current features and processes present in the Yucca Mountain region.

FEPs associated with igneous activity and addressed by information in this report are identified in Section 6.1.2. The analysis report describes the volcanic history of the YMR and separates the Miocene eruptions of huge volumes of silicic tephra from the Pliocene and Quaternary eruptions of very modest amounts of basalt that ended with the eruption(s) at the Lathrop Wells cone about 80,000 years ago. Characteristics of the Crater Flat structural domain are described in Section 6.4.1. The correlation of volcanism with features of the structural domain is described in Section 6.4.1.5. The relationship of volcanic source zones described in the Probabilistic Volcanic Hazards Analysis for Yucca Mountain, Nevada (PVHA) to the structural domain are described in Section 6.4.2.

- (2) An adequate understanding is provided of future events and processes likely to be present in the Yucca Mountain region that could affect repository safety.

The PVHA established that the annual probability of intersection of the repository by a basaltic dike is very low but still large enough that volcanism must be considered in the TSPA-LA. The estimate of the annual probability of intersection of the repository by an ascending basaltic dike was done using an expert elicitation process described in the PVHA. Topics of special interest include (a) discussion of PVHA results and uncertainty (Section 6.3.1.5), (b) consideration of alternative conceptual models (Section 6.3.1.6), (c) discussion of the significance of buried volcanic centers on PVHA results (Section 6.3.1.7), (d) discussion of alternative estimates of intersection probabilities, (e) discussion of the definitions and parameters of a volcanic event and implications for alternative probability calculations (Section 6.3.2), and (f) discussion of conceptual models of volcanism and formulation of probability models (Section 6.3.3).

For TSPA-LA, volcanic disruption of the repository will be modeled by two disruption scenarios. The first is a direct release scenario, which features a basaltic eruption through the repository, and ejection and dispersal of contaminated ash to the location of the reasonably maximally exposed individual. The second is an indirect release scenario, which features intrusion of a basaltic dike into the repository without eruption, damage to waste packages and exposure of the waste to transport by normal groundwater mechanisms. In each case, the dose is multiplied by the annual probability to provide a probability-weighted mean annual dose. The annual probability is documented in this report, and other reports document the other parameters needed to complete the models for the two scenarios.

### Section 2.2.1.2.2.3 Identification of Events with Probabilities Greater Than $10^{-8}$ Per Year

#### Acceptance Criterion 1: Events Are Adequately Defined.

- (1) Events or event classes are defined without ambiguity and used consistently in probability models, such that probabilities for each event or event class are estimated separately.

For the PVHA, an expert panel was convened in 1995 to review all pertinent data relating to volcanism at Yucca Mountain and, based on these data, to quantify both the annual probability and associated uncertainty of a volcanic event intersecting a proposed repository sited at Yucca Mountain. The data the experts reviewed was comprehensive, consisting of two decades of data collected by volcanologists who conducted studies to quantify the probability that a future volcanic eruption would disrupt the proposed repository. PVHA methods and results are summarized in Section 6.3.1.5, and Section 6.3.2 describes how the experts defined a volcanic event. Based on the description in Section 6.3.2, although the experts defined a volcanic event differently, the product of the expert elicitation process was an unambiguous definition of a volcanic event, and the descriptions in Sections 6.3.2 and 6.3.3 show how the definitions were consistently used in the development and evaluation of probability models that supported the estimate of the probability of intersection of the proposed repository by a future igneous event.

- (2) Probabilities of intrusive and extrusive igneous events are calculated separately.

Section 6.5.3 describes the results of the estimation of the probability of intersection of the LA repository footprint by an ascending basaltic dike. The section also describes the results of the estimation of the number of eruptive centers that could occur within the repository footprint. Probability values, presented in Table 22, show the annual frequency of intersection of the repository by a dike, the conditional probability of at least one eruptive center (given intersection), and the annual frequency of occurrence of one or more eruptive centers within the proposed repository.

#### Acceptance Criterion 2: Probability Estimates For Future Events Are Supported By Appropriate Technical Bases.

- (1) Probabilities for future natural events have considered past patterns of the natural events in the Yucca Mountain region considering the likely future conditions and interactions of the natural and engineered system. These probability estimates have specifically included igneous events.

Section 6.2 describes the volcanic history of the YMR. Section 6.3.1 describes the PVHA process and includes documentation of the measures used to include information about past patterns of igneous activity in the YMR were incorporated into alternative spatial and temporal distributions of potential future volcanic activity in the region (Section 6.3.1.3). Section 6.3.1.7 describes the methods used to evaluate the significance of buried volcanic centers on the PVHA results, and Section 6.3.1.8 describes the measures used to include alternative estimates of the intersection probability. Section 6.3.2 includes examples of how information about vents and vent alignments in the YMR were incorporated into the probability calculations.

Acceptance Criterion 3: Probability Model Support Is Adequate.

- (1) Probability models are justified through comparison with output from detailed process-level models and/or empirical observations (e.g., laboratory testing, field measurements, or natural analogs, including Yucca Mountain site data). Specifically:
  - (a) For infrequent events, the U.S. Department of Energy justifies, to the extent appropriate, proposed probability models with data from reasonably analogous systems. Analog systems should contain significantly more events than the Yucca Mountain system, to provide reasonable evaluations of probability model performance.

Section 6.3.1.3 describes the temporal and spatial aspects of probability models and the methods that were used to ensure that alternative spatial and temporal models were considered by the experts and included in the development of probability models. Section 6.3.1.6 describes the consideration of alternative conceptual models of the tectonic environment of Yucca Mountain that have emerged since the PVHA was completed. Section 6.3.1.7 describes the methods used to consider the significance of buried volcanic centers on the PVHA results. Section 6.3.1.8 describes the alternative estimates of intersection probability and provides comments about the relevance of each of the models to estimating the probability of intersection. Section 6.3.2 describes definitions and parameters of a volcanic event and describes implications of these elements for alternative probability calculations. Section 6.3.2.1 specifically addresses use of analog information and describes evidence from analog sites related to determining whether dikes or dike systems can reach the near-surface without any portion of the system erupting. Data from the analog systems shows that field observations do not support the multipliers assigned for undetected intrusive events by the NRC. Rather, the analog information supports the interpretation that the intrusion/extrusion ratio is close to 1.

- (b) The U.S. Department of Energy justifies, to the extent appropriate, the ability of probability models to produce results consistent with the timing and characteristics (e.g., location and magnitude) of successive past events in the Yucca Mountain system.

The DOE probability estimate for intersection of the proposed repository by a basaltic dike is a combined estimate developed from inputs of 10 experts but modified to reflect the current design. The experts' models were based on the igneous characteristics of the YMR; hence, the probability models they developed were consistent with the timing and characteristics of past events in the YMR. The information used by the experts and the results of their deliberations are extensively documented in the PVHA (CRWMS M&O 1996 [100116]). The ability of the probability model to produce results consistent with timing and characteristics of past events is described in detail in Section 6.5.3, and the effects of new aeromagnetic information on the hazard estimate is evaluated in Section 6.5.4.

- (c) The U.S. Department of Energy probability models for natural events use underlying geologic bases (e.g., tectonic models) that are consistent

with other relevant features, events, and processes evaluated, using Section 2.2.1.2.1

Consistency of experts' models with tectonic models is discussed in Section 6.4, which presents a detailed description of the Crater Flat structural domain. Consideration of relevant features, events and processes is discussed in Section 6.1.2.

Acceptance Criterion 4: Probability Model Parameters Have Been Adequately Established.

- (1) Parameters used in probability models are technically justified and documented by the U.S. Department of Energy. Specifically:
  - (a) Parameters for probability models are constrained by data from the Yucca Mountain region and engineered repository system to the extent practical.

Section 6.2 describes the volcanic history of the YMR. Section 6.3.1 describes the PVHA process and includes documentation of the measures used to include information about past patterns of igneous activity in the YMR were incorporated into alternative spatial and temporal distributions of potential future volcanic activity in the region (Section 6.3.1.3). Section 6.3.1.7 describes the methods used to evaluate the significance of buried volcanic centers on the PVHA results, and Section 6.3.1.8 describes the measures used to include alternative estimates of the intersection probability. Section 6.3.2 includes examples of how information about vents and vent alignments in the YMR were incorporated into the probability calculations.

- (b) The U.S. Department of Energy appropriately establishes reasonable and consistent correlations between parameters.

The volcanic history of the YMR is described in Section 6.2. The correlations between volcanism and the internal structure and boundaries of the Crater Flat basin are described in Section 6.4.1.5, and the relationship between Crater Flat structural features and the probability of dike intersection with the repository is described in Section 6.4.2. The reasonableness and consistency of the relationship between intrusive and extrusive event, and the effects of consideration of alternative models of the relationship based on analog information, is described in detail in Section 6.3.2.1. Alternative event (dike) lengths and their consistency with data from the YMR and with data from analogs are considered in Section 6.3.2.2. Conceptual models of volcanism and the use of these models in the development of probability models are described in Section 6.3.3.

- (c) Where sufficient data do not exist, the definition of parameter values and conceptual models is based on appropriate use of other sources, such as expert elicitation conducted in accordance with appropriate guidance.

The DOE probability estimate is based on the results of formal elicitation of 10 experts (Section 6.3.1.1). The data considered by the experts was described in detail in the PVHA report (CRWMS M&O 1996 [100116], e.g., Table 3-1). The development of the probability estimate is summarized in Section 6.3 of this report, and the elicitation process is summarized in Section 6.3.1.4. Elicitation results are extensively documented in the PVHA report (CRWMS

M&O 1996 [100116], Sections 4.1 and 4.2) and are summarized in this report in Section 6.3.1.5. DOE and NRC guidance relevant to the elicitation process and adherence to that guidance during the elicitation process was described in the PVHA (CRWMS M&O 1996 [100116], Section 2.1.1).

Acceptance Criterion 5: Uncertainty In Event Probability Is Adequately Evaluated.

- (1) Probability values appropriately reflect uncertainties. Specifically:
  - (a) The U.S. Department of Energy provides a technical basis for probability values used, and the values account for the uncertainty in the probability estimates.

The technical basis for the probability values described in this report are extensively documented in Sections 6.3.2 and 6.4, and the PVHA process is summarized in Section 6.3.1. The formulations and methods used to recalculate the frequency of intersection, develop distributions for length and orientation of dikes, and estimate the number of eruptive centers within the proposed repository footprint are described in Sections 6.5.1 and 6.5.2. The results of the calculations are described in Section 6.5.3.

Uncertainties in the PVHA elicitation process are summarized in Section 6.3.1.5, and uncertainties in the technical basis supporting the probability values calculated in this report are described in Sections 6.3.2 and 6.3.3. The correlation of volcanism in the YMR with the Crater Flat structural domain is discussed in Section 6.4.1.5, and the relationship of the PVHA volcanic source zones to Crater Flat structural features and the probability of dike intersection is described in Section 6.4.2. Propagation of uncertainties in the analyses are specifically described in Section 6.5.3 and are shown, for example, in Figure 20.

- (b) The uncertainty for reported probability values adequately reflects the influence of parameter uncertainty on the range of model results (i.e., precision) and the model uncertainty, as it affects the timing and magnitude of past events (i.e., accuracy).

Propagation of uncertainties in the analyses are specifically described in Section 6.5.3 and are shown, for example, in Figure 20. Methods to include uncertainties associated with specific parameter are described in the formulation of the probability models in Section 6.5.1.

Acceptance criteria related to the volcanic disruption of waste packages are presented in Section 2.2.1.3.10.3 of the YMRP (NRC 2003 [163274] NUREG-1804). Because this section of the review plan addresses the consequences of an igneous event intersecting the repository, the applicability of the information in this report to the acceptance criteria is limited. Information in this report about the segment lengths and orientations of dikes that intersect the repository, the number of eruptive centers that could form along a dike segment within the repository footprint, and the spacing between centers is needed to evaluate eruptive processes. However, this report does not address issues related to the nature of the possible interactions between a dike and repository drifts; nor does this report address waste package damage caused by exposure to magmatic conditions or the incorporation of such damage models into TSPA-LA.

Acceptance Criterion 1: System Description And Model Integration Are Adequate.

- (1) Total system performance assessment adequately incorporates important design features, physical phenomena, and couplings, and uses consistent and appropriate assumptions throughout the volcanic disruption of waste packages abstraction process.

The element is not addressed by information in this report. Information about the effects of exposure of waste packages to the environmental conditions attending intersection of the repository by a basaltic dike will be provided in a new report, *Igneous Intrusion Impacts on Waste Package and Waste Form*.

- (2) Models used to assess volcanic disruption of waste packages are consistent with physical processes generally interpreted from igneous features in the Yucca Mountain region and/or observed at active igneous systems.

Information in this report addresses the relationship between an ascending dike and the number of eruptive centers that could occur within the repository footprint (Section 6.5.3). The formulations and implementation methods needed to support the analyses are described in Sections 6.5.1 and 6.5.2, respectively. Models that are used to support the analysis of the effects of exposure of waste packages to the environmental conditions attending intersection of the repository by a basaltic dike will be described in a new report, *Igneous Intrusion Impacts on Waste Package and Waste Form*.

- (3) Models account for changes in igneous processes that may occur from interaction with engineered repository systems.

Changes in igneous processes that may occur from interactions with the engineered repository systems are not addressed in this report. Changes in igneous processes will be addressed in the update of the report, *Dike Propagation Near Drifts* and in the new report, *Igneous Intrusion Impacts on Waste Package and Waste Form*.

- (4) Guidance in NUREG-1297 and NUREG-1298 (Altman et al. 1998 a, b) or other acceptable approaches is followed.

This acceptance criterion is not applicable to this report. The information in this report was not developed using peer review methods (NUREG-1297), and no preexisting data was qualified (NUREG-1298) to support the analyses in this report.

Acceptance Criterion 2: Data Are Sufficient For Model Justification

- (1) Parameter values used in the license application to evaluate volcanic disruption of waste packages are sufficient and adequately justified. Adequate descriptions of how the data were used, interpreted, and appropriately synthesized into the parameters are provided.

The parameters developed in this report and needed in the analysis of volcanic disruption of waste packages are the results of calculations of the length and orientation of dikes and the

number of eruptive centers within the repository. These parameters are documented in Section 6.5.3.

- (2) Data used to model processes affecting volcanic disruption of waste packages are derived from appropriate techniques. These techniques may include site-specific field measurements, natural analog investigations, and laboratory experiments.

Information about, and modeling of, processes affecting volcanic disruption of waste packages will be provided in the following analysis reports:

- Characterize Eruptive Processes and Ash Redistribution at Yucca Mountain, Nevada
- Dike Propagation Near Drifts
- Igneous Intrusion Impacts on Waste Package and Waste Form.

Provides the results of calculations of the length and orientation of dikes and the number of eruptive centers within the repository. These parameters are documented in Section 6.5.3.

- (3) Sufficient data are available to integrate features, events, and processes, relevant to volcanic disruption of waste packages into process-level models, including determination of appropriate interrelationships and parameter correlations.

Table 9 identifies the features, events and processes (FEPs) that are included in this analysis report and provides a summary of the disposition of each FEP in the TSPA-LA. However, this report does not provide that FEPs disposition documentation. That documentation will be provided in the update of the disruptive events FEPs analysis report (CRWMS M&O 2000 [151553]).

- (4) Where sufficient data do not exist, the definition of parameter values and associated conceptual models is based on appropriate use of expert elicitation, conducted in accordance with NUREG-1563 (Kotra et al 1996). If other approaches are used, the U.S. Department of Energy adequately justifies their use.

The DOE probability estimate is based on the results of formal elicitations of 10 experts (Section 6.3.1.1). The data considered by the experts was described in detail in the PVHA report (CRWMS M&O 1996 [100116], e.g., Table 3-1). The development of the probability estimate is summarized in Section 6.3 of this report, and the elicitation process is summarized in Section 6.3.1.4. Elicitation results are extensively documented in the PVHA report (CRWMS M&O 1996 [100116], Sections 4.1 and 4.2) and are summarized in this report in Section 6.3.1.5. DOE and NRC guidance relevant to the elicitation process and adherence to that guidance during the elicitation process was described in the PVHA (CRWMS M&O 1996 [100116], Section 2.1.1).

Acceptance Criterion 3: Data Uncertainty Is Characterized And Propagated Through The Model Abstraction.

- (1) Models use parameter values, assumed ranges, probability distributions, and bounding assumptions that are technically defensible, and reasonably account for uncertainties and variabilities, and do not result in an under-representation of the risk estimate.

The formulations support the probability estimate and propagate parameter uncertainties, methods used to implement the analyses, and results of the analyses are described in detail in Sections 6.5.1, 6.5.2, and 6.5.3, respectively, of this report. In addition, the definitions and parameters of a volcanic event and their implications for alternative probability calculations are described in Section 6.3.2. PVHA results and associated uncertainties are discussed in Section 6.5.1.3. Consideration of alternative probability models in the PVHA process is described in Section 6.5.1.4, and the significance of buried volcanic centers on the PVHA results is described in Section 6.5.1.5. Alternative estimates of the intersection probability are described in Section 6.5.1.6. The robustness of the estimate of the probability of intersection has been demonstrated through sensitivity analyses (e.g., Brocoum 1997 [147772]), and some published estimates of the probability of intersection of the repository by a dike are presented in Table 13.

- (2) Parameter uncertainty accounts quantitatively for the uncertainty in parameter values observed in site data and the available literature (i.e., data precision), and the uncertainty in abstracting parameter values to process-level models (i.e., data accuracy).

The uncertainties associated with the temporal and spatial aspects of models of the probability of intersection are described in Section 6.3.1.3. PVHA results and uncertainty are described in Section 6.3.1.5. Similarly, the formulations, implementation, and results of the recalculation of the frequency of intersection and the development of distributions for length and orientation of dikes are explained in Sections 6.5.1, 6.5.2, and 6.5.3, respectively. These sections also explain the development of the probability distributions for the number of eruptive center that could occur within the repository. The process for abstracting the recalculated values is not addressed in this report.

- (3) Where sufficient data do not exist, the definition of parameter values and associated uncertainty is based on appropriate use of expert elicitation, conducted in accordance with NUREG-1563 (Kotra et al 1996). If other approaches are used, the U.S. Department of Energy adequately justifies their use.

The DOE probability estimate is based on the results of formal elicitation of 10 experts (Section 6.3.1.1). The data considered by the experts was described in detail in the PVHA report (CRWMS M&O 1996 [100116], e.g., Table 3-1). The development of the probability estimate is summarized in Section 6.3 of this report, and the elicitation process is summarized in Section 6.3.1.4. Elicitation results are extensively documented in the PVHA report (CRWMS M&O 1996 [100116], Sections 4.1 and 4.2) and are summarized in this report in Section 6.3.1.5. DOE and NRC guidance relevant to the elicitation process and adherence to that guidance during the elicitation process was described in the PVHA (CRWMS M&O 1996 [100116], Section 2.1.1).

Acceptance Criterion 4: Model Uncertainty Is Characterized And Propagated Through The Model Abstraction.

- (1) Alternative modeling approaches to volcanic disruption of the waste package are considered and are consistent with available data and current scientific understandings, and the results and limitations are appropriately considered in the abstraction.

This report does not address modeling of the volcanic disruption of waste packages. That modeling will be described in the report, *Igneous Intrusion Impacts on Waste Package and Waste Form*.

- (2) Uncertainties in abstracted models are adequately defined and documented, and effects of these uncertainties are assessed in the total system performance.

This report does not address abstractions of models and propagation of uncertainty through the abstraction process.

- (3) Consideration of conceptual model uncertainty is consistent with available site characterization data, laboratory experiments, field measurements, natural analog information and process-level modeling studies; and the treatment of conceptual model uncertainty does not result in an under-representation of the risk estimate.

This report does not directly address the processes and associated models of volcanic disruption of waste packages. The processes and modeling will be described in the report, *Igneous Intrusion Impacts on Waste Package and Waste Form*.

Uncertainties in conceptual models used to estimate the probability of intersection of the repository, distributions of dike length and orientation, and the number of eruptive centers within the proposed repository are explained in Section 6.5.1, which describes the formulation of the analyses.

Acceptance Criterion 5: Model Abstraction Output Is Supported By Objective Comparisons.

This report does not address model abstraction.

**ATTACHMENT II**  
**DEVELOPMENT OF FOOTPRINT POLYGON**  
**FOR THE PROPOSED REPOSITORY**

INTENTIONALLY LEFT BLANK

## ATTACHMENT II

### DEVELOPMENT OF FOOTPRINT POLYGON FOR THE PROPOSED REPOSITORY

The coordinates of the emplacement drifts for the LA repository design were obtained from the Repository/PA IED Subsurface Facilities Plan (BSC 2002 [159527]). These coordinates are given in terms of the Nevada State Plane Coordinate System, Central Zone. The coordinate system used in the PVHA hazard assessment is UTM. The Nevada State Plane coordinates for the emplacement drifts were transformed to UTM (Zone 11) using the coordinate conversion utility in EarthVision 5.1 (STN: 10174-5.1-00 [152614]). The transformed coordinates are listed in Table II-1.

The calculations performed in this scientific analysis input data from files that contain the vertices of a polygon for the proposed repository footprint. For the purpose of this analysis, the repository footprint is defined as the outline of the waste emplacement area. A polygon was constructed to encompass the emplacement drifts in panels 1, 2, 3, and 5 of the LA repository design. A buffer zone was added around the emplacement area defined by the drift coordinates in Table II-1 to account for the effect of eruptive conduit size on the calculation of the frequency of dike intersection and the distribution for number of eruptive centers within the repository footprint. The mean of the distribution for conduit diameter given in CRWMS M&O (2000 [151551]) is approximately 52.2 meters. Adding the emplacement drift half-width of 2.75 meters gives a buffer zone width of 55 meters. The resulting polygon vertices were placed in input file LA2002.FP used in the calculations presented in this report. The footprint polygon file is listed below and is shown in Figure 16, Section 6.5.

```
**** File: LA2002.fp****  
LA 2002 Footprint Panels 1, 2, 3, & 5  
31  
547.741 4078.280  
547.735 4077.339  
547.755 4076.323  
547.840 4076.095  
547.909 4076.060  
548.354 4076.207  
548.389 4076.276  
548.468 4076.473  
548.530 4077.601  
548.577 4078.554  
548.619 4079.420  
548.688 4079.474  
549.066 4079.595  
549.101 4079.664  
549.216 4080.213  
549.662 4081.128  
549.584 4081.272  
549.441 4081.365  
548.997 4081.219  
549.018 4081.512  
548.949 4081.547  
548.434 4081.375  
547.959 4081.134  
547.782 4080.990  
547.658 4080.810
```

# Characterize Framework for Igneous Activity at Yucca Mountain, Nevada

547.394 4080.211  
 547.328 4079.167  
 547.384 4078.588  
 547.418 4078.513  
 547.528 4078.410  
 547.741 4078.280

Table II-1. Proposed Repository Drift Coordinates for License Application Design

Zone	Drift	East Side		West Side	
		UTM Easting (km)	UTM Northing (km)	UTM Easting (km)	UTM Northing (km)
2	1	548.966	4081.495	548.434	4081.320
2	2	548.962	4081.408	548.392	4081.221
3	2	548.364	4081.212	547.959	4081.079
2	3	548.921	4081.310	548.351	4081.122
3	3	548.323	4081.113	547.782	4080.935
2	4	548.879	4081.211	548.309	4081.023
3	4	548.281	4081.014	547.711	4080.827
2	1	549.441	4081.310	548.997	4081.164
2	5	548.837	4081.112	548.267	4080.925
3	5	548.239	4080.915	547.669	4080.728
3	6	547.627	4080.629	548.198	4080.816
2	6	548.226	4080.826	548.796	4081.013
2	2	548.956	4081.065	549.532	4081.255
2	3	549.582	4081.186	548.914	4080.966
2	7	548.754	4080.913	548.184	4080.726
3	7	548.156	4080.717	547.586	4080.529
3	8	547.544	4080.431	548.114	4080.618
2	8	548.142	4080.627	548.713	4080.815
2	4	548.872	4080.868	549.610	4081.110
2	5	549.563	4081.009	548.831	4080.769
2	9	548.671	4080.716	548.101	4080.528
3	9	548.073	4080.519	547.503	4080.332
3	10	547.446	4080.228	548.032	4080.421
2	10	548.061	4080.430	548.626	4080.616
2	6	548.770	4080.664	549.511	4080.907
2	7	549.459	4080.805	548.738	4080.567
2	11	548.622	4080.529	548.046	4080.340
3	11	547.994	4080.323	547.425	4080.136
3	12	547.421	4080.049	547.990	4080.236
2	12	548.042	4080.253	548.618	4080.443
2	8	548.735	4080.481	549.408	4080.703
2	9	549.356	4080.601	548.730	4080.394
2	13	548.613	4080.356	548.038	4080.167
3	13	547.986	4080.150	547.417	4079.963

Table II-1. Proposed Repository Drift Coordinates for License Application Design (Continued)

Zone	Drift	East Side		West Side	
		UTM Easting (km)	UTM Northing (km)	UTM Easting (km)	UTM Northing (km)
3	14	547.412	4079.876	547.981	4080.063
2	14	548.033	4080.080	548.609	4080.269
2	10	548.726	4080.307	549.304	4080.498
2	11	549.253	4080.395	548.722	4080.221
2	15	548.605	4080.183	548.030	4079.993
3	15	547.978	4079.977	547.407	4079.789
3	16	547.404	4079.703	547.973	4079.890
2	16	548.025	4079.907	548.601	4080.096
2	12	548.718	4080.134	549.201	4080.293
2	13	549.164	4080.196	548.713	4080.048
2	17	548.596	4080.009	548.021	4079.820
3	17	547.969	4079.803	547.399	4079.616
3	18	547.395	4079.529	547.965	4079.717
2	18	548.016	4079.733	548.593	4079.923
2	14	548.710	4079.962	549.142	4080.104
2	15	549.115	4080.010	548.705	4079.875
2	19	548.588	4079.836	548.012	4079.647
3	19	547.961	4079.630	547.391	4079.443
3	20	547.387	4079.356	547.956	4079.543
2	20	548.008	4079.560	548.584	4079.750
2	16	548.701	4079.789	549.106	4079.921
2	17	549.087	4079.830	548.696	4079.702
2	21	548.580	4079.663	548.003	4079.474
3	21	547.951	4079.457	547.382	4079.269
3	22	547.381	4079.184	547.948	4079.370
2	22	548.000	4079.387	548.575	4079.576
2	18	548.693	4079.615	549.067	4079.738
2	19	549.049	4079.647	548.688	4079.529
2	23	548.571	4079.490	547.995	4079.300
3	23	547.946	4079.284	547.389	4079.101
3	24	547.396	4079.018	547.962	4079.204
1	1	548.112	4079.254	548.566	4079.403
1	2	548.563	4079.316	548.012	4079.135
3	25	547.959	4079.118	547.403	4078.935
3	26	547.411	4078.852	547.954	4079.031
1	3	548.006	4079.048	548.558	4079.230
1	4	548.554	4079.143	548.002	4078.961
3	27	547.950	4078.944	547.419	4078.770
3	28	547.426	4078.687	547.946	4078.858
1	5	548.003	4078.877	548.550	4079.056

Table II-1. Proposed Repository Drift Coordinates for License Application Design (Continued)

Zone	Drift	East Side		West Side	
		UTM Easting (km)	UTM Northing (km)	UTM Easting (km)	UTM Northing (km)
1	6	548.546	4078.970	548.044	4078.805
3	29	547.944	4078.772	547.437	4078.605
3	30	547.470	4078.531	547.977	4078.697
1	7	548.541	4078.883	548.128	4078.747
3	31	548.074	4078.645	547.528	4078.465
1	8	548.538	4078.796	548.215	4078.691
5	1	548.525	4078.537	547.794	4078.297
5	2	547.793	4078.211	548.520	4078.450
5	3	548.516	4078.363	547.791	4078.125
5	4	547.790	4078.040	548.511	4078.277
5	5	548.508	4078.190	547.789	4077.954
5	6	547.788	4077.869	548.503	4078.103
5	7	548.499	4078.017	547.786	4077.783
5	8	547.786	4077.697	548.495	4077.930
5	9	548.491	4077.843	547.784	4077.612
5	10	547.783	4077.526	548.486	4077.757
5	11	548.483	4077.670	547.785	4077.441
5	12	547.787	4077.356	548.478	4077.583
5	13	548.473	4077.497	547.788	4077.272
5	14	547.789	4077.187	548.469	4077.410
5	15	548.465	4077.324	547.792	4077.102
5	16	547.793	4077.018	548.461	4077.237
5	17	548.456	4077.150	547.795	4076.933
5	18	547.800	4076.849	548.453	4077.064
5	19	548.448	4076.977	547.805	4076.766
5	20	547.807	4076.681	548.444	4076.890
5	21	548.440	4076.804	547.807	4076.596
5	22	547.805	4076.510	548.436	4076.717
5	23	548.431	4076.630	547.806	4076.425
5	24	547.807	4076.340	548.428	4076.544
5	25	548.416	4076.455	547.815	4076.257
5	26	547.843	4076.181	548.381	4076.358
5	27	548.337	4076.259	547.892	4076.113

OUTPUT DATA. DTN: LA0303BY831811.001 [163985]

**ATTACHMENT III**

**DEVELOPMENT OF DISTRIBUTIONS FOR NUMBER OF  
ERUPTIVE CENTERS PER VOLCANIC EVENT AND AVERAGE SPACING  
BETWEEN ERUPTIVE CENTERS**

INTENTIONALLY LEFT BLANK

## ATTACHMENT III

### DEVELOPMENT OF DISTRIBUTIONS FOR NUMBER OF ERUPTIVE CENTERS PER VOLCANIC EVENT AND AVERAGE SPACING BETWEEN ERUPTIVE CENTERS

#### III.1 INTRODUCTION

This attachment presents the derivation of discrete distributions for the number of eruptive centers per volcanic event,  $n^{EC}$ , and the average spacing between eruptive centers. These assessments are derived from the PVHA experts' assessments of the number of volcanic events at the three Quaternary volcanic centers in the site region, Lathrop Wells (LW), Sleeping Butte (SB), and Northwest Crater Flat (NWCF) using the first two assumptions described in Section 5. As defined in the PVHA (CRWMS M&O 1996 [100116]), the number of eruptive centers at each of these sites is: two at Sleeping Butte (Little Black Peak and Hidden Cone); five at Crater Flat (Little Cones southwest, Little Cones northeast, Red Cone, Black Cone, and Makani Cone); and one at Lathrop Wells.

#### III.2 ILLUSTRATION OF THE PROCESS

The process is illustrated using the assessments of Alex McBirney (AM) [from Table AM-1, p. AM-13 of Appendix E in CRWMS M&O (1996 100116)]. For Lathrop Wells (LW), AM assigned probabilities of 0.3, 0.2, 0.4, and 0.1 to there having been 1, 2, 3, or 4 volcanic events, respectively. If only one event occurred, then the data from LW are one event with one eruptive center per event ( $n^{EC} = 1$ ). If there were two events, then the data are two events with  $n^{EC} = 1$ . For the three and four volcanic event scenarios the data are three events with  $n^{EC} = 1$  and four events with  $n^{EC} = 1$ , respectively. These assessments are summarized in Table III-1.

For Sleeping Butte (SB), AM assigned probabilities of 0.05, 0.8, and 0.15 to there being 1, 2, or 3 volcanic events, respectively. For the one event scenario, the data are one event with  $n^{EC} = 2$  (Hidden Cone and Little Black Peak). For the two-event scenario, the data are two events with  $n^{EC} = 1$ . For the three-event scenario, the data are three events with  $n^{EC} = 1$ .

For Northwest Crater Flat (NWCF), AM assigned probabilities of 0.9, 0.05, 0.025, 0.015, and 0.01 to there having been 1, 2, 3, 4, or 5 volcanic events, respectively. For the one event scenario, the data are one event with  $n^{EC} = 5$  (Little Cones SW, Little Cones NE, Red Cone, Black Cone, and Makani Cone). For the two-event scenario, AM linked Little Cones (SW and NE), Red Cone, and Black Cone into one event and considered Makani Cone to be the second event. Thus, the data are one event with  $n^{EC} = 4$  and one event with  $n^{EC} = 1$ . For the three-event scenario, AM considered Red Cone and Black Cone to be one event, Little Cones SW and NE to be one event, and Makani Cone to be the third event. Thus, the data are two events with  $n^{EC} = 2$  and one event with  $n^{EC} = 1$ . For the four-event scenario, AM considered Little Cones SW and NE to be one event, and Red Cone, Black Cone, and Makani Cone to each be separate events. Thus, the data are one event with  $n^{EC} = 2$  and four events with  $n^{EC} = 1$ . Finally, for the five-event scenario, the data are five events with  $n^{EC} = 1$ .

The PVHA experts defined their assessments at each of the volcanic centers to be independent of the assessments at the other centers. As a result, for the assessments from Alex McBirney, there

are  $4 \times 3 \times 5 = 60$  possible combined scenarios for the number of Quaternary volcanic events. Each of these combined scenarios represents a possible empirical data set for evaluating the distribution for  $n^{EC}$ . For example, if LW scenario 1, SB scenario 1, and NWCF scenario 1 are the correct assessments for the number of events, then the combined data set consists of one event with  $n^{EC} = 1$ , one event with  $n^{EC} = 2$ , and one event with  $n^{EC} = 5$ . The resulting empirical distribution defining the relative frequency for various values of  $n^{EC}$  is:

$$P(n^{EC} = 1) = 1/3 = 0.333$$

$$P(n^{EC} = 2) = 1/3 = 0.333$$

$$P(n^{EC} = 3) = 0/3 = 0$$

$$P(n^{EC} = 4) = 0/3 = 0$$

$$P(n^{EC} = 5) = 1/3 = 0.333$$

The joint probability that this combined scenario represents the correct data is the product of the three independent probabilities for each scenario and is equal to  $0.3 \times 0.05 \times 0.9 = 0.0135$ . There are 59 other possible combined data sets, each resulting in an empirical distribution for  $n^{EC}$ . The weighted average of these is used to represent the expected distribution for  $n^{EC}$  based on the assessments of Alex McBirney.

A similar process is followed to compute the average spacing between eruptive centers. Whenever a volcanic event is defined to contain more than one of the eruptive centers, then the assessment provides a data point that can be used to evaluate the average spacing between eruptive centers. In the above combined scenario, there are two volcanic events with multiple eruptive centers. The single event at Sleeping Butte consists of eruptive centers at Little Black Peak and Hidden Cone. These cones are located 2.45 kilometers apart. The single event at Crater Flat consists of five eruptive centers. The distance between Makani Cone and Little Cones SW is 11.19 kilometers. Dividing this by 4, which is the number of intervals between eruptive centers, gives an average spacing of 2.80 kilometers. Thus, the combined scenario provides an average value of 2.6 kilometers based on two data points. The process is repeated for the 59 other scenarios, and the weighted average provides the expected average spacing between eruptive centers. In performing this calculation, those scenarios that result in only volcanic events with no multiple eruptive centers are removed from the weighting process.

### **Calculation of Empirical Distribution for Average Spacing of Eruptive Centers**

Both the previous revision to this scientific analysis report and this current revision incorporate the empirical distribution for the average spacing between eruptive centers into the calculation of the conditional probability for the number of eruptive centers within the repository footprint. For the example scenario presented in the previous paragraph, the empirical distribution consists of a sample of two points, 2.45 kilometers with a probability of 0.5 and 2.80 kilometers, with a probability of 0.5. This distribution is weighted by the probability for the scenario of 0.0135. Repeating the process for the 59 other scenarios, weighting each empirical distribution by its scenario probability provides a composite empirical distribution for the average spacing between eruptive centers in future volcanic events.

### III.3 CALCULATION INPUT AND RESULTS

The inputs to the calculation are the distributions for the number of volcanic events represented by the mapped Quaternary volcanoes defined by the PVHA experts and the locations of the volcanoes. Tables III-1 through III-10 summarize the interpretations of the assessments made by the 10 PVHA experts.

Table III-1. Assessments from Alex McBirney's Volcanic Hazard Model

Volcanic Center	Scenario	Number of Events *	Probability	Number of Events with $n^{EC} =$				
				1	2	3	4	5
Lathrop Wells	1	1 LW	0.3	1				
	2	2 LW, LW	0.2	2				
	3	3 LW, LW, LW	0.4	3				
	4	4 LW, LW, LW, LW	0.1	4				
Sleeping Butte	1	1 LBP+HC	0.05		1			
	2	2 LBP, HC	0.8	2				
	3	3 LBP, HC, ?	0.15	3				
Crater Flat	1	1 MC+BC+RC+ LCne+LCsw	0.9					1
	2	2 MC, BC+RC+ LCne+LCsw	0.05	1			1	
	3	3 MC, BC+RC, LCne+LCsw	0.025	1	2			
	4	4 MC, BC, RC, LCne+LCsw	0.015	3	1			
	5	5 MC, BC, RC, LCne, LCsw	0.01	5				

DTN: MO0002PVHA0082.000 [148234]

Source: CRWMS M&O (1996 [100116], Appendix E, Table AM-1, p. AM-13)

NOTE: \*LW = Lathrop Wells; HC = Hidden Cone; LBP = Little Black Peak; MC = Makani Cone; BC = Black Cone; RC = Red Cone; LCne = Little Cones North East; LCsw = Little Cones southwest, ? undetected. A + indicates eruptive centers considered to be part of a single volcanic event.

Table III-2. Assessments from Bruce Crowe's Volcanic Hazard Model

Volcanic Center	Scenario	Number of Events *	Probability	Number of Events with $n^{EC} =$				
				1	2	3	4	5
Lathrop Wells	1	1 LW	0.9	1				
	2	2 LW, LW	0.06	2				
	3	3 LW, LW, LW	0.03	3				
	4	4 LW, LW, LW, LW	0.01	4				
Sleeping Butte	1	1 LBP+HC	0.35		1			
	2	2 LBP, HC	0.45	2				
	3	3 LBP, HC, ?	0.2	3				
Crater Flat	1	1 MC+BC+RC+ LCne+LCsw	0.1					1
	2	2 MC+BC, RC+LCne+LC sw	0.1		1	1		
	3	3 MC, BC+RC, LCne+LCsw	0.45	1	2			
	4	4 MC, BC, RC, LCne+LCsw	0.2	3	1			
	5	5 MC, BC, RC, Lcne, LCsw	0.1	5				
	6	6 MC, BC, RC, Lcne, LCsw, ?	0.025	6				
	7	7 MC, BC, RC, Lcne, LCsw, ?, ?	0.025	7				

DTN: MO0002PVHA 0082.000 [148234]

Source: CRWMS M&O (1996 [100116], Appendix E, Table BC-3, p. BC-39)

NOTE: \* LW = Lathrop Wells; HC = Hidden Cone; LBP = Little Black Peak; MC = Makani Cone; BC = Black Cone; RC = Red Cone; Lcne = Little Cones North East; LCsw = Little Cones southwest, ? undetected. A + indicates eruptive centers considered to be part of a single volcanic event.

Table III-3. Assessments from George Thompson's Volcanic Hazard Model

Volcanic Center	Scenario	Number of Events*	Probability	Number of Events with $n^{EC} =$				
				1	2	3	4	5
Lathrop Wells	1	1 LW	0.75	1				
	2	2 LW, LW	0.09	2				
	3	3 LW, LW, LW	0.08	3				
	4	4 LW, LW, LW, LW	0.08	4				
Sleeping Butte	1	1 LBP+HC	0.35		1			
	2	2 LBP, HC	0.65	2				
Crater Flat	1	1 MC+BC+RC+ LCne+LCsw	0.2					1
	2	2 MC, BC+RC+ LCne+LCsw	0.15	1			1	
	3	3 MC, BC+RC, LCne+LCsw	0.1	1	2			
	4	4 MC, BC, RC, LCne+LCsw	0.5	3	1			
	5	5 MC, BC, RC, Lcne, LCsw	0.05	5				

DTN: MO0002PVHA0082.000 [148234]

Source: CRWMS M&O (1996 [100116], Appendix E, Table GT-1, p. GT-11)

NOTE: \* LW = Lathrop Wells; HC = Hidden Cone; LBP = Little Black Peak; MC = Makani Cone; BC = Black Cone; RC = Red Cone; Lcne = Little Cones North East; LCsw = Little Cones southwest, ? undetected. A + indicates eruptive centers considered to be part of a single volcanic event.

Table III-4. Assessments from George Walker's Volcanic Hazard Model

Volcanic Center	Scenario	Number of Events*	Probability	Number of Events with $n^{EC} =$				
				1	2	3	4	5
Lathrop Wells	1	1 LW	0.9	1				
	2	2 LW, LW	0.07	2				
	3	3 LW, LW, LW	0.02	3				
	4	4 LW, LW, LW, LW	0.01	4				
Sleeping Butte	1	1 LBP+HC	0.4		1			
	2	2 LBP, HC	0.6	2				
Crater Flat	1	1 MC+BC+RC+ LCne+LCsw	0.1					1
	3	3 MC, BC+RC, LCne+LCsw	0.35	1	2			
	4	4 MC, BC, RC, LCne+LCsw	0.55	3	1			

DTN: MO0002PVHA0082.000 [148234]

Source: CRWMS M&O (1996 [100116], Appendix E, Table GW-1, p. GW-11).

NOTE: \* LW = Lathrop Wells; HC = Hidden Cone; LBP = Little Black Peak; MC = Makani Cone; BC=Black Cone; RC = Red Cone; Lcne = Little Cones North East; LCsw = Little Cones southwest, ? undetected. A + indicates eruptive centers considered to be part of a single volcanic event.

Table III-5. Assessments from Mel Kuntz's Volcanic Hazard Model

Volcanic Center	Scenario	Number of Events *	Probability	Number of Events with $n^{EC} =$				
				1	2	3	4	5
Lathrop Wells	1	1 LW	0.95	1				
	2	2 LW, LW	0.03	2				
	3	3 LW, LW, LW	0.019	3				
	4	4 LW, LW, LW, LW	0.001	4				
Sleeping Butte	1	1 LBP+HC	0.6		1			
	2	2 LBP, HC	0.3	2				
	3	3 LBP, HC, ?	0.1	3				
Crater Flat	1	1 MC+BC+RC+ LCne+LCsw	0.6					1
	2	2 MC, BC+RC+ LCne+LCsw	0.3	1			1	
	3	3 MC, BC+RC, LCne+LCsw	0.05	1	2			
	4	4 MC, BC, RC, LCne+LCsw	0.05	3	1			

DTN: MO0002PVHA0082.000 [148234]

Source: CRWMS M&O (1996 [100116], Appendix E, Table MK-1, p. MK-18).

NOTE: \* LW = Lathrop Wells; HC = Hidden Cone; LBP = Little Black Peak; M = Makani Cone; BC = Black Cone; RC = Red Cone; Lcne = Little Cones North East; LCsw = Little Cones southwest, ? undetected. A + indicates eruptive centers considered to be part of a single volcanic event.

Table III-6. Assessments from Michael Sheridan's Volcanic Hazard Model

Volcanic Center	Scenario	Number of Events *	Probability	Number of Events with $n^{EC} =$				
				1	2	3	4	5
Lathrop Wells	1	1 LW	0.9	1				
	2	2 LW, LW	0.1	2				
Sleeping Butte	1	1 LBP+HC	0.67		1			
	2	2 LBP, HC	0.33	2				
Crater Flat	1	1 MC+BC+RC+ LCne+LCsw	0.7					1
	2	2 MC, BC+RC+ LCne+LCsw	0.2	1			4	
	3	3 MC, BC+RC, LCne+LCsw	0.1	1	2	2		

DTN: MO0002PVHA0082.000 [148234]

Source: CRWMS M&O (1996 [100116], Appendix E, Table MS-1, p. MS-16 and from text on pages MS-6 to MS-7).

NOTE: \* LW = Lathrop Wells; HC = Hidden Cone; LBP = Little Black Peak; MC = Makani Cone; BC = Black Cone; RC = Red Cone; Lcne = Little Cones North East; LCsw = Little Cones southwest, ? undetected. A + indicates eruptive centers considered to be part of a single volcanic event.

Table III-7. Assessments from Richard Carlson's Volcanic Hazard Model

Volcanic Center	Scenario	Number of Events *	Probability	Number of Events with $n^{EC} =$				
				1	2	3	4	5
Lathrop Wells	1	1 LW	0.95	1				
	2	2 LW, LW	0.05	2				
Sleeping Butte	1	1 LBP+HC	0.7		1			
	2	2 LBP, HC	0.2	2				
	3	3 LBP, HC, ?	0.1	3				
Crater Flat	1	1 MC+BC+RC+ LCne+LCsw	0.6					1
	3	3 MC, BC+RC, LCne+LCsw	0.3	1	2			
	5	5 MC, BC, RC, Lcne, LCsw	0.01	5				

DTN: MO0002PVHA0082.000 [148234]

Source: CRWMS M&O (1996 [100116], Appendix E, Table RC-1, p. RC-16).

NOTE: \* LW = Lathrop Wells; HC = Hidden Cone; LBP = Little Black Peak; MC = Makani Cone; BC = Black Cone; RC = Red Cone; Lcne = Little Cones North East; LCsw = Little Cones southwest, ? undetected. A + indicates eruptive centers considered to be part of a single volcanic event.

Table II-8. Assessments from Richard Fisher's Volcanic Hazard Model

Volcanic Center	Scenario	Number of Events *	Probability	Number of Events with $n^{EC} =$				
				1	2	3	4	5
Lathrop Wells	1	1 LW	0.6	1				
	2	2 LW, LW	0.3	2				
	3	3	0.05	3				
	4	4	0.05	4				
Sleeping Butte	1	1 LBP+HC	0.7		1			
	2	2 LBP, HC	0.25	2				
	3	3 LBP, HC, HC	0.05	3				
Crater Flat	1	1 MC+BC+RC+ LCne+LCsw	0.8					1
	2	2 MC+BC, RC+LCne+LCs w	0.05		1	1		
	3	3 MC, BC+RC, LCne+LCsw	0.05	1	2			
	4	4 MC, BC, RC, LCne+LCsw	0.1	3	1			

DTN: MO0002PVHA0082.000 [148234]

Source: CRWMS M&O (1996 [100116], Appendix E, Table RF-1, p. RF-12).

NOTE: \* LW = Lathrop Wells; HC = Hidden Cone; LBP = Little Black Peak; MC = Makani Cone; BC = Black Cone; RC = Red Cone; LCne = Little Cones North East; LCsw = Little Cones southwest, ? undetected. A + indicates eruptive centers considered to be part of a single volcanic event.

Table III-9. Assessments from Wendell Duffield's Volcanic Hazard Model

Volcanic Center	Scenario	Number of Events*	Probability	Number of Events with $n^{EC} =$				
				1	2	3	4	5
Lathrop Wells	1	1 LW	0.9	1				
	2	2 LW, LW	0.1	2				
Sleeping Butte	1	1 LBP+HC	0.05		1			
	2	2 LBP, HC	0.95	2				
Crater Flat	1	1 MC+BC+RC+ LCne+LCsw	0.07					1
	2	2 MC+BC+RC, LCne+LCsw	0.14		1	1		
	3	3 MC, BC+RC, LCne+LCsw	0.26	1	2			
	4	4 MC, BC, RC, LCne+LCsw	0.34	3	1			
	5	5 MC, BC, RC, Lcne, LCsw	0.19	5				

DTN: MO0002PVHA0082.000 [148234]

Source: CRWMS M&O (1996 [100116], Appendix E, Table WD-1, pp. WD-11 and page WD-5).

NOTE: \* LW = Lathrop Wells; HC = Hidden Cone; LBP = Little Black Peak; MC = Makani Cone; BC = Black Cone; RC = Red Cone; Lcne = Little Cones North East; LCsw = Little Cones southwest, ? undetected. A + indicates eruptive centers considered to be part of a single volcanic event.

Table III-10. Assessments from William Hackett's Volcanic Hazard Model

Volcanic Center	Scenario	Number of Events*	Probability	Number of Events with $n^{EC} =$				
				1	2	3	4	5
Lathrop Wells	1	1 LW	0.4	1				
	2	2 LW, LW	0.1	2				
	3	3 LW, LW, LW	0.4	3				
	4	4 LW, LW, LW, LW	0.05	4				
	5	5 LW, LW, LW, LW, LW	0.05	5				
Sleeping Butte	1	1 LBP+HC	0.4		1			
	2	2 LBP, HC	0.5	2				
	3	3 LBP, HC, ?	0.1	3				
Crater Flat	1	1 MC+BC+RC+ LCne+LCsw	0.1					1
	2	2 MC+BC+RC, LCne+LCsw	0.3		1	1		
	3	3 MC, BC+RC, LCne+LCsw	0.4	1	2			
	4	4 MC, BC, RC, LCne+LCsw	0.1	3	1			
	5	5 MC, BC, RC, Lcne, LCsw	0.05	5				
	6	6 MC, BC, RC, Lcne, LCsw, ?	0.05	6				

DTN: MO0002PVHA0082.000 [148234]

Source: CRWMS M&O (1996 [100116], Appendix E, Table WH-1, pp. WH-16).

NOTE: \* LW = Lathrop Wells; HC = Hidden Cone; LBP = Little Black Peak; MC = Makani Cone; BC = Black Cone; RC = Red Cone; Lcne = Little Cones North East; LCsw = Little Cones southwest, ? undetected. A + indicates eruptive centers considered to be part of a single volcanic event.

The locations of the Quaternary volcanoes are listed in Table III-11. These values were used in the PVHA calculation (CRWMS M&O 1996 [100116]) and were taken from Connor and Hill (1995 [102646]).

Table III-11. Volcano Locations

UTM East (km)	UTM North (km)	Volcano
543.780	4060.380	Lathrop Wells
523.230	4112.530	Hidden Cone
522.130	4110.340	Little Black Peak Cone
540.330	4079.130	Makani Cone (North Cone)
538.840	4073.990	Black Cone
537.450	4071.470	Red Cone
535.500	4069.490	Little Cone northwest
535.131	4069.220	Little Cone southeast

DTN: MO0002PVHA0082.000 [148234]

The calculation of the distribution for the number of eruptive centers per volcanic event and the average spacing between eruptive centers was performed using the software routine NECPDS V1.0 (STN: 10272-1.0-00 [148555]). The data in Tables III-1 through III-11 were used to create the following input files. The resulting output files are listed after each input file.

\*\*\*\* File: AMNECPDS.IN \*\*\*\*

```
vxy.dat
amnecpds.out
AM no ec on dikes at LW, SB, NWCF
4 0.3 0.2 0.4 0.1
1 1 1
2 1 1 1 1
3 1 1 1 1 1 1
4 1 1 1 1 1 1 1 1
3 0.05 0.8 0.15
1 2 2 3
2 1 2 1 3
3 1 2 1 3 1 3
5 0.9 0.05 0.025 0.015 0.01
1 5 4 5 6 7 8
2 4 5 6 7 8 1 4
3 2 7 8 2 5 6 1 4
4 2 7 8 1 5 1 6 1 4
5 1 4 1 5 1 6 1 7 1 8
q
```

\*\*\*\* File: AMNECPDS.OUT \*\*\*\*

```
AM no ec on dikes at LW, SB, NWCF
NEC 1 2 3 4 5
0.797067 0.020689 0.000000 0.008057 0.174188
average spacing = 2.69
```

\*\*\*\* File: BCNECPDS.IN \*\*\*\*

```
vxy.dat
bcnecpds.out
BC no ec on dikes at LW, SB, NWCF
4 0.9 0.06 0.03 0.01
1 1 1
2 1 1 1 1
3 1 1 1 1 1 1
4 1 1 1 1 1 1 1 1
3 0.35 0.45 0.2
1 2 2 3
2 1 2 1 3
```

# Characterize Framework for Igneous Activity at Yucca Mountain, Nevada

---

3 1 2 1 3 1 3  
7 0.1 0.1 0.45 0.2 0.1 0.025 0.025  
1 5 4 5 6 7 8  
2 3 6 7 8 2 4 5  
3 2 7 8 2 5 6 1 4  
4 2 7 8 1 4 1 5 1 6  
5 1 4 1 5 1 6 1 7 1 8  
6 1 4 1 5 1 6 1 7 1 8 1 8  
7 1 4 1 5 1 6 1 7 1 8 1 8 1 8  
q

\*\*\*\* File: BCNECPDS.OUT \*\*\*\*  
BC no ec on dikes at LW, SB, NWCF  
NEC 1 2 3 4 5  
0.681609 0.271645 0.020588 0.000000 0.026158  
average spacing = 1.87

\*\*\*\* File: GTNECPDS.IN \*\*\*\*  
vxy.dat  
GTnecpds.out  
GT no ec on dikes at LW, SB, NWCF  
4 0.75 0.09 0.08 0.08  
1 1 1  
2 1 1 1 1  
3 1 1 1 1 1 1  
4 1 1 1 1 1 1 1 1  
2 0.35 0.65  
1 2 2 3  
2 1 2 1 3  
5 0.2 0.15 0.1 0.5 0.05  
1 5 4 5 6 7 8  
2 4 5 6 7 8 1 4  
3 2 7 8 2 5 6 1 4  
4 2 7 8 1 5 1 6 1 4  
5 1 4 1 5 1 6 1 7 1 8  
q

\*\*\*\* File: GTNECPDS.OUT \*\*\*\*  
GT no ec on dikes at LW, SB, NWCF  
NEC 1 2 3 4 5  
0.744308 0.174364 0.000000 0.030266 0.051062  
average spacing = 1.53

\*\*\*\* File: GWNECPDS.IN \*\*\*\*  
vxy.dat  
gwnecpds.out  
GW no ec on dikes at LW, SB, NWCF  
4 0.9 0.07 0.02 0.01  
1 1 1  
2 1 1 1 1  
3 1 1 1 1 1 1  
4 1 1 1 1 1 1 1 1  
2 0.4 0.6  
1 2 2 3  
2 1 2 1 3  
3 0.1 0.35 0.55  
1 5 4 5 6 7 8  
3 2 7 8 2 5 6 1 4  
4 2 7 8 1 4 1 5 1 6  
q

\*\*\*\* File: GWNECPDS.OUT \*\*\*\*

# Characterize Framework for Igneous Activity at Yucca Mountain, Nevada

---

GW no ec on dikes at LW, SB, NWCF  
NEC 1 2 3 4 5  
0.690211 0.282237 0.000000 0.000000 0.027552  
average spacing = 1.36

\*\*\*\* File: MKNECPDS.IN \*\*\*\*

vxy.dat  
MKnecpds.out  
MK no ec on dikes at LW, SB, NWCF  
4 0.95 0.03 0.019 0.001  
1 1 1  
2 1 1 1 1  
3 1 1 1 1 1 1  
4 1 1 1 1 1 1 1 1  
3 0.6 0.3 0.1  
1 2 2 3  
2 1 2 1 3  
3 1 2 1 3 1 3  
4 0.6 0.3 0.05 0.05  
1 5 4 5 6 7 8  
2 4 5 6 7 8 1 4  
3 2 7 8 2 5 6 1 4  
4 2 7 8 1 4 1 5 1 6  
q

\*\*\*\* File: MKNECPDS.OUT \*\*\*\*

MK no ec on dikes at LW, SB, NWCF  
NEC 1 2 3 4 5  
0.559011 0.199381 0.000000 0.067184 0.174424  
average spacing = 2.40

\*\*\*\* File: MSNECPDS.IN \*\*\*\*

vxy.dat  
MSnecpds.out  
MS no ec on dikes at LW, SB, NWCF  
2 0.9 0.1  
1 1 1  
2 1 1 1 1  
2 0.67 0.33  
1 2 2 3  
2 1 2 1 3  
3 0.7 0.2 0.1  
1 5 4 5 6 7 8  
2 4 5 6 7 8 1 4  
3 2 7 8 2 5 6 1 4  
q

\*\*\*\* File: MSNECPDS.OUT \*\*\*\*

MS no ec on dikes at LW, SB, NWCF  
NEC 1 2 3 4 5  
0.509542 0.235628 0.000000 0.045810 0.209020  
average spacing = 2.49

\*\*\*\* File: RCNECPDS.IN \*\*\*\*

vxy.dat  
RCnecpds.out  
RC no ec on dikes at LW, SB, NWCF  
2 0.95 0.05  
1 1 1  
2 1 1 1 1  
3 0.7 0.2 0.1  
1 2 2 3

# Characterize Framework for Igneous Activity at Yucca Mountain, Nevada

---

2 1 2 1 3  
3 1 2 1 3 1 3  
3 0.6 0.3 0.1  
1 5 4 5 6 7 8  
3 2 7 8 2 5 6 1 4  
5 1 4 1 5 1 6 1 7 1 8  
q

\*\*\*\* File: RCNECPDS.OUT \*\*\*\*  
RC no ec on dikes at LW, SB, NWCF  
NEC 1 2 3 4 5  
0.518637 0.301513 0.000000 0.000000 0.179850  
average spacing = 2.40

\*\*\*\* File: RFNECPDS.IN \*\*\*\*  
vxy.dat  
RFnecpds.out  
RF no ec on dikes at LW, SB, NWCF  
4 0.6 0.3 0.05 0.05  
1 1 1  
2 1 1 1 1  
3 1 1 1 1 1 1  
4 1 1 1 1 1 1 1 1  
3 0.7 0.25 0.05  
1 2 2 3  
2 1 2 1 3  
3 1 2 1 3 1 3  
4 0.8 0.05 0.05 0.1  
1 5 4 5 6 7 8  
2 3 6 7 8 2 4 5  
3 2 7 8 2 5 6 1 4  
4 2 7 8 1 4 1 5 1 6  
q

\*\*\*\* File: RFNECPDS.OUT \*\*\*\*  
RF no ec on dikes at LW, SB, NWCF  
NEC 1 2 3 4 5  
0.540624 0.232107 0.010571 0.000000 0.216698  
average spacing = 2.51

\*\*\*\* File: WDNECPDS.IN \*\*\*\*  
vxy.dat  
WDnecpds.out  
WD no ec on dikes at LW, SB, NWCF  
2 0.9 0.1  
1 1 1  
2 1 1 1 1  
2 0.05 0.95  
1 2 2 3  
2 1 2 1 3  
5 0.07 0.14 0.26 0.34 0.19  
1 5 4 5 6 7 8  
2 2 7 8 3 4 5 6  
3 2 7 8 2 5 6 1 4  
4 2 7 8 1 4 1 5 1 6  
5 1 4 1 5 1 6 1 7 1 8  
q

\*\*\*\* File: WDNECPDS.OUT \*\*\*\*  
WD no ec on dikes at LW, SB, NWCF  
NEC 1 2 3 4 5  
0.782655 0.172043 0.027872 0.000000 0.017430

average spacing = 1.40

\*\*\*\* File: WHNECPDS.IN \*\*\*\*

```
vxy.dat
WHnecpds.out
WH no ec on dikes at LW, SB, NWCF
5 0.4 0.1 0.4 0.05 0.05
1 1 1
2 1 1 1 1
3 1 1 1 1 1 1
4 1 1 1 1 1 1 1 1
5 1 1 1 1 1 1 1 1 1 1
3 0.4 0.5 0.1
1 2 2 3
2 1 2 1 3
3 1 2 1 3 1 3
6 0.1 0.3 0.4 0.1 0.05 0.05
1 5 4 5 6 7 8
2 3 4 5 6 2 7 8
3 2 5 6 2 7 8 1 4
4 2 7 8 1 4 1 5 1 6
5 1 4 1 5 1 6 1 7 1 8
6 1 4 1 5 1 6 1 7 1 8 1 8
q
```

\*\*\*\* File: WHNECPDS.OUT \*\*\*\*

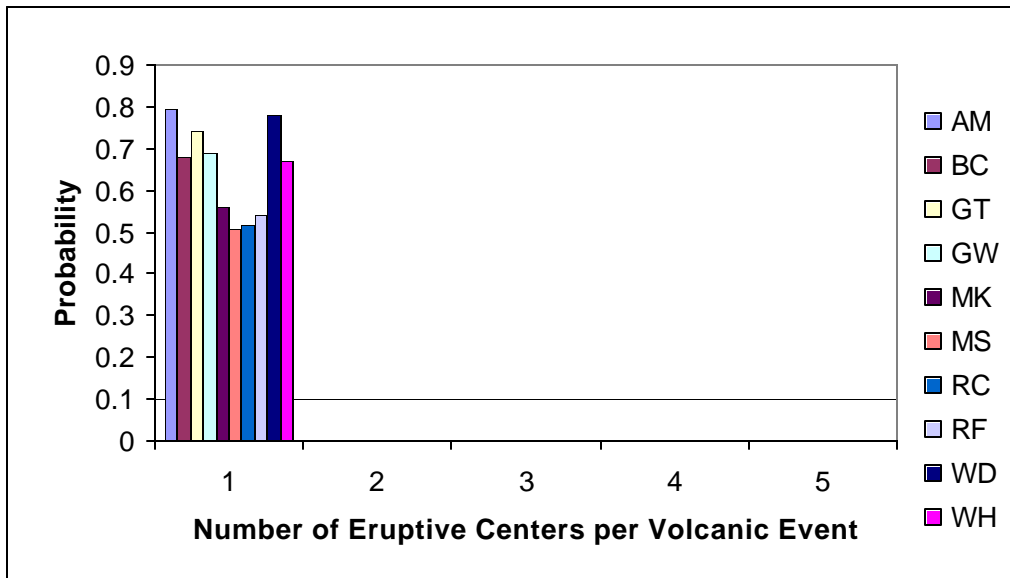
```
WH no ec on dikes at LW, SB, NWCF
NEC 1 2 3 4 5
0.668581 0.256513 0.053095 0.000000 0.021812
average spacing = 1.97
```

The distributions for  $n^{EC}$  for each expert are plotted in Figure III-1. The expected value for the average spacing between eruptive centers computed from each PVHA expert's hazard model is listed in Table III-12.

Table III-12. Summary of Expected Average Spacing Between Eruptive Centers Calculation Results

PVHA Expert	Expected Average Spacing Between Eruptive Centers (km)
Alex McBirney (AM)	2.7
Bruce Crowe (BC)	1.9
George Thompson (GT)	1.5
George Walker (GW)	1.4
Mel Kuntz (MK)	2.4
Michael Sheridan (MS)	2.5
Richard Carlson (RC)	2.4
Richard Fisher (RF)	2.5
Wendell Duffield (WD)	1.4
William Hackett (WH)	2.0

Output Data. DTN: LA0009FP831811.001 [164712]



Output Data. DTN: LA0009FP831811.001 [164712]

NOTE: The two-letter code indicates the PVHA expert's initials from Table III-12.

Figure III-1. Distributions for Number of Eruptive Centers per Volcanic Event,  $n^{EC}$ , Derived from the Probabilistic Volcanic Hazard Analysis Experts' Interpretations

### Computed Empirical Distributions for Average Spacing of Eruptive Centers

The calculation of the empirical distribution for the average spacing between eruptive centers was performed using the software routine NECPDS V1.1 (STN: 10272-1.1-00 [148555]). The software routine uses the same input files listed above and outputs all of the same data plus the empirical distribution for average spacing of eruptive centers. The resulting output files are listed below.

\*\*\*\* File: AMNECPDS.OUT \*\*\*\*

```
AM no ec on dikes at LW, SB, NWCF
NEC 1 2 3 4 5
0.797067 0.020689 0.000000 0.008057 0.174188
average spacing = 2.69
Average spacing distribution
5 0.46 0.0272 2.01 0.0492 2.45 0.0253 2.80 0.8859 2.88 0.0124
average spacing from distribution = 2.69
```

\*\*\*\* File: BCNECPDS.OUT \*\*\*\*

```
BC no ec on dikes at LW, SB, NWCF
NEC 1 2 3 4 5
0.681609 0.271645 0.020588 0.000000 0.026158
average spacing = 1.87
Average spacing distribution
6 0.46 0.4030 1.62 0.0489 2.45 0.1874 2.80 0.0914 2.88 0.2202 5.35 0.0489
average spacing from distribution = 1.88
```

\*\*\*\* File: GTNECPDS.OUT \*\*\*\*

```
GT no ec on dikes at LW, SB, NWCF
```

## Characterize Framework for Igneous Activity at Yucca Mountain, Nevada

---

NEC 1 2 3 4 5  
0.744308 0.174364 0.000000 0.030266 0.051062  
average spacing = 1.53  
Average spacing distribution  
5 0.46 0.4720 2.01 0.1279 2.45 0.1839 2.80 0.1705 2.88 0.0457  
average spacing from distribution = 1.53

\*\*\*\* File: GWNECPDS.OUT \*\*\*\*  
GW no ec on dikes at LW, SB, NWCF  
NEC 1 2 3 4 5  
0.690211 0.282237 0.000000 0.000000 0.027552  
average spacing = 1.36  
Average spacing distribution  
4 0.46 0.5917 2.45 0.1767 2.80 0.0800 2.88 0.1517  
average spacing from distribution = 1.37

\*\*\*\* File: MKNECPDS.OUT \*\*\*\*  
MK no ec on dikes at LW, SB, NWCF  
NEC 1 2 3 4 5  
0.559011 0.199381 0.000000 0.067184 0.174424  
average spacing = 2.40  
Average spacing distribution  
5 0.46 0.0550 2.01 0.2100 2.45 0.2950 2.80 0.4200 2.88 0.0200  
average spacing from distribution = 2.40

\*\*\*\* File: MSNECPDS.OUT \*\*\*\*  
MS no ec on dikes at LW, SB, NWCF  
NEC 1 2 3 4 5  
0.509542 0.235628 0.000000 0.045810 0.209020  
average spacing = 2.49  
Average spacing distribution  
5 0.46 0.0388 2.01 0.1330 2.45 0.3238 2.80 0.4655 2.88 0.0388  
average spacing from distribution = 2.49

\*\*\*\* File: RCNECPDS.OUT \*\*\*\*  
RC no ec on dikes at LW, SB, NWCF  
NEC 1 2 3 4 5  
0.518637 0.301513 0.000000 0.000000 0.179850  
average spacing = 2.40  
Average spacing distribution  
4 0.46 0.1186 2.45 0.3608 2.80 0.4021 2.88 0.1186  
average spacing from distribution = 2.41

\*\*\*\* File: RFNECPDS.OUT \*\*\*\*  
RF no ec on dikes at LW, SB, NWCF  
NEC 1 2 3 4 5  
0.540624 0.232107 0.010571 0.000000 0.216698  
average spacing = 2.51  
Average spacing distribution  
6 0.46 0.0842 1.62 0.0192 2.45 0.3383 2.80 0.5200 2.88 0.0192 5.35 0.0192  
average spacing from distribution = 2.51

\*\*\*\* File: WDNECPDS.OUT \*\*\*\*  
WD no ec on dikes at LW, SB, NWCF  
NEC 1 2 3 4 5  
0.782655 0.172043 0.027872 0.000000 0.017430  
average spacing = 1.40  
Average spacing distribution  
5 0.46 0.6445 2.45 0.0322 2.80 0.0833 2.88 0.1560 4.09 0.0840  
average spacing from distribution = 1.40

\*\*\*\* File: WHNECPDS.OUT \*\*\*\*

## Characterize Framework for Igneous Activity at Yucca Mountain, Nevada

---

WH no ec on dikes at LW, SB, NWCF

NEC 1 2 3 4 5

0.668581 0.256513 0.053095 0.000000 0.021812

average spacing = 1.97

Average spacing distribution

5 0.46 0.4078 2.45 0.1844 2.80 0.0851 2.88 0.1844 4.09 0.1383

average spacing from distribution = 1.97

The empirical distributions for the average spacing between eruptive centers computed from each PVHA expert's hazard model are listed in Table III-13.

Table III-13. Empirical Distribution for Average Spacing Between Eruptive Centers Calculation Results

PVHA Expert	Empirical Distribution for Average Spacing between Eruptive Centers (km)
Alex McBirney (AM)	0.46 (0.0272), 2.01 (0.0492), 2.45 (0.0253), 2.80 (0.8859), 2.88 (0.0124)
Bruce Crowe (BC)	0.46 (0.4031), 1.62 (0.0489), 2.45 (0.1874), 2.80 (0.0914), 2.88 (0.2203), 5.35 (0.0489)
George Thompson (GT)	0.46 (0.4720), 2.01 (0.1279), 2.45 (0.1839), 2.80 (0.1705), 2.88 (0.0457)
George Walker (GW)	0.46 (0.5916), 2.45 (0.1767), 2.80 (0.0800), 2.88 (0.1517)
Mel Kuntz (MK)	0.46 (0.0550), 2.01 (0.2100), 2.45 (0.2950), 2.80 (0.4200), 2.88 (0.0200)
Michael Sheridan (MS)	0.46 (0.0388), 2.01 (0.1330), 2.45 (0.3238), 2.80 (0.4656), 2.88 (0.0388)
Richard Carlson (RC)	0.46 (0.1186), 2.45 (0.3608), 2.80 (0.4020), 2.88 (0.1186)
Richard Fisher (RF)	0.46 (0.0842), 1.62 (0.0192), 2.45 (0.3383), 2.80 (0.5199), 2.88 (0.0192), 5.35 (0.0192)
Wendell Duffield (WD)	0.46 (0.6445), 2.45 (0.0322), 2.80 (0.0833), 2.88 (0.1560), 4.09 (0.0840)
William Hackett (WH)	0.46 (0.4078), 2.45 (0.1844), 2.80 (0.0851), 2.88 (0.1844), 4.09 (0.1383)

Output Data. DTN: LA0009FP831811.002 [164714]

NOTE: The values in ( ) are the empirical probability for the preceding value of average spacing.